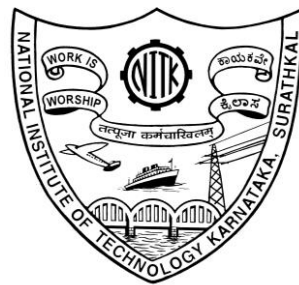# STUDIES ON THE EFFECTS OF AN EMERGED IMPERMEABLE AND SEASIDE PERFORATED QUARTER CIRCLE BREAKWATER ON NEAR FIELD HYDRODYNAMICS

Thesis

Submitted in partial fulfillment of the requirement for degree of

DOCTOR OF PHILOSOPHY

by

BINUMOL S

DEPARTMENT OF APPLIED MECHANICS AND HYDRAULICS

NATIONAL INSTITUTE OF TECHNOLOGY KARNATAKA

SURATHKAL, MANGALORE- 575 025

September 2017

D E C L A R A T I O N

I hereby *declare* that the Research Thesis entitled "**Studies on the effects of an emerged impermeable and seaside perforated quarter circle breakwater on near-field hydrodynamics",** which is being submitted to the **National Institute of Technology Karnataka, Surathkal** in partial fulfilment of the requirements for the award of the Degree of **Doctor of Philosophy** in **Civil Engineering** is a *bonafide report of the research work carried out by me*. The material contained in this Research Thesis has not been submitted to any University or Institution for the award of any degree.

112028AM11P04, BINUMOL.S.

(Register Number, Name & Signature of the Research Scholar)

Department of Applied Mechanics and Hydraulics
National Institute of Technology Karnataka, India

Place: NITK-Surathkal
Date: 05-09-2017

C E R T I F I C A T E

This is to *certify* that the Research Thesis entitled "**Studies on the effects of an emerged impermeable and seaside perforated quarter circle breakwater on near-field hydrodynamics",** submitted by **BINUMOL.S**. (Register Number: 112028AM11P04) as the record of the research work carried out by her, is *accepted as the Research Thesis submission* in partial fulfilment of the requirements for the award of degree of **Doctor of Philosophy**.

Prof. Subba Rao   **Prof. Arkal Vittal Hegde**
(Research Guide)   **(Research Guide)**

(Chairman – DRPC)

**DEPARTMENT OF APPLIED MECHANICS AND HYDRAULICS
NATIONAL INSTITUTE OF TECHNOLOGY KARNATAKA
SURATHKAL, MANGALORE-575025**

ACKNOWLEDGEMENT

ABSTRACT

Breakwaters are structures which are mainly used for the purpose of withstanding and dissipating the dynamic energy of ocean waves and thereby provide tranquility conditions on the lee side. Breakwaters are constructed either shore connected or detached to the coast. The main function of breakwaters is to create a tranquil medium on its leeside by reflecting the waves and also dissipating the wave energy arriving from seaside, resulting in ease of maneuverability to boats or ships to their berthing places. In modern times breakwaters are constructed for the purpose of protecting structures near to the coast and offshore, shoreline stabilization, forming an artificial harbour with a water area so protected from the ocean waves as to provide safe accommodation for ships and for preventing the siltation of river mouths.

Different types of breakwaters have been developed in the past for the harbour development and protection of valuable coastal property, commercial activity and beach morphology. Among these, rubble mound breakwaters are the most common and provide good wave attenuation. In the beginning, primitive reefs and dykes of gentle slopes were built with natural stones. Later to save the material, steeper sloped structures with rubble mound, concrete block mound, rock fill over mound, caisson type etc. were tried. However, with time breakwaters with a variety of caisson designs have been proposed and developed. Later with development of technology various innovative types of breakwaters such as semicircular breakwater and quarter circle breakwater have been developed.

Quarter circle breakwater (QBW) is a new-type breakwater first proposed by Xie et al. (2006) on the basis of semicircular breakwater. Quarter circle breakwater is usually placed on rubble mound foundation and its superstructure consists of a precast reinforced concrete quarter circular surface facing incident waves, a horizontal bottom slab and a rear vertical wall.

A series of experiments are conducted in a two dimensional monochromatic wave flume on impermeable and seaside perforated quarter circle breakwater model. The present study investigates the wave reflection, loss characteristics, wave runup,

wave rundown and sliding stability on an emerged seaside perforated quarter circle breakwater of three different radii 0.55 m, 0.575 m and 0.60 m with ratio of spacing to diameter of perforations (S/D) equal to 5, 4, 3, 2.5 and 2 for different water depths and wave conditions.

A 1:30 scale model of quarter circle breakwater of 0.55 m radius is fabricated using Galvanized Iron (GI) sheet of 0.002 m thickness. The sheet is fixed to the slab with the help of stiffeners made up of flat plates of cross section 0.025 m x 0.005 m. The model is then placed over the rubble mound foundation of thickness 0.05m and stones weighing from 50 to 100 grams.

Initially, impermeable quarter circle breakwater of different radius is tested for wave reflection and loss characteristics using regular waves of heights 0.03 m to 0.18 m and periods 1.2 s to 2.2 s in water depths of 0.30 m, 0.35 m and 0.40 m. Then runup and run down height on the curved QBW surface is noted and the vertical distance above and below the still water level is estimated. Later tests were conducted for determining minimum weight to be added to the QBW structure to prevent sliding. All the models were tested in the predetermined QBW dimensions as mentioned earlier.

In the second phase, perforated QBW with different S/D ratios were tested to determine the reflection, loss characteristics, runup, rundown and stability with the same wave conditions and using the same structural parameters.

Based on the experiments conducted, it was found that the reflection coefficient (K_r) increases but the loss coefficient (K_l) decreases with increase in incident wave steepness (H_i/gT^2). The minimum K_r and the maximum K_l observed are 0.5054 and 0.8629 respectively for QBW of radius equal to 0.55 m at $H_i/gT^2 = 9.439 \times 10^{-4}$. The results shows that the value of K_r decreases but K_l increases as the relative water depth (d/h_s) increases for all values of H_i/gT^2 and S/D ratio. The maximum percentage reduction in the value of K_r is observed for QBW of 0.55 m radius S/D= 2.5 and varies from 31.66% to 44.50% when the water depth increases from 0.35 m to 0.45 m. For seaside perforated QBW with $d/h_s= 0.732$, percentage reduction in

K_r for S/D equal to 5, 4, 3, 2.5, 2 varies from 47% to 49%, 54% to 58%, 60% to 71%, 72% to 86% and 68% to 84% when compared to impermeable QBW. For all d/h_s and H_i/gT^2, the values for relative wave runup (R_u/H_i) and relative wave rundown (R_d/H_i) decreases with decrease in S/D ratio. But in the case of seaside perforated QBW with S/D = 2 the values of R_u/H_i and R_d/H_i are found to slightly more than that of S/D = 2.5 due to back propogation of waves from inside the chamber.

Finally based on the studies on the sliding stability characteristics, it was observed that for all values of d/h_s and S/D ratio, stability parameter ($W/\gamma H_i^2$) decreases with increase in H_i/gT^2. The minimum values for $W/\gamma H_i^2$ for QBW of radius 0.55 m, 0.575 m and 0.60 m with S/D = 2.5 are 2.110, 1.998 and 1.967 respectively for $H_i/gT^2 = 6.241 \times 10^{-3}$ and at 0.35 m water depth.

Key words: Quarter circle breakwater, spacing to diameter of perforations, relative water depth, incident wave steepness, water depth, reflection coefficient, loss coefficient, wave runup, wave rundown, stability parameter.

CONTENTS

LIST OF TABLES

LIST OF FIGURES

LIST OF PLATES

NOMENCATURE

R	=	Radius of quarter circle breakwater
S/D	=	Spacing between perforations/ diameter of perforations
H_i	=	Incident wave height
H_r	=	Reflected wave height
R_u	=	Wave runup
R_d	=	Wave rundown
d	=	Depth of water
T	=	Wave period
L	=	Wave length
W	=	Weight of QBW per unit length
h_s	=	Height of structure
ρ	=	Mass density
g	=	Acceleration due to gravity
γ	=	Weight density
K_r	=	Reflection coefficient
K_l	=	Loss coefficient
d/h_s	=	Relative water depth
H_i/gT^2	=	Incident wave steepness parameter
R_u/ H_i	=	Relative wave runup
R_d/ H_i	=	Relative wave rundown
$W/\gamma H_i^2$	=	Stability parameter

1.1 GENERAL

Ports are considered to be the most important transit locations to carry out the world trade through seaways, which need to be protected from the disturbances due to the incoming waves. A seaport plays an important role in the sector of sea transportation, exports, imports, tourism, and travel, and thus is an important ingredient of economic growth. Water transport is a major economy input for a nation with over 82% of world trade in tons and 94% of world trade in tons-kilometers which are moved by shipping and thereby through ports (Frankel 1987).

The basic requirement of any port, harbour or marina is a sheltered area free from the waves. In the coastal areas where natural protection from waves is not available, the development of harbour requires an artificial protection for the creation of calm areas. For harbours, where perfect tranquility conditions are required, large structures such as rubble mound breakwaters or vertical wall breakwaters are used. Most of the breakwaters are used to create tranquil conditions in the lagoon and at the entrance channel of ports, for maneuvering of ships and port operations. Mostly breakwaters are also used as berthing structures along with protecting the harbour area. Sometimes they are used to protect beaches from erosion due to the destructive wave forces (Verhagen et al. 2009).

There are three main types of breakwaters: rubble mound, vertical wall and composite breakwaters. Rubble mound breakwaters are the oldest type and consist of natural rubble, undressed stone blocks or artificial blocks placed in various layers. Due to the development of these blocks, modern day rubble mound breakwaters can strongly resist the destructive power of waves, even in deep waters. Composite breakwaters consist of rubble mound foundation and vertical wall. By using caissons as the vertical wall, composite breakwaters provide an extremely stable structure even in rough, deep seas. Such strength has led to their use throughout the world. The selection of the type of breakwater will be primarily

based on the function of the breakwater, wave climate of that area, depth of water, availability of construction materials and local labour, geotechnical characteristics of sea bed, environmental concerns, aesthetics and available contractor potential.

Due to fast growing need of the universe and advances in technology different types of composite breakwater are being developed. One of the most recent developments is the evolution of semicircular breakwater. Semicircular breakwater is a composite structure first developed in Japan at the beginning of the Nineties and first adopted for the formation of the harbor in Miyazaki Port, Japan. Quarter circle breakwater is a new-type breakwater first proposed by Xie et al. (2006) on the basis of semicircular breakwater.

1.2 BREAKWATERS

1.2.1 History of breakwaters

The development of breakwater construction is closely related to the development of ports around the world over the centuries. The first breakwaters built can be linked to the ancient Egyptian, Phoenician, Greek and Roman cultures. Some of them were simple mound structures, composed of locally found rock. As early as 2000 BC, mention was made of a stone masonry breakwater in Alexandria, Egypt (Takahashi 1996). The Roman emperor Trajan (AD53 - 117) initiated the construction of a rubble mound breakwater in Civitavecchia, which still exists today (Fig. 1.1) (D'Angremond and van Roode 2004).
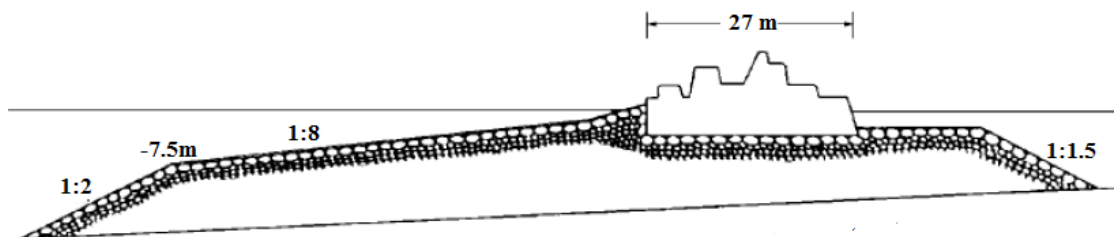
Fig. 1.1 Rubble mound breakwater at Civitavecchia

The standards for design and construction of a breakwater remained those developed primarily by the Romans, later a great leap in technology was achieved through the development of mechanical equipment and hydraulic sciences including maritime hydraulics (Franco 1996). De Cessart undertook rather complex work of a breakwater construction in Cherbourg harbor in comparatively deep waters. The

Plymouth breakwater started in 1811 showed a remarkable similarity of profile with the Cherbourg breakwater (Bruun 1985). The characteristic feature of these breakwaters was that they were periodically and partially damaged due to storms.

Later need for ports and harbours has resulted in construction of breakwater in deepwater and hence the failures of large rubble mound breakwaters. The large weights of stones were uneconomical to quarry or transport or were not available in the quarries nearby and hence later replaced by concrete blocks. Artificial armour units were being used from 19th century only. At the initial stage, artificial armour blocks used were cubic or rectangular shaped and used in the same manner as natural stone units.

Various studies conducted led to the development of new types of artificial armour units like tetrapods developed by Danel in 1950. The research since then has resulted in development of different types of rubble mound breakwaters with artificial armour units to suit to different marine conditions. Vertical wall breakwater originated at Dover U.K in 1847 (Refer Fig. 1.2). Erection of that vertical wall breakwater was extremely difficult; thus its construction was slow and performed at great expense.
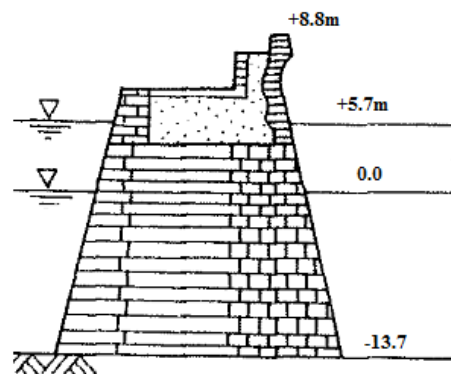
Fig. 1.2 Vertical wall breakwater at Dover, U. K

Later vertical wall breakwater was changed to composite breakwater with different rubble mound heights (Takahashi 1996). The development of composite breakwaters following 1945 was rapid due to the advancement of the design technology for concrete structures and that of in-sea construction technology using large working vessels (Takahashi 1996).The first modern breakwater was built in Japan in 1897: the north breakwater at the Port of Otaru designed by Hiroi (Refer Fig. 1.3).
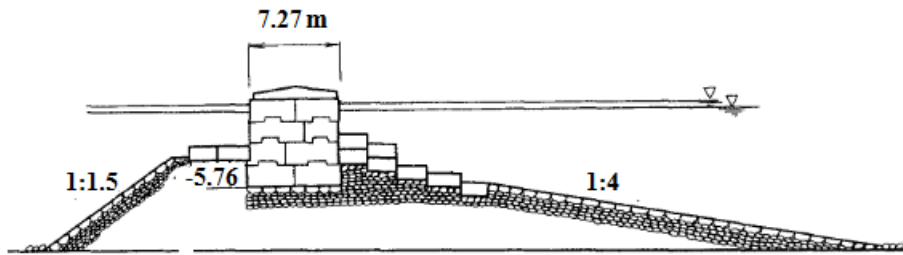
Fig. 1.3 Breakwater at the Port of Otaru

Many breakwaters constructed in Europe around this time were rubble mound breakwaters or composite breakwaters with block masonry. The technology introduced in Japan was primarily related to the composite breakwater, which has been developed into the currently used caisson composite breakwater. Caisson breakwater is one of the composite type breakwater first proposed by walker in 1840's and with technology developed into current status (Tanimoto et al. 1994). A metal caisson was employed in Bilbao, Spain, in 1894, and was later adopted in several other ports. Concrete caissons were also erected in Barcelona, Spain, and other ports, while reinforced concrete caissons were employed, vice using a rock fill crib, around 1901 in America's Great Lakes. In Japan, the reinforced concrete caisson was used for the first time in Kobe in 1907. Perforated wall caisson breakwater is one of the advanced type of caisson breakwater invented by Jarlan (1961). The first perforated wall caisson breakwater built in Takamatsu Port in 1970 (Takahashi, 1996) (Refer Fig. 1.4). The perforated wall caisson breakwater is usually employed with in a bay having relatively small waves since the forces on the caisson members are relatively small in such area. This type of construction also meets the need for providing low reflectivity.
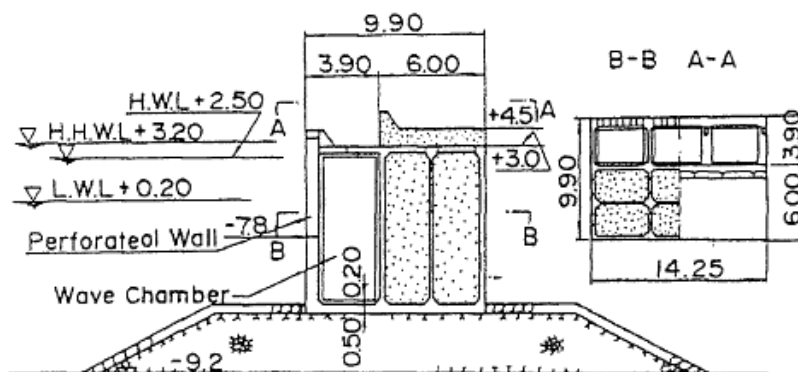
Fig. 1.4 Perforated wall caisson breakwater built in Takamatsu port

A curved-slit caisson was proposed to apply the wave-dissipating caisson to rough seas in 1976 by K. Tanimoto. After successful laboratory and field tests, the first curved slit caisson breakwater, with a length of 150 m, was constructed in 1984 at Funakawa Port, Japan. Fig. 1.5 shows the cross section of curved silt caisson breakwater. This geometry allows the decomposition of the wave forces along horizontal and a vertical direction, which favours the stability of the whole caisson.
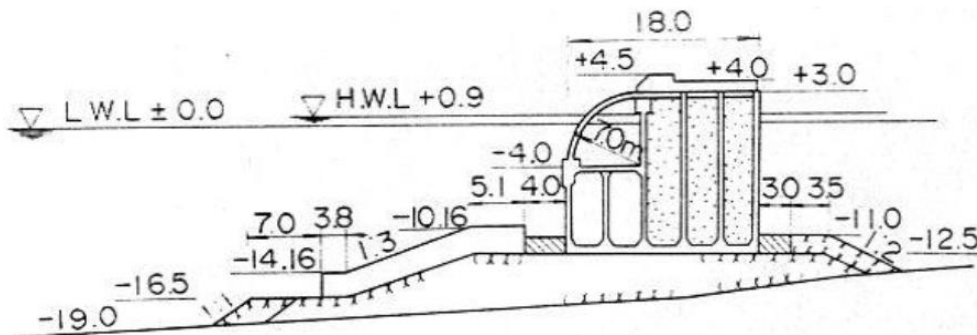
Fig. 1.5 Cross section of a caisson with curved wall, Funakawa port, Japan

In parallel the fast growing need of the universe and advances in technology resulted in development of different types of caisson breakwaters. Table 1.1 summarizes the historical development of breakwater especially during the 19th and 20th century.

Table 1.1 Summary of historical development of breakwater (Takahashi, 1996)

Most recent developments in breakwater construction are the evolution of semicircular and quarter circle breakwater. Some of these types of breakwater are constructed as impermeable while the others as perforated utilizing the merits of perforated type breakwaters.The semicircular breakwater was initially created in Japan at the beginning of the 1990s as reported by Tanimoto and Takahashi (1994), and a prototype semicircular breakwater of 36 m length was constructed at Miyazaki Port from 1992 -93 (Refer Fig. 1.6). This type has a high stability against wave action and can also be applied to protect beaches from erosion.Wave pressures on the semicircle face act towards the centre. The resultant force acts toward the centre and makes no rotational moment. It results in uniform distribution of the reaction at the bottom of the slab. So this can be used on very soft ground, because of the high stability against waves and the soft feature with the round top.
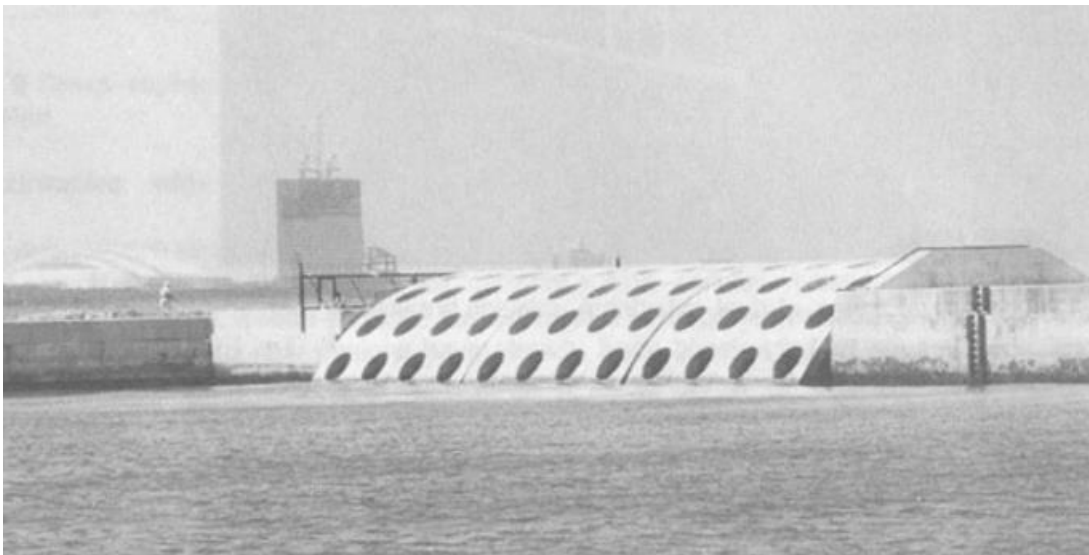
Fig. 1.6 Breakwater with semicircular caisson, Miyazaki Port, Japan

In China, a 527 m long semicircular breakwater was built at Tianjin Port in 1997, and after that an 18 km long semicircular estuary jetty was finished for the first stage works of the Deep Channel Improvement Project of the Yangtze River Estuary in 2000. The semicircular jetty structure was likewise proposed for utilization in the second Period of the Deep Channel Improvement Project of the Yangtze River Estuary. This new sort of breakwater is made out of a precast reinforced concrete structure manufactured with a semicircular caisson and a bottom section. The caisson comprises of a hollow structure and has a semicircular cross section. It is made up of pre-stressed concrete, cast in distinctive components, and joined by dry

joint method. The prefabricated structure is put on an arranged rubble mound foundation. The front and back sides of the semicircular caisson could be perforated either on one side or on both sides as per particular necessities.

At present, various types of breakwaters are in use throughout the world for the purpose of coastal protection, harbor activities, water sports and temporary construction activities. Research activities are in progress to study the hydrodynamic performance characteristics of new types of breakwaters in order to recommend them for the prevailing environmental and economic conditions.

1.2.2 Types of breakwaters

Breakwaters are mainly classified as:

1. Rubble mound or heap breakwaters.
2. Upright or vertical wall breakwaters.
3. Mound with superstructure or composite breakwaters.
4. Special types of breakwaters.

A breakwater may be constructed some distance away from the coast, or built with one end linked to the coast. Offshore breakwaters, also called bulkheads reduce the intensity of wave action in inshore waters and thereby reduce coastal erosion. Breakwater construction is usually parallel or perpendicular to the coast to maintain tranquility conditions in the port. Most of breakwater construction depends upon wave approach and considering some other environmental parameters. Breakwaters may be either fixed or floating; the choice depends on normal water depth and tidal range. A breakwater structure is designed to absorb the energy of the waves that hit it. This is done either by using mass (e.g. with caissons) or by using a revetment slope (e.g. with rock or concrete armour units). Caisson breakwaters typically have vertical sides and are usually used where it is desirable to berth one or more vessels on the inner face of the breakwater. They use the mass of the caisson and the fill within it to resist the overturning forces applied by waves hitting them. They are relatively expensive to construct in shallow water, but in deeper sites, they can offer a significant saving over revetment breakwaters. Breakwaters can be also divided into two principle categories: submerged and emerged. Submerged breakwaters lie entirely beneath the surface of the water while emerged breakwaters' crest protrudes

above the mean water level (MWL). Emerged breakwaters are designed to offer protection on their seaward face (armour layer), by inducing runup, breaking, and partial reflection of incident waves. Similarly, submerged breakwaters are designed to offer protection by inducing breaking and partial reflection-transmission of large waves (Grilli et al. 1994).

1. **Rubble mound or heap breakwaters:** It is a heterogeneous assemblage of natural rubble, undressed stone blocks, riprap, supplemented in many cases by artificial blocks of huge bulk and the whole being deposited without any regard to bond or bedding. This is the simplest type and is constructed by tipping or dumping of rubble stones into the sea till the heap or mound emerges out of the water, the mound being consolidated and its side slopes regulated by the action of the waves.

Rubble mound breakwaters are suitable for all types of foundations. Even though initial and maintenance cost is high, construction does not necessitate skilled labor or specialized equipment. Rubble mound breakwaters are further classified based on its variation in structural configuration as Multi layer rubble mound breakwater, submerged breakwaters, berm breakwaters, reef breakwaters and tandem breakwaters (Refer Fig. 1.7).
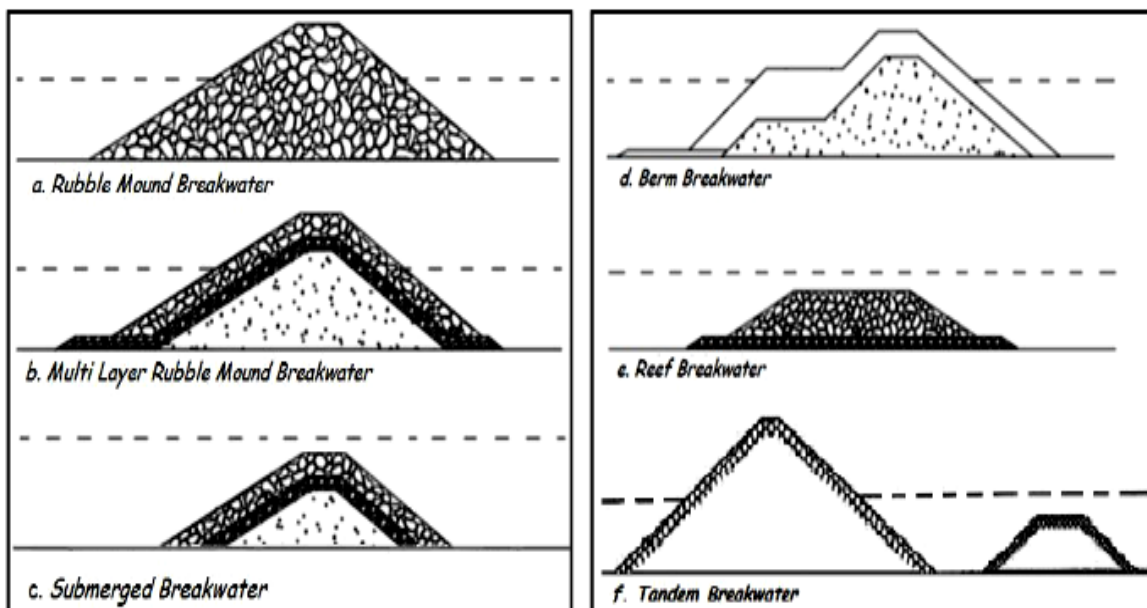
Fig. 1.7 Types of rubble mound breakwater

Multi-layer rubble mound breakwaters are made of three layers namely primary layer, secondary layer and a core. The primary layer is directly exposed to waves

and also acts a protective layer for secondary and core layers. A submerged breakwater is similar to multi-layer breakwater with only its crest at or below sea level. A breakwater with a horizontal berm at some elevation is called a berm breakwater. The berm breakwater may be reshaping type or non-reshaping type. The traditional rubble mound is a reef structure constructed as a heap of bulky stones laid at some stable slope to resist the wave action. A reef breakwater is a low-crested group of stones without a filler layer or core. Reef breakwater is allowed to reshape under wave attack. The concept of rubble mound breakwater and submerged reef breakwater, operating together as a single unit, is called the tandem breakwater.

2. **Upright or vertical wall breakwaters:** Vertical wall breakwaters are of different types such as huge concrete blocks, gravity walls, concrete caissons, concrete or sheet pile walls etc. (Refer Fig. 1.8). Caisson breakwaters typically have vertical sides and are usually used where it is desirable to berth one or more vessels on the inner face of the breakwater. The main purpose of the vertical breakwater was to reflect a major portion of the incident waves thereby creating tranquility in the protected area, while that for the rubble mound breakwater was to dissipate the incident wave energy.
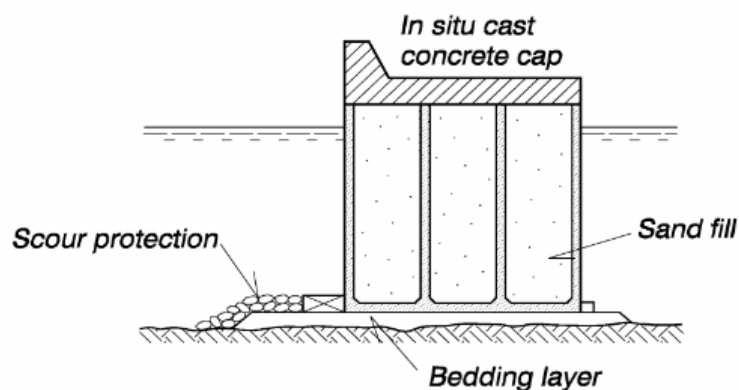
Fig. 1.8 Conventional Caisson breakwaters with vertical front

3. **Mound with superstructure or composite breakwaters:** Composite breakwaters are combination of rubble mound and vertical wall breakwaters. These are used in locations where either the depth of water is large or there is a large tidal range and in such situations, the quantity of rubble stone required to construct a breakwater to the full height would be too large. In such conditions, a composite

breakwater is constructed as a structure with rubble mound base and a super structure of vertical wall as shown in Fig.1.9. These breakwaters tend to fail when the waves break near the mound and then slam against the vertical wall, which damages the structure.
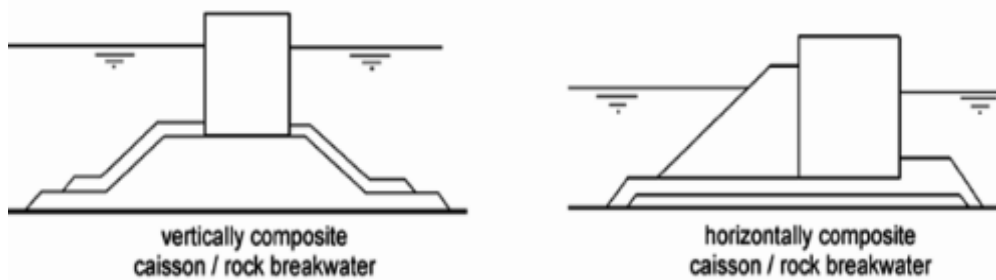
Fig. 1.9 Composite breakwaters

4. Special type of breakwaters: These breakwaters are for specific purposes with special features and are not commonly used. Depending on the site condition these are designed. Some special type of breakwaters are

i. Pneumatic and Hydraulic breakwaters: Pneumatic breakwater was first developed by Philip Brasher in 1907. The essence of idea is that a curtain of air bubbles blown up from the seabed through a row of perforated nozzles acts as a barrier to the movement of waves over the surface.
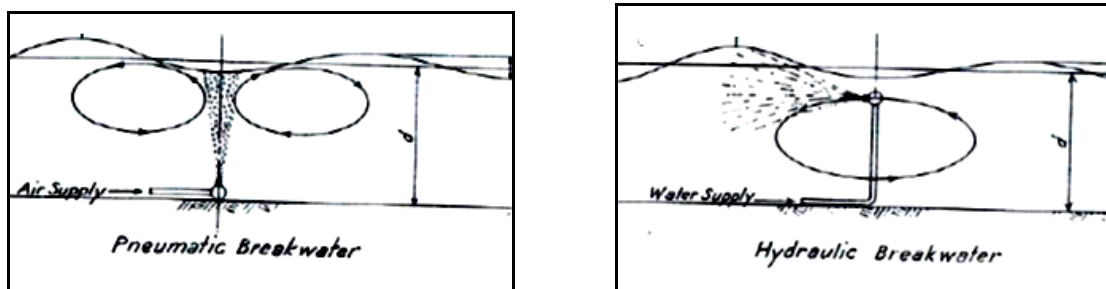
Fig. 1.10 Pneumatic and Hydraulic breakwaters

William and Weigel in 1963 introduced the hydraulic breakwater which consists of a series of water jets issued by forcing water through a number of nozzles mounted on a pipe installed at the water surface perpendicular to the direction of incident waves. The jets create a surface current which results in breaking of the incident wave and its attenuation.

ii. Floating breakwaters: This type of breakwater is an alternative to conventional fixed breakwaters and may be preferred in relatively low wave energy environments or where water depth or foundation considerations preclude the use of a bottom-

founded structure. Furthermore, in certain applications, aesthetic or water circulation considerations may require that the breakwater does not pierce the free surface and or extend down to the seabed.
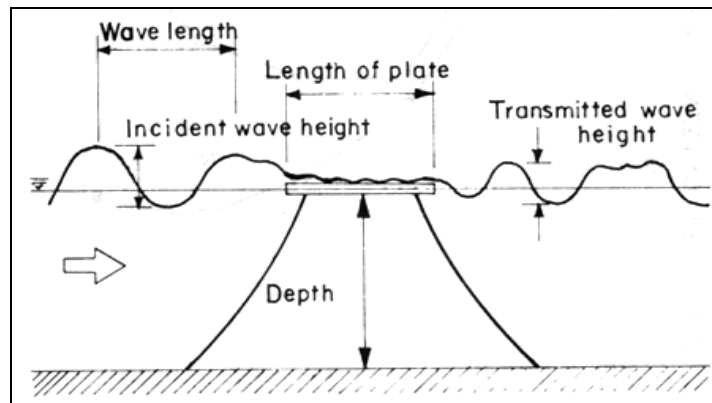
Fig. 1.11 Typical Floating breakwater

iii. Quadrant front face pile supported breakwater: It is a combination of semicircular and closely spaced pile breakwaters, which couples the advantages of these two types. This type of structure consists of two parts. The bottom portion consists of closely spaced piles and the top portion consists of a quadrant solid front face on the seaside. The leeward side of the top portion with a vertical face would facilitate the berthing of vessels.
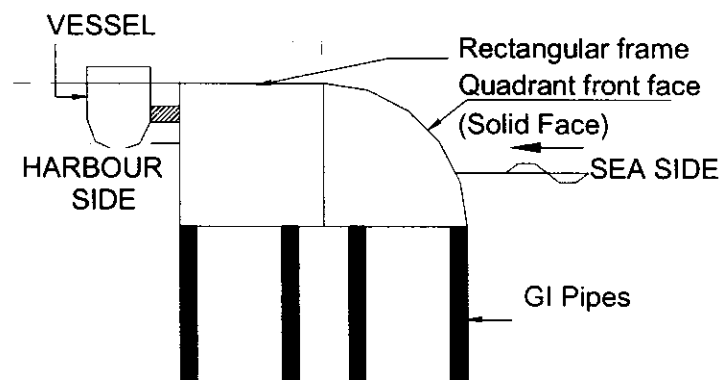
Fig. 1.12 Quarter front face pile supported breakwater

iv. Mobile breakwaters: These are structures that combine the stability to appreciably reduce the height of ocean waves on its lee side with a degree of mobility sufficient to permit its ready transportation for considerable distance and its speedy installation when arrived at the site.

v. Pile breakwater: It is formed by a series of piles placed in rows. When constructed in the marine environment experiencing littoral drift dominant in a

particular direction, pile breakwaters allow the free passage of sediments to some extent, thus reducing the shoreline erosion on its down-drift side compared with what would occur with conventional rubble mound breakwaters.
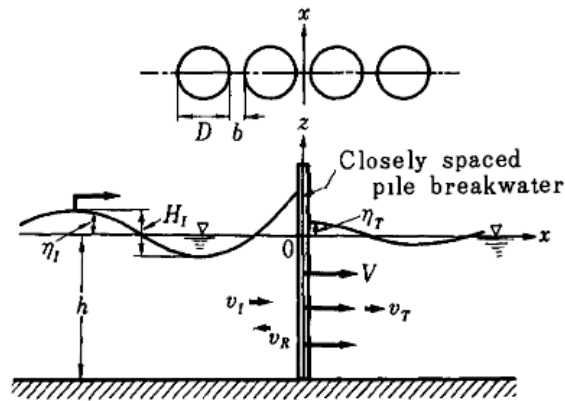
Fig. 1.13 Pile breakwater

vi. Horizontal plate breakwater: It can reflect and break waves, and it is sometimes supported by a steel jacket. Horizontal plate breakwater is applicable in less severe wave climates on sites with weak and soft subsoils.
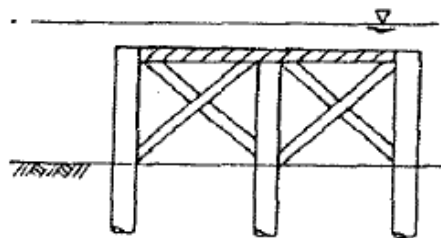
Fig. 1.14 Horizontal plate breakwater

vii. Curtain wall breakwater: It is commonly used as secondary breakwater to protect small craft harbors.
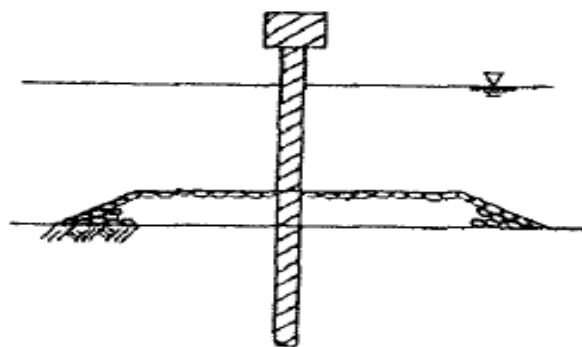
Fig. 1.15 Curtain wall breakwater

1.2.3 Semicircular breakwater

Semicircular breakwater (SBW) consists of a semicircle shaped hollow caisson and base slab cast as different elements made of pre-stressed concrete and founded on a rubble mound base. The semicircular caisson structure is hollow, therefore the weight and materials required are less and it is suited to sites with poor ground conditions. As the caisson is a prefabricated structure, it can easily be transported, handled and placed at the site. In addition to the above, it has the following excellent hydraulic characteristics compared with other types of breakwater.

The stability against sliding for SBW is good, since the horizontal component of a wave force applied to a semicircular surface is smaller than that applied to an upright wall; the vertical component of the wave force is applied downwards along the wall. Its curved configuration is exceptionally scenery enhancing, and its curved structure provides increased member strength. It is expected that a semicircular caisson is well suited for offshore breakwaters designed to protect beaches from erosion. SBW's are classified as

1. Submerged and emerged
2. Impermeable and perforated

1. Submerged and emerged: SBW serves as submerged breakwater at low water levels and emerged breakwater at high water levels (Refer Fig.1.16). By introducing breaking, partial reflection and transmission of incident wave (Grilli et al., 1994) it provides protection to the shore and other structures. It maintains the landward flow of water, it is important for water quality consideration (Kobayashi et al., 2007). According to Burcharth et al., (2006) submerged breakwater are much stable than emerged breakwater under the same wave condition.

Submerged   Alternately submerged   Emerged
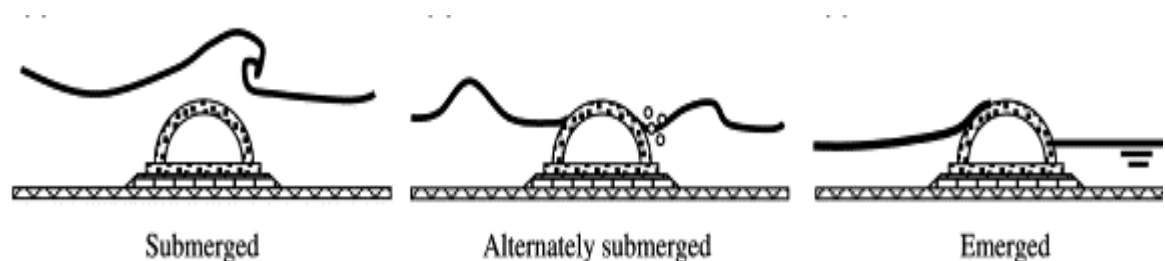
Fig. 1.16 Types of Semicircular breakwater based on depth of submergence.

SBW is commonly used for coastal protection on many eroding coasts. A desirable feature of submerged breakwaters (and low crested structures, in general) is that they do not interrupt the clear view of the sea from the beach. This aesthetic feature is important for maintaining the tourist value of many beaches and it is usually one of the considerations in using such structures for shoreline protection. When the SBW is fully submerged, it results in premature breaking of high waves, and hence waves with lower energy impinge on the beach.

Emerged breakwaters act as barriers and create a tranquility condition on the lee side for safe handling of cargo and passengers. The main function of these type breakwaters is to offer protection on their seaward face by introducing runup, breaking and partial reflection of incident waves.

2. Impermeable and perforated:

Sasajima et al. (1994) classified the SBW into four types: (i) the 'solid type' having impermeable front and rear walls; (ii) the 'front wave-dissipating type' having only a perforated front wall; (iii) the 'permeable type' having perforated front and rear walls; and (iv) the 'rear wave-dissipating type' having only a perforated rear wall.
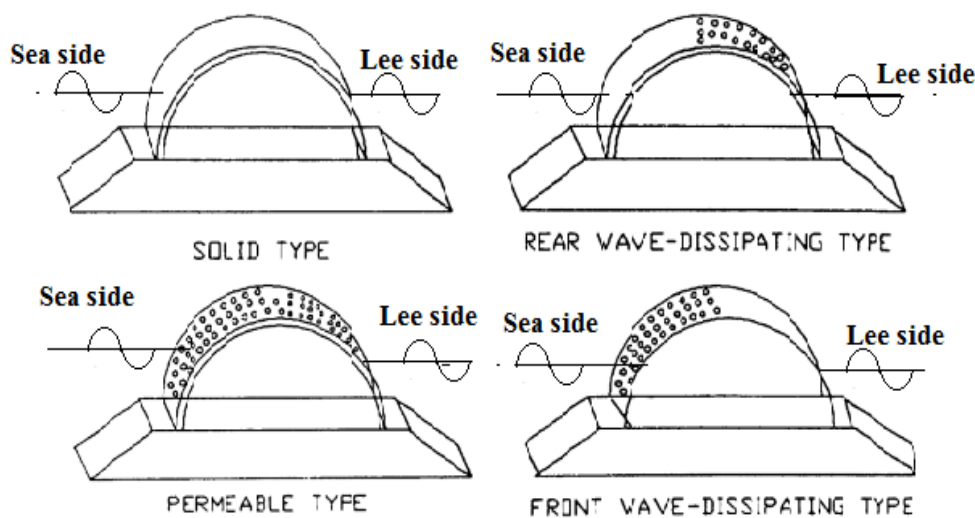
Fig. 1.17 Types of Semicircular breakwater

The solid-type is impermeable (0% perforations) with highly reflective characteristics. In rear wave dissipating type SBW, the openings on the rear side of the breakwater will permit the overtopped water to infiltrate the interference chamber.

The 'front wave-dissipative-type' reduces the amount of reflection by energy dissipation, while the 'permeable-type' permits entire water to penetrate to the rear side of the breakwater. By the provision of perforations, the energy is dissipated owing to the formation of eddies and turbulence created inside the hollow chamber. If a perforated SBW is placed in front of a structure experiencing a higher force and pressures due to waves, there will be a reduction in the wave force and wave pressure on the structure because of the presence of the SBW and the provision of perforations in it.

1.2.4 Quarter circle breakwater

Quarter circle breakwaters (QBW) are new type breakwaters first proposed by Xie et al. (2006) on the basis of SBW concept. The superstructure of QBW consists of a quarter circular surfaces facing incoming wave, a horizontal bottom and a rear vertical wall mounted on rubble mound foundation (Refer Fig. 1.18). The most important benefit of QBW is the reduction in the volume of concrete as well as rubble mound foundation, because of the smaller bottom width (Hanbin Gu et al., 2008).
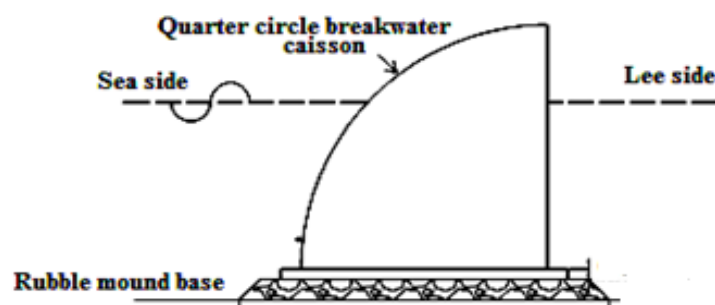
Fig. 1.18 Typical QBW section

Quarter circle breakwaters may be either submerged or emerged. When the crest level of QBW is below the still water level, it serves as submerged breakwater and emerged breakwater when the crest of QBW is above the still water level. QBW are classified as solid type having impermeable front and front wave-dissipating type having only a perforated front wall (Refer Fig. 1.19). In the case of solid type or impermeable type, the total wave energy is dissipated by wave reflection and runup /rundown. But in the perforated QBW having front side perforated, major portion of the wave energy is dissipated by the turbulence caused by the waves entering the chamber.
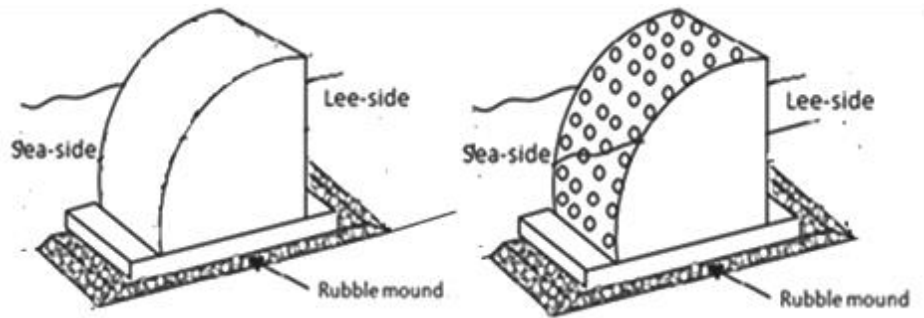
(a) Impermeable QBW   (d) Perforated QBW

Fig. 1.19 Types of QBW

1.3 NEED AND SCOPE OF THE PRESENT STUDY

Breakwaters have been built throughout the centuries but their structural development as well as their design procedure is under massive change. New ideas and developments are in the process of being tested regarding breakwater layout for reducing wave loads and failures. Breakwater design is increasingly influenced by environmental, social and aesthetical aspects and new types of structures are being proposed and built. There is a need to develop a safe and economical breakwater, as it represents a significant portion of capital investment in a port.

At the same time, breakwaters' vulnerability to extreme events such as storms is a reality and we have ample number of such cases in literature. One of the things engineers can do is to design a stable structure, which will withstand, resist and manage such destructive extreme events at least to some extent, mitigate catastrophic damage to the shoreward structures. Innovative concepts were experimented and a variety of perforated breakwaters were evolved.

Quarter circle breakwater is a new type evolved is found to possess merits of caisson as well as perforated breakwaters such as low weight, requires less materials, suited for poor soil conditions, easily transported, handled and placed at the site, aesthetically pleasing, cost effective, eco- friendly and stable. Studies conducted so far on QBW are related to the wave forces and hydrodynamic performance criteria under submerged conditions on impermeable QBW. In most cases, emerged breakwaters are required to be provided based on the prevailing site conditions and for better tranquillity in the harbour area, perforations of the

breakwater surface works better. Therefore it is necessary to carry out detailed studies to investigate various types of quarter circle breakwaters both impermeable and perforated under emerged condition. In the case of quarter circle breakwater, horizontal wave force is the major force which causes sliding of the structure. Hence a detailed experimental investigation has to be conducted in the laboratory on the hydrodynamic performance characteristics as well as stability of the QBW by using a suitable physical model under varying site conditions.

The design of QBW is complex and requires detailed information on various parameters such as water level changes, wave steepness, wave reflection, loss characteristics, wave runup and wave rundown etc.

In the present research, an attempt has been made to study the performance of a QBW both impermeable as well as seaside perforated using physical models. Studies were conducted on QBW models with varying radii, size of perforations and spacing between the perforations. Certain combinations of QBW with varying radii, S/D ratio are tested at different water levels for varying wave conditions and a QBW with better hydrodynamic performance is identified.

1.4 ORGANIZATION OF THE THESIS

The information gathered from the work is presented in seven chapters.

Chapter 1 introduces the history of breakwaters and types of breakwaters with special emphasis on semicircular breakwater and quarter circle breakwater. Further it also includes need and scope of the present research work.

Developments in the design, construction and performance of semicircular and quarter circle breakwater are surveyed in Chapter 2 which in turn leads to the selection of quarter circle breakwater as a topic of the present research work.

Chapter 3 describes the formulation of the present research problem and objectives. It discusses model scale selection, physical models, and limitations of model testing and describes the methodology of the present experimental work.

Chapter 4 discusses the results obtained from the experiments on the reflection and loss characteristics of impermeable and seaside perforated quarter circle breakwater.

It also includes the equation developed on the impermeable and perforated quarter circle breakwater based on the reflection and loss characteristics.

Chapter 5 discusses the results obtained from the experiments on the runup and rundown characteristics of impermeable and seaside perforated quarter circle breakwater. It also includes the equation developed on the impermeable and perforated quarter circle breakwater based on the runup and rundown characteristics.

Chapter 6 discusses the results obtained from the experiments on the stability analysis of impermeable and seaside perforated quarter circle breakwater. It also includes the equation developed on the impermeable and perforated quarter circle breakwater based on the stability characteristics.

The conclusions drawn from the present study and future recommendations are presented in Chapter 7

References follow up after the Measurement of wave reflection presented in Appendix 1, Uncertainty analysis which is presented in Appendix 2 and breakwater design example in Appendix 3. A list of publications based on the present research work and a brief resume are put at the end of report.

2.1 GENERAL

Breakwaters have been widely constructed to prevent coastal erosion, to provide a calm basin by reducing wave induced disturbances for ships and to protect harbour facilities from rough seas. Rubble mound breakwaters are the oldest type and have been widely used for sheltering harbours. However, with time, innovative vertical structures like vertical caisson perforated breakwaters became popular among coastal engineers providing a better alternative to the classical types. One of the most recent developments is the evolution of semicircular breakwater. Quarter circle breakwater is a new-type breakwater first proposed by Xie et al. (2006) on the basis of semicircular breakwater.

This chapter outlines a comprehensive review of previous studies on semicircular breakwater and quarter circle breakwaters. Various researches conducted on reflection and runup characteristics of perforated type breakwaters were also briefly discussed.

2.2 SEMICIRCULAR BREAKWATERS

Research activities on the development of a curved water front surface led to the development of semicircular breakwater which was initiated by a joint research group formed by the Port and Harbour Research Institute of the Ministry of Transport of Japan, Coastal Development Institute of Technology and several other corporations in the early 1990s (Tanimoto and Takahashi, 1994).

From 1992 to 1993, a prototype semicircular breakwater having length 36 m was built at Miyazaki port. It was a precast reinforced concrete structure built with a semicircular vault and a bottom slab (Yuan and Tao, 2003), and was placed on a prepared rubble mound foundation. The breakwater built in Miyazaki Port was an emerged type structure and was of rear wave dissipating type. Opening ratios of 0% (no perforations) and 25% were adopted for the front wall, the rear wall respectively, and 10% for the bottom slab.
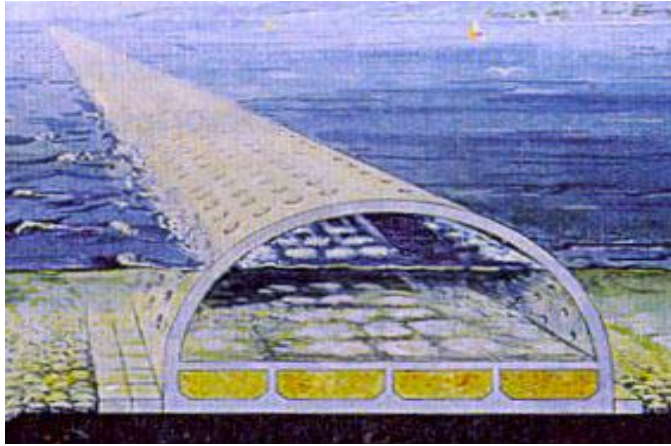
Fig. 2.1 Breakwater at Miyazaki port in Japan (Sasajima et al., 1994)

Before erecting the breakwater, field demonstration tests were conducted using test breakwaters at Miyazaki port from 1991 to 1995 to check the stability and safety of the SBW under actual site conditions. Length of the semicircular caisson used for the SBW was 12 m, radius 9.8 m, thickness of the curved arch 0.50 m and the base slab thickness was 0.70 m. The total height of the structure was 15.5 m with rubble mound foundation of thickness 2.5 m. The low water level and high water level used for the SBW design considering the site condition for the Miyazaki port was 7.5 m and 9.5 m respectively.

Fig. 2.2 Lowering of semicircular breakwater caisson from a floating crane

For the breakwater constructed at Miyazaki port in Japan, Sasajima et al. (1994) presented the results of the measured pressures and forces on the semicircular caisson. The variation of measured highest 1/3rd wave pressure and maximum wave pressure at different elevations along the seaward face were found to be less than the results of modified theoretical formulation of Goda (1974).

The success of semicircular breakwater at Miyazaki port in Japan led to the application of this type of breakwater in other harbour projects especially in China. In 1997, a front wave dissipating type SBW of length 527 m was built for Tianjin Port in the Peoples Republic of China and 18 km long semicircular estuary jetty was completed for the Deep Channel Improvement Project of the Yangtze Estuary in 2000 (Xie, 1999). According to the master plan of Tianjin Port, a new north breakwater shall be constructed on the north of the original north breakwater to protect the new harbour basin. The slope of the sea bottom is very mild and the depth of the seabed is about 1.0 m calculated from the lowest tide level. The first layer of soil underneath the seabed is mud for about 7 m to 11 m depth. Second layer is muddy clay, about 12.7 m to 14.3 m. The soil under the second layer is relatively compact, which is sandy clay or loam. The design high and low water levels are 4.30 m and 0.5 m respectively. The design wave height, H = 3.2 m and wave period, T = 8.1 s was considered for the study. The cost of rubble mound breakwater is relatively high due to lack of rock material in the locality. The conventional type of composite breakwater is also not economical because the foundation soil should be treated and compacted. Therefore finally the option of semicircular breakwater was recommended in the preliminary design of New North Breakwater Project in 1995.

Fig. 2.3 Semicircular breakwater in Tianjin Port, China

The crest elevation of the breakwater was 5.2 m and the radius of the semicircular part was 4.5 m. There are circular holes on the front part of the arch as well as on the bottom slab for relieving the wave uplift. The design length of the semicircular element is 4.8 m with weight of 176.6 tonnes. The wave forces acting on

semicircular breakwater were calculated using modified Goda's formula (Tanimoto and Takahashi, 1994). Then, the design section of the breakwater was tested in two harbours and coastal engineering laboratories.

In 1998 with the rapid development of China's economy, the demand for cargo transport increased dramatically. After studying the site conditions, North Passage was selected as the deep-draft navigation channel. Dredging was done in various phases; 7.0 m to 8.5 m, 10 m and 12.5 m. The semicircular caisson structure was installed for the second-phase works of the Deep Channel Improvement Project of the Yangtze Estuary. The lengths of the south and north jetties of the first phase works of the Project are 20 km and 16.5 km respectively. The crest elevation of the jetty structure was selected as 2.0 m, wave height of 3.9 m with mean wave period of 7.5 s for the design high water level condition.

After designing selecting suitable parameters, the radius of the semi-circular jetty was selected as 4.0 m, with front part and the slab at the bottom with perforations 4.7% and 11.3% respectively. The weight of the precast element was about 180 tonnes. Combination of geotextile and sand as well as geotextile and small concrete blocks are placed on the sea bed to prevent scouring. For calculating the wave force acting on the caisson, modified Goda's wave force formula (Tanimoto and Takahashi, 1994) was not found to be good. Therefore, Shi-Leng Xie (1999), proposed a new calculation method for the wave forces acting on submerged semicircular breakwater.

Fig. 2.4 Semicircular breakwater in Yangtze River Estuary, China

Later many studies are being carried out to evaluate the performance of both impermeable and perforated types of SBW under the emerged as well as the submerged condition. Many researchers focused on the hydrodynamic behavior of the semicircular breakwaters verified by experimental studies and only few of them are numerical studies. The breakwaters models are tested for their performance characteristics under the action of both regular and random waves.

The research on emerged (breakwaters constructed with their crest level above the still water level) semicircular breakwater was initiated by Tanimoto et al. (1987 - 1989) by conducting a two dimensional model test on semicircular breakwater. The results obtained from their experiments were presented as the coefficients of transmission K_T, reflection K_R and energy dissipation K_L plotted against the ratio of breakwater freeboard to incident wave height ($h_c/H_{1/3}$), ratio of the incident wave height to water depth ratios ($H_{1/3}/d$) and the ratio of chamber width to wavelength ratio ($B_o/L_{1/3}$). The effects of porosity at the front wall, ε_f, at the rear wall, ε_r and at the bottom, ε_b are also investigated. It was concluded that the 'rear wave dissipating type' breakwater is a better wave attenuator than the 'solid type' breakwater due to infiltration of the overtopping waves allowed by the rear perforated wall; whereas the 'front wave-dissipating type' outperforms the 'permeable type' significantly. The 'solid type' breakwater was found to be more reflective than the 'front wave-dissipating type'. Finally it was concluded that the porosity of the structure has an outstanding effect on the hydraulic performance of the semicircular breakwaters.

Tanimoto et al. (1987–1989) also investigated the wave loadings behaviours of the 'solid type semicircular breakwaters which was found smaller than that on upright wall, and the vertical force component applied downward along the wall provided additional stability against the waves. There is no uplift wave pressure acting on the bottom slab was when the porosity of the bottom slab was more than 10%; and the wave chamber was not airtight.

Sasajima et al. (1994) conducted tests on semicircular breakwater installed at the Miyazaki Port from 1993 to 1994 in order to verify the structural stability and safety of the structure under severe waves. The results were in accordance with the findings of Tanimoto (1989) and confirmed that the reduction in the horizontal wave

force component due to phase difference in the wave pressure on curved surface of the breakwater; and almost equal amount of uplift and inner wave pressure applied to the bottom slab of 10% porosity in which they offset each other by being in the opposite directions. They also found that an increase of the sliding resistance and stability of the structure is due to simultaneity of the peak occurrence between the horizontal wave component and the vertical downward wave force component.

Sasajima et al. (1994) reported that the dissipation of incident wave energy due to the presence of an SBW is mainly due to reflection and arises because part of the energy is dissipated while the wave run over the curved front face of the breakwater. This resulted in looking into alternative means of dissipating the wave energy and reducing the wave runup and overtopping.

Tanimoto and Takahashi (1994) compared the forces on vertical caisson and semicircular caisson and concluded that the Goda formula derived for vertical composite breakwaters could be applied successfully to calculate the design wave forces on the caisson of a SBW. They introduced a phase-modification coefficient and an angle modification coefficient to address the geometry of the semicircular structures. The average intensity of wave force on the vertical wall caisson varies with the height of the rubble mound foundation, while the horizontal and vertical components of forces on the semicircular caisson are almost constant.

Aburatani et al. (1996) reported the field tests on the semicircular breakwater built at Miyazaki port in Japan and concluded that the wave pressure data confirmed a reduction in the horizontal force component due to the occurrence of a phase difference in the wave pressure on the circumference. They analyzed the wave pressure exerted on the semicircular caisson and stresses on the members by conducting a field test on SBW at Miyazaki port in Japan. From their experiments, it was concluded that stability is increased due to horizontal wave force component is smaller and vertical wave force component is applied downwards along the wall.

In India, the research activities on the performance characteristics of semicircular breakwater initiated with the works using the 2D wave flume of the Department of Ocean Engineering, Indian Institute of Technology in Madras from 1997 to 2002. Their studies mainly emphasized on the evaluation of the hydrodynamic

characteristics of the impermeable and perforated semicircular breakwaters under various wave conditions and water depths.

Sundar and Raghu (1997) conducted tests on an impermeable semicircular breakwater subjected to regular waves and concluded that, the reflection coefficient K_r varied from 0.5 to 0.9 for relative water depth h_w/L (ratio of water depth to wavelength) ranging between 0.1 and 0.4 for waves with steepness (H/L) up to 0.12. The dynamic pressures at still water level were reported to be less than the theoretical solution of Goda (1974). It was also found that at elevations below SWL, the measured pressures were found to be slightly more than the theoretical value for intermediate water conditions, whereas a reverse trend in its variation was observed for deepwater conditions.

Jia (1997) investigated the interaction of steep waves with semicircular breakwater with the complex plane's Cauchy boundary integral theorem. The boundary integral method was used to transform the calculation in fluid domain into its boundary alone. In the calculation, the computation domain is moved with the propagation of waves. Jia (1997) obtained a numerical solution for incident Stokes waves passing the submerged obstacles and extended the method of calculation of the wave run-up on a slope for estimation of over-topping.

Sundar and Raghu (1998) conducted tests on dynamic pressures and runup on semicircular breakwaters due to random waves. The dynamic pressures due to random waves of predefined spectral characteristics exerted on a semicircular breakwater model at five different elevations along the depth are measured. In addition, the wave run-up on the model and its reflection characteristics are also measured. The results on the variation of frequency pressure spectra along the depth and the runup spectra were plotted in graphs.

The variation of zero[th] spectral moment of elevation $(m_o)_\eta$ with the zero[th] spectral moment of pressure $(m_o)_p$ and zero[th] spectral moment of runup $(m_o)_{Ru}$ for various values of z/d (where z and d stands for the location of pressure gauge and depth of water below still water level) were plotted.

The results indicate that $(m_o)_p$ increases with increase in $(m_o)_\eta$ for all z/d. It was also concluded that the pressure spectrum at the SWL has a lesser peak with lesser

energy compared to that of pressures sensed at locations immediately below the SWL, that is z/d = - 0.1.
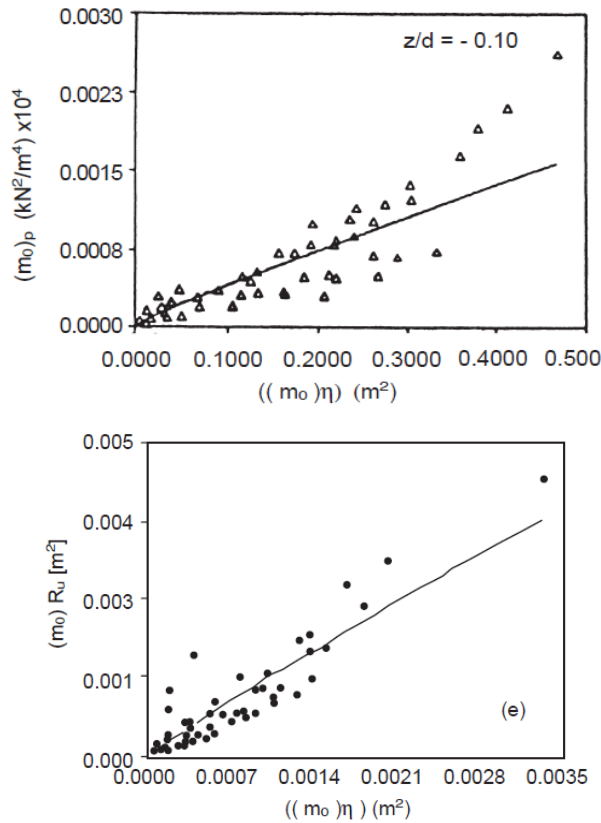
Fig. 2.5 Variation of zeroth spectral moment of wave elevation and zeroth spectral moment for pressures and runup. (Sundar and Raghu, 1998)

This was due to the intermittence effect with its absence of seaward pressure in the pressure time history. Similar conclusions were drawn by Isaacson and Subbiah (1991) in their studies on random wave forces at SWL on a vertical cylinder and by Mallayachari and Sundar (1994) for the random wave pressures exerted on walls.

The equation of the line of best fit takes the form

$$[(m_o)_p]^A = [(m_o)_\eta]^B \dots\dots\dots\dots\dots\dots\dots\dots\dots\dots\dots\dots\dots\dots\dots\dots\dots\dots\dots\dots\dots \text{(2.1)}$$

Where A and B are constants varying for different values of z/d. The variation of zeroth spectral moment of the runup with surface elevation along with the line of best fit reveals that the energy under the runup spectra increases with increase in energy in the incident wave spectrum. The equation of the line of best fit is obtained as

$$[(m_o)_{Ru}] = 0.7648[(m_o)_\eta]^{0.93} \dots\dots\dots\dots\dots\dots\dots\dots\dots\dots\dots\dots\dots\dots\dots\dots\dots \text{(2.2)}$$

The plot shows a wide scatter in K_r with respect to its variation with wave steepness. K_r is seen to vary from 0.6 to 0.95 over a wave steepness range of 0.2 to 0.095.
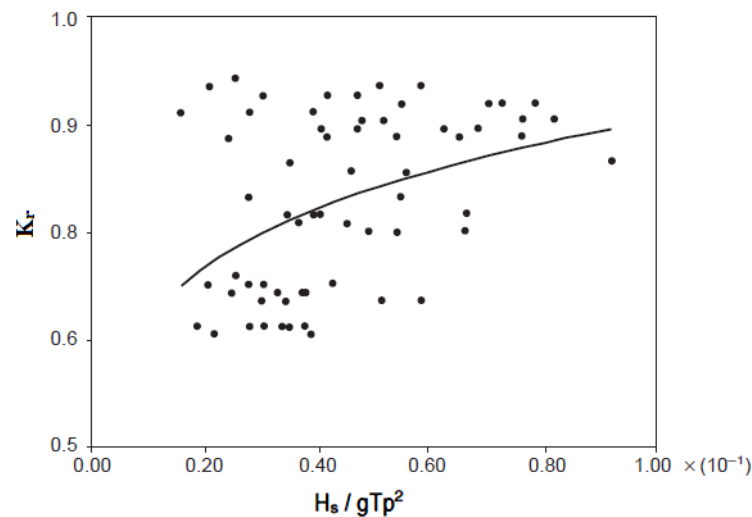
Fig. 2.6 Variation of reflection coefficient K_r with wave steepness. (Sundar and Raghu, 1998)

The results indicate that the SBW is quite effective in reflecting the incident wave energy. The major conclusions are pressure spectrum at still water level (SWL) experiences lesser energy compared to that at a location immediately below the SWL, which is due to the intermittence effect. The pressure spectra decay towards the seabed. The zero[th] spectral moment at a location (z/d = - 0.10) immediately below the SWL is nearly 60 to 75% more than that exerted at the SWL. The shape of the pressure spectra is slightly broader than the corresponding wave spectrum. The shoreward peak pressures follow a Raleigh distribution. The zero[th] spectral moment of run-up increases with increase in the zero[th] moment of the incident wave spectra. The reflection coefficient for the SBW model ranges from 0.6 to 0.95, suggesting that the shape of the breakwater considered in this study is quite effective in dissipating the incident wave energy.

Krishna Priya et al. (2000) measured the wave pressures along the seaward side of the impermeable breakwater at different water depths and under the action of regular waves. They observed that the dynamic pressure decay exponentially from still water level towards the bed and the pressure will be higher on the structure with longer period waves and at smaller water depths. They further commented that the modified Goda's method is not valid for the pressure measured near to the still water level. Similar studies on SBW was undertaken by Graw et al. (1998), who

reported that the modified Goda's formula is not valid for the pressure on impermeable SBW at the relative water depth, d/L < 0.35, and at d/L > 0.58.

Studies on the perforated SBW with perforations on the seaside of the breakwater under emerged as well as submerged condition were undertaken Dhinakaran et al. (2002-2010). Dhinakaran et al. (2002) investigated the reflection characteristics, hydrodynamic pressures and the horizontal and vertical forces on the seaside perforated SBW model with 7 % and 11% perforations due to the action of regular waves. The results for the reflection characteristics and dimensionless pressure for the seaside perforated SBW models are compared with an impermeable SBW model (SBW0) of Krishna Priya et al. (2000).
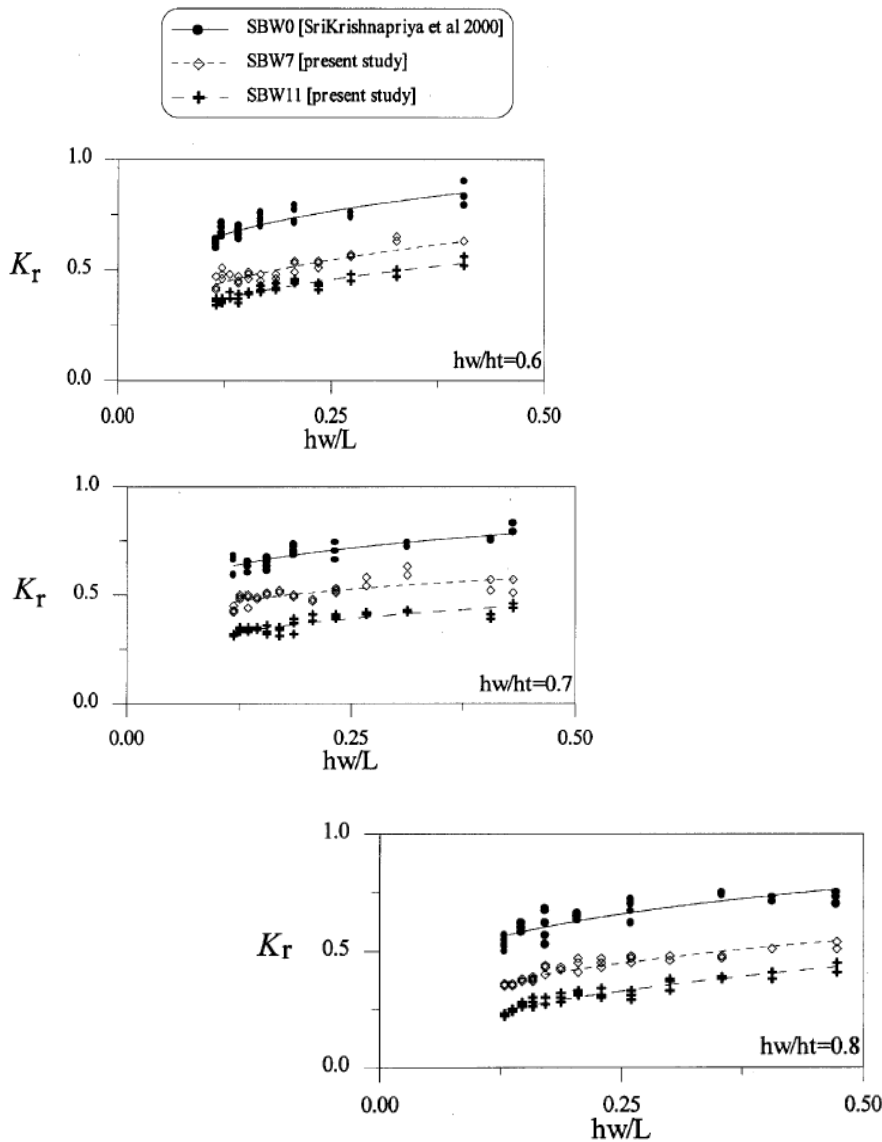
Fig. 2.7 Variation of reflection coefficient K_r with h_w/L (Dhinakaran et al., 2002)

The reflection coefficient K_r is found to slightly increase with increase in h_w/L (ratio of water depth to wave length) and for higher h_w/h_t (water depth / total height of breakwater), K_r is found to be less. The value of K_r for SBW7 (SBW with 7% of the exposed area perforated) varies from 0.35 to 0.65, and for SBW11 (SBW with 11% of the exposed area perforated) it varies from 0.22 to 0.59, which are both less than the range for SBW0 (impermeable SBW), for which K_r ranges between 0.5 and 0.9. The percentage reduction in K_r for SBW7 ranges from 15 to 39% and for SBW11 it ranges from 29 to 57% compared to SBW0.

The dimensionless pressure (dynamic pressure/static pressure head) decreases with increase in relative water depth. It was observed that the dimensionless pressure is less for higher h_w/h_t. The maximum dynamic pressure exerted on SBW7 and SBW11 is about 0.6 times the static pressure head due to wave height, whereas this value for an impermeable SBW is about 0.75. The dimensionless vertical and horizontal forces decrease with increase in relative water depth and percentage of perforations. The percentage reduction in horizontal force for SBW7 ranges from 10% to 65% and for SBW11 it ranges from 34% to 86% compared with SBW0. The percentage reduction in vertical force for SBW7 ranges from 10% to 53% and for SBW11 it ranges from 29% to 85% compared with SBW0.
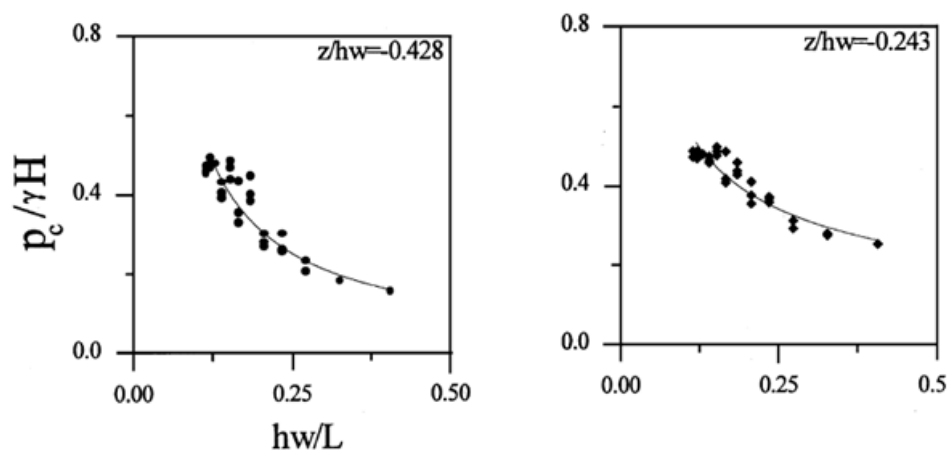
Fig. 2.8 Variation of dimensionless pressure with h_w/L (Dhinakaran et al., 2002)

Similar experiments on semicircular breakwater under emerged condition and due to the action of random waves are repeated by research group headed by Dhinakaran. Again Dhinakaran et al. (2008) conducted tests to investigate the reflection characteristics, runup, hydrodynamic pressures, horizontal and vertical forces on the

seaside perforated SBW models with 7%, 11% and 17% perforations due to the action of random waves. The experimental studies were conducted for surface piercing conditions and the results were compared with the SBW0 model of Krishna priya et al. (2000). The variations of K_r for SBW7, SBW11, and SBW17 for h_w/h_t ratios equal to 0.6, 0.7 and for constant h_r / h_t (ratio of rubble mound height to total structure height) equal to 0.18 were analysed. The results indicate that K_r increases with the increase in h_w/L for all the h_w/h_t and decrease with the increase in perforations from to 7% to 11%. Experiments on runup were analysed and shown that the runup (R_u /H_s, R_u = runup and H_s = significant wave height) decrease with the increase in h_w/h_t and also decrease with the increase in percentage of perforations from 7% to 11%.
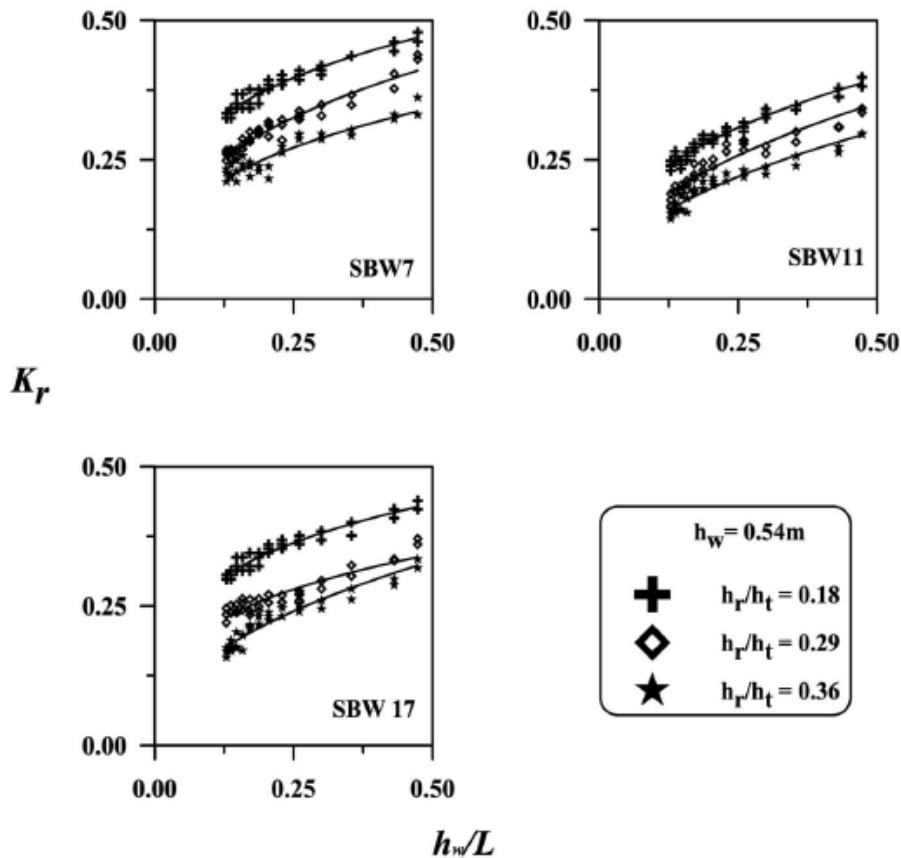
Fig. 2.9 Variation of reflection coefficient K_r with h_w/L (Dhinakaran et al., 2008)

The experimental studies on pressure states that the increase in percentage of perforations from 0% to 11% decreases the dimensionless pressures and forces on the structure and further increase in perforation shows a reverse trend. The rate of

reduction in dimensionless pressures, horizontal and vertical forces, and run up by varying h_r/h_t from 0.18 to 0.29 is significant, whereas it is insignificant for further increase in h_r/h_t equal to 0.36. The effect of water depth on hydrodynamic characteristics of seaside perforated SBW models was found to be less significant compared to the effect of perforations and the effect of rubble mound height. The optimum percentage of perforation arrived at is 11% for seaside perforated SBW from the experiments conducted. The total height of the model recommended being about 1.25 times the water depth and height of the rubble mound which is 0.29 times the total height of the model.

Dhinakaran et al. (2009) investigated how the perforations, water depth and rubble mound height on fully perforated semicircular breakwater (SBW) affects non-breaking wave transformations. SBW model with surface piercing condition for three different perforation ratios with 7 %, 11 % and 17 % were considered.
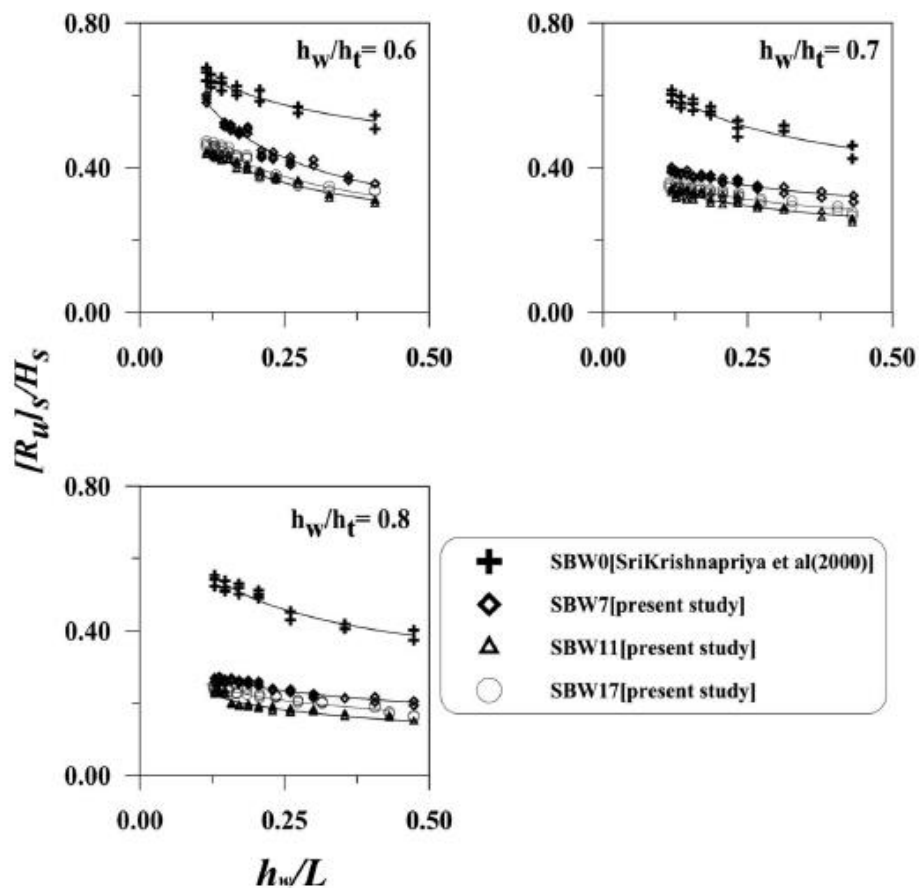
Fig. 2.10 Variation of dimensionless runup with h_w/L (Dhinakaran et al., 2009)

Studies were conducted on the variation of reflection, transmission, runup characteristics and dimensionless horizontal and vertical forces as a function of relative water depth and the results are compared with an impermeable SBW and seaside perforated SBW models. The major conclusions of the work are increase in percentage of perforations from 0% to 11% causes decrease in the reflection coefficient and dimensionless runup. In the case of seaside perforated SBW having 17 % perforation, the dimensionless runup and reflection coefficient increases with increase in relative water depth. The increase in rubble mound height resulted significant reduction in reflection and run-ups from h_r/h_t (height of rubble mound/total height of breakwater) from 0.18 to 0.29 and it is less significant for further increase in h_r/h_t to 0.36

In parallel research activities on submerged (crest level of the breakwater above the still water level) SBW's are also started which was initiated by Xie et al. in Peoples Republic of China. Submerged semicircular breakwater was first built at the Yangtze River Estuary, China from 1998 to 2000. Xie (1999) proposed new calculation method for the wave forces acting on submerged semi-circular breakwater, which is based on Goda's formula and new experimental data. This was verified by physical model tests and adopted in the design of southern estuary jetty of the Yangtze River estuary in the Peoples Republic of China. Tests were also conducted on the stability of the submerged structures with and without perforations. Experiment showed that for submerged case, larger wave force would act on rear part inside the chamber or arch of the SBW when the perforations on the front side of the SBW was increased and this situation had an adverse effect on the stability of the structure.

Later in India, Krishna priya et al. (2000) investigated the reflection and transmission characteristics, hydrodynamic pressures and forces on a submerged semicircular breakwater model due to the action of regular waves. The hydrodynamic pressures are compared with the two-dimensional finite element model of Sundar et al. (2000) and the agreement was found good. The reflection coefficient, K_r is found decreasing with increase in water depth. Further, the dimensionless pressures were found to reduce with increase in the scattering parameter, ka, where, 'k' is the wave number and 'a' is the radius of the

semicircular caisson. The dimensionless pressure is slightly less for the location closer to SWL than results from the formulation of Goda. The dimensionless horizontal and vertical force on semicircular caisson drastically decreases with increase in ka.

Numerical model study on SBW started in the early 2000 when Yuan and Tao (2003) studied the wave force acting on SBWs under submerged, alternately submerged and emerged conditions. A numerical model based on the hybrid method of the boundary element method and the finite difference method and fluid motion described by the velocity potential was used to study the wave force on SBW. Five sets of laboratory experimental data that consist of semicircular breakwaters with different diameters and shapes have been used to calibrate and verify the numerical model, and good agreements are obtained between the numerical results and the experimental data. For the convenient use in practical projects, a simplified formula for calculating the total wave forces on the breakwaters has been derived from the numerical results. Later Liu and Tao (2004) developed a 2-D numerical wave model based on unsteady Reynolds equations. In this model, the k-epsilon models were used to close the Reynolds equations and volume of fluid (VOF) method was used to reconstruct the free surface. The model was used to simulate solitary wave interaction with submerged, alternative submerged and emerged semicircular breakwaters. The process of velocity field, pressure field and the wave surface near the breakwaters was obtained. It was found that when the semicircular breakwater is submerged, a large vortex will be generated at the bottom of the leeside wall of the breakwater; when the still water depth is equal to the radius of the semicircular breakwater, a pair of large vortices will be generated near the shoreward wall of the semicircular breakwater due to wave impacting, but the velocity near the bottom of the leeside wall of the breakwater is always relatively small. When the semicircular breakwater is emerged, and solitary wave cannot overtop it, the solitary wave surface will run up and down secondarily during reflecting from the breakwater.

Zhang et al. (2005) studied the hydraulic characteristics of the semicircular breakwater based on oblique irregular wave physical model tests. The variations of wave forces on unit length of semicircular breakwater with the factors including

wave steepness H_s/L_s, relative wave height H_s/d or d/H_s and the angle of incidence are studied. They found that the maximum horizontal wave forces under both wave crests, F_c and troughs, F_t were almost identical when the structure was either largely emerged or submerged; however, F_t were much larger than F_c when the breakwater was at the alternately submerged situation.

Young and Testik (2009 & 2011) investigated the two-dimensional onshore scour along the base of submerged vertical and semicircular breakwaters. They investigated the effects of submerged vertical and semicircular breakwaters on local wave characteristics, particularly with the aim of determining the parameterizations for the wave reflection coefficients for submerged vertical and semicircular breakwaters. Experiments were conducted with normally incident monochromatic waves breaking at the breakwater on both sloping and horizontal sandy bottoms. The reflection coefficient (C_r) is observed to rely mainly on the dimensionless submergence parameter, a/H_i (a, the breakwater's depth of submergence and H_i, the height of the incident wave at the breakwater).

Two semi-empirical parameterizations are proposed to predict reflection coefficients for submerged vertical and semicircular breakwaters. While both parameterizations share the same functional dependency on a/H_i, the functions have different constant coefficients. For the limiting case when 'a' approaches zero (breakwater crest is at the mean water level), the C_r value tends toward 0.53 for both breakwaters. However, as 'a' increases, the submerged vertical breakwaters reflect more energy than submerged semicircular breakwaters for the same a/H_i value.

Teh et al. (2010) conducted experiments on solid and perforated free surface SBW with varying perforations that was particularly suitable to be used in shallow waters. The test models of SBW with four different perforations of 0 %, 9 %, 18 % and 27 % was studied and based on this the characteristics such as wave transmission, reflection and energy dissipation was evaluated. For the free surface semicircular breakwater, the horizontal wave forces acting on the front face of the structure were estimated based on Goda's method incorporating a correction coefficient called phase modification coefficient λ_p developed by Tanimoto et al. (1994).
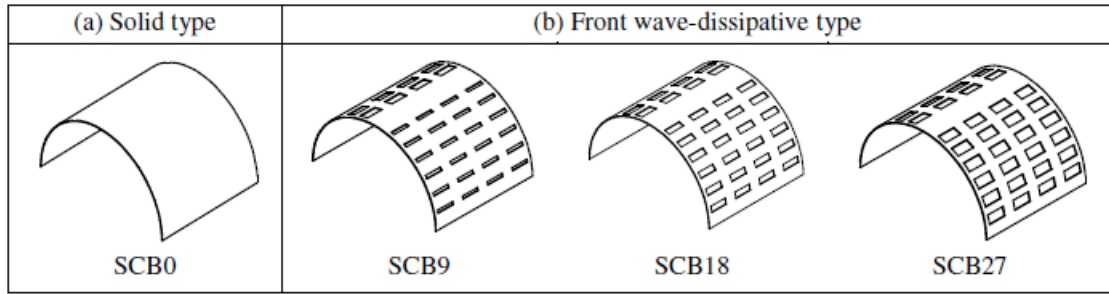
Fig. 2.11 Semicircular breakwater models (Teh et al., 2010)

(a) Wave run up at the front wall

(b) Wave overtopping over the breakwater

(c) Wave penetration and turbulence in the breakwater's chamber

(d) Formation of eddies in the vicinity of the bottom of the breakwater

(e) Exchange of water jet flow at the porous front wall

(f) Water level variation due to pressure difference
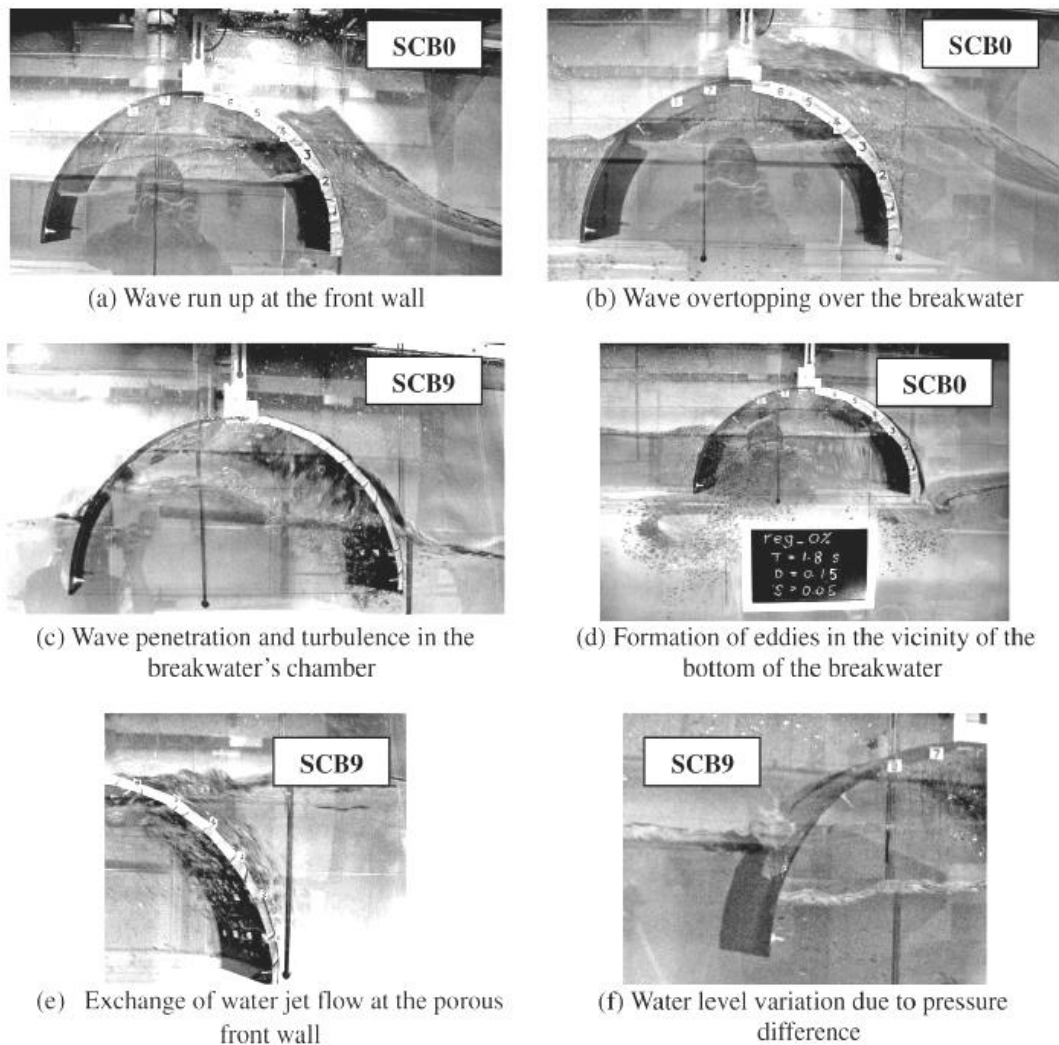
Fig. 2.12 Hydraulic processes observed in the experiment (Teh et al., 2010)

The semicircular breakwater with different arrangement of screens and porosities are examined for various hydrodynamic performance characteristics under the action of irregular waves in a wave flume. The main aim of the conducting experiments was to determine the effect of lower water depth on the performance of such type of SBW. From the results obtained it was concluded that the wave

attenuation characteristics of the model was less satisfactory at lower water depths and longer wave period due to more transmission of waves below the structure. The wave transmission for the structure at lower water depths varies from 60% − 98%, which is higher for many coastal and marine related applications.

The effectiveness of the semicircular breakwater models was determined by comparing the hydraulic characteristics other type of free surface breakwaters developed by other researchers. The solid breakwaters was found to highly reflective structures but the reflectivity of quadrant front face supported breakwater was very low due to the breakwater geometry and energy dissipation under the influence of closely spaced piles.

The breakwater with impermeable wall − SCB0 model offered higher wave attenuation efficiency (with C_T values as low as 0.01 in regular waves and 0.05 in irregular waves) than the perforated models; also it was also highly reflective to incident waves (with C_R values as high as 0.87 in regular waves and 0.78 in irregular waves) subjected to severe wave climate in front of the breakwater (with C_F values as high as 2.20 in regular waves and 1.94 in irregular waves).

Dhinakaran et al. (2010) conducted experiments to evaluate hydrodynamic characteristics such as the reflection characteristics, hydrodynamic pressures and forces on a submerged semicircular breakwater model with varying perforations such as 0%, 7%, 11% and 17% at different water depths and due to regular waves.
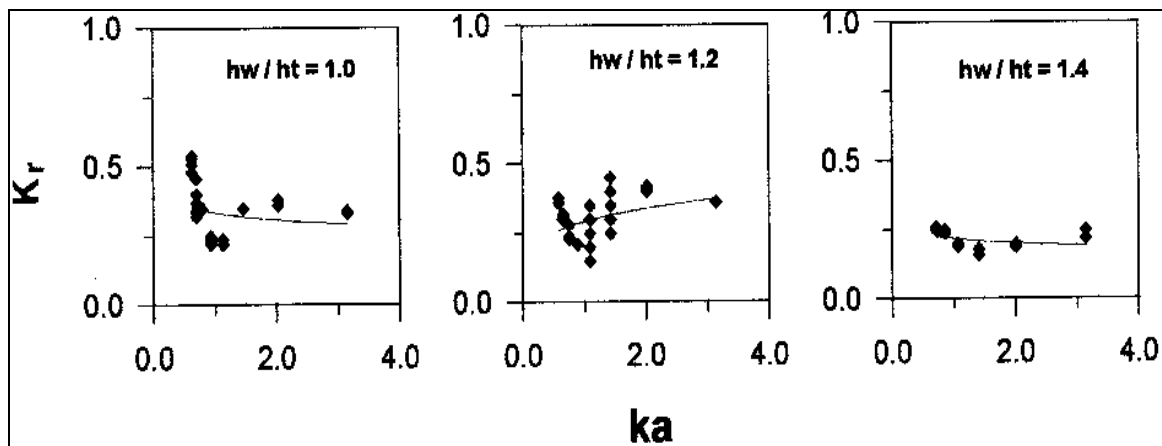
Fig. 2.13 Variation of reflection coefficient with scattering parameter for three different h_w/h_t for $h_s/h_r = 4.6$ (Dhinakaran et al., 2010)
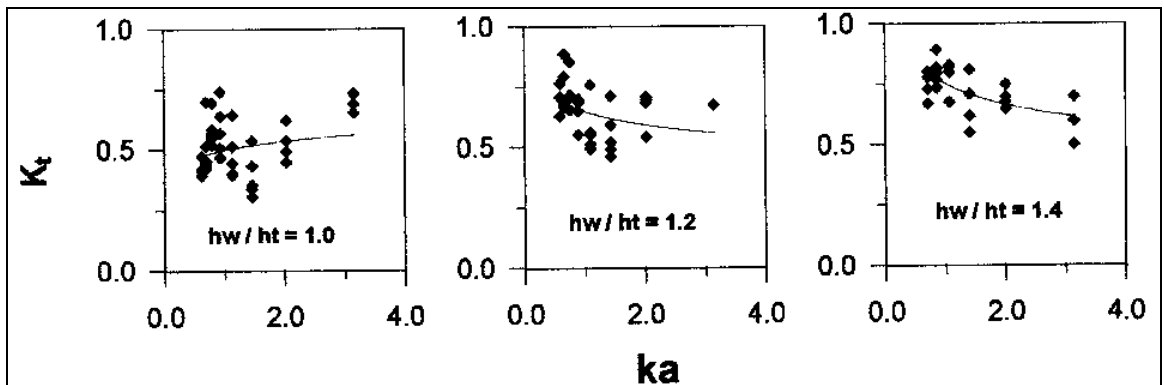
Fig. 2.14 Variation of transmission coefficient with scattering parameter for three different h_w/h_t for h_s/h_r = 4.6 (Dhinakaran et al., 2010)
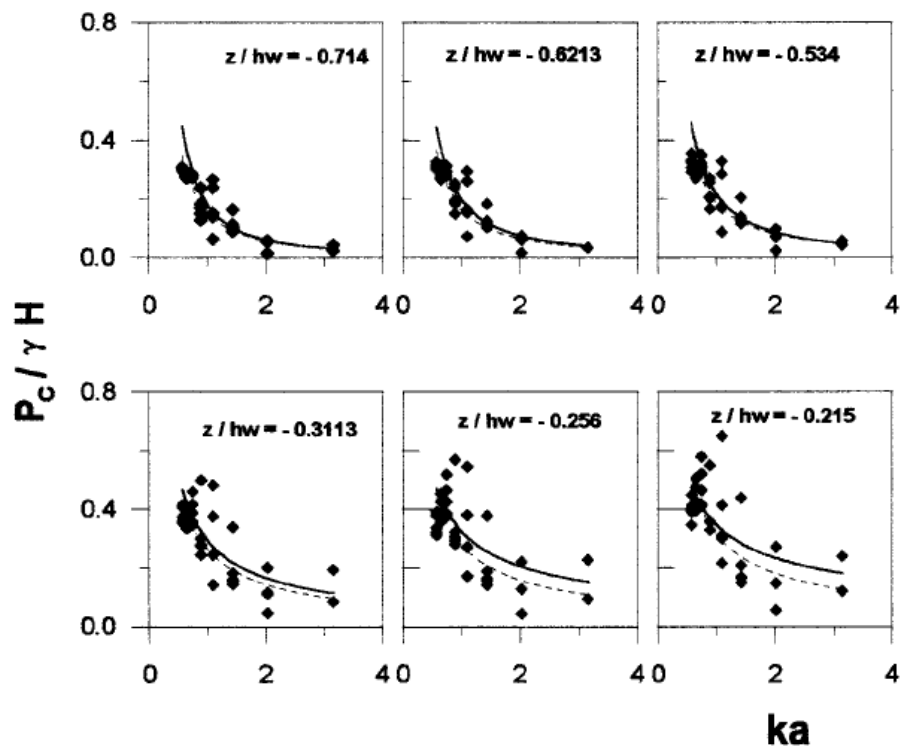
Fig. 2.15 Variation of dimensionless pressure with scattering parameter for h_w/h_t =1.2 and h_s/h_r = 4.6 (Dhinakaran et al., 2010)

The results for seaside perforated SBWs are compared with the results of an impermeable SBW to study the effect of perforations. It was concluded that the reflection coefficient K_r decreases with an increase in the water depth for seaside perforations of up to 11% and further increasing perforation shows a reverse trend (increase in K_r value). The dimensionless pressure and forces decreases with increase in ka and the percentage of perforations. From the studies conducted sea

side perforated SBW with 11% perforations is recommended for the intermediate water depth conditions with the total height of breakwater equal to 0.83 times of water depth to enable maximum energy dissipation resulting in lesser pressures and forces on a structure or harbour on its leeward side.

Liu and Li (2012) developed multipoles with singularities on the seabed on the basis of the linear potential theory and used the multipole expansions to obtain a solution of water wave interaction with submerged perforated semi-circular breakwaters. A submerged perforated semicircular breakwater with suitable porosity may work well reducing the transmission and reflection coefficients. Perforating the semi-circular arc can significantly reduce the total horizontal and vertical wave forces acting on the breakwater. The major conclusions are maximum total horizontal and vertical wave forces acting on a perforated or impermeable semi-circular breakwater has a significant phase difference, which is beneficial to enhancing the stability against sliding. The maximum wave pressure difference on the semicircular arc generally occurs at the seaside top area of the arc.

Ever since the world's first semicircular breakwater was constructed at Miyazaki Port in Japan in 1993, the concept of semicircular breakwater receives considerable attention by researchers worldwide, particularly those from Japan, India and China. A review of these breakwaters is vital in this study because it provides some useful reference for the development of the quarter circle breakwater in this study.

2.3 QUARTER CIRCLE BREAKWATERS

The success of semicircular breakwater led researchers in Peoples Republic of China to investigate the performance of quarter circle breakwater whose front side is similar to that of semicircular breakwater. Initial studies on quarter circle breakwater were mainly related to the comparative study between SBW and QBW. Quarter circle breakwater (QBW) was first proposed by Xie et al. (2006) based on semicircular breakwater (SBW) concept. The following section describes a few studies on quarter circle breakwater and other relevant works for breakwater having quadrant front face. Most of these works are experimental studies on the hydraulic performance characteristics of quarter circle breakwater and only a few of them are numerical studies.

Subba Rao and Sundar (2002) conducted experiments on hydrodynamic pressures and forces on quadrant front face pile supported breakwater. Quadrant front face pile supported breakwater is a combination of semicircular and closely spaced pile breakwaters, which couples the advantages of these two types. The bottom portion of quadrant front face pile supported breakwater consists of closely spaced piles and the top portion consists of a quadrant solid front face on the seaside. The leeward side of the top portion with a vertical face would facilitate the berthing of vessels.
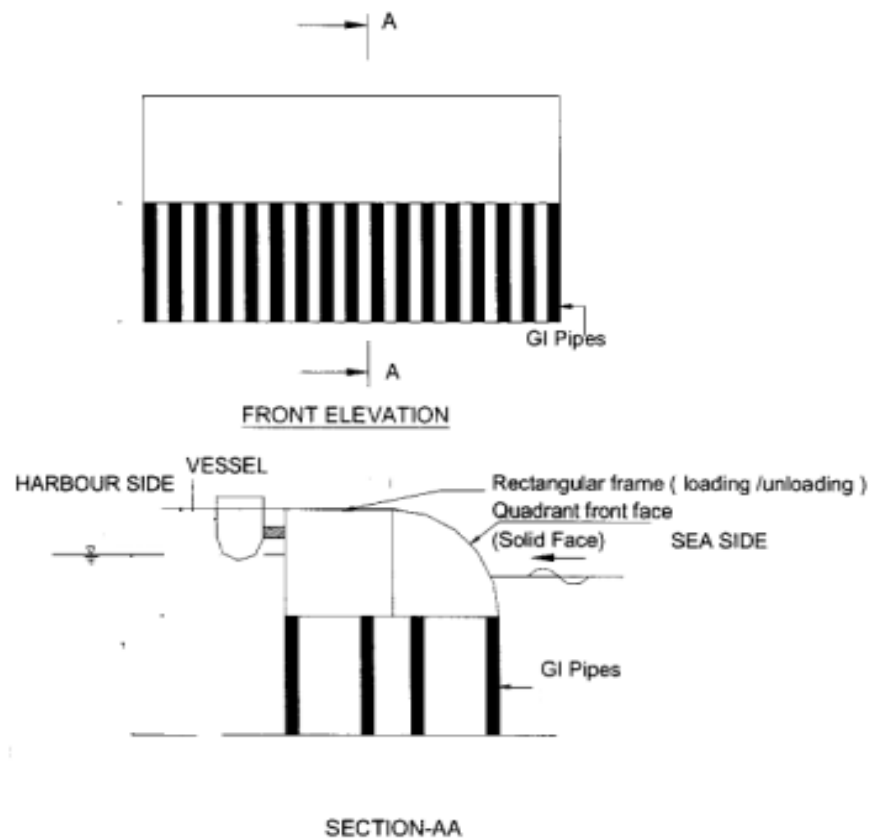
Fig. 2.16 Details of quadrant front-face pile-supported breakwater model (Subba Rao and Sundar, 2002)

The breakwater model was tested in a wave flume for different water depths. For each water depth, three different spacing between the piles were adopted for the investigation. The dynamic pressures exerted along the quadrant front face due to regular waves were measured.

The variation of dimensionless pressure with scattering parameter for different gap ratio (spacing between the pile/diameter of pile (s/D) and for relative pile depth

(water depth/pile height, d/h) are investigated under different water depths. In addition, the dimensionless total forces exerted on the breakwater model as well as its reflection characteristics as a function of scattering parameter was presented. The reflection coefficient, K_r varies from 0.25 to 0.85 for regular waves and 0.3 to 0.7 for random waves.
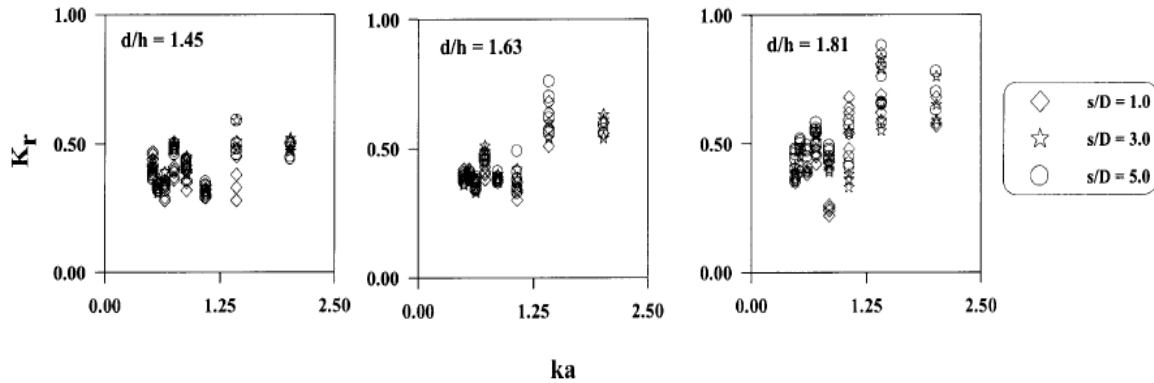
Fig. 2.17 Variation of reflection coefficient with scattering parameter for s/D =1, 3, 5   for different d/h (Subba Rao and Sundar, 2002)

For a constant s/D, the transmission coefficient K_t is found to be more for a lesser water depth. The study on the effect of spacing between the piles reveals no significant variation of K_t, but it is observed that the transmission of energy increases with an increase in spacing between the piles for a particular water depth; K_t is found to vary from 0.1 to 0.55 for both regular and random waves.
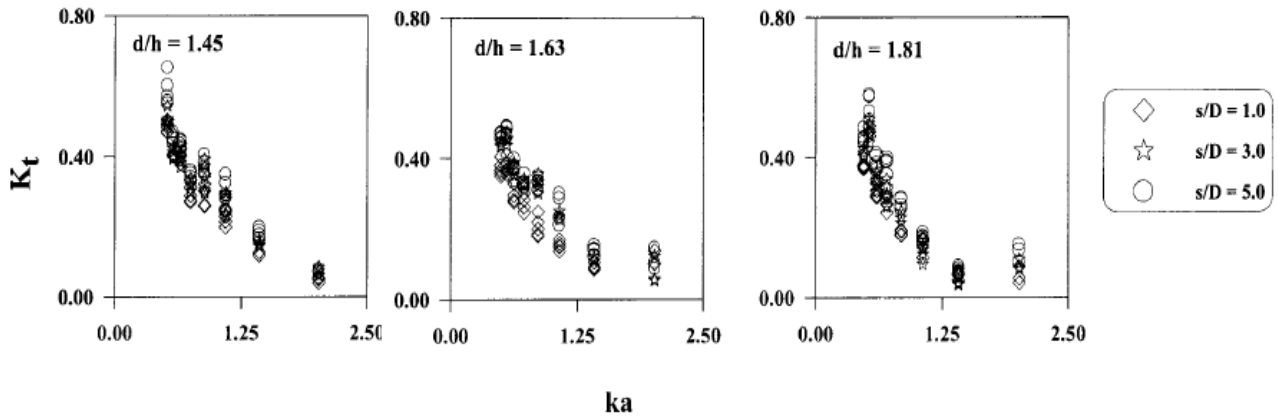
Fig. 2.18 Variation of transmission coefficient with scattering parameter

(Subba Rao and Sundar, 2002)

For a constant s/D, the loss coefficient K_l is found to increase with an increase in ka for a lesser d/h and decreases with an increase in ka for the higher d/h; K_l is found to vary between 0.5 and 0.95 for regular wave tests and 0.5 to 0.9 in the case of random waves. The dimensionless peak shoreward pressure decreases with an increase in scattering parameter for both regular and random waves. The shoreward peak pressures are observed to be lower than the seaward peak pressures for regular waves, which is due to the existence of a secondary harmonic component. Both horizontal and vertical components of dimensionless force also decrease with an increase in the scattering parameter for both the regular and random wave tests.
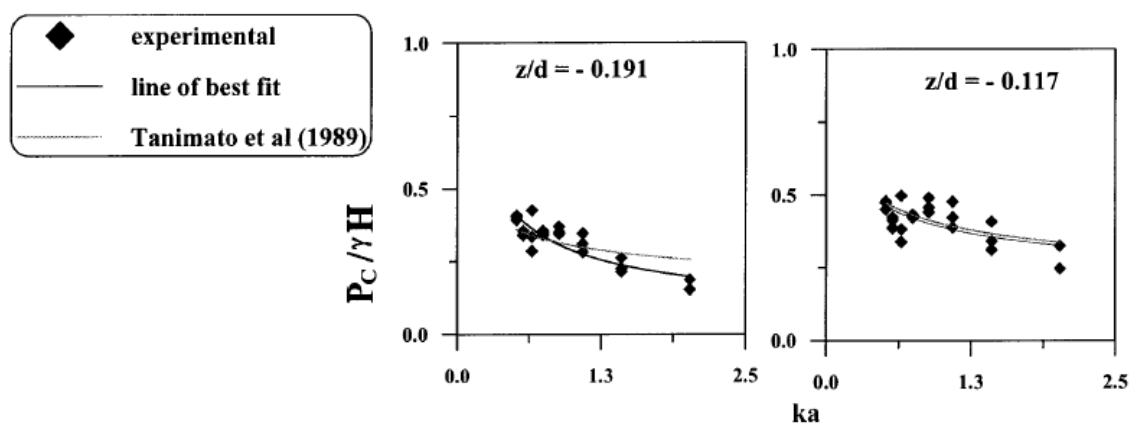
Fig. 2.19 Variation of dimensionless pressure with scattering parameter for different z/d (Subba Rao and Sundar, 2002)

Xie (1999) and Xie et al. (2006) evaluated the hydraulic characteristics of quarter circle breakwater and concluded the main reason for the difference of wave forces on the quarter circle and the semi circular breakwater (SBW). Based on comparison tests of wave forces acting on these two types of breakwaters, a simplified calculation method of wave forces on the quarter circle breakwater was also proposed. The horizontal wave force for quarter circle breakwater was found out by applying a modification coefficient to that for the semicircular breakwater. The modification coefficient can be taken as 1.3 for submerged condition or 1.1 for the breakwater with a freeboard.

Hanbin Gu et al. (2008) developed a numerical wave flume for impressible viscosity fluid based on Reynolds averaged Navier-Stokes equations in order to simulate the hydraulic behaviors of QBW and SBW. Based on the experiments, they evaluated the major difference between hydraulic behaviours of QBW and SBW.
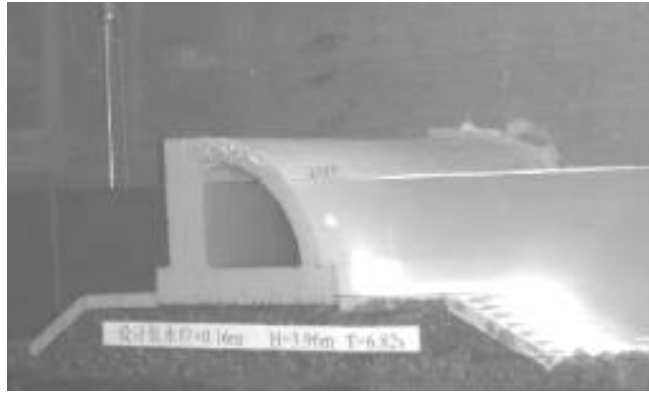
Fig. 2.20 Test model of Quarter circle breakwater (Hanbin Gu et al., 2008)

The hydraulic performances of both QBW and SBW, such as wave forces and reflection coefficients are evaluated using the characteristics of flow field which was developed numerically. Both in submerged and emerged cases, the reflection coefficients of QBW and SBW are found to be closer under similar conditions, which increase with increase in relative free board, h_c/H (where h_c is the free board height of breakwater and H is the incident wave height).
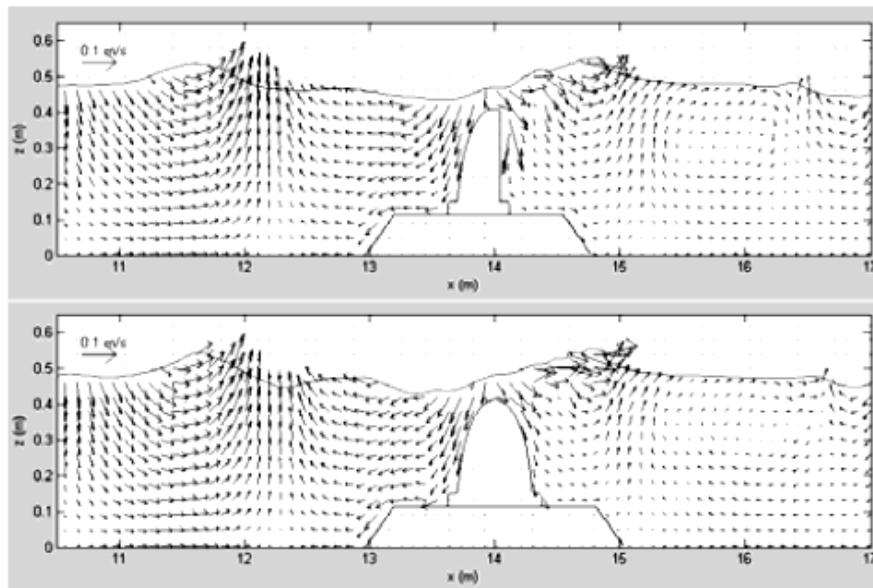
Fig. 2.21 Flow fields around submerged QBW and SBW (Hanbin Gu et al., 2008)

The non-dimensional horizontal component of wave force ($F_x/\gamma H^2$) was found to be decreasing with increase in wave steepness for both QBW and SBW. Under submerged condition, high flow velocity and vortexes was observed near the rear wall of QBW during wave overtopping. This may be caused by the top sharp corner of and sudden expansion of flow field around QBW which makes the horizontal

components of wave force on QBW larger than those on SBW. They concluded that the similarity in flow fields in front of both submerged and emerged cases is due to the similarity of reflection coefficients for both breakwaters.
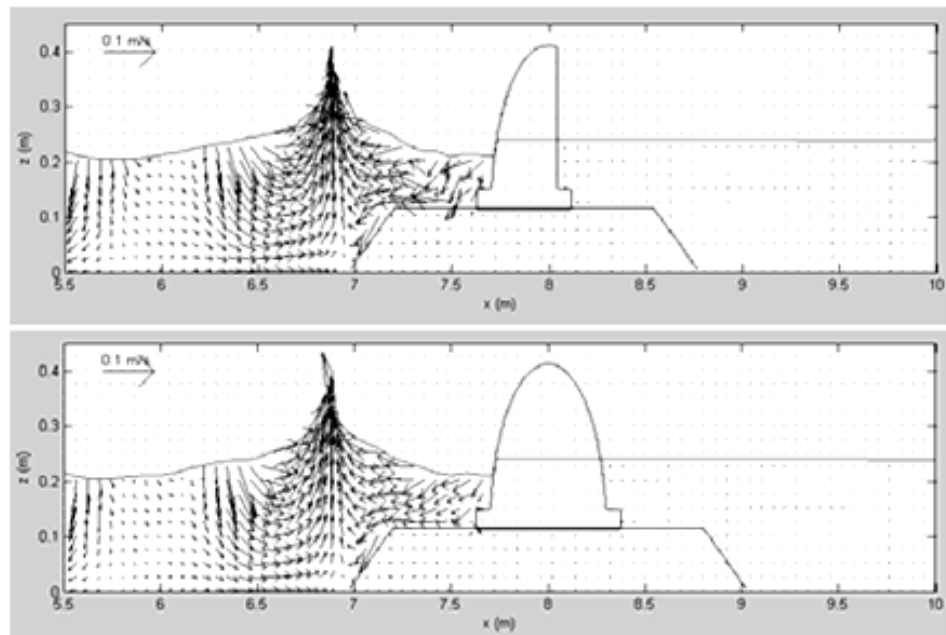
Fig. 2.22 Flow fields around emerged QBW and SBW (Hanbin Gu et al., 2008)

Jiang et al. (2008) conducted two dimensional wave numerical model and physical model studies to research the performances of QBW by comparing the hydraulic behaviours of SBW and QBW under same hydraulic conditions. They found that the reflection coefficients of QBW and SBW are close to each other with values less than 1.0, even if h_c reaches 2 to 3 times of incident wave height. They also concluded that the reflection coefficient K_r was increasing with increase in h_c/H_i for both SBW and QBW.

The numerical and experimental studies on QBW performed by Jiang et al. (2008) were limited to regular wave conditions. The experiments on similar type QBW was repeated by other researchers based on both regular and irregular wave experiments. Jiao et al. (2011) conducted a series of regular and irregular wave experiments to study the reflective and transmitting performances of quarter circle breakwater in comparison with those of semi circular breakwater. In irregular wave experiments, the reflection coefficients of QBW and their spectrums are studied. They discussed the two types of reflection coefficient, resolution reflection coefficient (based on standard reflection concept, $K_r = H_r/H_i$) and circular surface reflection coefficient

(K_{rc}, used to describes the reflective effect by circular surface on the adjacent flow). They observed that for QBW, both reflective and transmitting performances are more sensitive to the relative freeboard height (h_c /H_i) than the wave steepness. For QBW under the action of regular waves, the resolution reflection coefficients (K_r) was found to be varying from about 0.17 to 0.5 and the range of the circular surface reflection coefficients (K_{rc}) was about 0.02 to 0.4.
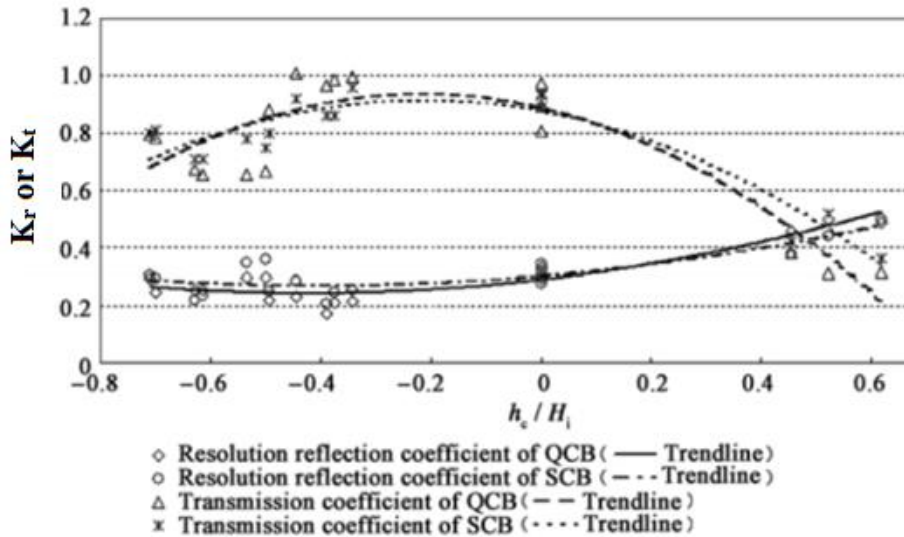
Fig. 2.23 K_r or K_t for QBW under regular waves (Jiao et al., 2011)

In the case of submerged QBW, both reflection coefficients decreases as h_c /H_i increases and conversely under emerged cases increases when h_c /H_i increases. The influence of the wave steepness upon the resolution reflection coefficients (K_r) is found to be small under regular wave conditions. Based on the results, an expression for the resolution reflection coefficient of QBW was deduced by use of the linear regression of experimental results. Based on experimental results, they concluded that the hydraulic performances of QBW and SBW are almost the same, which may be resulted from the similar wave profiles in front of both breakwaters.

$$K_r = 0.19 \frac{h_c}{H_i} + 0.35; -0.7 \le \frac{h_c}{H_i} \le 0.6 \, and \, 0.055 \le \frac{H_i}{L_i} \le 0.085 \ldots\ldots\ldots\ldots\ldots (2.3)$$

By conducting experiments under irregular waves, they concluded that the influence of the wave steepness upon the reflection coefficients under irregular wave conditions is stronger than those under regular wave conditions.

The synthesis reflection coefficients for QBW can be calculated by:

$$K_r = 0.23\frac{h_c}{H_{si}} + 0.35; -1.0 \le \frac{h_c}{H_{si}} \le 1.0 \, and \, 0.033 \le \frac{H_{si}}{L_{si}} \le 0.062 \dots\dots\dots (2.4)$$

Where H_{si} and L_{si} stands for the wave height and wave period corresponding to significant wave.
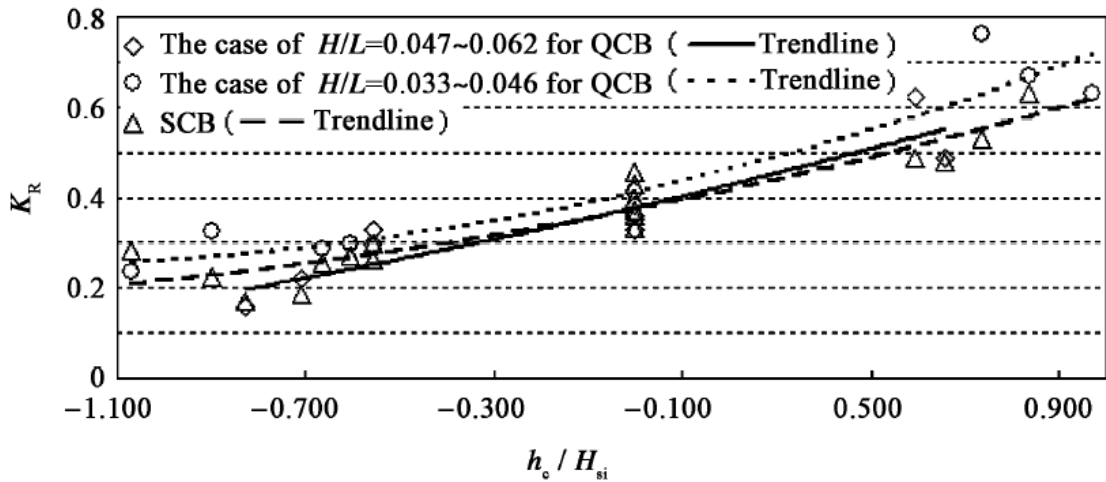
Fig. 2.24 K_r or K_t for QBW under irregular waves (Jiao et al., 2011)

Qie et al. (2013) conducted a series of physical model tests acted by irregular waves to investigate the wave force distribution on the seaward side of QBW. Through their research for wave force distribution on QBW, a modified Goda formula is proposed to calculate the wave forces on the QBW.
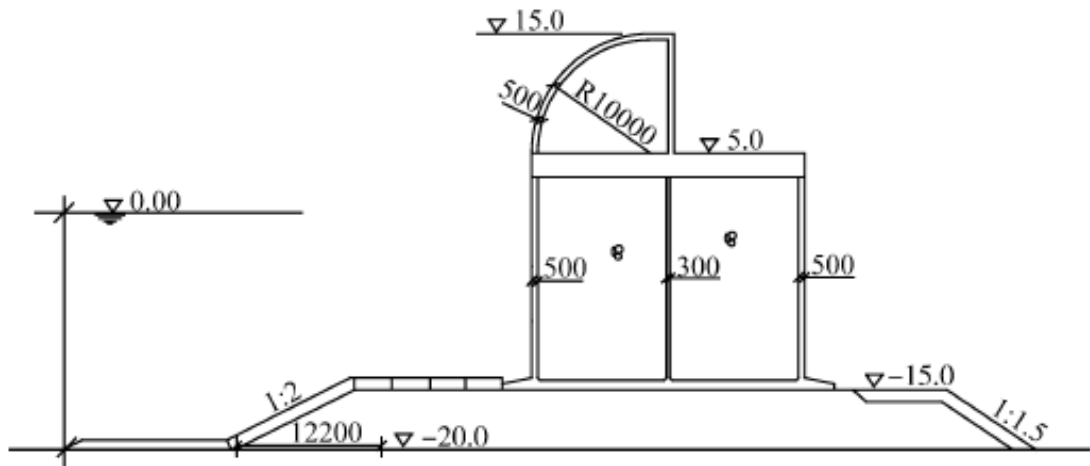
Fig. 2.25 Cross section of QBW (Qie et al., 2013)

Based on the observed wave data, they proposed a reliability index and failure probability of QBW, as well as they proposed partial coefficients of wave loadings.

Finally, a factor Q = 0.9 is given to modify the zero pressure height above still water level of QBW, and wave force partial coefficient 1.34 to the design expressions of QBW for anti-sliding, as well as 1.67 for anti-overturning.

Using the wave data statistical method, they studied the horizontal wave force, vertical downward force on the quarter-circular crest and the uplift force on the QBW. The wave forces on the quarter-circular crest test points are decomposed into horizontal and vertical components and the wave force P_{2H} and vertical force P_{2V} are integrated on the quarter-circular part. The total horizontal wave force P_H on QBW is composed of P_1 (wave force on caisson) and P_{2H}, *i.e.* $P_H = P_1 + P_{2H}$. The downward vertical wave force on QBW is $P_V = P_{2V}$, and the uplift force on the caisson bed is P_U (Refer figure 2.26).
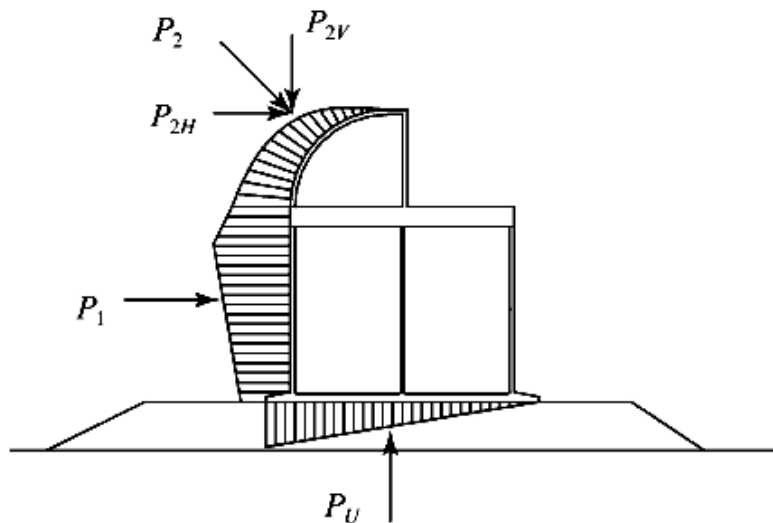
Fig. 2.26 Wave force distribution on QBW (Qie et al., 2013)

They calculated the wave forces on QBW using the combined method of caisson breakwaters and semicircular breakwaters. The wave forces on caisson of QBW were calculated using the Goda formula for caisson breakwater.

By using this, wave pressure on the still water level is given by the relation,

$$p_s = 0.5(1 + cos\beta).(\alpha_1 + \alpha_2 cos^2\beta)\rho_0 \qquad (2.5)$$

The wave pressure at front toe of caisson,

$$p_b = \alpha_3 p_s \qquad (2.6)$$

The wave pressure at sea bed,

$$p_d = \frac{p_s}{\cosh kd} \ \text{..} \ (2.7)$$

The wave pressure on the slab seaward,

$$p_u = 0.5(1 + \cos\beta)\alpha_1\alpha_3\rho_0 H \ \text{...} \ (2.8)$$

$$\alpha_1 = 0.6 + 0.5\left[\frac{4\pi \frac{d}{L}}{\sinh\left(4\pi \frac{d}{L}\right)}\right]$$

$$\alpha_2 = \min\left\{\frac{H'-d}{3H'}\left(\frac{H}{d}\right)^2, \frac{2d}{H}\right\}$$

$$\alpha_3 = 1 - \frac{d_1}{d}\left[1 - \frac{1}{\cosh\left(2\pi \frac{d}{L}\right)}\right]$$

Where H = design wave height, L the wave length, d the water depth in front of breakwater, and ρ_0 the density of water. Wave number, k= $2\pi/L$, d_1 is the water depth above bedding, H′ is the water depth 5 times of H_S (effective wave height) away from the breakwater, β is the angle between wave direction and the normal direction of breakwater axes.

In order to calculate the wave forces acting on the quarter-circular crest of QBW, they adopted the Goda formula on semi-circular breakwater which was recommended by Japan harbor Institute. By using this, the zero pressure height above still water level (SWL) is given by,

$$\eta = 0.75(1 + \cos\beta)H \ \text{..} \ (2.9)$$

With the phase difference between the vertical and the quarter-circular breakwaters, the wave pressure at the bottom of crest point pa (kPa, based on the Goda fomula) on QBW was modified as given by the equation,

$$p'_a = \lambda_p p_a \ \text{.................................,.....................................} \ (2.10)$$

Where λ_p is the correction factor for phase, and $\varDelta l$ is the horizontal distance between action points p'_a and p'_s.

$$\lambda_p = cos^4\left(\frac{2\pi\Delta l}{L}\right) \dots\dots\dots\dots\dots\dots\dots\dots\dots\dots\dots\dots\dots\dots\dots\dots\dots \text{ (2.11)}$$

They expressed modified wave pressure as $p'(Z)$, where Z indicates the height from the bottom of quarter-circular curve. The wave pressure acting on the normal direction of quarter-circular curve was given by the expression,

$$p(\theta) = p'(Z)cos(\theta) \dots\dots\dots\dots\dots\dots\dots\dots\dots\dots\dots\dots\dots\dots\dots\dots \text{ (2.12)}$$

Where θ denotes the central angle.
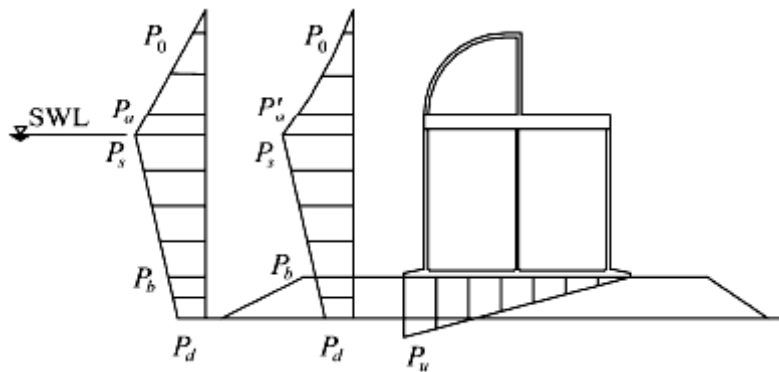
Fig. 2.27 Wave force distribution on QBW (Qie et al., 2013)

They developed a new method for calculating the wave force on QBW based on utilizing the combined Goda formula.

The water height above SWL (m) is given by the relation,

$$\eta' = Q.\eta = 0.675(1 + cos\beta)H \dots\dots\dots\dots\dots\dots\dots\dots\dots\dots\dots\dots\dots \text{ (2.13)}$$

When the angle $\beta = 0$, the η value of QBW was simplified as $\eta = 1.35H$.

The wave pressure at SWL ps' becomes equal to ps, at the toe of caisson $pb' = pb$, at sea bed, at sea side of caisson slab $pu' = pu$, at the joint point of caisson and quarter-circular crest $pa'' = pa'$

The wave pressure at the quarter-circular crest: $p'(\theta) = p(\theta)$

2.4 WAVE REFLECTION

Coastal structures reflect some proportion of the incident wave energy. If reflection is significant, the interaction of incident and reflected waves can create an extremely confused sea with very steep waves that often are breaking. This is a difficult problem for many harbor entrance areas where steep waves can cause considerable

maneuvering problems for smaller vessels. Strong reflection also increases the sea bed erosion potential in front of protective structures. Waves reflected from some coastal structures may contribute to erosion of adjacent beaches (CEM, Part VI, 2006).

Water waves may be either partially or totally reflected from both natural and manmade barriers. Wave reflection may often be as important a consideration as refraction and diffraction in the design of coastal structures, particularly for structures associated with harbor development (SPM, Volume I, 1984).

Reflection of waves implies a reflection of wave energy as opposed to energy dissipation. Consequently, multiple reflections and absence of sufficient energy dissipation within a harbor complex can result in a buildup of energy which appears as wave agitation and surging in the harbour. These surface fluctuations may cause excessive motion of moored ships and other floating facilities, and result in the development of great strains on mooring lines. Therefore seawalls, bulkheads, and revetments inside of harbors should dissipate rather than reflect incident wave energy whenever possible.

Natural beaches in a harbor are excellent wave energy dissipaters, and proposed harbor modifications which would decrease beach areas should be carefully evaluated prior to construction. Hydraulic model studies are often necessary to evaluate such proposed changes.

A measure of how much a barrier reflects waves is given by the ratio of the reflected wave height H_r to the incident wave height H_i which is termed the reflection coefficient (K_r). The magnitude of K_r varies from 1.0 for total reflection to 0 for no reflection; however, a small value of K_r does not necessarily imply that wave energy is dissipated by a structure since energy may be transmitted through some structures such as permeable, rubble-mound breakwaters.

The reflection characteristics depend on the geometry and composition of a structure and the incident wave characteristics such as wave steepness and relative depth d/L at the structure site. Non-overtopped impermeable smooth vertical walls reflect almost all the incident wave energy, whereas permeable, mild slope, rubble-mound structures absorb a significant portion of the energy. Structures that absorb wave

energy are well suited for use in harbour basins. The incident wave energy can be partly dissipated by wave breaking, surface roughness and porous flow; partly transmitted into harbour basins due to wave overtopping and penetration; and partly reflected back to the sea. The incident wave energy E_i is generally considered as the sum of energy dissipated (E_d), energy transmitted (E_t) and reflected energy(E_r) (CEM Part VI, 2006).

Reflection can be quantified by the reflection coefficient C_r given by the equation,

$$C_r = H_{sr}/H_s = \{E_r/E_i\}^{1/2}$$ .... (2.14)

Where H_s and H_{sr} are the significant wave heights of incident and reflected waves and E_r and E_i are the relative wave energies.

For past few years, investigators have experimentally and analytically studied wave energy dissipation and reflection characteristics for a variety of structures. Various prediction techniques have been proposed to estimate reflection coefficients for specific types of energy dissipation.

Miche (1951) proposed a wave reflection coefficient prediction technique. He assumed that there is some critical deepwater wave steepness below which the reflection coefficient is a constant. For conditions where wave steepness is greater than the critical value, the reflection coefficient is proportional to the ratio of the wave steepness to the critical value of wave steepness.

$$\left(\frac{H_0}{L_0}\right)_{crit} = \left(\frac{2\theta}{\pi}\right)^{1/2} \frac{sin^2\theta}{\pi}$$ (Miche, 1951) .... (2.15)

Where H_0 is the deep water wave height and θ, the angle the structure slope makes with the horizontal in radians.

For vertical breakwater on rubble mound foundation, the wave reflection was investigated by Tanimoto, Takahashi and Kimura (1987). The reflection coefficient K_r of vertical wall breakwaters is high, though less than 1.0 due to the effects of the rubble mound foundation and wave overtopping.

Studies on the reflection characteristics of perforated breakwater were initiated by Jarlan (1961, 1965) by conducting experiments using a low-reflectivity structure.

Other low reflectivity designs, similar to the original idea, have been proposed in Japan (Takahashi, 1996), in Italy (Franco, 1994) and Spain (Esteban and Llamas, 2007). Perforated wall caissons are the most widely used solutions for low-reflectivity vertical structures. Typically, perforated walls may have vertical or horizontal slots as well as circular or rectangular holes. Jarlan (1961) tested at 1/30 scale, a caisson with a perforated front wall with holes having porosity of 49% and concluded that the reduction of wave reflection was significant for certain values of wavelength. Marks and Jarlan (1968) included tests with irregular waves to study the forces on perforated structures.
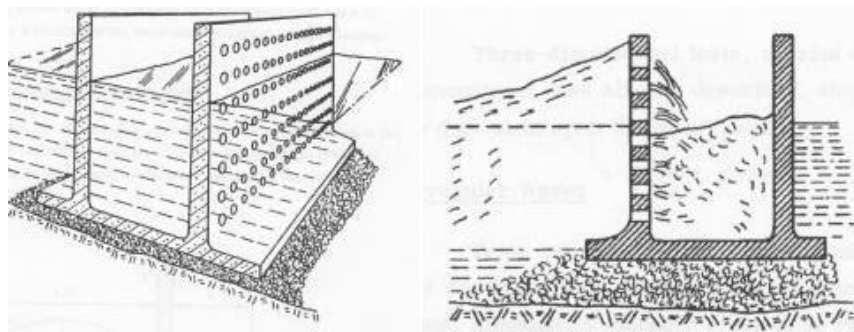
Fig. 2.28 Perforated breakwater at Comoeau bay (Jarlan, 1961)

Later investigations for quantifying the reflection on perforated type breakwaters were carried out. The following section outlines a brief summary of the studies conducted on the reflection characteristics of perforated type breakwater.

Terrett et al. (1968) developed an equation for reflection coefficient after conducting model studies on perforated breakwater using continuity and momentum balance theory. The reflection coefficient, R is given by

$R^2 = N_1 / D_1$, (Terrett, 1968)**………...………..…………………………………...**
(2.16)

$$N_1 = \left[\cos k_2 l \quad a^1 k_2 \sin k_2 l\right]^2 + \left(\frac{f}{c_2} \quad \frac{k_1}{k_2}\right)^2 \sin^2 k_2 l$$

$$D_1 = \left[\cos k_2 l \quad a^1 k_2 \sin k_2 l\right]^2 + \left(\frac{f}{c_2} + \frac{k_1}{k_2}\right)^2 \sin^2 k_2 l$$

k_1= wave number inside the breakwater = $2\pi / L_1$

k_2 = wave number outside the breakwater = $2\pi / L_2$

L_1 and L_2 are wave lengths in front of the screen and behind the screen.

l = chamber length and a^1 = virtual mass constant.

$$\frac{f}{c_2} = \frac{8}{3\pi} k_* \frac{A}{h_2} 2 \sin k_2 l / D_1$$

k_* = drag coefficient.

A and B are constants representing the amplitude of incident and reflected waves.

Kondo(1970) used linearize equations of motion similar to that of Terrett et al, to develop an analytical solution for flow in homogeneous vertical faced permeable breakwaters and derived equation for reflection and transmission coefficients , mean rate of energy flux and mean rate of energy dissipation. Hattori (1972) derived equations for reflection and transmission coefficients on a perforated wall breakwater from momentum and continuity equations.

$$K_r = H_r / H_i = \left| \{1 - \tau \, tanh(ikl)\} / \{1 + tanh(ikl)\} \right|, \text{ (Hattori, 1972)} \ldots\ldots\ldots\ldots\text{ (2.17)}$$

$$\tau = \varepsilon(S - if)^{-1/2}$$

Where H_r and H_i are height of incident and reflected waves, S = constant of momentum equation, ε = porosity, f = friction factor and l = width of the block mound.

Sollit and Cross (1972) analyzed the problem of small amplitude wave incident upon a permeable breakwater and obtained the solutions for velocity potential, pressure field, reflection and transmission coefficients. The reflection coefficient is given by,

$$C_r = \frac{S - if - \varepsilon 2}{S - if + \varepsilon 2 - i2\varepsilon \dfrac{\sqrt{gh}}{\sigma b}}, \text{ (Sollit \& Cross, 1972)} \ldots\ldots\ldots\ldots\text{ (2.18)}$$

Where S = inertial constant, f = damping coefficient, ϵ = porosity of the medium, σ = angular frequency of periodic motion, g = acceleration due to gravity, h = water depth and b = width of the breakwater.

Kondo and Toma (1972) conducted experiments on porous breakwater composed of vertical and circular cylinders to determine the effect of variations in longitudinal structural width.

$$K_r = \frac{\sqrt{K_{rf}^2 + K_{tf}^2 . K_{rb}^2 . K_{rf}^2 . e^{-2(n_i+n_r)B} + 2K_{rf} . K_{tf} . K_{rb} . K_{tf}}}{xe^{-(n_i+n_r)B} \cos(-2m_i B + \alpha_{tf} + \alpha_{rb} + \alpha_{tf} - \alpha_{rf})} \qquad \text{...............} \quad (2.19)$$

Where K_{rf}, K_{tf} = reflection and transmission coefficient at the front face, K_{rb} = reflection coefficient at the rear face and m, n = constants for incident and reflected waves.

Kondo (1979) developed an analytical model for calculating the reflection coefficient of a perforated wall caisson breakwater with one or two perforated wall, which was verified with his experimental data. Nagai (1976) conducted experimental investigations of the wave attenuation characteristics of a perforated box mounted to a rigid permeable vertical wall. A box-type wave absorber, which is composed of a perforated vertical front-wall and a perforated, horizontal bottom-wall, has been proved by a number of experiments to show lower coefficients of reflection than the perforated vertical wall breakwater.

Ijima et al. (1976) investigated several configurations of porous structure in conjunction with reflecting quay walls and found reflection coefficient using one dimensional small amplitude long wave equations of momentum and mass continuity. They concluded that the permeable or perforated wall with reservoir in total width of about 0.18 times the wave length has the same degree of wave absorbing ability as the permeable sloped-face seawall, even for long period waves.

Massel and Mei (1977) presented an analytical theory for random waves passing a perforated and porous breakwater. Sawaragi and Iwata (1979) considered the dissipation characteristics of wave energy of porous structures under irregular waves based on the reflection and transmission coefficient of a single slit wall and wave surface equations.

Massel and Butowski (1980) investigated various aspects of wave interaction of rectangular porous breakwater assuming that the incident wave spectrum is arbitrary. Tanimoto and Yoshimoto (1982) conducted a series of experiments to investigate the phenomenon of wave reflection of the perforated wall caisson.

Madsen (1983) derived an analytical solution for the reflection of monochromatic waves from a vertical homogenous wave absorber on a horizontal bottom.

Vidal et al. (1988) formulated a semi-empirical theory to predict wave reflection and transmission at a porous breakwater of rectangular cross section for normally incident solitary waves.

Twu and Lin (1991) conducted a research on the reflection of normal incident waves from multiple vertical porous plates. They assumed that the flow velocity passing through each porous plate obeys Darcy's Law.

Fugazza and Natale (1992) proposed a closed-form solution for wave reflection from a multi-chamber perforated-wall caisson, which overcame the calculating difficulty of the previous method. They concluded that the reflection is minimized when the wave chamber width is about one quarter of the wave length and the perforated-wall breakwater with a single wave chamber could provide the largest reduction of wave reflection in the range of practical applications.

Suh and Park (1995) developed a numerical model that computes the reflection of regular waves from a fully perforated-wall caisson breakwater. The numerical model based on a linear wave theory tends to over-predict the reflection coefficient of regular waves as the wave nonlinearity increases, but such an over-prediction is not observed in the case of irregular waves.

Isaacson et al. (2000) described a theoretical analysis for wave reflection from a breakwater consisting of a perforated front wall, an impermeable back wall, and a rock-filled core. Yip and Chwang (2000) proposed a theoretical solution to assess the hydrodynamic performance of a caisson with perforated front wall and a horizontal plate in it. Suh et al. (2001) developed a numerical model based on linear wave theory to predict the reflection coefficient from a full perforated wall caisson breakwater.

Garrido and Medina (2011) developed new semi-empirical model is used to estimate the coefficient of reflection for single and double perforated chambers in Jarlan-type breakwaters. Suh et al. (2011) evaluated hydrodynamic coefficients such as reflection and transmission coefficients of a perforated wall using the friction coefficient in the permeability parameter. An empirical formula for the friction coefficient is proposed in terms of the porosity and thickness of the perforated wall and the water depth.

Tae et al. (2012) analyzed the wave reflection of vertical and slit caissons with porous structures using the numerical model based on the Navier-Stokes equations. In the case of regular waves, the reflection coefficient was significantly reduced, whereas the reflection coefficient for irregular waves reduced by a relatively small amount by using porous structures. As the wave height was increased, the reflection coefficient was found to be decreasing for both vertical and slit caissons. The waves were observed to be more dissipated at the slit caisson than at the vertical caisson. The reflection coefficient was rarely affected by the variation of significant wave period.

The rectangular and trapezoidal porous structures showed obvious energy dissipation, whereas the triangular porous structure showed a little reduction effect on the slit caisson and almost no reduction on the vertical caisson. Because porous structure with low height is not able to dissipate wave energy effectively, a proper height is required for efficiency. Although rectangular and trapezoidal porous structures showed almost same energy dissipation, the trapezoidal structure is more preferred because it has superiority in the workability and stability.

(a) Combination of the vertical caisson and the porous structure

(b) Combination of the slit caisson and the porous structure
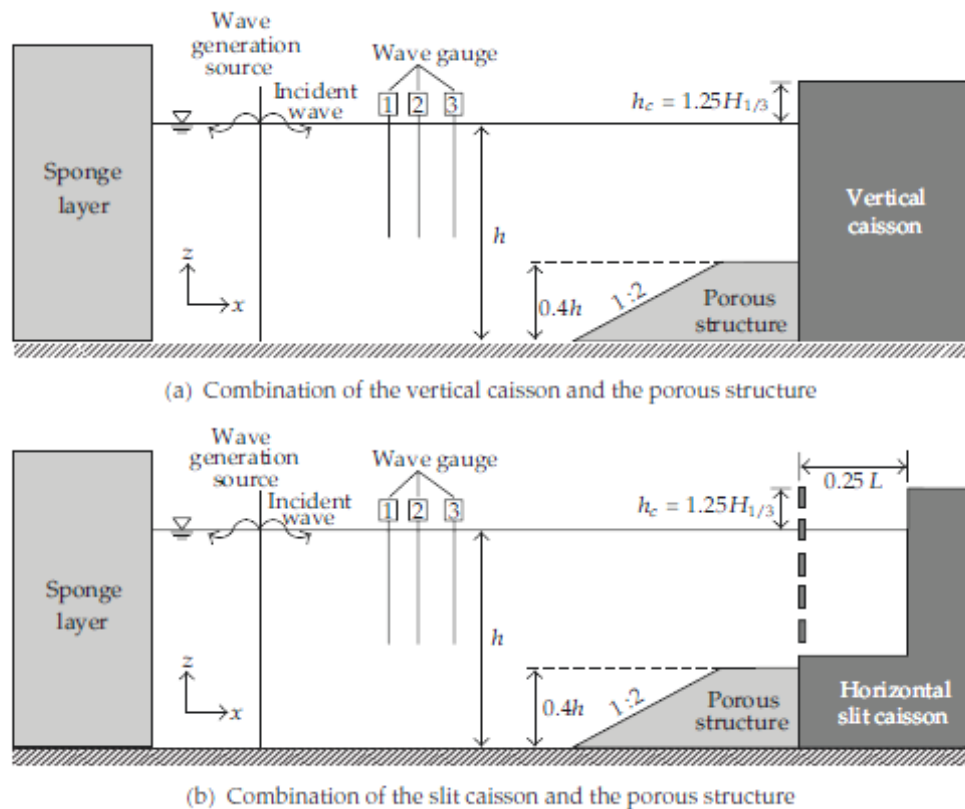
Fig. 2.29 Schematic diagram of Numerical wave flume (Tae et al., 2013)

2.5 WAVE RUNUP AND RUNDOWN

Wave runup is normally defined as the upper limit of wave up rush above the still water level in the field of coastal engineering. Wave runup on a beach determines the landward boundary of the area affected by wave action. Wave runup is hence important in delineating the area affected by storm waves and tsunamis. A quantitative understanding of the swash dynamics associated with wave up rush and down rush is essential for predicting sediment transport in the swash zone and establishing the landward boundary conditions of beach and dune erosion models (Kriebel,1990).

Wind generated waves have wave periods which trigger wave breaking on almost all sloping structures. The wave breaking causes runup (R_u) and rundown (R_d) defined as the maximum and minimum water surface elevation measured vertically from the still water level (SWL) (Refer Fig. 2.30). Runup and Rundown characteristics depend on the height and steepness of the incident wave and its interaction with the preceding reflected wave, the surface roughness, and the permeability and porosity of the structure. The wave runup level is one of the most important factors affecting the design of coastal structures because it determines the design crest level of the structure in cases where no (or only marginal) overtopping is acceptable. The prediction of wave runup on a coastal structure is necessary in determining the crest height of the structure required for no overtopping of design waves (Shore Protection Manual, 1984).
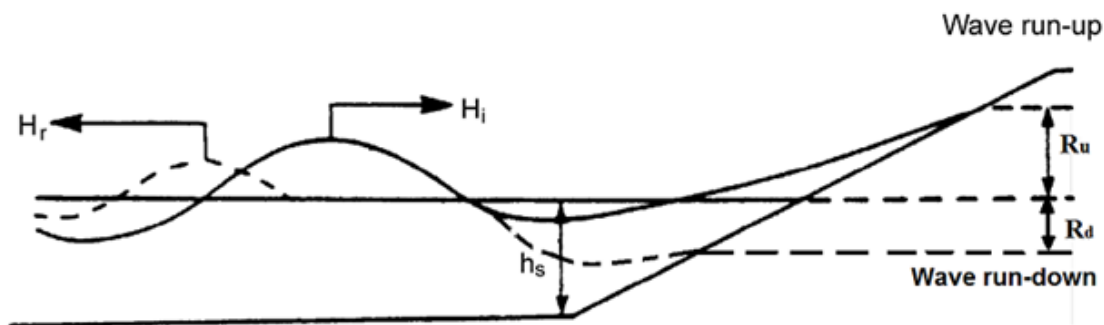
Fig. 2.30 Wave runup and rundown

The effects of the permeability and the roughness of the rubble mound face are important factors in wave run up (Hudson 1958). For a given structure slope, when the wave steepness decreases, the relative wave run up increases (CERC 1966).

Miche (1951) hypothesized that wave runup results from standing waves formed by the reflection of wave energy that is not dissipated by wave breaking. Based on this, Miche (1944) derived an equation for estimating wave runup based on the linear lagrangian equation of motion for shallow water.

$$R_u/H_0 = \sqrt{\pi/2\alpha}$$ .... (2.20)

Where R_u is the maximum runup height, H_0 is the wave height in deep water and α is the angle of the slope.

Saville (1957) suggested an iterative method for calculation of wave run up on composite slopes due to regular waves. The method proposed to consider an equivalent straight slope from the bottom to the point of maximum initial run up on the structure. The initial run up is estimated for the initial bottom slope of the breakwater. Early practical formulas for regular wave run up on smooth and rough plane slopes and composite slopes were presented by Hunt (1959).

Saville (1953) has concluded that effect of water depth is negligible when d/H > 3.0 for all wave steepness where d, the depth of water and H, the incident wave height. Wave run up increases with increasing ξ values and trends gets milder at high ξ values. Rundown also increases with increasing ξ values and becomes nearly constant at high ξ values ($\xi > 4.0$).

Ahrens (1981) and de Waal and Van der Meer (1992) conducted experiments on smooth, impermeable slopes and developed an equation for run up. Muttary et al. (2006) found that wave run-up is closely related to clapotis height in front of the breakwater. They also found an empirical equation relating wave run-up and reflection coefficient.

Wave run up and overtopping on coastal structures have historically being investigated using hydraulic models in the laboratories probably because storm waves occur infrequently and field measurements are expensive and difficult during storms. The runup elevation is also used to determine the base flood elevation for mapping purposes. Procedures used in the assessment of wave runup on vertical

structures are presented in Appendix D of the Guidelines and Specifications for Flood Hazard Mapping Partners (Section D.2.8.1.4 of the Atlantic Ocean and Gulf of Mexico Coastal Guidelines Update, Final Draft, February 2007). These procedures are also detailed in the Shore Protection Manual (USACE, 1984).

2.6 SUMMARY

The need for developing innovative structures for protecting the coast has led to the development of various types of breakwater. With the advancement in technology different types of breakwaters were developed in different parts of the world. Breakwaters are usually designed and constructed to satisfy a number of criteria such as functional performance, environmental impact, cost of construction and maintenance which adds challenge to the designer's task. Hence in order to economize the utilization of construction materials and to provide eco-friendly solution to coastal engineering problems alternative types of breakwater such as semicircular and quarter circle breakwater was developed.

The high construction cost of most coastal structures requires that risk analysis and life-cycle costing be an integral part of each design effort (SPM, Volume II, 1984). The performance of any type of breakwater depends on the primary objectives to be satisfied which in turn depends on the environmental conditions and purpose of construction. The analysis of breakwater after conducting a series of experiments is very significant to prevent the consequence of occasional damage particularly in the case of extreme events.

The types of failure associated with the quarter circle breakwater may be similar to that of caisson type breakwater. Failure of a caisson breakwater may be due to failure of caisson or monolith which includes slip surface failures, excess settlement, overturning, lateral displacement or sliding on foundation. It may be also due to hydraulic instability of rubble foundation, hydraulic instability of rubble-mound slope protection in front of caissons and breakage of blocks, seabed scour in front of the structure, breakage and displacement of structural elements (CEM, Part VI, 2006).

The hydraulic performance evaluation together with the structural stability is very significant while designing the structure. The extreme wave condition nearby the

breakwater structure and the resulting phenomena were to be studied in detail before designing a breakwater structure. Therefore in order to evaluate the performance of breakwater, characteristics such as wave reflection, wave transmission, wave runup and rundown are to be studied.

Perforated breakwaters are preferred over solid type breakwaters due to their advantage of dissipating wave energy in front of the breakwater. Dissipation of energy reduces both wave forces on the caisson and wave reflection (CEM, Part VI, 2006).

In this chapter the development of semicircular breakwaters and quarter circle breakwaters were briefly discussed. The outline of the research works conducted so far on different types of semicircular and quarter circle breakwater have been reviewed. The previous studies conducted on reflection and runup characteristics of perforated type breakwaters with the equations concerning each parameter were brought to attention. From the review of literature on quarter circle breakwater, it was observed that only a few researches were conducted on physical model studies which are very important to evaluate the functional performance. The studies on perforated type of quarter circle breakwater is not discussed anywhere.

PROBLEM FORMULATION AND EXPERIMENTAL DETAILS

3.1 GENERAL

Breakwaters have been built throughout the centuries but their structural development as well as their design procedure is under massive change. New ideas and developments are in the process of being tested regarding the breakwater layout, improve the performance and to reduce the failure of breakwaters. Designs are being increasingly influenced by environmental, social and aesthetical aspects transforming the breakwater into a complex structure. Under such situation where analysis and design of prototype structure is very complicated, the use of physical models is particularly advantageous.

In the past decades to design the hydraulic behaviour of coastal structures, physical models were only the possibility. Nowadays computer models are very powerful, but some complex flows and situations like wave breaking, overtopping and wave interaction with coastal structures cannot be easily handled by them. In such scenarios, physical modeling is used to obtain the hydrodynamic performance characteristics of emerged impermeable and perforated quarter-circle breakwater, with reasonable accuracy. In this chapter, problem formulation and objectives of the present study are briefed along with the details of laboratory conditions, experimental setup, dimensional analysis, hydraulic modeling, methodology and procedure adopted for the experimental investigation.

3.2 PROBLEM FORMULATION

The need for protecting the coast is continuously increasing ever since the man started interaction with the ocean for his livelihood. Trade and commerce has increased many fold in the last century which resulted in proliferation of ports and increase of the size of the vessels. This necessitated the construction of deep water harbours which are protected by breakwaters. Concerns of ecological damage and economical constraints directed the research for developing more cost effective and

eco-friendly technology for coastal protection. Researchers developed various innovative composite type structures based on all these considerations. One of the most recent achievements in breakwater technology was the development of semicircular and quarter circle breakwater.

The review of literature in the previous chapter shed light on the various studies conducted on reflection and runup characteristics of perforated type breakwaters with different size and shape of perforations. The present scenario of the development of innovative type breakwaters such as semicircular breakwater and quarter circle breakwater were highlighted. From the literature review presented, it was clear that physical model investigations conducted in the field of quarter circle breakwaters are very few. So, in the present work it was attempted to study the hydrodynamic performance characteristics of emerged perforated quarter circle breakwater by physical modeling.

The sliding of the quarter circle breakwater caused by the wave force exerted on the surface is an important phenomenon needs to be checked which was not discussed anywhere in the literature. Therefore sliding stability analysis of both impermeable and seaside perforated quarter circle breakwater was also carried out in the present research.

3.3 PHYSICAL MODELLING

Physical models have played a very crucial role in the development of complex hydrodynamic regime of the near shore region. Physical models are reproducing a physical system in the laboratory so that the major forces acting in nature are represented in the model in the correct proportion. A physical model is a precision device used to predict field behaviour. It can be regarded as reliable only if it is designed correctly. They can give a good simulation of the reality as they include all the processes that take place in the reality (Hughes, 1993).

Physical models are scaled representation of reality in which a prototype system is duplicated as closely as possible in a smaller scale. Laboratory studies are the diminutive reproduction of a physical system, so they are generally termed physical model studies. Model studies have their own technical and practical limitations, but

prove to be one of the best tools of the designer in arriving at a safe and stable design for breakwaters and other marine structures. The purpose of the model is to approximate and anticipate the prototype behaviour through certain prescribed modeling laws. There are many modeling approaches that are followed in the study of the natural systems. The most important of these are physical models and mathematical models. The physical model provides insight into a physical phenomenon which is not fully understood (Chakrabarthi 1996).

Physical modeling of coastal and harbour structures is based on the reproduction in the scale of gravity waves. Froude's model law is applied because the essential forces involved are inertia, pressure and gravity whereas viscous and surface tension forces are neglected and generally if wavelength is more than 0.05 m influence of surface tension can be neglected. The scale effects and uncertainty are the two major issues those decide the reliability of the model studies. To reduce scale effects the model should be as large as possible (Hughes 1993), so that the Reynolds number of flow is high and flow is turbulent (Ouellet 1970). And to minimize uncertainty the experiment has to properly planned, experimental procedures and extrapolation methods should be standardized and sources of errors have to be minimized (Mishra 2001).

3.4 OBJECTIVES

The present research work is intended to investigate the reflection and loss characteristics runup, rundown and sliding stability of an emerged impermeable and sea side perforated quarter circle breakwater model with varying radii and S/D (spacing between perforations/diameter of perforations) ratio.

The following are the objectives considered for the present study:

1) To investigate the hydrodynamic characteristics such as reflection and loss characteristics on an emerged impermeable as well as seaside perforated quarter circle breakwater with varying S/D ratio.
2) To investigate runup and rundown on an emerged impermeable as well as seaside perforated quarter circle breakwater with varying S/D ratio.

3) To study the effect of (S/D ratio) and water depth on hydrodynamic characteristics.

4) To compare the performance characteristics of an impermeable and sea-side perforated quarter circle breakwater under emerged conditions.

5) To study the sliding stability of impermeable and seaside perforated quarter circle breakwater against sliding.

3.5 DESIGN CONDITIONS

The wave climates off the Mangalore coast as given by KREC study team (1994) are considered while planning the present investigations. During the monsoon, the maximum recorded wave height off Mangalore coast is about 4.5 m to 5.4 m. During fair weather season wave height hardly exceeds 1 m. The predominant wave period during monsoon is 8 s to 11 s. Occasionally, during the fair weather season, wave periods up to 15 s are observed. The tides at Mangalore are mixed type with semi-diurnal components dominating. The tidal variation with respect to mean sea level is approximately ± 1.68 m. Hence, for the design of quarter circle breakwater model an equivalent of prototype design wave of height 4.5 m is assumed, while a maximum wave of height up to 5.4 m and period of 8 s to 14 s are considered for model study.

3.6 DIMENSIONAL ANALYSIS

In numerous engineering requisitions dimensional analysis is a normally utilized strategy to scale-up or down a process, and likewise to anticipate the results for distinctive conditions. It is not practical to conduct experiments for all conditions of a process to predict the data. Dimensional analysis is vital for learning fundamental dimensions and subsequent fundamental quantities which emerge in a true issue with a specific problem to plan fitting model investigations. It is a valuable procedure and is routinely utilized by physical researchers and designers to check the possibility of inferred comparisons and calculations. It provides a mathematical tool to supply both quantitative and qualitative relationships of a physical problem when combined with experimental procedures (Le Mehaute, 1990). Identification of the variables that influence the physics of the problem is important but difficult.

Unimportant variables must be eliminated to reduce expensive and time-consuming experiments; however, omitting important variables will likely result in incorrect conclusions (Hughes, 1993).

Dimensional analysis offers a method for reducing complex physical problems to the simplest (that is, most economical) form prior to obtaining a quantitative answer. Bridgman (1969) explains it thus: "The principal use of dimensional analysis is to deduce from a study of the dimensions of the variables in any physical system certain limitations on the form of any possible relationship between those variables. The method is of great generality and mathematical simplicity". Dimensional analysis is a rational procedure for combining physical variables in to dimensionless products, thereby reducing the number of variables those need to be considered (Hughes, 1993). In addition, depending of the results on the dimensions of the variables involved is estimated. The non-dimensional quantities in the results obtained from experiments on the model may be easily correlated to the corresponding quantities in the prototype.

There are two important methods used for dimensional analysis are

1   Rayleigh's method
2   Buckingham PI (π) theorem

The first step in modeling any physical phenomena is the identification of the relevant variables, then relating these variables by means of known physical laws. The Buckingham π theorem has a central importance in dimensional analysis. This theorem describes how any physically meaningful equation involving n variables can be rewritten as an equation of n–m dimensionless parameters. Where m is the number of fundamental dimensions used. Furthermore and most importantly, it provides a method for computing these dimensionless parameters from the given variables (Bridgman, 1963).

In the present case, the complex flow phenomenon responsible for energy dissipation cannot be easily represented by mathematical equations and one has to rely on experimental investigations. The results of such investigations are more useful when expressed in the form of non-dimensional relations. To arrive at such

non-dimensional relations involving different variables, dimensional analysis is carried out.

3.6.1 Predominant variables

The predominant variables influencing the performance of emerged perforated quarter-circle breakwater are shown in Table 3.1.

Table 3.1 Predominant variables influencing the performance of QBW

Predominant variables		Dimension
Wave parameters:	Incident wave height (H_i)	[L]
	Reflected wave height (H_r)	[L]
	Wave runup(R_u)	[L]
	Wave rundown(R_d)	[L]
	Depth of water (d)	[L]
	Wave period (T)	[T]
	Wave length (L)	[L]
Structure parameters:	Weight of QBW per unit length (W)	$[M] [T]^{-2}$
	Radius of structure (R)	[L]
	Height of structure (h_s)	[L]
	Diameter of perforations (D)	[L]
	Spacing between perforations (S)	[L]
Fluid Specific parameter	Mass density (ρ)	$[M] [L]^{-3}$
External Effects	Acceleration due to gravity (g)	$[L] [T]^{-2}$

3.6.2 Details of dimensional analysis

For deep-water wave conditions L_0 and T are related by the equation,

$$L_0 = gT^2 \big/ 2\pi \dots\dots\dots\dots\dots\dots\dots\dots\dots\dots\dots\dots\dots\dots\dots\dots\dots\dots \text{ (3.1)}$$

For intermediate and shallow water wave conditions L and T are related by the equation,

$$L = \left(gT^2 \big/ 2\pi\right) tanh\left(2\pi d/L\right) \dots\dots\dots\dots\dots\dots\dots\dots\dots\dots\dots\dots\dots\dots \text{ (3.2)}$$

'L_0' is the deep water wavelength and 'd' is the water depth. The term gT^2 is incorporated in the Eq. (3.1) to represent the wavelength L, instead of taking L directly. This is because, if L is utilized it would be depth specific, while gT^2 is independent of depth and represents the deep wave characteristics which might be effectively transformed to shallow waters depending on local bathymetry.

Wave reflections at and within a coastal harbour may make a significant contribution to wave disturbance in the harbour. Wave reflection and dissipation of wave energy can be measured in terms of reflection and loss coefficient. Reflection coefficient (K_r) is the ratio of reflected wave height (H_r) to the incident wave height (H_i). There is no transmission due to the impermeable wall on the lee side of the breakwater. The dissipation or loss coefficient is calculated by applying the energy balance equation,

$$E_i = E_r + E_t + E_L \quad\cdots\cdots\cdots\cdots\cdots\cdots\cdots\cdots\cdots\cdots\cdots\cdots\cdots\cdots\cdots\cdots\cdots\cdots\cdots\cdots\cdots\cdots \text{...... (3.3)}$$

Where, E_i - Incoming wave energy

E_r - Reflected wave energy

E_t - Transmitted wave energy

E_L - Dissipated wave energy

Hence $E_L = E_i - E_r - E_t$

Applying linear wave theory, per wavelength, per unit crest width (Dean and Dalrymple, 1992) where

$$E_i = 1/8\rho g\left(H_i\right)^2$$

$$E_r = 1/8\rho g\left(H_r\right)^2$$

$$E_t = 1/8\rho g\left(H_t\right)^2$$

$$E_L = 1/8\rho g\left(H_L\right)^2$$

$$E_L / \left(1/8\rho g\left(H_i\right)^2\right) = 1 - K_r^2 - K_t^2$$

Since K_t is equal to zero, loss coefficient, $K_l = \sqrt{\left(1 - K_r^2\right)}$ .... (3.4)

Runup and rundown characteristics determine the upper and lower limit for the rush of water on the breakwater structure. K_r, K_l, R_u and R_d are dimensionless numbers which depends on several parameters their relationships can be expressed as,

$$K_r = f(H_i, H_r, d, T, h_s, g, S, D) \quad\text{···}\quad (3.5)$$

$$K_l = f(H_i, H_r, d, T, h_s, g, S, D) \quad\text{···........}\quad (3.6)$$

$$R_u / H_i = f(H_i, d, T, h_s, g, S, D) \quad\text{·······································}\quad (3.7)$$

$$R_d / H_i = f(H_i, d, T, h_s, g, S, D) \quad\text{······································........................}\quad (3.8)$$

Variations of minimum weight required for sliding stability with different wave specific and structural specific parameters were studied using non-dimensional parameters obtained from a dimensional analysis by Buckingham's π theorem.

Stability of structure measured in terms of stability parameter S_n which depends on several parameters and their relationships can be expressed as,

$$S_n = f(H_i, d, T, h_s, W, \gamma, g, S, D) \quad\text{······················...}\quad (3.9)$$

By the application of Buckingham's theorem, equations of the form shown below were obtained.

$$K_r = H_r / H_i = f(H_i / gT^2, d / h_s, S / D) \quad\text{·····················...........................}\quad (3.10)$$

$$K_l = f(H_i / gT^2, d / h_s, S / D) \quad\text{··..............}\quad (3.11)$$

$$R_u / H_i = f(H_i / gT^2, d / h_s, S / D) \quad\text{·································..........................}\quad (3.12)$$

$$R_d / H_i = f(H_i / gT^2, d / h_s, S / D) \quad\text{····························..........··················}\quad (3.13)$$

$$S_n = W / \gamma H_i^2 = f(H_i / gT^2, d / h_s, S / D) \quad\text{······················..........................}\quad (3.14)$$

Where,

H_i/gT^2	Incident wave steepness parameter
d / h_s	Relative water depth
S/D	Ratio of spacing to diameter of perforations
R_u / H_i	Relative wave runup
R_d / H_i	Relative wave rundown
$W/\gamma H_i^2$	Stability parameter

Where W (weight of the structure) and $\gamma = \rho g$

3.7 SIMILITUDE CRITERIA AND MODEL SCALE SELECTION

Any physical model properly designed should represent the field conditions as nearly as possible for the proper interpretation of the test results. A physical model is a precision device used to predict the behavior of a physical phenomenon (Hughes, 1993). Similitude can be achieved when all the factors that influence the phenomenon are in proportion between the prototype and the model. According to Hughes (1993), model similitude can be achieved by,

  i   Calibration

  ii Differential equation

  iii Dimensional analysis

  iv Scale series.

In the present study, the similitude condition is attained by the method of dimensional analysis. This method alone is adopted because the method of calibration is time consuming and more appropriate for movable bed models. The method of differential equations is not suitable because the wave structure interaction is not clearly understood.

Scale series is mostly used to establish the scaling criteria for a complex phenomenon, and one has to be extremely careful in analyzing the results from the model tests and extrapolating them to prototype. In the method of dimensional analysis, similitude is achieved between the prototype and the model with the help of non-dimensional parameters of the phenomenon. These non-dimensional parameters must be same range for both the model and the prototype. Considering the wave climate off Mangalore coast, in the present study similitude is achieved by considering the non-dimensional parameter, incident wave steepness H_i/gT^2 as given in Table 3.2.

Table 3.2 Wave parameters of prototype and the model

Wave parameters	H_i (m)	T(sec)	H_i/gT^2
Prototype	1 to 5.4	8 to 12	0.0070 to 0.0086
Model	0.03 to 0.24	1 to 3	0.00033 to 0.0244

In the laboratory using the existing facilities of the two-dimensional wave flume, regular waves of heights ranging from 0.030 m to 0.24 m and periods ranging from 1 to 3 seconds can be produced.

For selecting a model-scale the range of wave heights and wave periods that can be generated in the wave flume accounting the wave climate off Mangalore coast are considered. To simulate the field conditions of wave height, period and diameter of perforation by application of Froude's law (Hughes, 1993) a geometrically similar model scale of 1:30 was selected for the present experimental investigations. The details for the selection of the model scale were presented in table 3.3.

Table 3.3 Selection of model scale

Scale	H_i (m)		T (s)		D (m)			
	1	5.4	8	12	0.25	0.5	0.75	1
1:10	0.1	0.54	2.53	3.8	0.025	0.05	0.075	0.10
1:20	0.05	0.27	2.68	2.68	0.0125	0.025	0.0375	0.05
1:30*	**0.033**	**0.18**	**1.46**	**2.19**	**0.0083**	**0.0166**	**0.025**	**0.033**
1:40	0.025	0.135	1.9	1.9	0.0063	0.0125	0.0188	0.025

* Scale selected for the present study

3.8 EXPERIMENTAL SETUP

The physical model study for regular waves was conducted in a two dimensional wave flume available in Marine Structures laboratory of Applied Mechanics Department, National Institute of Technology Karnataka, Surathkal, India. The facilities used for the investigations are briefly mentioned in the following sections.

3.8.1 Wave flume

The wave flume is 50 m long, 0.71 m wide and 1.1 m deep. It has a 41.5 m long smooth concrete bed. About 15 m length of the flume is provided with glass panels on one side. It has a 6.3 m long, 1.5 m wide and 1.4 m deep chamber at one end where the bottom hinged flap (or wave paddle) generates waves.

A ramp is provided between flume bed level and generating chamber for generation of waves. A series of vertical asbestos cement sheets are provided as wave filter

spaced at about 0.1 m centre to centre parallel to length of the flume. The flap is controlled by an induction motor of 11 KW power at 1450 rpm. This motor is regulated by an inverter drive (0 – 50 Hz) rotating in a speed range of 0–155 rpm. The desired wave heights and wave periods can be obtained by changing the eccentricity of bar-chain link (mounted on flywheel of motor) and by changing the frequency of inverter respectively.

Waves of height ranging from 0.03 m to 0.24 m heights and periods from 1.0 s to 3.0 s in a maximum water depth of 0.5 m can be generated with this facility. Fig. 3.1 shows the line diagram of wave flume.
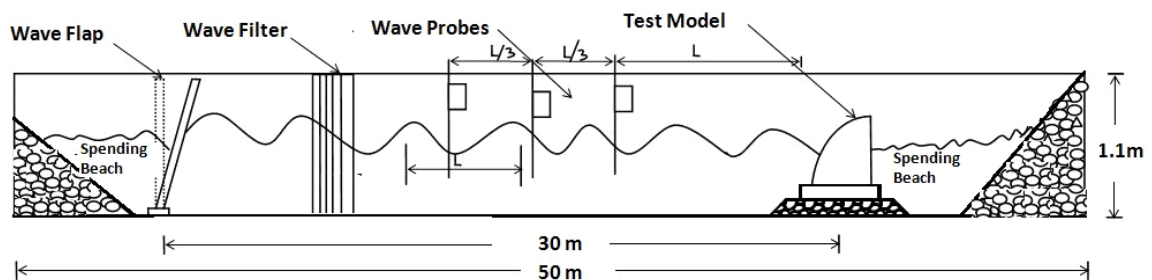
Fig. 3.1 Longitudinal Section of Wave Flume (Not to scale)

3.8.2   Wave probes

The capacitance type wave probes are used in the present study. The accuracy of the measurements is 0.001 m. The probes were used to record the incident wave characteristics. The spacing of probes and decomposition of incident and reflected waves from superposed waves recorded by wave probes was done using the three probe method suggested by Isaacson (1991).

3.8.3   Data acquisition system

Capacitance type wave probe along with amplification units was used for acquiring the data. The probe will be used for acquiring incident wave height, along with computer data acquisition system. The main parameter, wave surface elevation on seaward side of model is converted into electrical signal using relevant instruments. The digital voltage signals are converted into wave heights and wave periods using the laboratory wave recorder software provided by EMCON (Environmental Measurements and Controls), Kochi, India.

The probes were calibrated before every setup. Silica gel is applied to the probes at interval of 4hrs in order to reduce the surface tension. For the particular water depth, spacing between the probes is the function of wavelength and is kept at distance L/3(Issacson, 1991).

The wave periods in the experiment are varied from 1.2 s to 2.2 s at the interval of 0.2 s and the particular wavelength is calculated. For each wave period, five different wave heights ranging from 0.03 m to 0.18 m at the interval of 0.03 m were generated. And the depths of water in flume were varied from 0.30 m to 0.45 m at the interval of 0.05 m.

3.9 CALIBRATION OF TEST FACILITIES

Calibration of the experimental set up and instruments were undertaken frequently to check and ensure accuracy. The method of calibration of each component is given below.

3.9.1 Wave flume

The aim of calibration of wave flume is to evaluate a relationship between frequency of the inverter and wave period and eccentricity and wave height for a particular water depth. Desired wave period can be generated by changing of frequency through inverter drive. The wave period is inversely proportional to the frequency of inverter. With increase in the frequency the value of wave period will decrease.

The regular waves of height (H) ranging from 0.03 m to 0.18 m with varying periods (T) from 1.2 sec to 2.2 sec for different water depths were required for the experiment.

Wave height for a particular wave period can be produced by changing the eccentricity of bar chain on the fly wheel. Combinations that produced secondary waves in the flume are not considered for the experiments.

Figures 3.2 shows a calibration charts for wave heights at different wave periods and at water depth of 0.35 m, 0.40 m and 0.45 m.
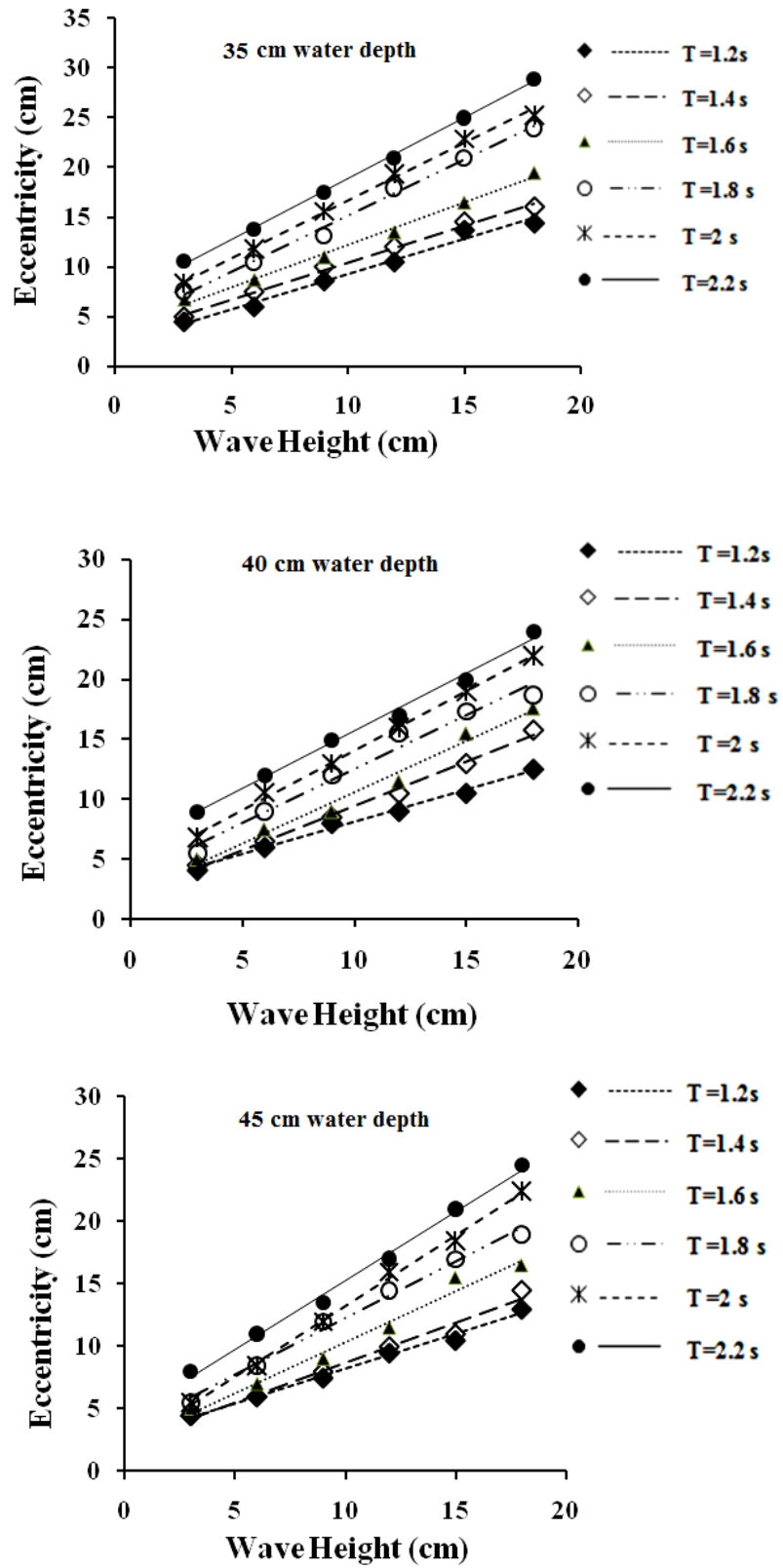
Fig. 3.2 Calibration curves for wave height at 35 cm, 40 cm and 45 cm water depth

3.9.2 Calibration of wave probes

The calibration of the wave probes has been done by lowering and raising the probe to a known depth of immersion and registering the changes in corresponding voltages. For obtaining, the average value, depth of immersion of the wave probes can be varied. The calibration graphs for wave probes are shown in Fig. 3.3.
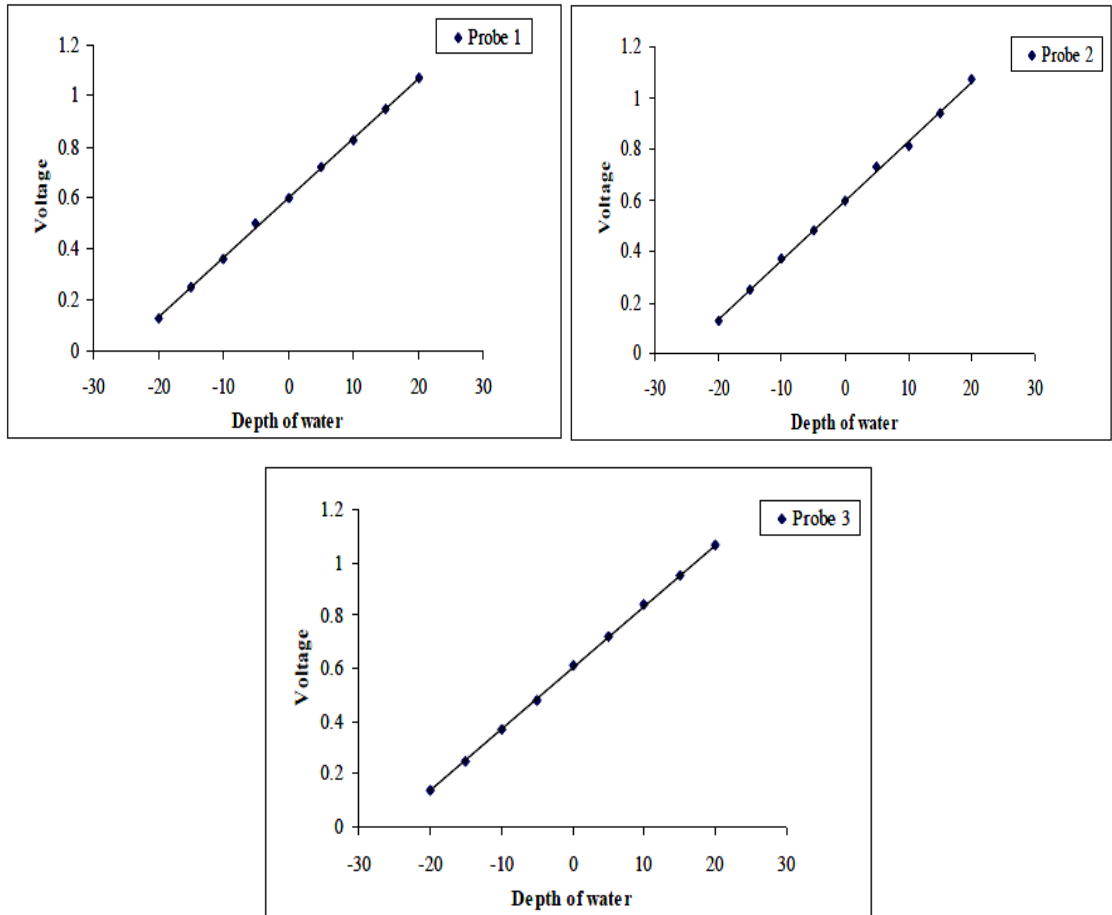
Fig. 3.3 Calibration curves for wave probe 1, 2 and 3

3.10   BREAKWATER TEST MODEL

3.10.1 Impermeable and Perforated quarter circle breakwater

Physical models were prepared to study the behaviour of the quarter-circle breakwater. Due to the predominant gravity effect in the free surface wave motion, Froude's model law was used for the physical modeling. A scale of 1:30 was used for testing of all physical models considering the Arabian Sea wave climate. For the experimental studies quarter circle breakwater (QBW) models of three different

caisson radii (R) 0.550 m, 0.575 m and 0.600 m are selected. The model dimensions are selected to satisfy the condition that the model will be emerged at all water depths (say 0.35 m, 0.40 m and 0.45 m) and remains non-overtopped under all wave conditions considered for the study. For each radius, the following types were tested,

1. Non perforated or Impermeable QBW
2. QBW with S/D = 5 (3% Perforations)
3. QBW with S/D = 4 (5% Perforations)
4. QBW with S/D = 3 (9% Perforations)
5. QBW with S/D = 2.5 (12% Perforations)
6. QBW with S/D = 2 (16% Perforations)

The percentage perforations is calculated as the percentage of the ratio of total area of the perforations (area of one perforation x number of perforations) to the surface area of the QBW considering the front face of QBW.

3.10.2 Casting and placing of QBW model

The proposed model of QBW consists of two parts, the bottom concrete slab and the top quarter circle shaped caisson. The casting of the model is done in two steps. Firstly concrete base slab is casted and then the curved wall of the caisson with or without perforations on front side and a rear impermeable vertical wall. The dimensions of concrete base slabs are 0.72 m × 0.65 m × 0.015 m, 0.72 m × 0.675 m × 0.015 m and 0.72 m × 0.70 m × 0.015 m for 0.550 m, 0.575 m and 0.600 m radii breakwaters respectively. Galvanized Iron (GI) sheet of 0.002 m thickness was used to fabricate the quarter circle caissons of radius 0.55 m, 0.575 m and 0.60 m and coated with cement slurry. The sheet is fixed to the slab with the help of stiffeners made up of flat plates of cross section 0.025 m x 0.005 m. The model is then placed over the rubble mound foundation of thickness 0.05m (minimum thickness as per CEM, 2001), and stones weighing from 50 to 100 gm.

The total height of the structure (h_s) is the sum of the radius (in m) of caisson, thickness of the concrete base slab (0.015 m) and rubble base foundation (0.05 m thick).

h_s= R+0.015+0.05 …………………………..……………………….………... (3.15)

The typical cross section of the QBW model both impermeable and perforated was shown in figures 3.4 and 3.5.
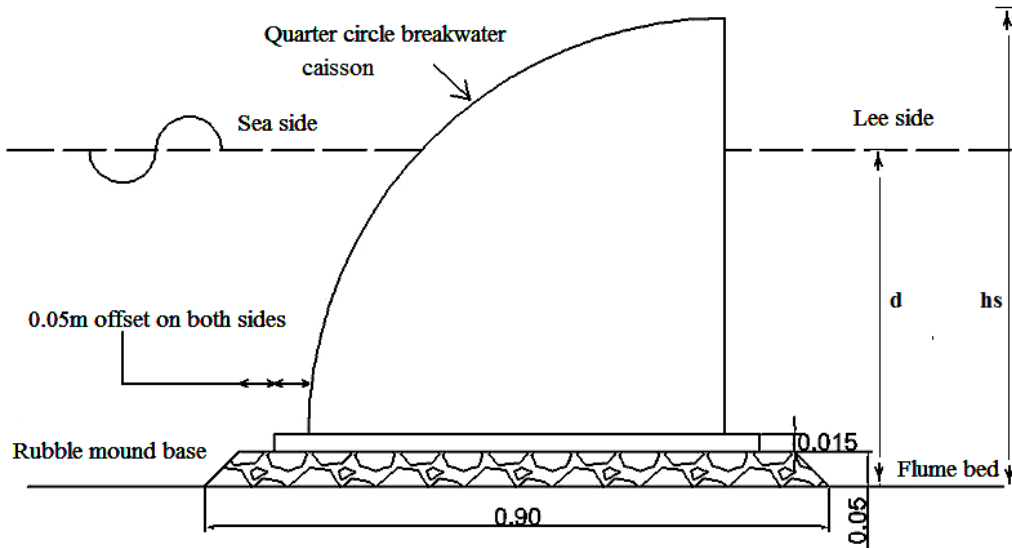
Fig. 3.4 Cross section of Impermeable QBW (All dimensions in m)
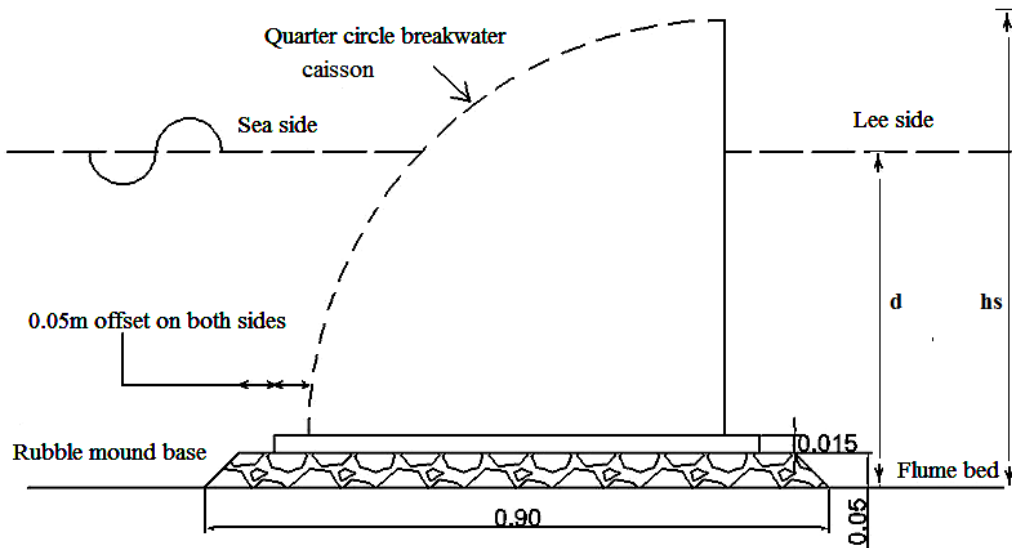
Fig. 3.5 Cross section of Perforated QBW(All dimensions in m)

The dimensions for QBW model were so chosen as to avoid the overtopping of incident waves and to ensure there is no transmission of waves. Also the dimensions of QBW structure were selected in such a way that the structure should slide for the least value of incident wave height (H_i) and wave period (T) used in the experiment,

so that additional weight may be added into the caisson body and thereby determine the minimum caisson weight (including the additional weight) required to resist the sliding.

3.11 RANGE OF EXPERIMENTAL VARIABLES

The ranges for experimental variables are to be selected at the earlier stage of experimental studies on any type of breakwater. The parameters may be either related to wave conditions or related to the structure and are described in table 3.4.

Table 3.4 Range of Experimental variables

Parameters	Experimental Range
Wave Specific Parameters	
Incident wave height, H_i	0.03, 0.06, 0.09, 0.12, 0.15, 0.18 m
Water depth, d	0.35, 0.40, 0.45 m
Time period, T	1.2, 1.4, 1.6, 1.8, 2.0, 2.2 s
Structure specific parameter	
Radius of the structure	0.55, 0.575, 0.6 m
S/D ratio	2, 2.5, 3, 4, 5
Diameter of perforation	0.016 m, 0.020 m

3.12 METHODOLOGY

The models were casted using GI sheet in suitable dimensions and the wave flume was prepared for the study as per the specifications. The wave flume is filled up with fresh water to the desired level and calibrated to produce the selected wave height and period without putting the model. The measuring instruments are also calibrated. The model is constructed at 30 m away from the generator flap.

First, 1:30 scale model of impermeable quarter circle breakwater were tested for wave reflection and loss characteristics. The runup and run down height on the curved QBW surface is noted and the vertical distance above and below the still water level is estimated. Then the model is tested for stability with regular waves of heights 0.03 m to 0.18 m and periods 1.2 s to 2.2 s in water depths of 0.35 m, 0.40 m

and 0.45 m. All the models were tested in the predetermined QBW dimensions as mentioned earlier. Later perforated QBW with different S/D ratios were tested to determine the reflection, loss characteristics, runup, rundown and stability.

After the tests, finally, the optimum dimension for the QBW radius and percentage of perforations were obtained from the analysis of the results.

The methodology adopted for the present research work is as follows:

1. The wave climates off the Mangalore coast as given by KREC study team (1994) are considered as the input parameters while planning the experimental investigations.

2. Dimensional analysis was carried out using Buckingham π theorem and non-dimensional parameters were identified.

3. The scale of the model was then selected based on the available site conditions and the predominant wave parameters.

4. Before conducting the experiment, calibration of the set up and instruments were undertaken frequently to check and ensure accuracy.

5. In the first phase, tests on reflection characteristics of both impermeable and seaside perforated QBW with varying S/D were conducted and the reflection coefficient, K_r is obtained. Since there is no transmission on the lee side, the loss coefficient was derived from the equation, $K_l = \sqrt{\left(1 - K_r^2\right)}$.

6. Then tests were conducted on runup and rundown characteristics and the dimensionless parameters relative wave runup (R_u/H_i), relative wave rundown (R_d/H_i) were determined.

7. Later test on sliding stability of both impermeable and seaside perforated QBW were conducted and the minimum weight required to avoid sliding of QBW was tabulated. Based on this non dimensional stability parameter ($W/\gamma H_i^2$) for different S/D ratio were found out.

8. For each experiment conducted, uncertainty analysis was done to check the errors occurred and based on the results, suitable equations were derived.

Wave run-up was measured as the vertical distance above the SWL and the maximum wave up rush when a wave impinges on breakwater. The vertical distance

below the SWL up to the minimum elevation attained by the wave on breakwater slope will be taken as the wave run-down.

The wave run-up, run-down was measured over the breakwater by the graduated graph sheet fixed over the glass panels of the flume. The QBW models were checked for any sliding and an incremented weight of 2.5 kg (24.52 N) was added to the caisson structure to resist the motion. The experiment was repeated till the structure stopped sliding and that is the minimum weight required for the sliding stability of the QBW model.

3.13 MODEL TEST CONDITIONS

Model after casting was tested for the hydraulic performance characteristics as well sliding stability and accuracy of the results will be checked. In order to design safe and economic structures, models are to be designed and operated correctly and the test conditions should be selected judiciously.

In the lab, the reflected waves from the breakwater strike the wave paddle and are almost totally re-reflected and create waves which may not represent the prototype condition truly. Further, the re-reflected waves may add-up or reduce the incident wave height and period thus resulting in undesired wave heights and periods. This results in erroneous output which is not desirable. This problem is eliminated by conducting experiments with series of wave bursts, such that, each burst of waves ending before re-reflected waves can again reach the testing section of the wave flume (Hughes 1993).

The present experimental investigations are carried out with the following test conditions:

1. The sea bed is rigid and horizontal and it is assumed that the sediment movement does not interfere with the wave motion and do not affect the model performance.

2. The waves are periodic and monochromatic.

3. Wave reflection from the structure does not interfere with freshly generated incident waves, since the waves are generated in bursts.

4. Secondary waves generated during the test are not considered.

5. Wave reflection from the flume bottom or flume side walls is not considered.

6. The density difference between freshwater and seawater is not considered.

7. Bottom frictional effects have not been accounted.

The experimental setup is prepared to produce ideal conditions as per the assumptions mentioned. However there may be some factors which cannot be satisfied fully. The errors due to them are small and do not have significant influence on the results of the study.

3.14 SOURCES OF ERRORS AND PRECAUTIONS EXERCISED

The following sources are identified which may cause error in the experimental study.

1. Error in linear dimensions: The model is constructed with an accuracy of linear dimensions up to ± 1.0 mm, which may contribute errors in between 0.2% to 0.3%.

2. Error in wave height measurement: The least count of the wave probe is 1.0 mm and may contribute to an error of 2% to 6% in the incident wave height.

3. Error due to change in water level: The water level is checked at the beginning and end of every day's work and maintained within ± 2 mm of the required level.

The following precautions are taken for minimizing the errors:

1. The model is constructed, as per the standard procedure, with a largest possible model with a scale of 1:30.

2. The depth of water in the flume is maintained exactly at the required level and was continuously monitored. Average variation of 2 mm was found after a full day of model testing. Any drop in the water level of more than 2 mm was immediately corrected.

3. Before the commencement of the experiments, calibration of flume and wave probes without the placement of model were undertaken to determine the proper wave height to assign to a particular combination of generator stroke and wave period. The wave heights to be used in the test runs are obtained

during calibration. This will exclude the losses due to interference of flume bed and side walls and therefore, eliminates these error sources.

4. Waves were run in short bursts of five during the tests. Between wave bursts there will be brief interval to allow reflected wave energy to dampen out.

5. All the wave characteristics were measured with more iteration and were statistically analyzed. Similar exercise was repeated for other parameters such as wave run-up and run-down over the breakwater.

3.15 PROCEDURE FOR THE EXPERIMENTAL STUDY

The experiments were conducted in the wave flume which generates regular waves and after carefully studying the model test conditions, following procedure is adopted.

1. The models to be tested were placed on a rubble mound foundation and 30 m away from the wave flap.

2. The wave flume was filled with tap water and the entire experimental setup including the wave probes were calibrated for each depth of water.

3. The superposed waves were measured by using three probes and the incident and reflected waves are decomposed from the superposed waves by using 3 probes method proposed by Michael Isaacson (1991). The details of the method are given in Appendix-1. For the particular depth, spacing between the probes is the function of wavelength and is kept at distance L/3. The first probe is placed at a distance L (wavelength) from the structure, and the distance between the probes is equal to L/3, where L is the wavelength.

4. Wave bursts each of five waves are generated to avoid the successive reflection. The surface elevation measured by the probes are recorded by the wave recorder and the signals are converted into wave heights and wave periods using the lab wave recorder software provided by EMCON, Kochi, India. The data is then analyzed by a MATLAB program and the reflected wave height was noted to obtain the reflection coefficient. Then the loss coefficient is deducted from the energy balance equation and by using the values for reflection coefficient.

Wave run-up will be measured as the vertical distance above the SWL and the maximum wave up rush when a wave impinges on breakwater. The vertical distance below the SWL up to the minimum elevation attained by the wave on breakwater slope will be taken as the wave run-down. The wave run-up, run-down will be measured over the breakwater by using graduated graph sheet fixed over the glass panels of the flume.

3.16   UNCERTAINITY ANALYSIS

Uncertainty is an estimate of experimental error. It describes the degree of goodness of a measurement or experimentally determined result. With the help of uncertainty analysis, it is possible to conduct experiments in a scientific manner and predict the accuracy of the result (Misra, 2001). Experimental error sources should be identified and the error (δ) should be determined from manufactures brochures, from calibration and conducting simple experiments respectively. The distribution of uncertainty between precision and bias is arbitrary. The confidence interval gives an estimated range of values, which is likely to include an unknown population parameter. The estimated range is calculated from a given set of observations. The 95% confidence interval limits must always be estimated and this concept of confidence level is fundamental to uncertainty analysis (Misra, 2001). The details of the uncertainty analysis are explained in Appendix I.

3.17   PHOTOS OF EXPERIMENTAL SETUP AND MODELS

Plate 3.1 A view of wave flume with QBW model

Plate 3.2 Arrangement of wave probes

Plate 3.3 Preparation of the base slab

Plate 3.4 QBW model after casting and fixing

Plate 3.5 Model placed in the flume

Plate 3.6 Data acquisition system
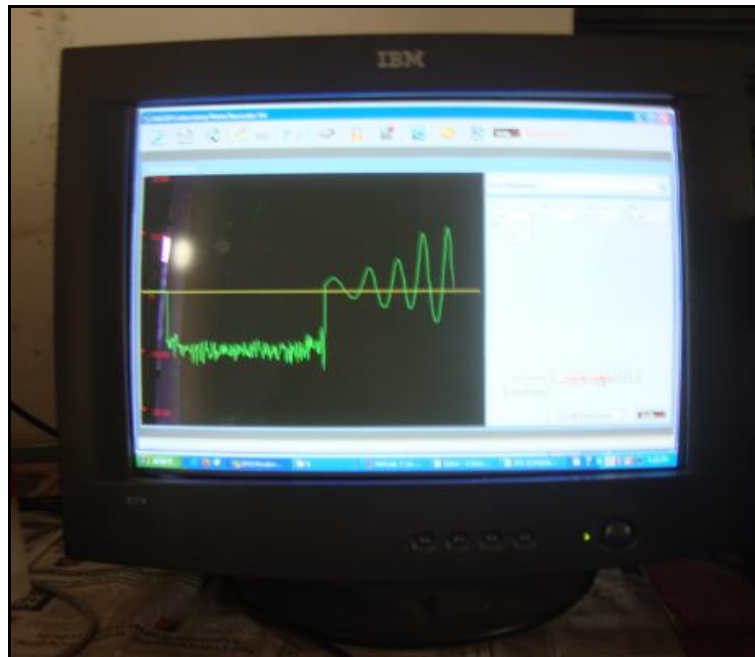
Plate 3.7 Wave recorder (EMCON software)
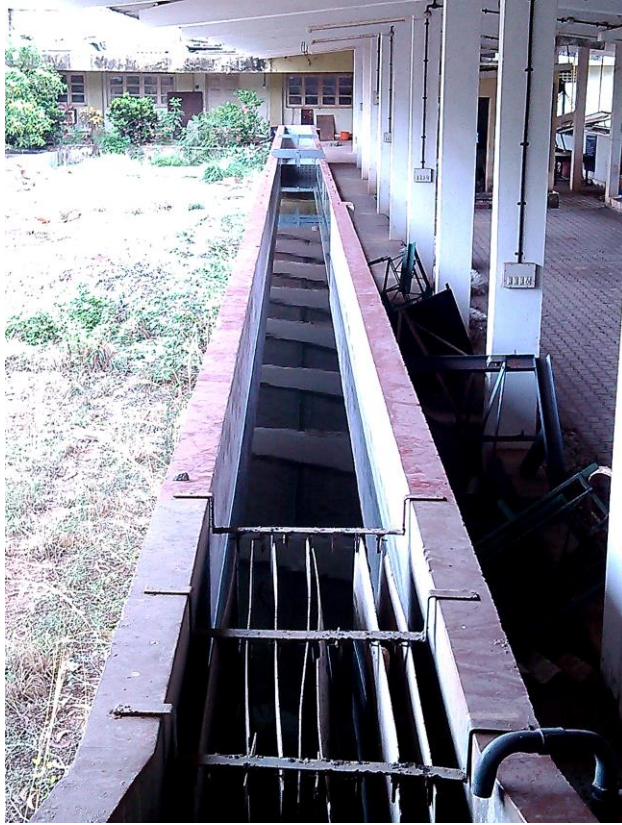
Plate 3.8 Wave Generating system

Plate 3.9 Wave structure interaction

INVESTIGATIONS ON REFLECTION AND LOSS CHARACTERISTICS OF EMERGED IMPERMEABLE AND SEASIDE PERFORATED QBW

4.1 GENERAL

The experiments are conducted on an emerged impermeable and seaside perforated quarter circle breakwater (QBW) models of three different radii 0.55 m, 0.575 m and 0.60 m with S/D ratio 2, 2.5, 3, 4 and 5. In this chapter the effect of various sea state parameters as well as structural parameters on the wave reflection and loss characteristics of an emerged impermeable and sea side perforated QBW model with varying perforations are discussed in detail.

After the completion of experiments, the results obtained have to be interpreted accurately to know the performance of a structure. The main objective of the study is to investigate the effect of varying water depth and the spacing / diameter of perforations (S/D) under different wave conditions. Finally a comparative analysis is done on the reflection and loss characteristics of impermeable and seaside perforated QBW.

4.2   STUDIES ON EMERGED IMPERMEABLE QBW

A 1:30 scale impermeable QBW model of different radius is fixed with the precast slab of suitable dimension and is placed on rubble mound foundation. The entire setup is placed at 30 m away from the wave flap. The model is subjected to regular waves of wave height varying from 0.03 m to 0.018 m and wave period ranging from 1.2 s to 2.2 s. For each breakwater radius, the model is tested at three different water depths (0.35 m, 0.40 m and 0.45 m).

The experiments are conducted on impermeable QBW of three different radii (say 0.55 m, 0.575 m and 0.60 m). The results obtained are analysed separately for different breakwater radii under different water depths and varying wave conditions. The graphs are plotted using non-dimensional parameters to study the effect of influencing parameters on each impermeable model.

The non-dimensional parameter reflection coefficient, K_r is plotted against wave steepness for $6.318 \times 10^{-4} < H_i/gT^2 < 6.3710 \times 10^{-3}$. For QBW radius equal to 0.55 m (height of the structure $h_s = 0.615$), corresponding to water depths of 0.35 m, 0.40 m and 0.45 m the graphs are plotted for each non-dimensional relative depth (d/h_s) of values 0.569, 0.650 and 0.732. Similarly for QBW of radius 0.575 m ($h_s = 0.640$), corresponding to water depths of 0.35 m, 0.40 m and 0.45 m the values of non-dimensional relative depth d/h_s obtained are 0.547, 0.625 and 0.703 respectively. When QBW radius is equal to 0.60 m ($h_s = 0.665$), the values for d/h_s are 0.526, 0.602 and 0.677 for water depths of 0.35 m, 0.40 m and 0.45 m.

4.3 VARIATION OF WAVE REFLECTION (K_r) FOR IMPERMEABLE QBW

4.3.1 Influence of incident wave steepness on reflection characteristics

(a) For radius 0.55 m   (b) For radius 0.575 m

(c) For radius 0.60 m
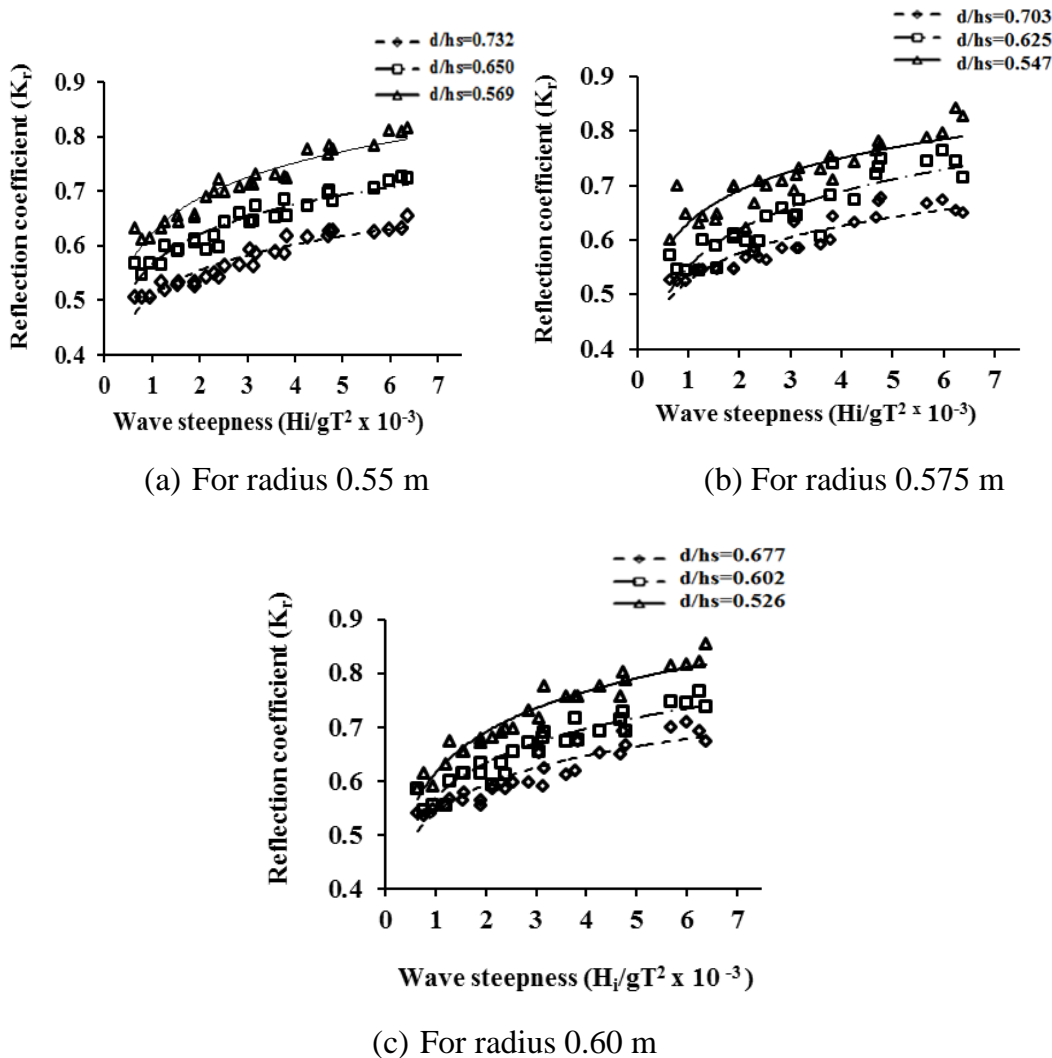
Fig. 4.1 Influence of H_i/gT^2 on K_r for different values of d/h_s and radius of QBW

Fig. 4.1 shows the variation of K_r with H_i/gT^2 for different water depths with radius of QBW 0.55 m, 0.575m and 0.60 m respectively. It is observed that K_r increases with increase in H_i/gT^2 for all breakwater radii and water depth or d/h_s. The increase in reflection coefficient with wave steepness may be because when the waves of shorter wave period run over the curved surface, they feel the surface of QBW for a shorter distance; because of this the energy dissipated due to turbulence is less and hence the reflection is greater for higher wave steepness.

Considering all water depths and for QBW of radius equal to 0.55 m (h_s equal to 0.615 m), K_r varies from 0.5054 to 0.8155 for $6.318 \times 10^{-4} < H_i/gT^2 < 6.3710 \times 10^{-3}$. The maximum value for K_r observed is 0.8155 at a wave height of 0.09 m and a wave period of 1.2 s ($H_i/gT^2 = 6.3710 \times 10^{-3}$) and at water depth equal to 0.35 m (d/h_s equal to 0.569). The minimum K_r observed is 0.5054 at a wave height of 0.03 m and a wave period of 1.8s ($H_i/gT^2 = 9.439 \times 10^{-4}$) and at water depth equal to 0.45 m ($d/h_s = 0.732$).

The experiments are repeated for QBW of radius 0.575 m ($h_s = 0.640$ m), K_r is found to be varying from 0.5263 to 0.8436 for $6.318 \times 10^{-4} < H_i/gT^2 < 6.3710 \times 10^{-3}$. The maximum value for K_r observed is 0.8436 for $H_i/gT^2 = 6.2410 \times 10^{-3}$ and d/h_s equal to 0.547. The minimum K_r observed is 0.5263 at $H_i/gT^2 = 7.645 \times 10^{-4}$ and d/h_s equal to 0.703. For QBW of radius equal to 0.60 m (h_s equal to 0.665 m), K_r varies from 0.5358 to 0.8541 for $6.318 \times 10^{-4} < H_i/gT^2 < 6.3710 \times 10^{-3}$. The maximum value for K_r observed is 0.8541 at $H_i/gT^2 = 6.3710 \times 10^{-3}$ and at water depth equal to 0.35 m (d/h_s equal to 0.526). The minimum K_r observed is 0.5358 at $H_i/gT^2 = 7.645 \times 10^{-4}$ and at water depth equal to 45cm ($d/h_s = 0.677$).

The percentage increase in K_r with H_i/gT^2 varies from 23% to 25% for QBW of radius equal to 0.55 m but it varies from 22% to 29% and 24% to 31% when QBW radius is 0.575 m and 0.60 m respectively.

4.3.2 Influence of water depth on reflection characteristics

The effect of water depth on reflection characteristics is obtained by plotting graphs between K_r and relative water depth, d/h_s for different ranges of wave steepness, H_i/gT^2 which is shown in Fig. 4.2.

From the trend line of the graph showing the relation between K_r and d/h_s, it is

observed that the values for K_r decreases with increase in relative water depth, d/h_s. This is because under higher water depth condition, waves run over the curved surface of the QBW leading to greater dissipation of energy and, thereby, resulting in lesser reflection.
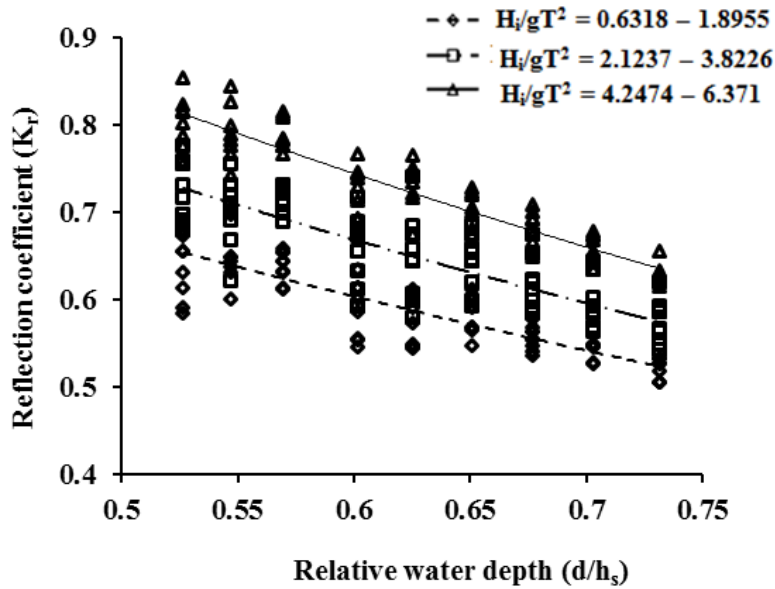
Fig. 4.2 Influence of d/h_s on K_r for different values of H_i/gT^2

From the experiments on impermeable QBW of radius 0.55 m, the minimum K_r value of 0.5054 is observed at d/h_s equal to 0.732 (0.45 m water depth) and maximum K_r obtained is 0.8155 when d/h_s equal to 0.569 (0.35 m water depth).

For QBW of radius 0.575m, the minimum K_r observed is 0.5263 at $d/h_s = 0.703$ (water depth of 0.45 m) and maximum K_r obtained is 0.8436 corresponding to $d/h_s = 0.547$ (water depth of 0.35 m). Considering QBW of radius 0.60 m, the minimum value for K_r is equal to 0.5358 observed at $d/h_s = 0.677$ (water depth of 0.45 m) and maximum K_r obtained is 0.8541.

For each radius of QBW considering different d/h_s and H_i/gT^2, minimum K_r is observed for a water depth of 0.45 m. The percentage reduction in K_r occurs when water depth is increased from 0.35 m to 0.45 m and it is found to be varying from 18% to 21%, 14% to 19% and 9% to 17% respectively for QBW of radius equal to 0.55 m, 0.575 m and 0.60 m respectively.

Considering all values of d/h_s and H_i/gT^2, values for K_r is observed to be increasing with increase in height of QBW (h_s) or QBW radius because effect of curvature is less predominant when the breakwater radius is more. Hence the effect of dissipating wave energy is more predominant in the QBW of radius equal to 0.55 m compared to QBW of radius 0.575 m and 0.60 m.

4.4 VARIATION OF LOSS COEFFICIENT (K_l) FOR IMPERMEABLE QBW

The wave energy dissipated is measured in terms of loss coefficient which is very significant for the design of all marine structures. In the case of emerged breakwater, there is no transmission on the rear side of the breakwater and hence the loss coefficient depends entirely on the reflection coefficient.

The values for non-dimensional loss coefficient K_l is obtained from the reflection coefficient using the equation 3.4. Then graphs are plotted between K_l and H_i/gT^2 for different values of d/h_s by keeping breakwater radius constant and at different water depths.

4.4.1 Influence of incident wave steepness on loss characteristics

Fig. 4.3 shows the variation of K_l with H_i/gT^2 for different water depths with radius of QBW 0.55 m, 0.575 m and 0.60 m respectively.

From the trend lines for the graphs plotted between K_l and H_i/gT^2 it is observed that K_l decreases with increase in H_i/gT^2 for all values of d/h_s. This may be because when the steep waves of shorter wave period run over the curved surface, they feel the curvature of QBW for a shorter distance; because of this the energy dissipated due to turbulence is less.

For QBW of radius equal to 0.55 m (h_s equal to 0.615 m), K_l varies from 0.5788 to 0.8629 for $6.318 \times 10^{-4} < H_i/gT^2 < 6.3710 \times 10^{-3}$. The maximum K_l observed is 0.8629 at a wave height of 0.03 m and a wave period of 1.8s ($H_i/gT^2 = 9.439 \times 10^{-4}$) and at water depth equal to 0.45 m ($d/h_s = 0.732$).

The minimum K_l observed is 0.5788 at a wave height of 0.09 m and a wave period of 1.2s ($H_i/gT^2 = 6.3710 \times 10^{-3}$) and at water depth equal to 0.35 m (d/h_s equal to 0.569).

(a) For radius 0.55 m

(b) For radius 0.575 m

(c) For radius 0.60 m
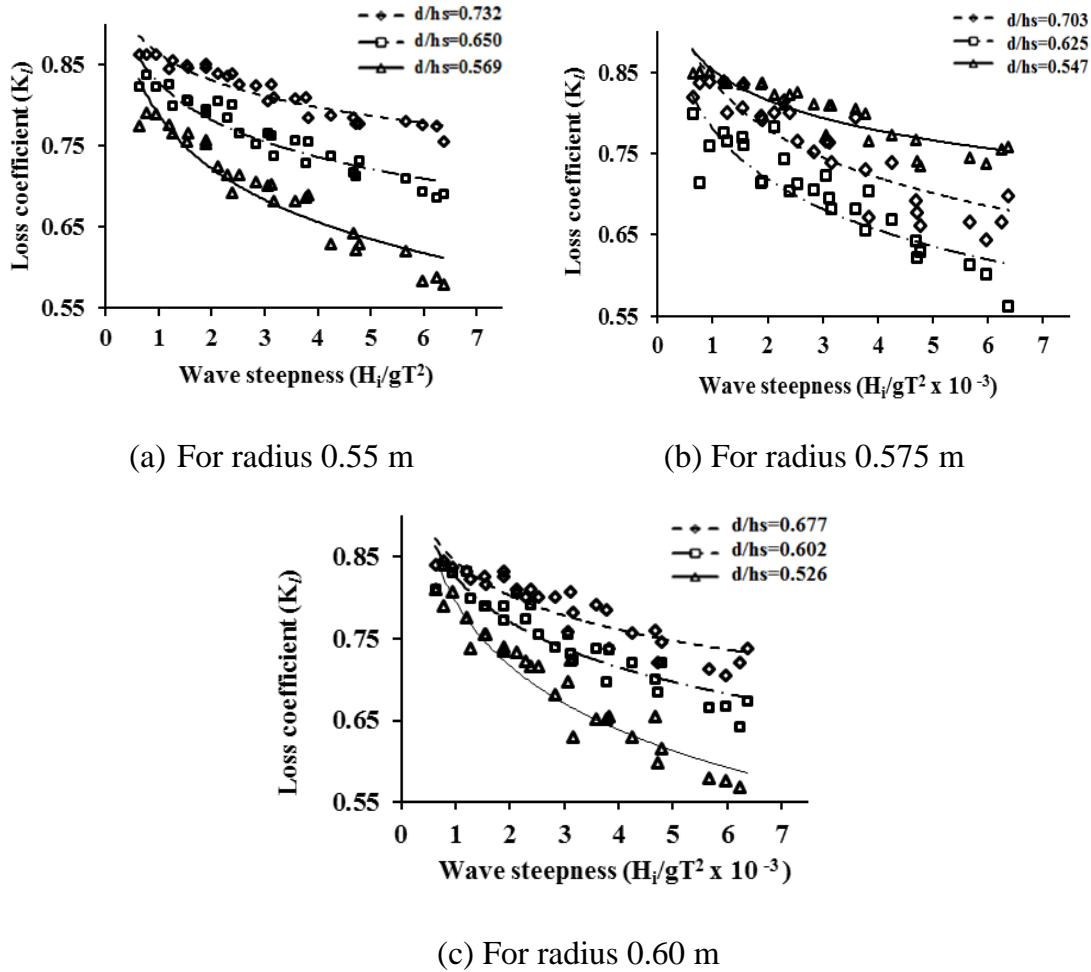
Fig. 4.3 Influence of H_i/gT^2 on K_l for different d/h_s and radius of QBW

When QBW of radius is increased to 0.575 m (h_s equal to 0.640 m), K_l varies from 0.5370 to 0.8503 for $6.318 \times 10^{-4} < H_i/gT^2 < 6.3710 \times 10^{-3}$. The maximum K_l observed is 0.8503 at a wave height of 0.03 m and a wave period of 2s ($H_i/gT^2 = 7.645 \times 10^{-4}$) and at water depth equal to 0.45 m ($d/h_s = 0.703$). The minimum value for K_l observed is 0.5370 at a wave height of 0.12 m and a wave period of 1.4 s ($H_i/gT^2 = 6.2410 \times 10^{-3}$) and at water depth equal to 0.35 m (d/h_s equal to 0.547).

For $6.318 \times 10^{-4} < H_i/gT^2 < 6.3710 \times 10^{-3}$ acting on QBW of radius equal to 0.60 m (h_s equal to 0.665 m), K_l varies from 0.5202 to 0.8443. The maximum K_l observed is 0.8443 at a wave height of 0.03 m and a wave period of 2s ($H_i/gT^2 = 7.645 \times 10^{-4}$) and at water depth equal to 0.45 m ($d/h_s = 0.677$). The minimum for K_l observed is 0.5202 for wave height of 0.09 m and a wave period of 1.2 s ($H_i/gT^2 = 6.3710 \times 10^{-3}$) and at water depth equal to 0.35 m (d/h_s equal to 0.526).

The percentage decrease in K_l with H_i/gT^2 varies from 9.52% to 26.85%, 13.58% to 32.84% and 16.44% to 35.83% for QBW of radius equal to 0.55 m, 0.575 m and 0.60 m respectively.

4.4.2 Influence of water depth on loss characteristics

$- \diamond - \ H_i/gT^2 = 0.6318 - 1.8955$
$-\square - \ H_i/gT^2 = 2.1237 - 3.8226$
$-\triangle - \ H_i/gT^2 = 4.2474 - 6.371$
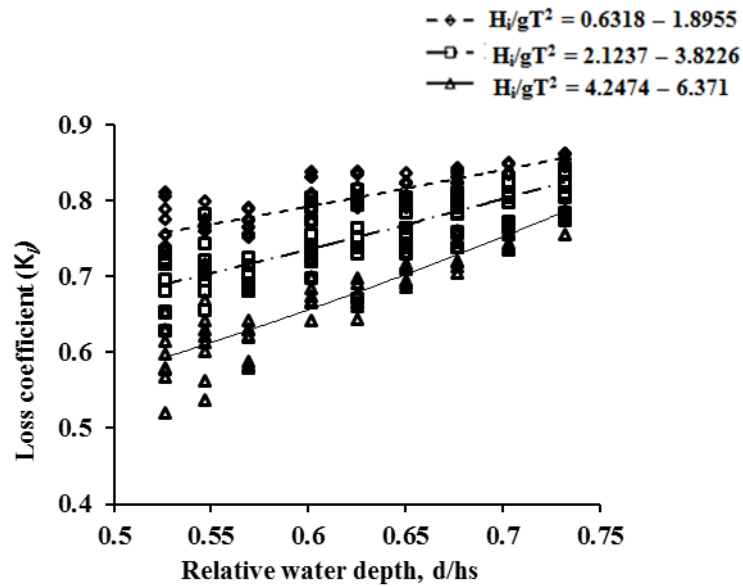
Fig. 4.4 Influence of d/h_s on K_r for different values of H_i/gT^2.

When QBW radius is equal to 0.55 m (h_s= 0.615), the minimum value for K_l is equal to 0.5788 observed at d/h_s =0.569 (water depth of 0.35 m) and maximum K_l obtained is 0.8629 corresponding to d/h_s = 0.732 (water depth of 0.45 m). The percentage increase in the value of K_l with respect to a water depth of 0.35 m (d/h_s = 0.569) is found to be varying from 8.33% to 27% for a water depth of 0.45 m (d/h_s = 0.732).

The minimum value for K_l is equal to 0.5370 observed at d/h_s= 0.547 (water depth of 0.35 m and QBW of radius 0.575 m) and maximum K_l obtained is 0.8503 d/h_s = 0.703, corresponding to a water depth of 0.45 m.

The percentage reduction in K_l with respect to a water depth of 0.35 m is found to be varying from 5.90% to 26.2% for a water depth of 0.45 m. For the tests conducted on QBW of radius 0.60 m, the minimum value for K_l is equal to 0.5202 observed at d/h_s = 0.526 and maximum K_l obtained is 0.8443 corresponding to d/h_s = 0.677. The percentage reduction in K_l with respect to a water depth of 0.35 m is found to be varying from 3.96% to 23.3% for a water depth of 0.45 m.

4.5 STUDIES ON EMERGED SEASIDE PERFORATED QBW

The results obtained from the studies on emerged QBW are analysed separately for different spacing to diameter (S/D) ratios as well as for different breakwater radii under different water depths (say 0.35 m, 0.40 m and 0.45 m) and varying wave conditions. The data collected from the experimental work are initially expressed as non dimensional parameters. The results are plotted as non-dimensional graphs to study the effect of influencing parameters of each seaside perforated models separately. Finally the percentage increase or decrease in wave reflection and loss characteristics with wave steepness water depth and S/D ratio are found out.

4.6 VARIATION OF REFLECTION COEFFICIENT (K_r) FOR QBW 0.55 m RADIUS (h_s= 0.615 m)

The reflection characteristics of QBW are usually expressed in terms of reflection coefficient, K_r which depends on water depth, structure parameters like breakwater radii, percentage perforations and wave parameters. For the analysis of the results, data obtained from the experimental studies on wave flume are plotted as non-dimensional graphs showing the variation of reflection coefficient with wave steepness and ratio of water depth to height of breakwater structure (d/ h_s) for each S/D ratio.

4.6.1 Influence of incident wave steepness on reflection characteristics

4.6.1.1 Seaside perforated QBW with S/D ratio equal to 2

The influence of wave steepness on the reflection characteristics of emerged seaside perforated quarter circle are obtained by plotting non-dimensional graphs showing variation of reflection coefficient, K_r with wave steepness, H_i/gT^2 for each S/D ratio. For a constant S/D ratio, results obtained for K_r are analyzed for different values of H_i/gT^2 and d/h_s. In all cases, radius of breakwater (R) or breakwater structure height (h_s) is kept constant and water depth is varied (0.45 m, 0.40 m and 0.35 m).

Fig. 4.5 shows the variation of K_r with H_i/gT^2 for different water depths with radius of QBW 0.55 m and S/D ratio equal to 2. It is clear from the graph that K_r increases with increase in H_i/gT^2 for all values of d/h_s. The increase in reflection coefficient with wave steepness may be because when the waves of shorter wave period or

wave length run over the curved surface, they feel the presence of perforations on the QBW for a shorter distance; because of this the energy dissipated due to turbulence is less and hence the reflection is greater for higher wave steepness.
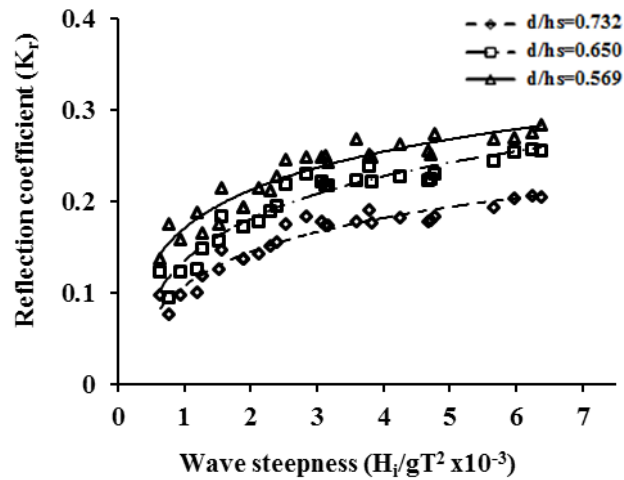
Fig. 4.5 Influence of H_i/gT^2 on K_r for S/D= 2 (R= 0.55 m)

Considering all values d/h_s, K_r varies from 0.0767 to 0.2757 for $6.24 \times 10^{-4} < H_i/gT^2 < 6.4 \times 10^{-3}$ and S/D = 2. The highest value for K_r observed is 0.2757 at a wave height of 0.12 m and a wave period of 1.4 s ($H_i/gT^2 = 6.241 \times 10^{-3}$) and at 0.35 m water depth ($d/h_s = 0.569$). The lowest K_r observed is 0.0767 at a wave height of 0.03 m and a wave period of 2 s ($H_i/gT^2 = 7.645 \times 10^{-4}$) and at water depth equal to 0.45 m ($d/h_s = 0.732$).

4.6.1.2 Seaside perforated QBW with S/D ratio equal to 2.5
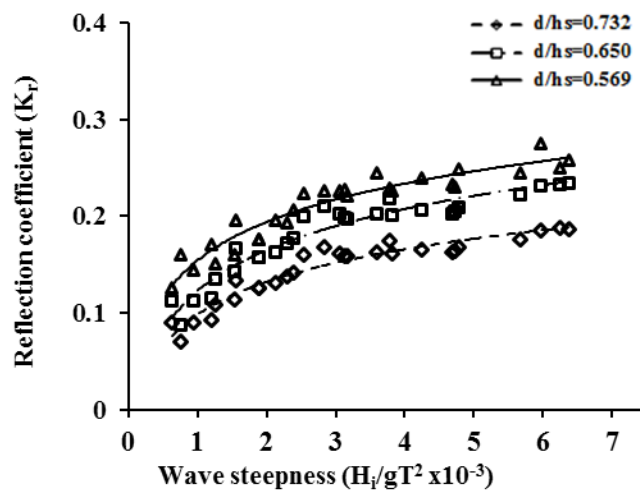
Fig. 4.6 Influence of H_i/gT^2 on K_r for S/D= 2.5 (R= 0.55 m)

Fig. 4.6 shows the variation of K_r with H_i/gT^2 for different water depths for QBW radius 0.55 m and S/D = 2.5. From the experiments conducted on QBW of radius 0.55 m and different values d/h_s , K_r varies from 0.0696 to 0.2745 for $6.24 \times 10^{-4} < H_i/gT^2 < 6.4 \times 10^{-3}$. The maximum K_r observed is 0.2745 at a wave height of 0.15 m and a wave period of 1.6 s ($H_i/gT^2 = 5.972 \times 10^{-3}$) and at water depth equal to 0.35 m ($d/h_s = 0.569$). The minimum K_r observed is 0.0696 at a wave height of 0.03 m and a wave period of 2 s ($H_i/gT^2 = 7.645 \times 10^{-4}$) and at 0.45 m water depth ($d/h_s = 0.732$).

4.6.1.3 Seaside perforated QBW with S/D ratio equal to 3
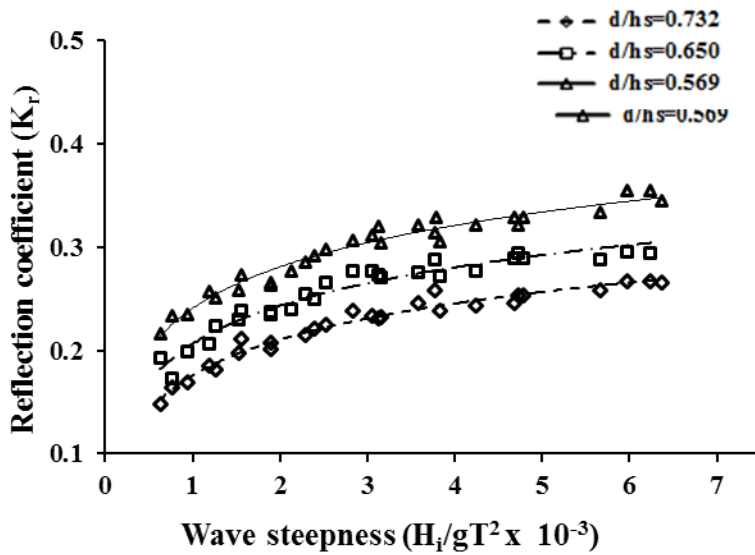
Fig. 4.7 Influence of H_i/gT^2 on K_r for S/D= 3 (R= 0.55 m)

Fig. 4.7 shows the variation of K_r with H_i/gT^2 for different water depths for QBW of radius 0.55 m (h_s= 0.615 m) and S/D ratio equal to 3. The value for K_r shows variation from 0.1480 to 0.3554 for $6.24 \times 10^{-4} < H_i/gT^2 < 6.4 \times 10^{-3}$. The highest value for K_r observed is 0.3554 at a wave height of 0.12 m and a wave period of 1.4 s ($H_i/gT^2 = 6.241 \times 10^{-3}$) and at water depth equal to 0.35 m ($d/h_s = 0.569$). The lowest K_r observed is 0.1480 at a wave height of 0.03 m and a wave period of 2.2 s ($H_i/gT^2 = 6.318 \times 10^{-4}$) and at water depth equal to 0.45 m ($d/h_s = 0.732$).

4.6.1.4 Seaside perforated QBW with S/D ratio equal to 4

Fig. 4.8 shows the variation of K_r with H_i/gT^2 for different d/h_s and S/D = 4. The results show that the reflection coefficient, K_r varies from 0.2090 to 0.3780 for $6.24 \times 10^{-4} < H_i/gT^2 < 6.4 \times 10^{-3}$. The maximum K_r observed is 0.3780 at $H_i/gT^2 =$

6.241 x10^{-3} and d/h$_s$ = 0.569. The minimum K$_r$ observed is 0.2090 at H$_i$/gT^2 = 7.645 x10^{-4} and d/h$_s$ = 0.732.
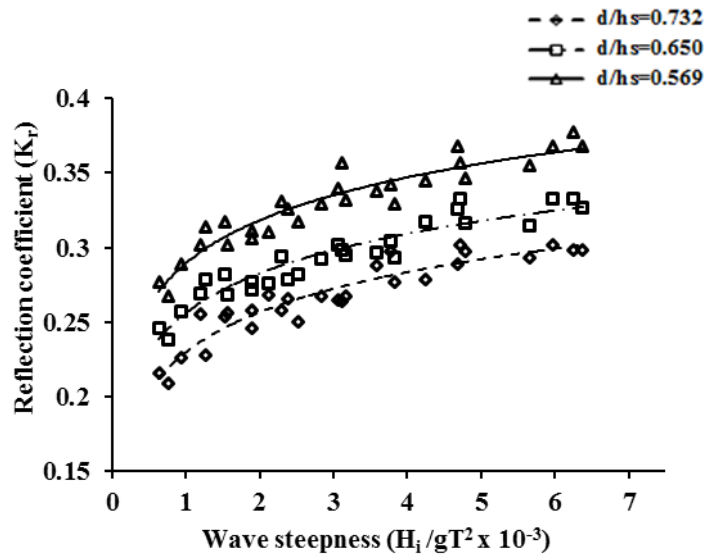
Fig. 4.8 Influence of H$_i$/gT^2 on K$_r$ for S/D= 4 (R= 0.55 m)

4.6.1.5 Seaside perforated QBW with S/D ratio equal to 5

From Fig 4.9, it is observed that for S/D= 5, K$_r$ varies from 0.2660 to 0.4353 for 6.24 x 10^{-4} < H$_i$/gT^2< 6.4x10^{-3}. Considering all the observations on QBW of radius 0.55 m with S/D= 5, the maximum and the minimum values for the reflection coefficient are 0.4353 and 0.2660 respectively obtained for wave steepness of 6.371 x10^{-3} and 9.439 x 10^{-4}.
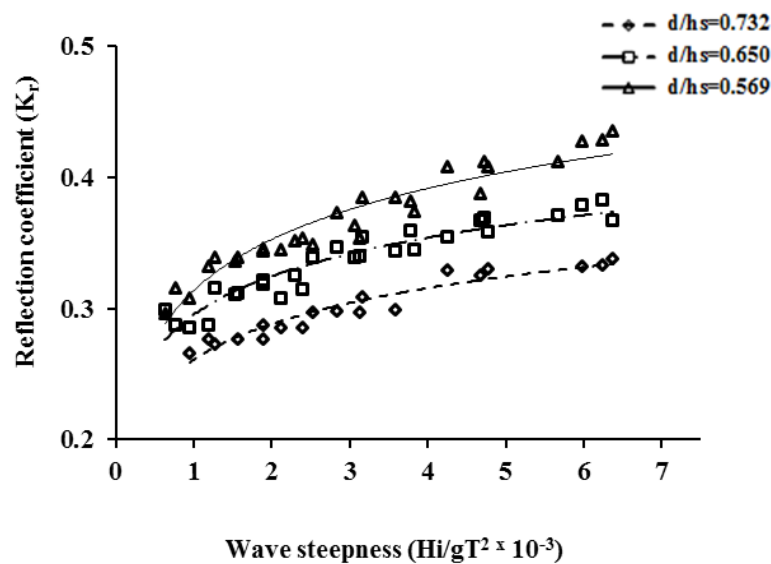
Fig. 4.9 Influence of H$_i$/gT^2 on K$_r$ for S/D=5 (R= 0.55 m)

Table 4.1 Variation Reflection coefficient, K_r (for R = 0.55 m or h_s= 0.615 m)

S/D ratio	Water depth in m	d/ h_s	Range of K_r values
2	0.45	0.732	0.0767 - 0.2063
	0.40	0.650	0.0958 - 0.2579
	0.35	0.569	0.1379 - 0.2757
2.5	0.45	0.732	0.0696 - 0.1876
	0.40	0.650	0.0871 - 0.2345
	0.35	0.569	0.1254 - 0.2745
3	0.45	0.732	0.1480 - 0.2667
	0.40	0.650	0.1734 - 0.2955
	0.35	0.569	0.2167 - 0.3554
4	0.45	0.732	0.209 - 0.3018
	0.40	0.650	0.238 - 0.333
	0.35	0.569	0.2677 - 0.378
5	0.45	0.732	0.2660 - 0.3380
	0.40	0.650	0.2860 - 0.3829
	0.35	0.569	0.2962 - 0.4353

The variation of K_r with H_i/gT^2 for different water depths or d/h_s and S/D ratio for QBW with 0.55 m radius is summarized in Table 4.1.

From the results obtained for the influence of H_i/gT^2 on K_r with different S/D, it is clearly understood that K_r always increases with increase in H_i/gT^2 with maximum K_r values under higher values of H_i/gT^2.

4.6.2 Influence of water depth on reflection characteristics

4.6.2.1 Seaside perforated QBW with S/D ratio equal to 2

When water depth is equal to 0.45 m and breakwater radius 0.55 m (d/h_s = 0.732), the maximum value for K_r is 0.2063 for wave height of 0.12 m and a wave period of 1.4 s (H_i/gT^2 = 6.241 x10^{-3}). At the same water depth, the minimum value of K_r obtained is 0.0767 for H_i/gT^2 = 7.645 x10^{-4}.
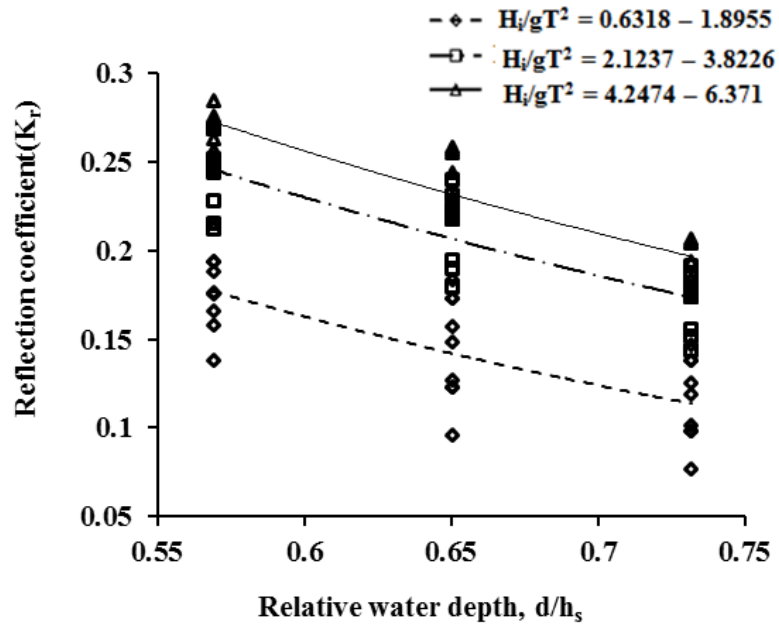
Fig. 4.10 Variation of K_r with d/h$_s$ for S/D= 2 (R= 0.55 m)

For water depth equal to 0.40 m (d/h$_s$ equal to 0.650), the maximum value for K_r observed is 0.2579 at $H_i/gT^2 = 6.371 \times 10^{-3}$. Under the same condition, the minimum value of K_r obtained is 0.0958 for $H_i/gT^2 = 7.645 \times 10^{-4}$. At a water depth equal to 0.35 m (d/h$_s$ equal to 0.569), the maximum and the minimum value for K_r observed are 0.2757 and 0.1379 for $H_i/gT^2 = 6.2410 \times 10^{-3}$ and 6.318×10^{-4} respectively. From all these results, it is clear that as the water depth increases, the value of K_r decreases and the minimum value for K_r are observed at a water depth of 0.45m.

Under higher water depth condition, in which case, the waves are exposed to greater area of perforations leading to greater dissipation of energy and, thereby, resulting in lesser reflection. In addition, the effect of curvature also plays a role in dissipating more energy by permitting waves to run over a longer distance.

As water depth increases from 0.35 m to 0.40m there is a reduction in wave reflection by 6.46% to 30.53%. When water depth increases from 0.35 m to 0.45 m there is a reduction in wave reflection by 25.17% to 44.38%.

4.6.2.2 Seaside perforated QBW with S/D ratio equal to 2.5

For a water depth equal to 0.45 m and breakwater radius equal to 0.55 m (d/h$_s$ equal to 0.732), the maximum value for K_r is 0.1876 at a wave height of 0.12m and a

wave period of 1.4 s ($H_i/gT^2 = 6.241 \times 10^{-3}$). At the same water depth, the minimum value of K_r obtained is 0.0696 for $H_i/gT^2 = 7.645 \times 10^{-4}$.
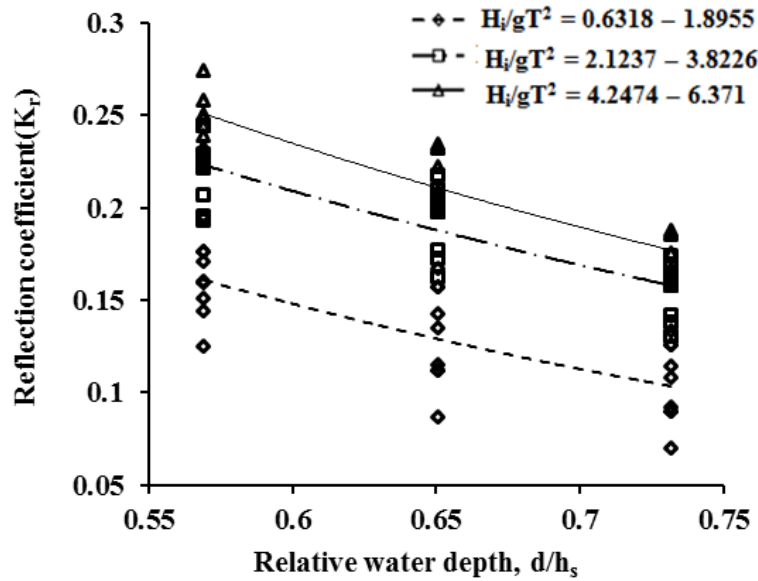
Fig. 4.11 Variation of K_r with d/h_s for S/D= 2.5 (R= 0.55 m)

When water depth is reduced to 0.40 m (d/h_s equal to 0.650), the maximum value for K_r observed is 0.2345 at $H_i/gT^2 = 6.371 \times 10^{-3}$. Under the same condition, the minimum value of K_r obtained is 0.0871 for $H_i/gT^2 = 7.645 \times 10^{-4}$. At 0.35 m water depth (d/h_s equal to 0.569), the maximum and the minimum value for K_r observed are 0.2745 and 0.1254 for $H_i/gT^2 = 5.972 \times 10^{-3}$ and 6.318 $\times 10^{-4}$ respectively. As water depth increases from 0.35 m to 0.40 m there is a reduction in wave reflection by 14.57% to 30.54%. When water depth increases from 0.35 m to 0.45 m there is a reduction in wave reflection by 31.66% to 44.50%.

4.6.2.3 Seaside perforated QBW with S/D ratio equal to 3

At water depth equal to 0.45 m and breakwater radius equal to 0.55 m (d/h_s equal to 0.732), the maximum value for K_r observed is 0.2667 at a wave height of 0.12m and a wave period of 1.4 s ($H_i/gT^2 = 6.241 \times 10^{-3}$). At the same water depth, the minimum value of K_r obtained is 0.148 for $H_i/gT^2 = 6.318 \times 10^{-4}$.

For 0.40 m water depth (d/h_s equal to 0.650), the maximum value for K_r observed is 0.2955 for $H_i/gT^2 = 5.972 \times 10^{-3}$. Under the same condition, the minimum value of K_r obtained is 0.1734 for $H_i/gT^2 = 7.645 \times 10^{-4}$.
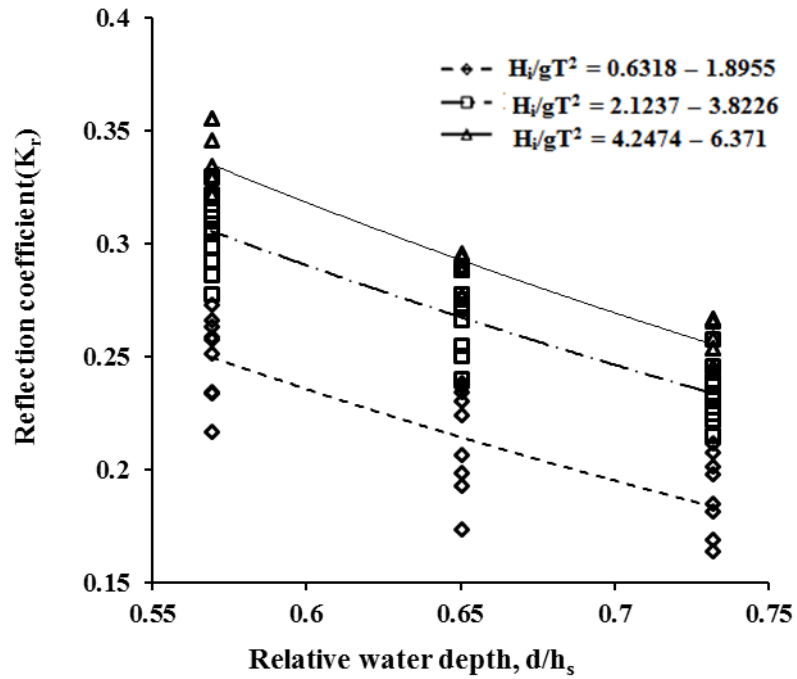
Fig. 4.12 Variation of K$_r$ with d/h$_s$ for S/D= 3 (R= 0.55 m)

At a water depth equal to 0.35 m (d/h$_s$ equal to 0.569), the maximum and the minimum value for K$_r$ observed are 0.3554 and 0.2167 for H$_i$/gT^2 = 5.972 x10^{-3} and 6.318 x10^{-4} respectively. When water depth is increased from 0.35 m to 0.40 m there is a reduction in wave reflection by 16.65% to 19.98% . Further increasing water depth from 0.35 m to 0.45m there is a reduction in wave reflection by 24.96 to 31.70%.

4.6.2.4 Seaside perforated QBW with S/D ratio equal to 4

For d/h$_s$ equal to 0.732, the maximum value for K$_r$ is 0.3018 at a wave height of 0.15m and a wave period of 1.8s (H$_i$/gT^2 = 4.7193 x10^{-3}). At the same condition, the minimum value of K$_r$ obtained is 0.2090 for H$_i$/gT^2 = 7.645 x10^{-4}.

For d/h$_s$ equal to 0.650, the maximum and minimum value for K$_r$ observed is 0.3330 and 0.238 for H$_i$/gT^2 = 6.241 x10^{-3} and 7.645 x10^{-4} respectively. At a water depth equal to 0.35 m (d/h$_s$ equal to 0.569), the maximum and the minimum value for K$_r$ observed are 0.3780 and 0.2667 for H$_i$/gT^2 = 6.241x10^{-3} and 7.645x10^{-4} respectively. When water depth increases from 0.35 m to 0.40 m there is a reduction in wave reflection by 11.09% to 11.90% . When water depth increases from 0.35 m to 0.45m there is a reduction in wave reflection by 20.16% to 21.93% .
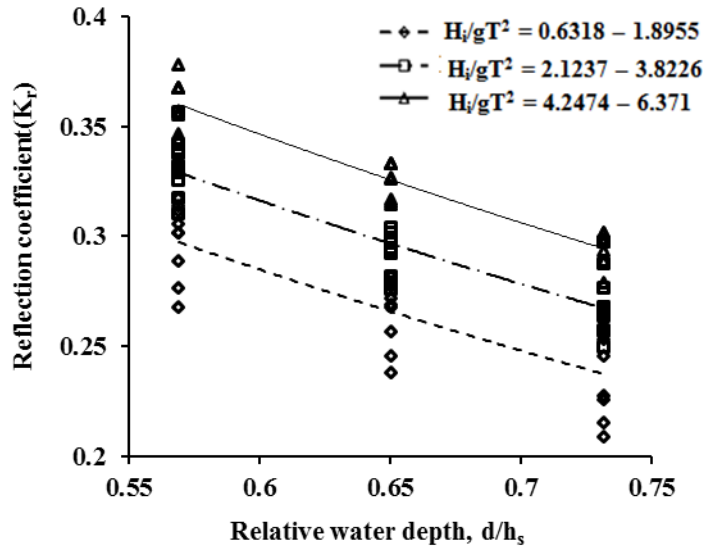
Fig. 4.13 Variation of K_r with d/h_s for S/D= 4 (R= 0.55 m)

4.6.2.5 Seaside perforated QBW with S/D ratio equal to 5

At 0.45 m water depth (d/h_s equal to 0.732), the maximum K_r observed is 0.3338 at a wave height of 0.09 m and a wave period of 1.2s ($H_i/gT^2 = 6.3710 \times 10^{-3}$). At the same water depth, the minimum value of K_r obtained is 0.2660 for $H_i/gT^2 = 9.439 \times 10^{-4}$.
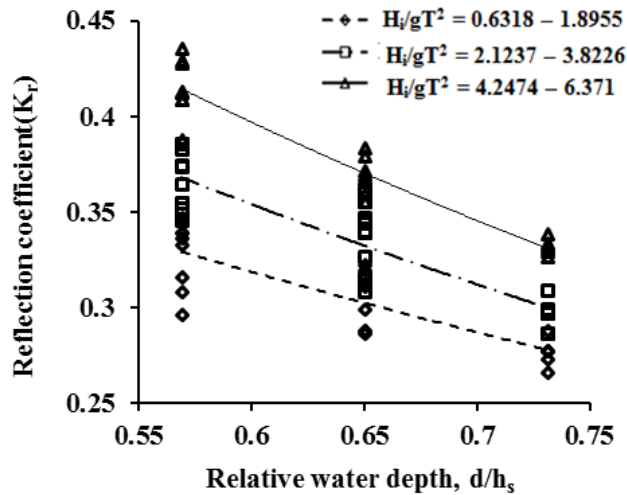
Fig. 4.14 Variation of K_r with d/h_s for S/D= 5 (R= 0.55 m)

For water depth equal to 0.40 m (d/h_s equal to 0.650), the maximum and minimum value for K_r observed are 0.3829 and 0.2860 for $H_i/gT^2 = 6.241 \times 10^{-3}$ and $H_i/gT^2 = 9.439 \times 10^{-4}$. At a water depth equal to 0.35 m (d/h_s equal to 0.569), the maximum and the minimum value for K_r observed are 0.4353 and 0.2962 for $H_i/gT^2 =$

6.371x10^{-3} and 6.318x10^{-4} respectively.

By increasing water depth from 0.35 m to 0.40 m, there is a reduction in wave reflection by 3.44% to 12.04%. When water depth increases from 0.35 m to 0.45 m there is a reduction in wave reflection by 10.20% to 22.35%.

4.6.3 Influence of S/D ratio on reflection characteristics

The studies on the reflection characteristics of seaside perforated QBW model shows that the effect of decrease in reflection coefficient with decreasing the values of S/D ratio is more predominant. At a constant breakwater radius (R) and different water depths, variations of K_r for different values of S/D ratio are analyzed separately. It is observed that K_r decreases with decrease in S/D for all values of d/h_s.

When the waves run over the curved surface with more perforations there may be higher dissipation of wave energy due to turbulence inside the breakwater chamber resulting in lesser refection coefficient. For the lower S/D values the perforations will be more compared to higher values of S/D. Therefore K_r value decreases with decrease in S/D for all values of d/h_s.

Fig. 4.15 shows the variation of K_r for different values of S/D ratio for a seaside perforated QBW of radius 0.55 m at a water depth of 0.45 m (d/h_s equal to 0.732). It is observed that for S/D ratio equal to 5, the value of K_r varies in the range 0.2660 to 0.338 for $6.24x10^{-4} < H_i/gT^2 < 6.4x10^{-3}$.

For the same radius of QBW and at the same water depth ($d/h_s = 0.732$), for S/D ratio equal to 4, K_r is observed to be in the range 0.2090 to 0.3018. The range of variation of K_r is from 0.1480 to 0.2667 for S/D = 3 and 0.0696 to 0.1876 for S/D = 2.5. For an S/D = 2, the range of variation of K_r is from 0.0767 to 0.2063 which has higher values compared to S/D = 2.5.

When the S/D ratio is reduced beyond the value 2.5, the spacing between the perforations will be decreasing and the diameter of the perforations or the number of perforations on the surface is increasing. This will result in back propagation of the waves from inside the chamber to the front side of the QBW which causes increase in the reflection.
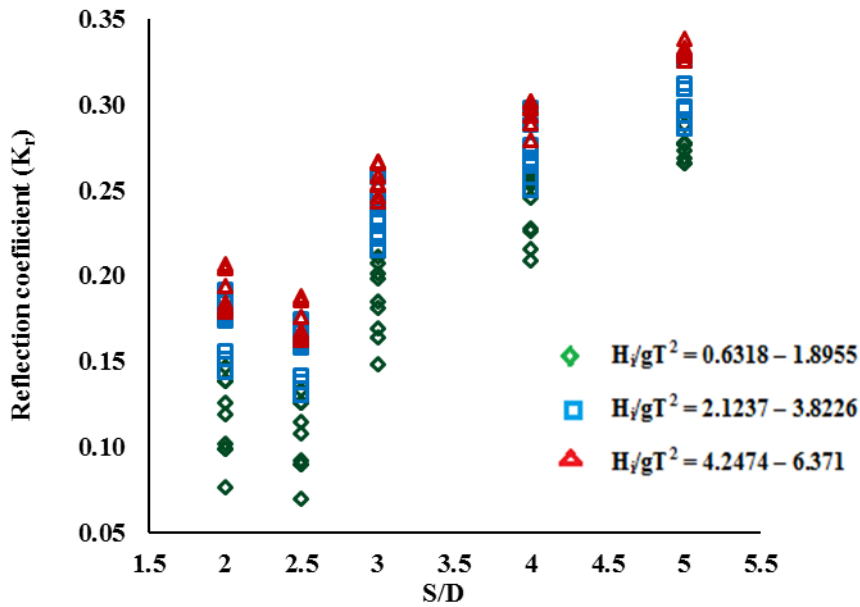
Fig. 4.15 Influence of S/D on K_r for d/h_s = 0.732 (water depth = 0.45 m)

At a water depth of 0.40 m (d/h_s = 0.650), for an S/D = 5, K_r varies in the range 0.2860 to 0.338 for $6.24 \times 10^{-4} < H_i/gT^2 < 6.4 \times 10^{-3}$. For S/D = 4, the range of variation of K_r is found to be 0.2380 to 0.3330. The variation of K_r for S/D = 3 is observed to be in the range 0.1734 to 0.2955; for S/D = 2.5, the value of K_r varies in the range 0.0871 to 0.2345 and for an S/D = 2, the range of variation of K_r is from 0.0958 to 0.2579 (Refer Fig. 4.16).
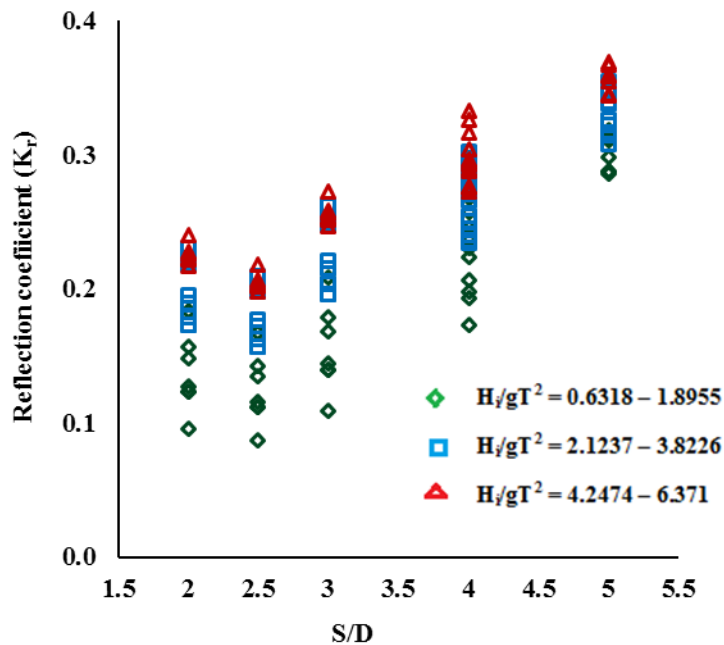
Fig. 4.16 Influence of S/D on K_r for d/h_s = 0.650 (water depth = 0.40 m)
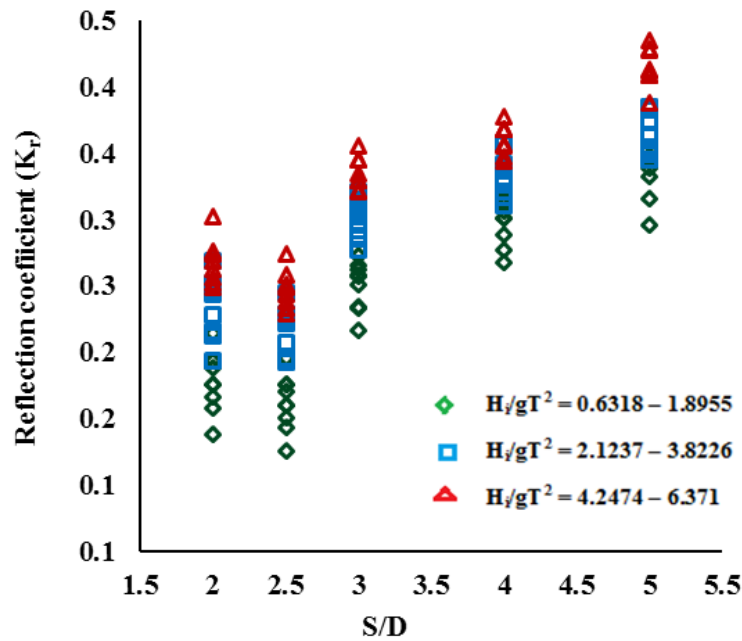
Fig. 4.17 Influence of S/D on K_r for d/h_s = 0.615 (water depth = 0.35 m)

For the same radius of QBW and at the same water depth, for S/D ratio equal to 4, K_r is observed to be in the range 0.2677 to 0.3780. The range of variation of K_r is from 0.2167 to 0.3554 for S/D ratio equal to 3, from 0.1254 to 0.2745 for S/D ratio equal to 2.5 and from 0.1379 to 0.2757 for S/D ratio equal to 2.

From the analysis of results for reflection coefficient for emerged seaside perforated QBW with 0.55 m radius; for different S/D ratios and at different water depths it is observed that the average value of K_r is decreasing with decrease in S/D ratio 5, 4, 3 and 2.5. But for an S/D ratio equal to 2 the values of K_r are more compared to that of S/D ratio equal to 2.5.

The percentage reduction in K_r for different S/D ratios and at different water depths for QBW of radius 0.55m are shown in Table 4.2.

From the analysis of data for average values of K_r, it is observed that at a water depth equal to 0.35 m (d/h_s = 0.569), the percentage reduction in K_r for S/D = 4 varies from 9.62% to 13.16% compared to S/D = 5.

The percentage reduction in K_r for S/D ratio equal to 3, 2.5 and 2 are found to be varying from 18.36% to 26.84% , 37.0% to 57.66% and 36.0% to 53.44% with respect to S/D equal to 5.

Table 4.2 Range of variation and percentage reduction in K_r with S/D for different d/h_s (for R=0.55 m or h_s= 0.615 m)

d/h_s	S/D	Range of variation in K_r	% Reduction in K_r
0.569	5	0.2962 to 0.4353	
	4	0.2677 to 0.3780	9.62% to 13.16%
	3	0.2167 to 0.3554	18.36% to 26.84%
	2.5	0.1254 to 0.2745	36.94% to 57.66%
	2	0.1379 to 0.2757	36.66% to 53.44%
0.650	5	0.2860 to 0.3380	
	4	0.2380 to 0.3330	13.03% to 16.78%
	3	0.1734 to 0.2955	22.83% to 39.37%
	2.5	0.0871 to 0.2345	38.75% to 69.54%
	2	0.0958 to 0.2579	32.64% to 66.50%
0.732	5	0.2660 to 0.3380	
	4	0.2090 to 0.3018	10.71% to 21.42%
	3	0.1480 to 0.2667	21.09% to 44.36%
	2.5	0.0696 to 0.1876	44.49% to 73.83%
	2	0.0767 to 0.2063	38.96% to 71.16%

Similarly at a water depth equal to 0.40 m (d/h_s = 0.650), the percentage reduction in K_r for S/D ratio = 4, 3, 2.5 and 2 varies from 13.03% to 16.78% , 22.83% to 39.37% , 38.75% to 69.54% and 32.64% to 66.50% with respect to S/D = 5. At 0.45 m water depth (d/h_s = 0.732), percentage reduction in K_r for S/D = 4 varies from 10.71% to 21.42% compared to S/D = 5. The percentage reduction in K_r for S/D = 3, 2.5 and 2 varies from 21.09% to 44.36%, 44.49% to 73.83% and 38.96% to 71.16% with respect to S/D = 5.

4.7 VARIATION OF REFLECTION COEFFICIENT (K_r) FOR QBW 0.575 m RADIUS (h_s= 0.640 m)

4.7.1   Influence of incident wave steepness on reflection characteristics

4.7.1.1 Seaside perforated QBW with S/D ratio equal to 2

For S/D = 2, considering all values d/h_s and for breakwater radius of 0.575 m, the reflection coefficient, K_r varies from 0.0783 to 0.3030 for $6.24 \times 10^{-4} < H_i/gT^2 < 6.4 \times 10^{-3}$ and S/D = 2 (Refer Fig. 4.18).
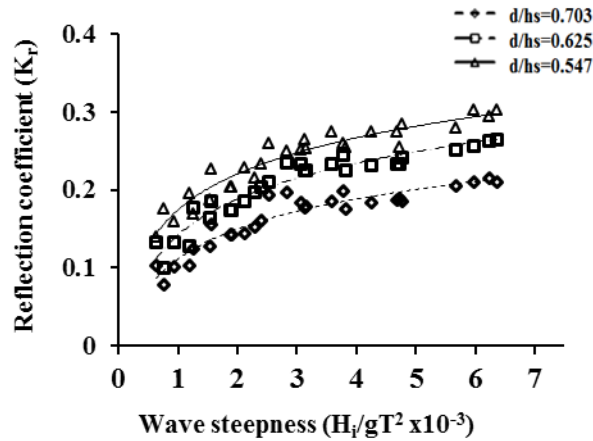
Fig. 4.18 Influence of H_i/gT^2 on K_r for S/D = 2 (R= 0.575 m)

The highest K_r value observed is 0.3030 for $H_i/gT^2 = 5.972 \times 10^{-3}$ and at 0.35 m water depth ($d/h_s = 0.547$). The lowest K_r observed is 0.0783 for $H_i/gT^2 = 7.645 \times 10^{-4}$ and at water depth equal to 0.45m ($d/h_s = 0.703$).

Similar to QBW of radius 0.55 m, it is observed that K_r increases with increase in H_i/gT^2 for all values of d/h_s. This may be because when the waves of shorter wave period run over the curved surface, they feel the presence of perforations on the QBW for a shorter distance. Hence the energy dissipated due to turbulence is less and the reflection is greater for higher wave steepness.

4.7.1.2 Seaside perforated QBW with S/D ratio equal to 2.5

For S/D = 2.5, considering all values d/h_s and for QBW of radius 0.575 m, K_r varies from 0.0712 to 0.2755 for $6.24 \times 10^{-4} < H_i/gT^2 < 6.4 \times 10^{-3}$ and S/D = 2 (Refer Fig. 4.19).
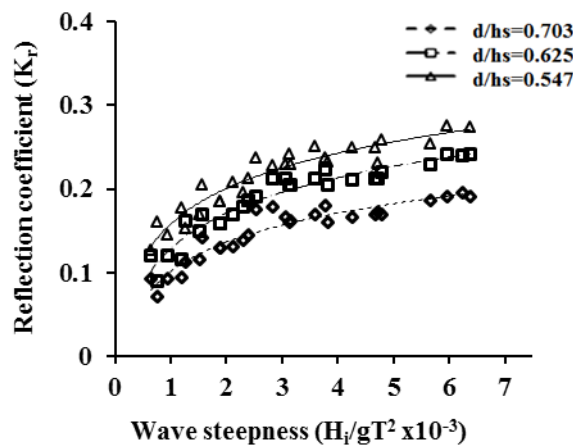
Fig. 4.19 Influence of H_i/gT^2 on K_r for S/D = 2.5 (R= 0.575 m)

The maximum observed K_r is 0.2755 at H_i/gT^2 = 5.972 $\times 10^{-3}$ and d/h_s equal to 0.547. The minimum K_r observed is 0.0712 for a wave height of 0.03 m and a wave period of 2 s (H_i/gT^2 = 7.645 $\times 10^{-4}$) and at water depth equal to 0.45 m (d/h_s equal to 0.703).

4.7.1.3 Seaside perforated QBW with S/D ratio equal to 3
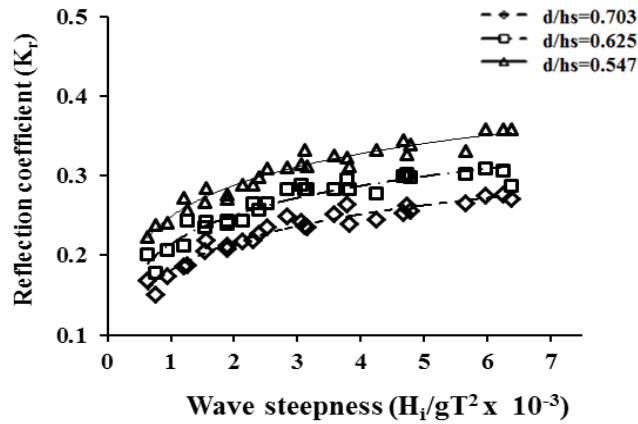
Fig. 4.20 Influence of H_i/gT^2 on K_r for S/D = 3 (R= 0.575 m)

From Fig. 4.20, it is clear that for all values d/h_s and for breakwater radius of 0.575 m, K_r varies from 0.1502 to 0.3587 for $6.24 \times 10^{-4} < H_i/gT^2 < 6.4 \times 10^{-3}$ and S/D = 3. The highest value for K_r observed is 0.3587 at a wave height of 0.15 m and a wave period of 1.6 s (H_i/gT^2 = 5.972 $\times 10^{-3}$) and at water depth equal to 0.35 m (d/h_s = 0.547). The lowest K_r observed is 0.1502 for a wave height of 0.03 m and a wave period of 2 s (H_i/gT^2 = 7.645 $\times 10^{-4}$) and at water depth equal to 0.45 m (d/h_s = 0.703).

4.7.1.4 Seaside perforated QBW with S/D ratio equal to 4
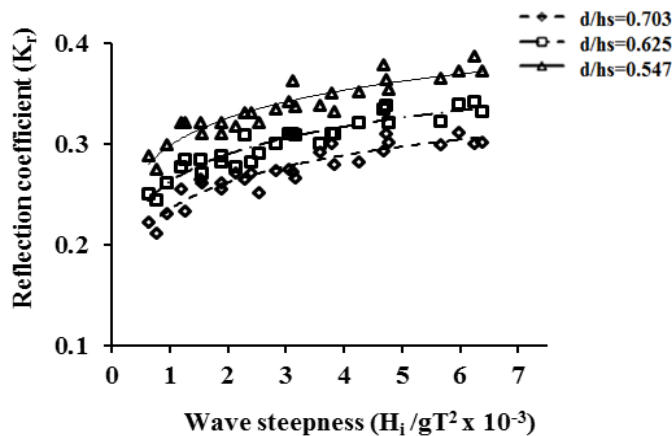
Fig. 4.21 Influence of H_i/gT^2 on K_r for S/D=4 (R= 0.575 m)

From the experiments it is observed that the value of K_r varies from 0.2113 to 0.3880 for $6.24 \times 10^{-4} < H_i/gT^2 < 6.4 \times 10^{-3}$ for S/D ratio equal to 4 (Refer Fig. 4.21). The maximum K_r observed is 0.3880 at a wave height of 0.12 m and a wave period of 1.4s ($H_i/gT^2 = 6.241 \times 10^{-3}$) and at water depth equal to 0.35 m (d/h_s equal to 0.547). The lowest K_r observed is 0.2113 for a wave height of 0.03 m and a wave period of 2 s ($H_i/gT^2 = 7.645 \times 10^{-4}$) and at water depth equal to 0.45 m (d/h_s equal to 0.703).

4.7.1.5 Seaside perforated QBW with S/D ratio equal to 5

For S/D ratio equal to 5, K_r for QBW of radius equal to 0.575 m, varies from 0.2770 to 0.4440 for $6.24 \times 10^{-4} < H_i/gT^2 < 6.4 \times 10^{-3}$. The maximum K_r observed is 0.4440 at a wave height of 0.12 m and a wave period of 1.4 s ($H_i/gT^2 = 6.241 \times 10^{-3}$) and at 0.35 m water depth (d/h_s equal to 0.547). The minimum K_r observed is 0.2770 for a wave height of 0.03 m and a wave period of 2 s ($H_i/gT^2 = 7.645 \times 10^{-4}$) and at water depth equal to 0.45 m (d/h_s equal to 0.703).
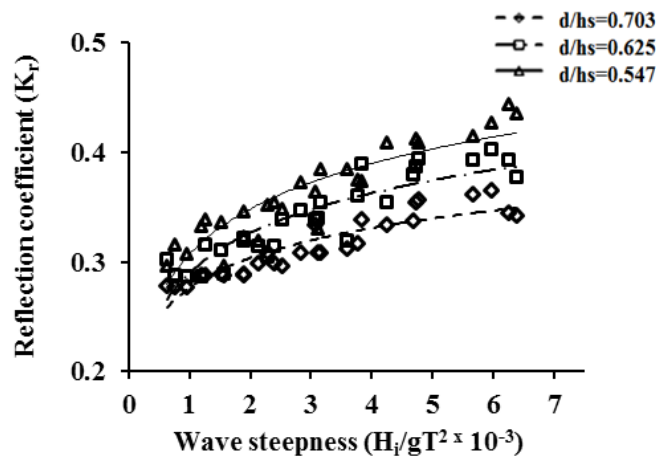
Fig. 4.22 Influence of H_i/gT^2 on K_r for S/D = 5 (R= 0.575 m)

The variation of reflection coefficient with wave steepness for different water depths and S/D ratio for QBW with 0.575 m radius are summarized in Table 4.3.

From the graphs plotted on reflection coefficient for different values of H_i/gT^2 and d/h_s, it is observed that in all cases K_r increases with increase in H_i/gT^2. The values for K_r for QBW of radius equal to 0.575 m is found to be more compared to that of QBW of radius equal to 0.55 m. This may be because when the breakwater radius is

more, the effect of curvature is less predominant and the waves encounter lesser perforations resulting in lesser dissipation and more reflection.

Table 4.3 Variation Reflection coefficient, K_r (for R = 0.575 m or h_s= 0.640 m)

S/D ratio	Water depth in cm	d/ h_s	Range of K_r values
2	0.45	0.703	0.0783 - 0.2147
	0.40	0.625	0.0994 - 0.2648
	0.35	0.547	0.1397 - 0.3030
2.5	0.45	0.703	0.0712 - 0.1952
	0.40	0.625	0.0904 - 0.2408
	0.35	0.547	0.1270 - 0.2755
3	0.45	0.703	0.1502 - 0.2747
	0.40	0.625	0.1785 - 0.3088
	0.35	0.547	0.2234 - 0.3587
4	0.45	0.703	0.2113 - 0.3115
	0.40	0.625	0.2440 - 0.3430
	0.35	0.547	0.2750 - 0.3880
5	0.45	0.703	0.2770 - 0.3660
	0.40	0.625	0.2869 - 0.4030
	0.35	0.547	0.2968 - 0.4440

4.7.2 Influence of water depth on reflection characteristics

For each S/D ratio, the efffect of water depth on the reflection characteristics for QBW of radius equal to 0.575 m is analysed seperately. The graphs are plotted showing the variation of K_r with d/h_s for different values of H_i/gT^2 and for different S/D values. Similar to QBW of radius equal to 0.55 m the reflection coefficient, K_r decreases with increase in water depth for all values of S/D.

Fig 4.23 shows the variation of K_r with d/h_s for different values of H_i/gT^2 and for S/D equal to 2. In the case of QBW of radius 0.575 m and S/D ratio equal to 2, the minimum value for K_r observed is 0.0783 at a water depth of 0.45 m. At the same condition for water depth equal to 0.40 m, the minimum observed value for K_r is

0.0994 and for a water depth equal to 0.35 m, the minimum observed value for K_r is 0.1397.
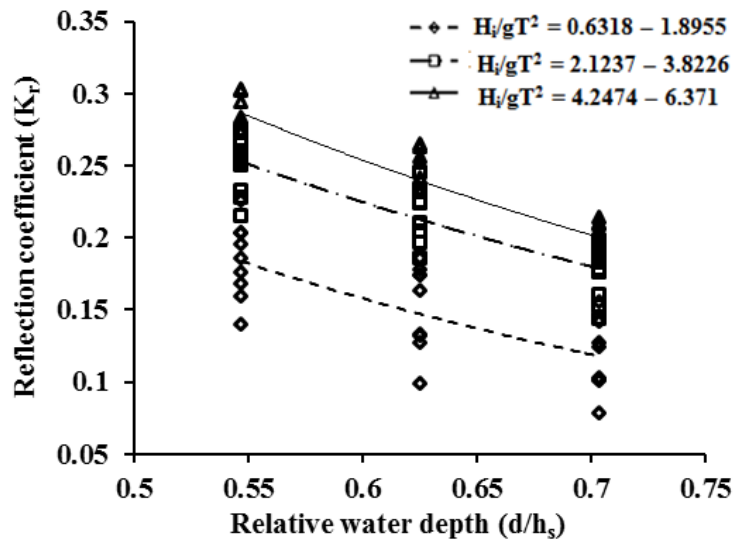
Fig. 4.23 Variation of K_r with d/h_s for S/D = 2 (R= 0.575 m)

For S/D = 2.5, the minimum K_r observed is 0.0712 at 0.45 m water depth. For water depth equal to 0.40 m, the minimum observed value for K_r is 0.0904 and for water depth equal to 0.35 m, the minimum observed value for K_r is 0.1270.
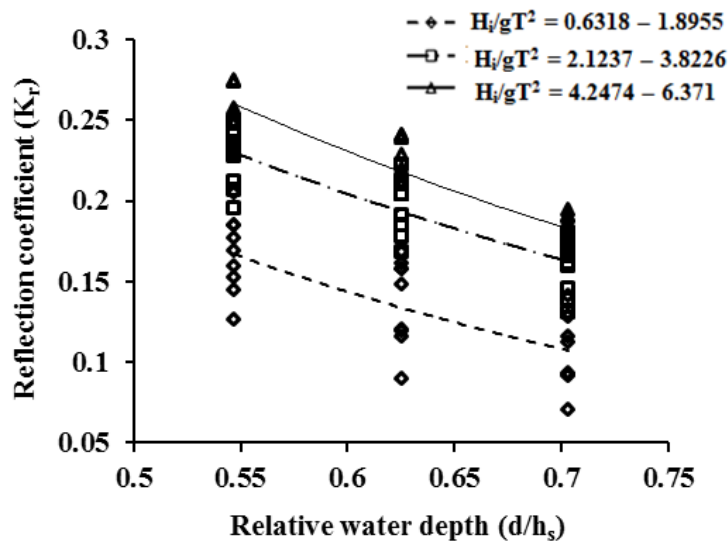
Fig. 4.24 Variation of K_r with d/h_s for S/D = 2.5 (R= 0.575 m)

When S/D is increased to 3 and under similar condition, the minimum observed value for K_r was 0.1502 at a water depth of 0.45 m. For water depth equal to 0.40 m, the minimum observed value for K_r is 0.1785 and for water depth equal to 0.35 m, the minimum observed value for K_r is 0.2234.
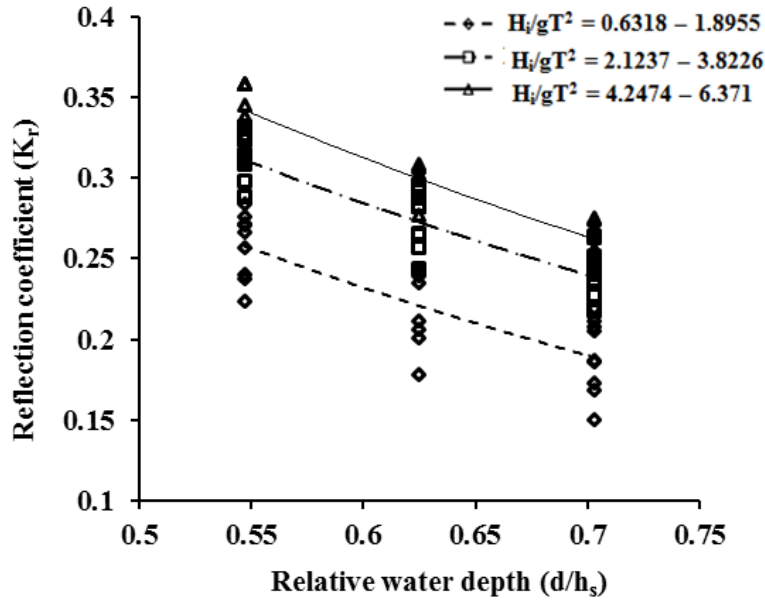
Fig. 4.25 Variation of K_r with d/h_s for S/D = 3 (R= 0.575 m)

For QBW of radius 0.575 m for S/D ratio equal to 4, the minimum observed value for K_r is 0.2113 at a water depth of 0.45 m. At the same condition for water depth equal to 0.40 m, the minimum observed value for K_r is 0.2440 and for a water depth equal to 0.35 m, the minimum observed value for K_r is 0.2750.
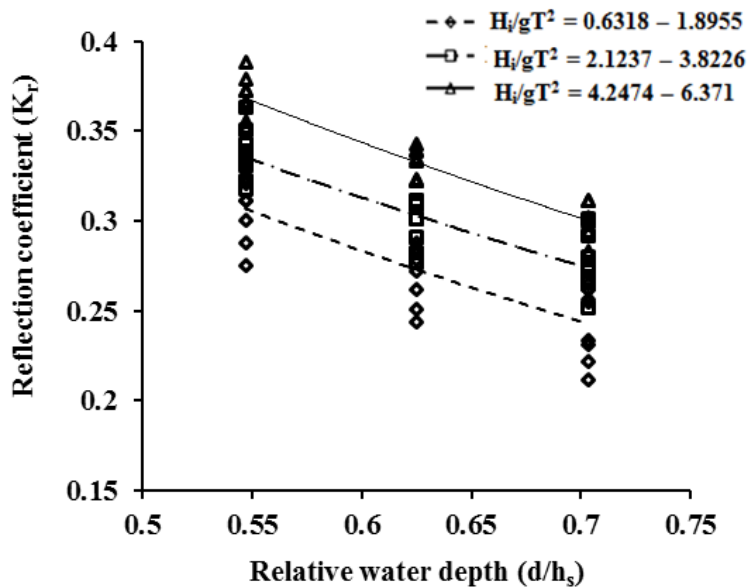
Fig. 4.26 Variation of K_r with d/h_s for S/D = 4 (R= 0.575 m)

For S/D ratio equal to 5 and under similar condition, the minimum observed value for K_r is 0.2770 at a water depth of 0.45 m. For water depth equal to 0.40 m, the minimum observed value for K_r is 0.2869 and for water depth equal to 0.35m, the minimum observed value for K_r is 0.2968.
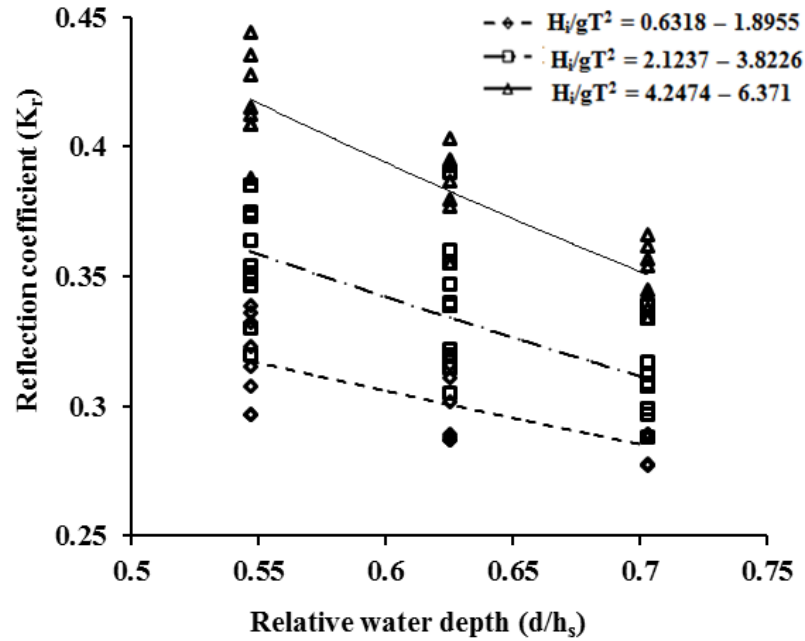
Fig. 4.27 Variation of K_r with d/h_s for S/D = 5 (R= 0.575 m)

For S/D =2, when water depth increases from 0.35 m to 0.40 m there is a reduction in K_r by 12.61% to 28.85% . When water depth increases from 0.35 m to 0.45m there is a reduction in K_r by 29.15% to 30.98% .

Similarly for S/D equal to 2.5, 3, 4 and 5 when water depth increases from 0.35 m to 0.40 m there is a reduction in K_r by 13.23% to 30.56%, 13.91% to 20.10%, 10.94% to 11.60% and 3.34% to 9.23% respectively. When water depth increases from 0.35 m to 0.45m there is a reduction in K_r by 30.19% to 43.94%, 23.42% to 32.77%, 21.98% to 23.16% and 6.67% to 17.57% respectively.

4.7.3   Influence of S/D ratio on reflection characteristics

The graphs are plotted showing the variation of K_r with H_i/gT^2 for different S/D ratios and under different water depths for a QBW of radius equal to 0.575 m. It is observed that the value K_r decreases with decrease in S/D ratios 5, 4, 3 and 2.5 but increases for S/D= 2 for all values of d/h_s and different ranges of H_i/gT^2 considered for the study. This may be due to the reason that when the S/D decreases the perforations encountered by the waves will be more resulting in more dissipation of wave energy and lesser reflection. But increasing S/D beyond 2.5 causes the back propogation of the waves from inside the chamber resulting in more reflection compared to S/D = 2.5.
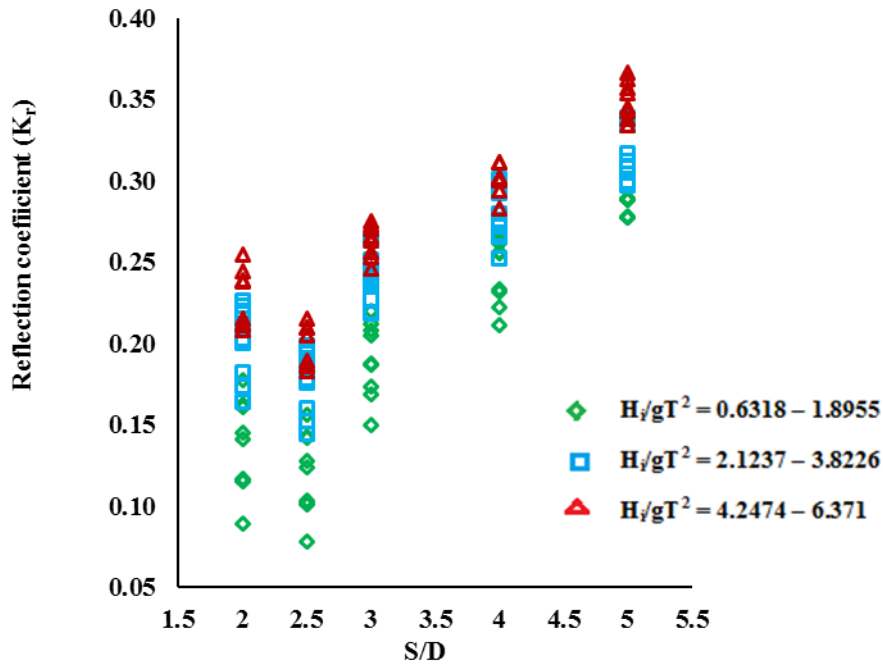
Fig. 4.28 Variation of K_r with S/D for $d/h_s = 0.703$

For a seaside perforated QBW of radius 0.575 m at a water depth of 0.45 m (d/h_s equal to 0.703) and S/D = 2, the range of variation of K_r is from 0.0783 to 0.2147 for $6.24 \times 10^{-4} < H_i/gT^2 < 6.4 \times 10^{-3}$. For the same radius of QBW and at the same water depth, for S/D ratio = 2.5, K_r varies from 0.0712 to 0.1952 and S/D = 3, the range of variation of K_r is found to be 0.1502 to 0.2747. The variation of K_r for S/D = 4 is observed to be in the range 0.2113 to 0.3115 and for S/D = 5, the value of K_r varies in the range 0.2770 to 0.3660.
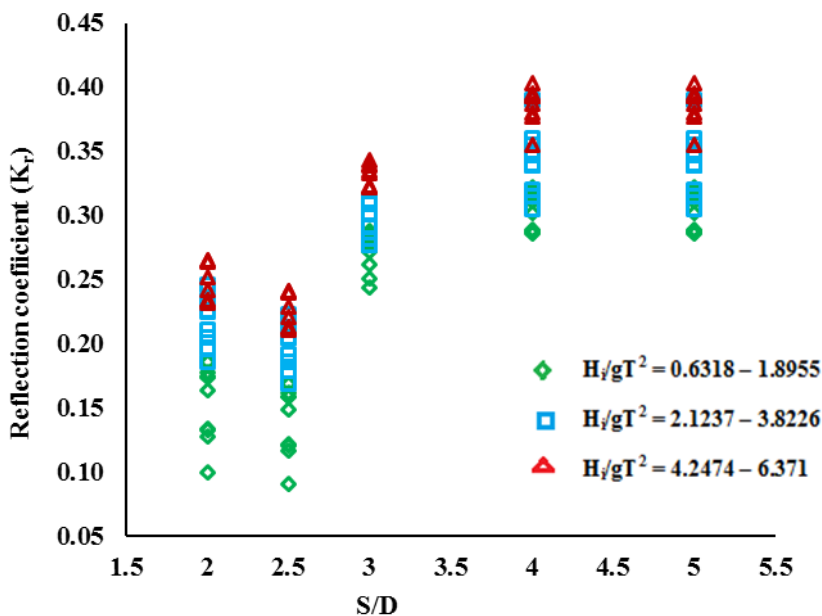
Fig. 4.29 Variation of K_r with S/D for $d/h_s = 0.625$

113

For QBW of radius 0.575 m at a water depth of 0.40 m (d/h_s equal to 0.625) and S/D equal to 2, the range of variation of K_r is from 0.0994 to 0.2648.

For the same radius of QBW and at the same water depth, S/D = 2.5, the range of variation of K_r is found to be 0.0904 to 0.2408 and for S/D = 3, K_r varies from 0.1785 to 0.3088. The variation of K_r for S/D = 4 is observed to be in the range 0.2440 to 0.3430 and for S/D ratio equal to 5, the value of K_r varies in the range 0.2869 to 0.4030.
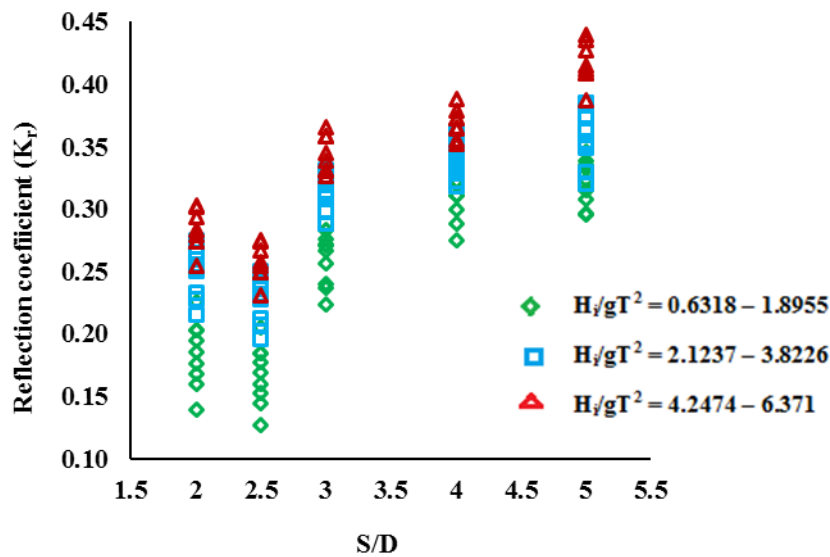
Fig. 4.30 Variation of K_r with S/D for d/h_s = 0.547

For a seaside perforated QBW of radius 0.575 m at a water depth of 0.35 m (d/h_s equal to 0.547) and S/D = 2, the range of variation of K_r is from 0.1397 to 0.3030 for $6.24 \times 10^{-4} < H_i/gT^2 < 6.4 \times 10^{-3}$.

For the same radius of QBW and at the same water depth, S/D = 2.5, the range of variation of K_r is found to be 0.1270 to 0.2755 and for S/D ratio = 3, K_r varies from 0.2234 to 0.3587. The variation of K_r for S/D = 4 is observed to be in the range 0.2750 to 0.3880 and for an S/D = 5, the value of K_r varies in the range 0.2968 to 0.4440. The percentage reduction in K_r for different S/D ratios with respect to a S/D ratio equal to 5 and at different water depths are shown in Table 4.4.

From the analysis of data for average values of K_r, it is observed that at a water depth equal to 0.35 m ,the percentage reduction in K_r for S/D = 4 is 7.53%

compared to S/D = 5. The percentage reduction in K_r for S/D = 3, 2.5 and 2 are 16.73% , 41.06 and 34.61 % with respect to S/D = 5.

Table 4.4 Range of variation and percentage reduction in K_r for various S/D
(for R=0.575 m and h_s= 0.640)

d/h_s	S/D	Range of Variation in K_r	% Reduction in K_r
	5	0.2968 to 0.4440	
	4	0.2750 to 0.3880	7.34% to 12.61%
0.547	3	0.2234 to 0.3587	19.21% to 24.73%
	2.5	0.1270 to 0.2755	37.95% to 57.21%
	2	0.1397 to 0.3030	21.90% to 49.20%
	5	0.2869 to 0.4030	
	4	0.2440 to 0.3430	14.95% to 39.45%
0.625	3	0.1785 to 0.3088	23.37% to 37.78%
	2.5	0.0904 to 0.2408	40.25% to 68.49%
	2	0.0994 to 0.2648	34.29% to 59.26%
	5	0.2770 to 0.3660	
	4	0.2113 to 0.3115	14.89% to 23.72%
0.703	3	0.1502 to 0.2747	24.95% to 45.77%
	2.5	0.0712 to 0.1952	46.67% to 74.29%
	2	0.0783 to 0.2147	41.33% to 71.73%

Similarly at a water depth equal to 0.40 m, the percentage reduction in K_r for S/D = 4, 3, 2.5 and 2 are 11.67% , 22.22% , 44.96% and 39.55 % with respect to S/D = 5. At a water depth equal to 0.45 m ,the percentage reduction in K_r for S/D ratio equal to 4 is 13.25% compared to S/D ratio equal to 5. The percentage reduction in K_r for S/D ratio equal to 3, 2.5 and 2 are 26.85% , 52.39% and 47.64 % with respect to S/D equal to 5. The percentage reduction in K_r was observed to be maximum when S/D= 2.5 due to more dissipation of wave energy caused by turbulence inside the QBW chamber.With respect to S/D=2.5, the percentage reduction is less for S/D= 2 due to back propogation of waves from inside the chamber.

4.8 VARIATION OF REFLECTION COEFFICIENT (K_r) FOR QBW 0.60 m RADIUS (h_s= 0.665 m)

4.8.1 Influence of incident wave steepness on reflection characteristics

4.8.1.1 Seaside perforated QBW with S/D ratio equal to 2

For S/D ratio equal to 2, considering all values d/h_s and for QBW radius of 0.60 m,

the reflection coefficient, K_r varies from 0.0987 to 0.3045 for $6.24 \times 10^{-4} < H_i/gT^2 < 6.4 \times 10^{-3}$ and S/D ratio equal to 2.
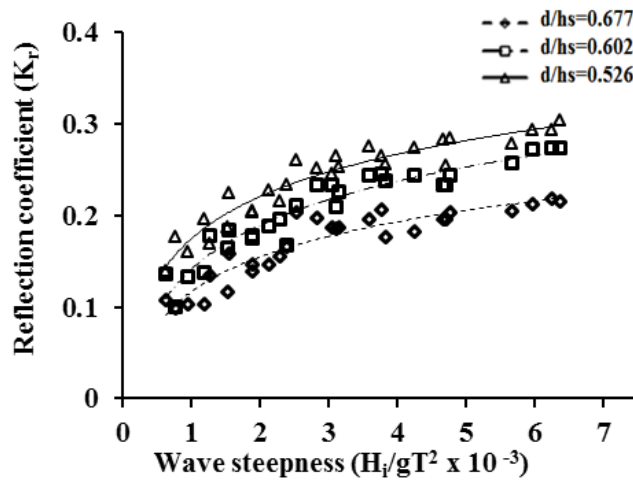
Fig. 4.31 Influence of H_i/gT^2 on K_r for S/D = 2 (R= 0.60 m)

The maximum value for K_r observed is 0.3045 at a wave height of 0.09 m and a wave period of 1.2 s ($H_i/gT^2 = 6.3710 \times 10^{-3}$) and at water depth equal to 0.35 m ($d/h_s = 0.526$). The minimum K_r observed is 0.0987 for a wave height of 0.03 m and a wave period of 2.2 s ($H_i/gT^2 = 6.318 \times 10^{-4}$) and at water depth equal to 0.45 m ($d/h_s = 0.677$).

4.8.1.2 Seaside perforated QBW with S/D ratio equal to 2.5
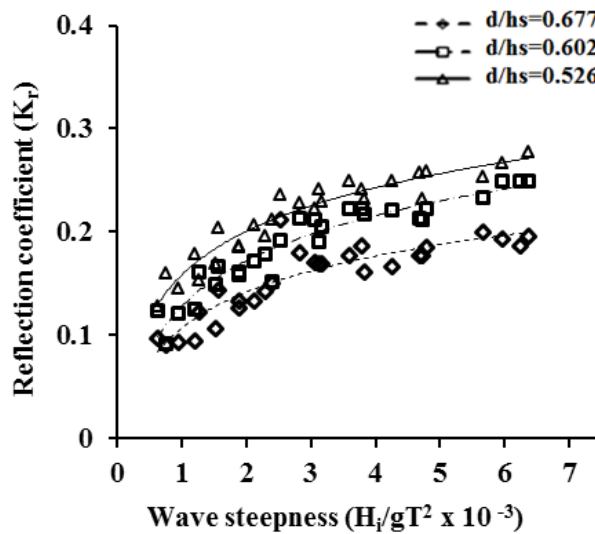
Fig. 4.32 Influence of H_i/gT^2 on K_r for S/D = 2.5 (R= 0.60 m)

For experiments conducted on seaside perforated QBW of 0.60 m radius and S/D ratio equal to 2.5, K_r varies from 0.0904 to 0.2767 for $6.24 \times 10^{-4} < H_i/gT^2 < 6.4 \times 10^{-3}$.

The maximum and the minimum values for K_r observed are 0.2767 and 0.0904 at $H_i/gT^2 = 6.3710 \times 10^{-3}$ and $H_i/gT^2 = 7.645 \times 10^{-4}$ respectively.

4.8.1.3 Seaside perforated QBW with S/D ratio equal to 3

From the results, it is observed that for all values d/h_s and for breakwater radius of 0.60 m, K_r varies from 0.1562 to 0.3596 for $6.24 \times 10^{-4} < H_i/gT^2 < 6.4 \times 10^{-3}$ when S/D ratio is increased to 3.
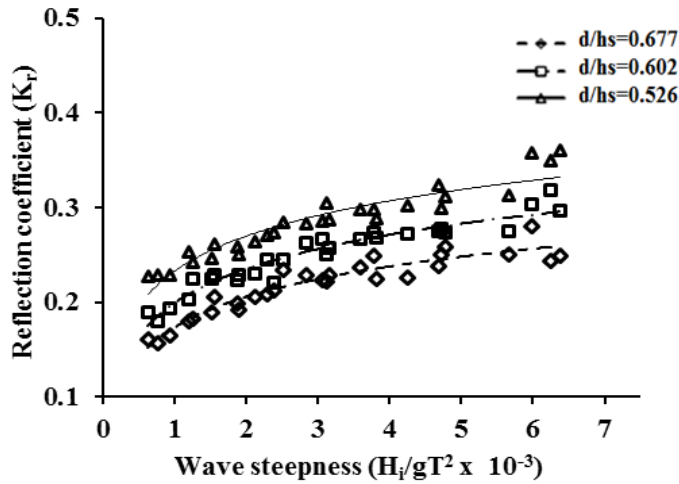
Fig. 4.33 Influence of H_i/gT^2 on K_r for S/D = 3 (R= 0.60 m)

The maximum K_r observed is 0.3596 at a wave height of 0.09 m and a wave period of 1.2 s ($H_i/gT^2 = 6.3710 \times 10^{-3}$) and at 0.35 m water depth ($d/h_s = 0.526$). The minimum K_r observed is 0.1562 for a wave height of 0.03 m and a wave period of 2 s ($H_i/gT^2 = 7.645 \times 10^{-4}$) and at 0.45 m water depth. ($d/h_s = 0.677$).

4.8.1.4 Seaside perforated QBW with S/D ratio equal to 4
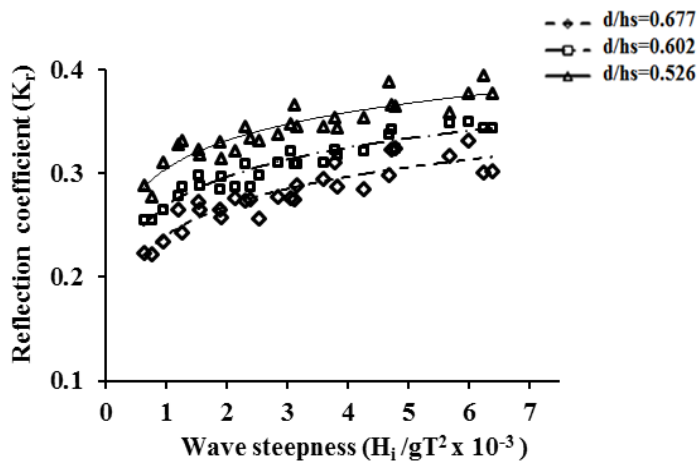
Fig. 4.34 Influence of H_i/gT^2 on K_r for S/D= 4 (R= 0.60 m)

For S/D ratio equal to 4, considering all values d/h_s and for breakwater radius of 0.60 m, K_r varies from 0.2220 to 0.3950 for $6.24 \times 10^{-4} < H_i/gT^2 < 6.4 \times 10^{-3}$ and S/D equal to 4. The maximum value for K_r observed is 0.3950 at a wave height of 0.12 m and a wave period of 1.4 s ($H_i/gT^2 = 6.241 \times 10^{-3}$) and at water depth equal to 0.35 m (d/h_s equal to 0.526). The minimum K_r observed is 0.2220 for a wave height of 0.03 m and a wave period of 2 s ($H_i/gT^2 = 7.645 \times 10^{-4}$) and at water depth equal to 0.45 m.

4.8.1.5 Seaside perforated QBW with S/D ratio equal to 5

From the results of the experiments conducted on QBW of radius 0.575 m and S/D ratio equal to 5, considering all values d/h_s, K_r varies from 0.2820 to 0.4495 for $6.24 \times 10^{-4} < H_i/gT^2 < 6.4 \times 10^{-3}$ and S/D = 5. The maximum and minimum value for K_r observed is 0.4495 and 0.2820 for $H_i/gT^2 = 7.645 \times 10^{-4}$ and $H_i/gT^2 = 6.3710 \times 10^{-3}$ respectively.
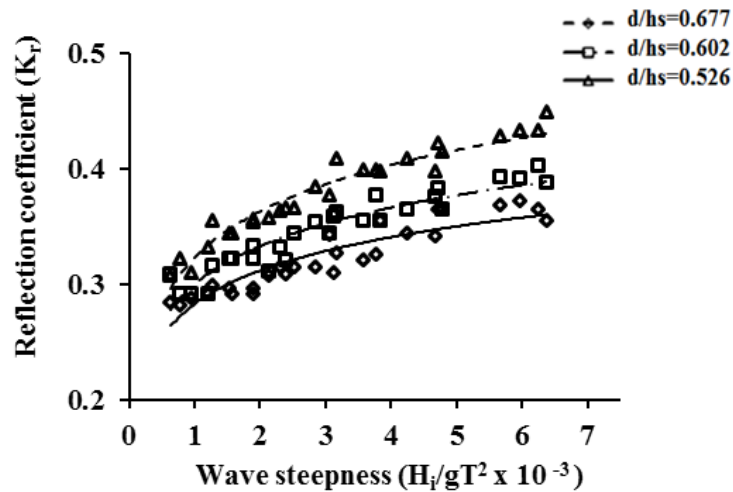
Fig. 4.35 Influence of H_i/gT^2 on K_r for S/D = 5 (R= 0.60 m)

From all the graphs plotted for the variation of K_r with H_i/gT^2, it is observed that the reflection coefficient K_r increases with increase in H_i/gT^2 for all values of d/h_s (i.e., for all water depth keeping a constant radius of 0.60 m and height of the structure, h_s equal to 0.665 m). Therefore it is clearly understood that the wave steepness has greater influence on the reflection characteristics of sea side perforated quarter circle breakwater with varying perforation. Also steeper waves will have less impact on dissipation of the wave energy compared to waves of lesser steepness. The curved

surface of the QBW is found to be having more influence on the wave reflection characteristics.

Table 4.5 Variation Reflection coefficient, K_r (for R = 0.60 m or h_s= 0.665 m)

S/D ratio	Water depth in m	d/h_s	Range of K_r values
2	0.45	0.677	0.0987 - 0.2193
	0.40	0.602	0.1006 - 0.2737
	0.35	0.526	0.1399 - 0.3045
2.5	0.45	0.677	0.0904 - 0.2120
	0.40	0.602	0.0915 - 0.2576
	0.35	0.526	0.1272 - 0.2767
3	0.45	0.677	0.1562 - 0.2796
	0.40	0.602	0.1796 - 0.3188
	0.35	0.526	0.2276 - 0.3596
4	0.45	0.677	0.2220 - 0.3730
	0.40	0.602	0.2550 - 0.3510
	0.35	0.526	0.2780 - 0.3950
5	0.45	0.677	0.2820 - 0.3820
	0.40	0.602	0.2920 - 0.4035
	0.35	0.526	0.3080 - 0.4495

4.8.2 Influence of water depth on reflection characteristics
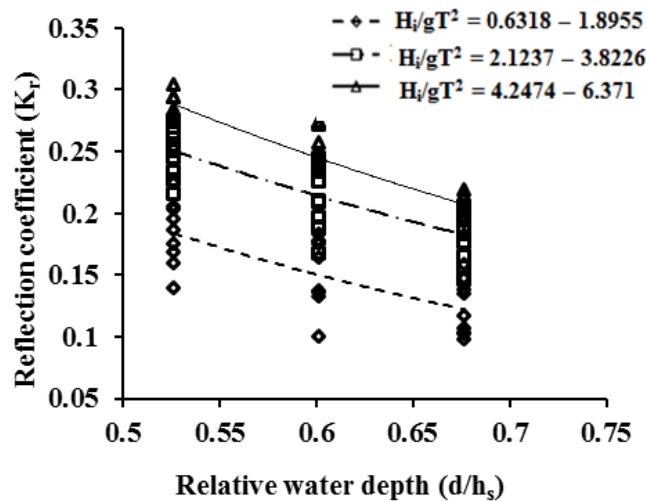
Fig. 4.36 Influence of d/h_s on K_r for S/D = 2 (R= 0.60 m)

119
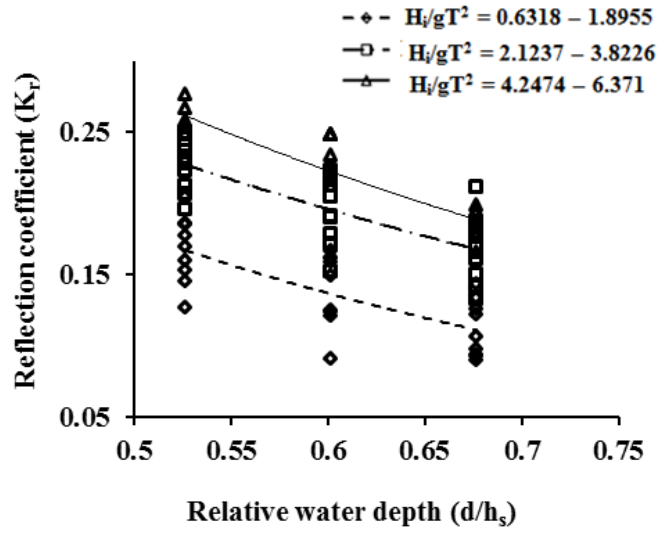
Fig. 4.37 Influence of d/h_s on K_r for S/D = 2.5 (R= 0.60 m)
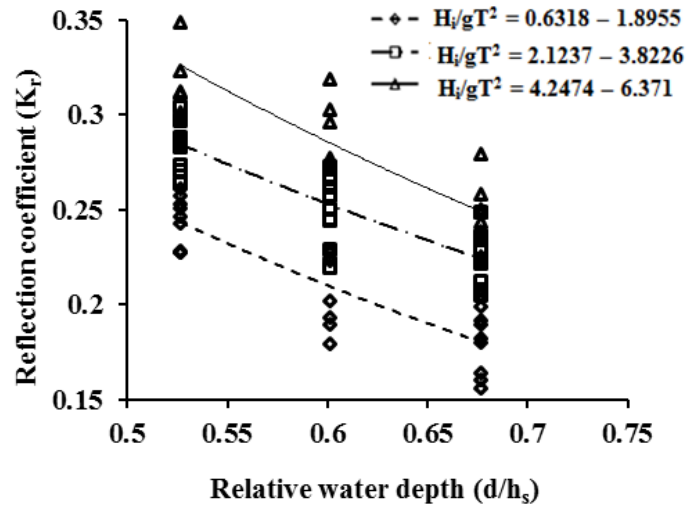
Fig. 4.38 Influence of d/h_s on K_r for S/D = 3 (R= 0.60 m)
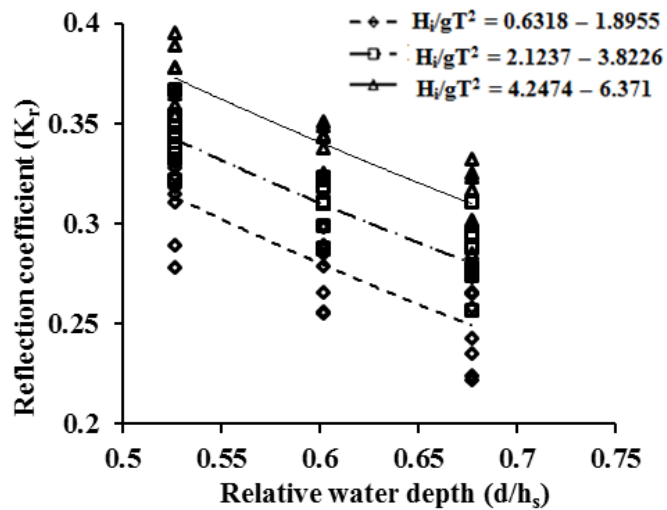
Fig. 4.39 Influence of d/h_s on K_r for S/D = 4 (R= 0.60 m)
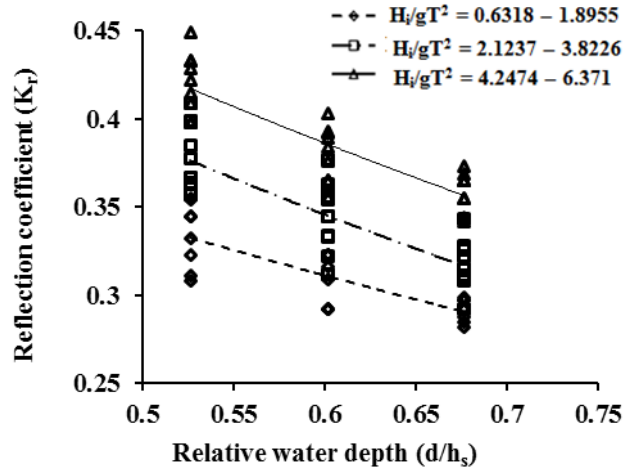
Fig. 4.40 Influence of d/h$_s$ on K$_r$ for S/D = 5 (R= 0.60 m)

For QBW of radius 0.60 m and for various values of S/D ratio, the minimum value for K$_r$ is observed at a water depth of 0.45 m and maximum corresponding to a water depth of 0.35 m. At a water depth of 0.45 m, the minimum values for K$_r$ obtained for S/D values of 2, 2.5, 3, 4 and 5 are 0.09876, 0.0904, 0.1562, 0.2220 and 0.2820 respectively. The maximum K$_r$ values observed at a water depth equal to 0.35 m and for S/D values of 2, 2.5, 3, 4 and 5 are 0.3045, 0.2767, 0.3596, 0.3950 and 0.4495 respectively.

With respect to water depth of 0.35 m the percentage reduction in K$_r$ for S/D values of 2, 2.5, 3, 4 and 5 is found to be varying from 10.11% to 28.09%, 12.08% to 31.06%, 11.12% to 21.19%, 8.27% to 11.14% and 5.19% to 10.23% respectively for a water depth of 0.40 m. But the percentage reduction in K$_r$ with respect to a water depth of 0.35 m for S/D values of 2, 2.5, 3, 4 and 5 is found to be varying from 27.98% to 29.41%, 23.38% to 39.76%, 22.05% to 28.07%, 15.95% to 20.14% and 8.44% to 17.02% respectively for a water depth of 0.40 m.

4.8.3 Influence of S/D ratio on reflection characteristics

Figure 4.41 shows the variation of K$_r$ with H$_i$/gT^2 for different S/D ratios and under different water depths for a QBW of radius equal to 0.60 m. Similar to other radius of QBW, K$_r$ decreases with decrease in S/D ratio for all values of d/h$_s$ and different ranges of H$_i$/gT^2 considered for the study. For d/h$_s$ equal to 0.677, the maximum K$_r$ obtained for S/D= 2, 2.5, 3, 4 and 5 are 0.2193, 0.2120, 0.2796, 0.3730 and 0.3820. Therefore it is clear that the reflection coefficient has higher values for S/D =5

compared to other lower values of S/D. This may be due to lesser dissipation of wave energy for higher values of S/D.
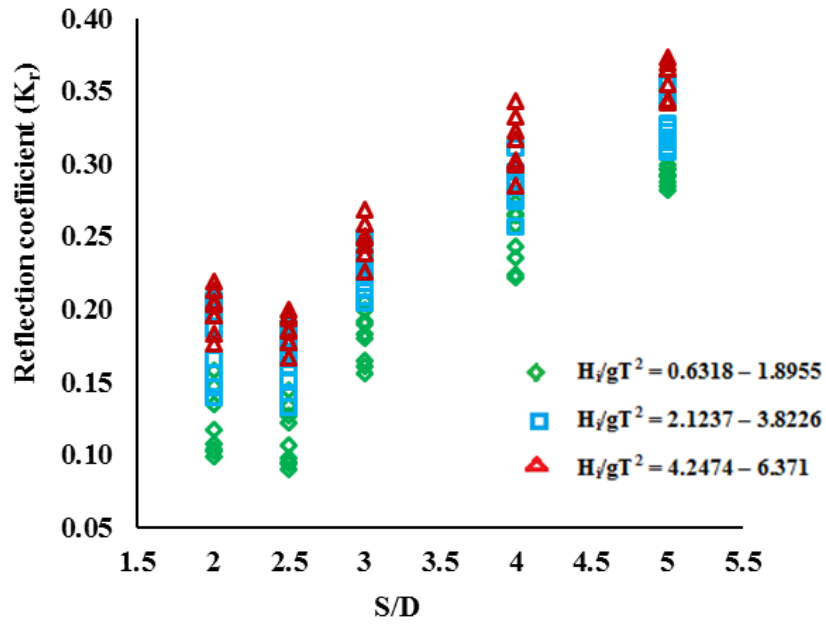
Fig. 4.41 Influence of S/D on K_r for $d/h_s = 0.677$
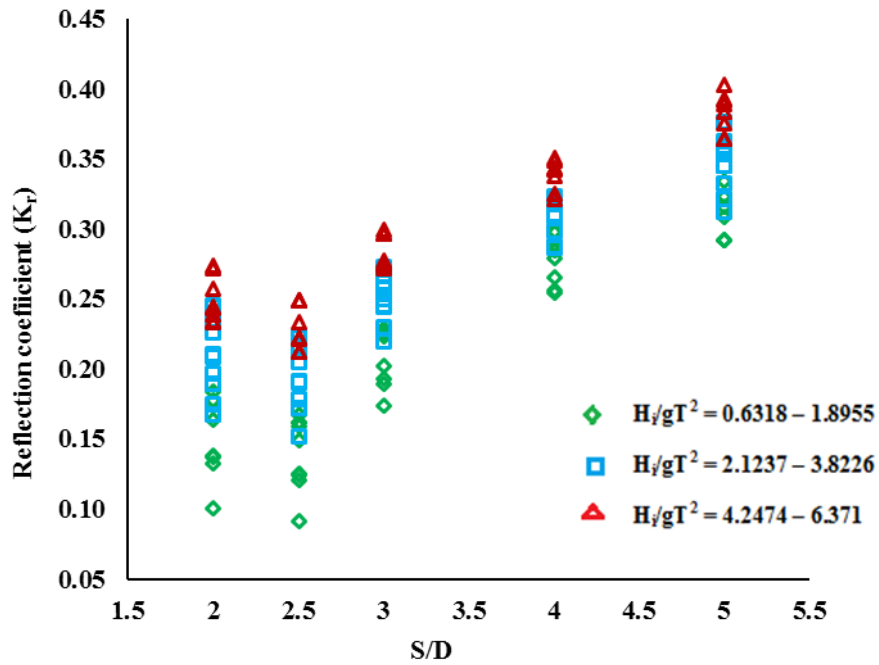
Fig. 4.42 Influence of S/D on K_r for $d/h_s = 0.602$

When d/h_s is equal to 0.602, the maximum K_r obtained for S/D= 2, 2.5, 3, 4 and 5 are 0.2737, 0.2576, 0.3188, 0.3510 and 0.4035.
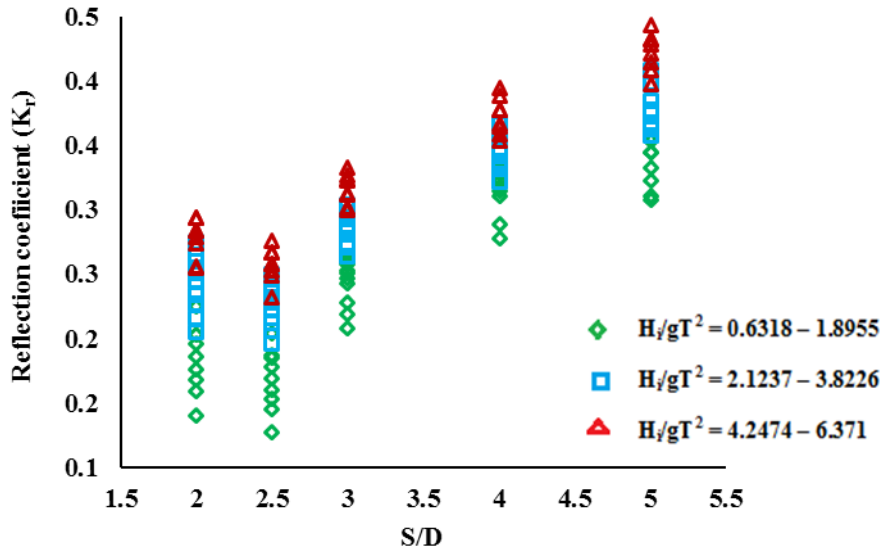
Fig. 4.43 Influence of S/D on K_r for d/h_s = 0.526

For d/h_s is equal to 0.526, the maximum K_r obtained for S/D= 2, 2.5, 3, 4 and 5 are 0.3045, 0.2767, 0.3188, 0.3596 and 0.4495.

Table 4.6 Range of variation and percentage reduction in K_r for various S/D

(for R=0.60 m and h_s= 0.665)

d/h_s	S/D	Range of Variation in K_r	% Reduction in K_r
0.526	5	0.3080 to 0.4495	
	4	0.2780 to 0.3950	9.74% to 12.12%
	3	0.2276 to 0.3596	20.0% to 26.10%
	2.5	0.1272 to 0.2767	38.44% to 58.70%
	2	0.1399 to 0.3045	32.25% to 54.58%
0.602	5	0.2920 to 0.4035	
	4	0.2550 to 0.3510	12.67% to 13.01%
	3	0.1796 to 0.3188	21.1% to 38.49%
	2.5	0.0915 to 0.2576	36.16% to 68.66%
	2	0.1006 to 0.2737	32.17% to 65.54%
0.677	5	0.2820 to 0.3820	
	4	0.2220 to 0.3730	21.98% to 23.56%
	3	0.1562 to 0.2796	26.80% to 44.61%
	2.5	0.0904 to 0.2120	44.50% to 67.94%
	2	0.0987 to 0.2193	42.59% to 65.10%

Therefore it is clear that in all cases the maximum values of K_r is obtained for S/D= 5 compared to other lower S/D values. The percentage reduction in K_r for S/D ratios

= 4, 3, 2.5 and 2 with respect to S/D= 5 and at different water depths and for QBW of radius 0.60 m are shown in Table 4.6.

From the analysis of data for K_r, it is observed that at a water depth equal to 0.35 m, the percentage reduction in K_r for S/D = 4 varies from 9.74% to 12.12% compared to S/D = 5. The percentage reduction in K_r for S/D ratio equal to 3, 2.5 and 2 varies from 20.0% to 26.10%, 38.44% to 58.70% and 32.25% to 54.58% with respect to S/D = 5.

The maximum percentage reduction corresponds to a water depth equal to 0.45 m. For S/D = 4, percentage reduction in K_r varies from 21.98% to 23.56% compared to S/D ratio = 5. The percentage reduction in K_r for S/D = 3, 2.5 and 2 varies from 26.80% to 44.61%, 44.50% to 67.94% and 42.59% to 65.10% with respect to S/D equal to 5.

4.9 VARIATION OF LOSS COEFFICIENT (K_l) FOR QBW 0.55 m RADIUS

When incident wave of height (H_i) strikes the curved surface of quarter circle breakwater, it will lose some part of its energy due to the perforations provided on the curved surface and the remaining wave energy tends the wave reflect back as reflected wave height (H_r). The amount of energy dissipated is usually measured in terms of amount of energy reflected and transmitted. In emerged breakwater, since there is no transmission, the amount of energy dissipated merely depends on the reflection characteristics. The dissipated energy is usually measured in terms of loss coefficient (K_l) and it depends on reflection coefficient which is given the equation.

$$K_l = \sqrt{\left(1 - K_r^{\,2}\right)}$$

4.9.1 Influence of incident wave steepness on loss characteristics

For a constant ratio of spacing to diameter of the perforations, loss coefficient, K_l is calculated from reflection coefficient for different values of H_i/gT^2 and d/h_s. Fig. 4.44 shows the variation of K_l with H_i/gT^2 for various S/D ratios.

Considering all values d/h_s for QBW of radius 0.55 m, K_l varies from 0.9612 to 0.9970 for $6.24 \times 10^{-4} < H_i/gT^2 < 6.4 \times 10^{-3}$ and S/D= 2. The maximum value of K_l observed is 0.9970 at a wave height of 0.03 m and a wave period of 2 s ($H_i/gT^2 = 7.645 \times 10^{-4}$) and at water depth equal to 0.45 m ($d/h_s = 0.732$).

For S/D=2.5, value of K_l varies from 0.9620 to 0.9980 for $6.24 \times 10^{-4} < H_i/gT^2 < 6.4 \times 10^{-3}$. The maximum value of K_l observed is 0.9980 at a wave height of 0.03 m and a wave period of 2 s ($H_i/gT^2 = 7.645 \times 10^{-4}$) and at water depth equal to 0.45 m ($d/h_s = 0.732$). It is observed that K_l varies from 0.9347 to 0.9889 for $6.24 \times 10^{-4} < H_i/gT^2 < 6.4 \times 10^{-3}$ when S/D ratio was increased to 3. The maximum value of K_l observed is 0.9889 for a wave height of 0.03 m and a wave period of 2.2 s ($H_i/gT^2 = 6.318 \times 10^{-4}$) and at water depth equal to 0.45 m (d/h_s equal to 0.732).

(a) For S/D =2

(b) For S/D =2.5

(c) For S/D =3

(d) For S/D =4

(e) For S/D =5

Fig. 4.44 Influence of H_i/gT^2 on K_l for various S/D and d/h_s (R= 0.55 m)

125

When S/D = 4, K_l varies from 0.9258 to 0.9779 for $6.24 \times 10^{-4} < H_i/gT^2 < 6.4 \times 10^{-3}$. The maximum value of K_l observed is 0.9779 for a wave height of 0.03 m and a wave period of 2 s ($H_i/gT^2 = 7.645 \times 10^{-4}$) and at water depth equal to 0.45 m ($d/h_s = 0.732$). For S/D ratio equal to 5, K_l varies from 0.9003 to 0.9640 for $6.24 \times 10^{-4} < H_i/gT^2 < 6.4 \times 10^{-3}$. The maximum value of K_l observed is 0.9640 for a wave height of 0.03 m and a wave period of 1.8 s ($H_i/gT^2 = 9.439 \times 10^{-4}$) and at water depth equal to 0.45 m ($d/h_s = 0.732$).

From the trend lines for the graphs plotted between K_l and H_i/gT^2 for the different S/D values, it is observed that K_l decreases with increase in H_i/gT^2 for all values of d/h_s. This may be because when the waves of higher steepness or shorter wave period run over the curved surface, they feel the perforations on QBW only for a shorter distance; because of this the energy dissipated due to turbulence is less. The percentage decrease in K_l with H_i/gT^2 considering all values of d/h_s and for S/D = 5, 4, 3, 2.5 and 2 varies from 10.48% to 35.71%, 11.76% to 37.40%, 12.75% to 38.08%, 13.62% to 41.20% and 13.45% to 39.70% respectively for QBW of radius 0.55 m.

4.9.2 Influence of water depth on loss characteristics

For all S/D ratio and wave steepness, loss coefficient K_l increases with increase in ratio of depth of water to height of the structure or relative water depth (d/h_s). At higher water depths, the waves are exposed to greater area of perforations leading to greater dissipation of energy and, thereby, resulting in higher loss coefficient.
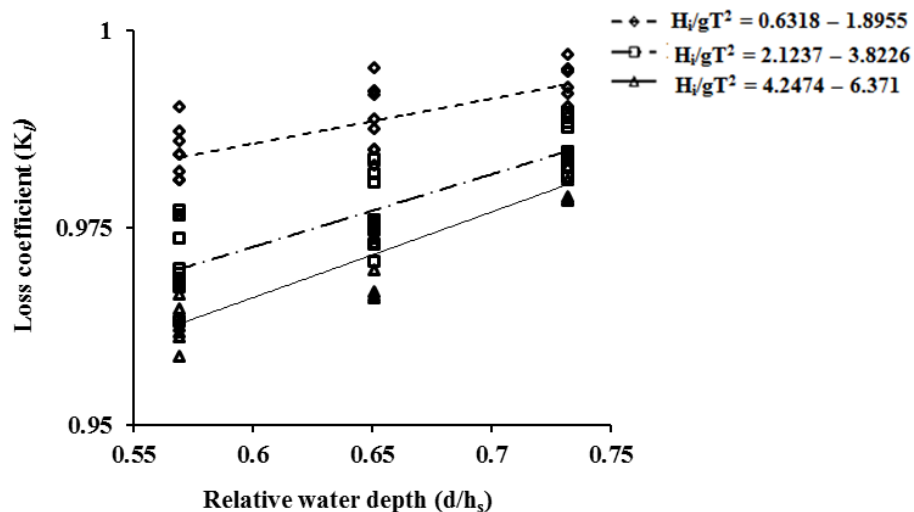
Fig. 4.45 Influence of d/h_s on K_l for S/D = 2 (R= 0.55 m)
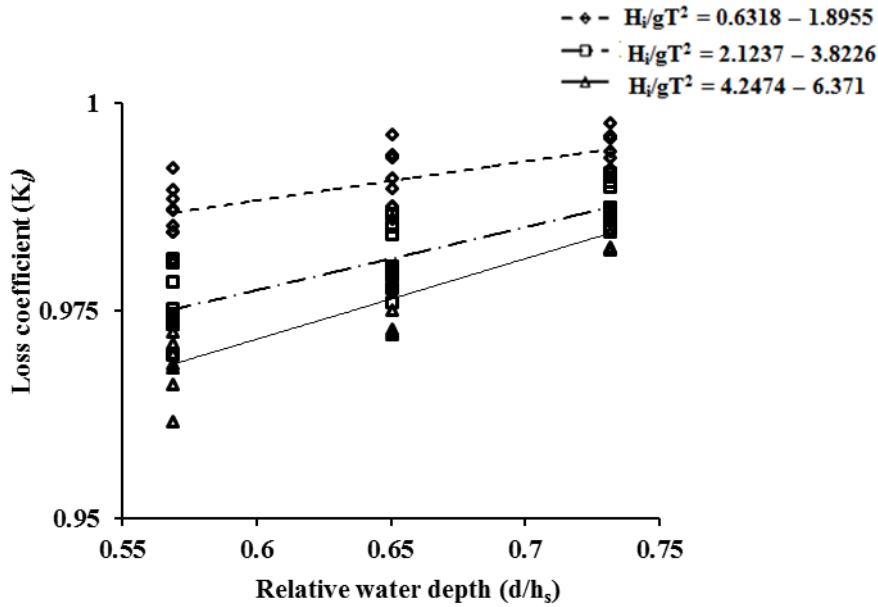
Fig. 4.46 Influence of d/h$_s$ on K$_l$ for S/D = 2.5 (R= 0.55 m)

In the case of QBW of radius 0.55 m and S/D ratio equal to 2, the maximum value for K$_l$ observed is 0.9970 at a water depth of 0.45 m. At the same condition for 0.40 m water, K$_l$ obtained is 0.9954 and for a water depth equal to 0.35 m, the maximum observed value for K$_l$ is 0.9904.

For S/D = 2.5, the maximum K$_l$ observed is 0.9980 at a water depth of 0.45 m. At the same condition for water depth equal to 0.40 m, maximum K$_l$ obtained is 0.9960 and for a water depth equal to 0.35 m, the maximum observed value for K$_l$ is 0.0.992.
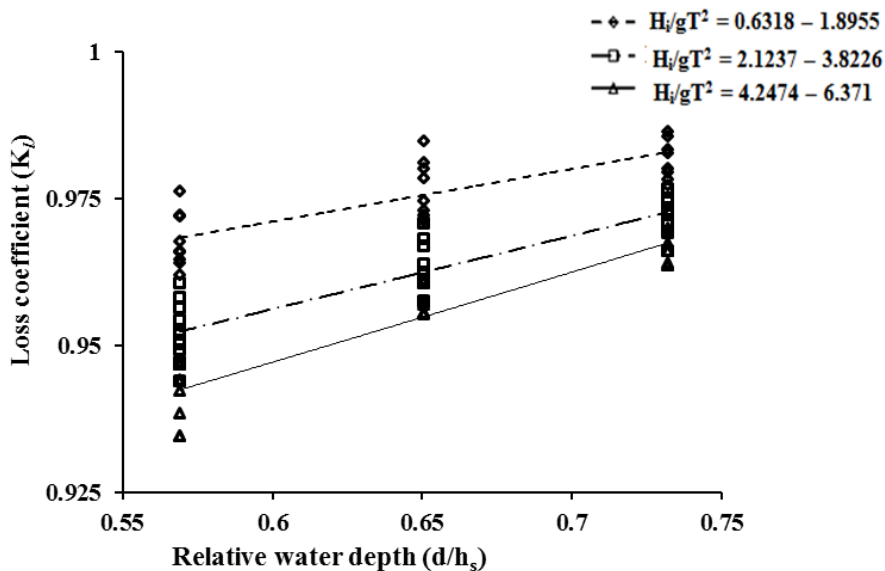
Fig. 4.47 Influence of d/h$_s$ on K$_l$ for S/D = 3 (R= 0.55 m)
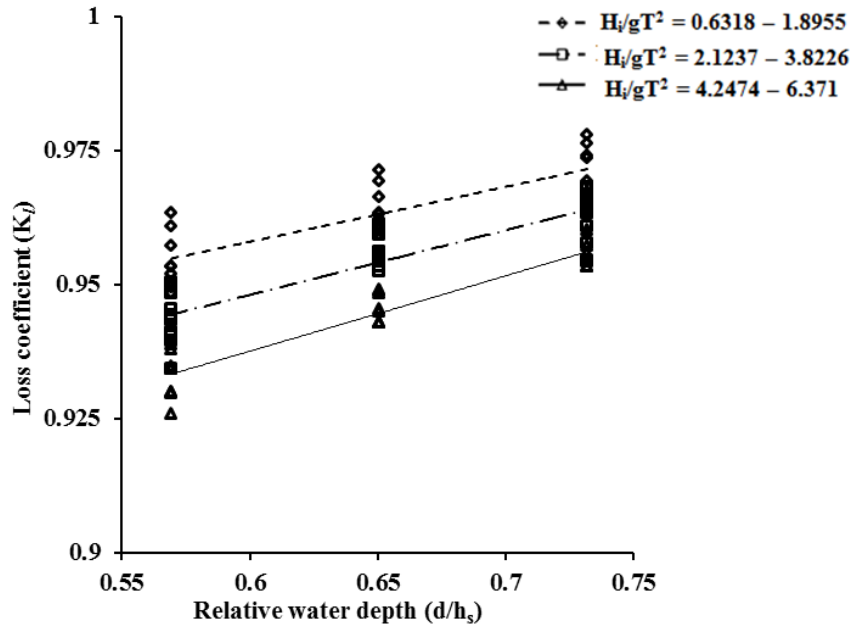
Fig. 4.48 Influence of d/h$_s$ on K$_l$ for S/D = 4 (R= 0.55 m)

For S/D ratio equal to 3, the maximum observed values for K$_l$ are 0.9889, 0.9848 and 0.976 for water depths 0.45 m, 0.40 m and 0.35 m respectively. The maximum K$_l$ values are 0.9779, 0.9713 and 0.9634 for water depths 0.45 m, 0.40 m and 0.35 m respectively for S/D = 4. For S/D = 5, the maximum observed values for K$_l$ are 0.9640, 0.9582 and 0.9551 for water depths 0.45 m, 0.40 m and 0.35 m respectively.
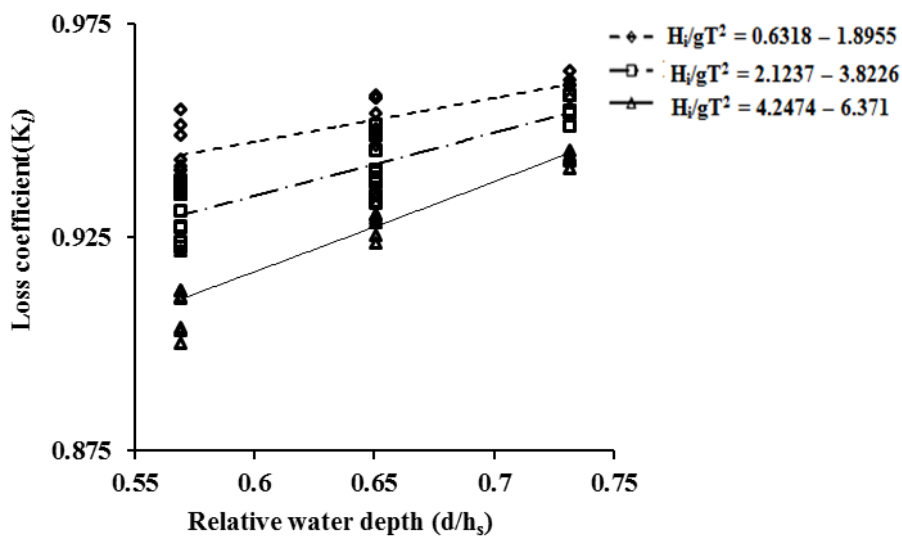
Fig. 4.49 Influence of d/h$_s$ on K$_l$ for S/D = 5 (R= 0.55 m)

From all these results, it is clear that as the water depth increases, the value of K$_l$ increases and the maximum value for K$_l$ are observed at a water depth of 0.45 m. As

water depth increases from 0.35 m to 0.40 m and for S/D ratio equal to 2, there is an increase in K_l from 22.10% to 41.80%. When water depth increases from 0.35 m to 0.45m there is an increase in K_l by 20.51% to 39.10%. Similar trend is observed for K_l on all other values of S/D ratio and when water depth increases from 0.35 m to 0.40 m and from 0.35 m to 0.45 m.

4.9.3 Influence of S/D ratio on loss characteristics

The variation of K_l with H_i/gT^2 for QBW of radius 0.55 m at different water depths for various values of S/D ratio are analyzed separately. It is observed that the loss coefficient, K_l decreases with increase in S/D values 2.5, 3, 4 and 5 for all values of d/h_s and at constant water depths for the range of wave steepness studied. But for S/D equal to 2, the values of K_l are lower than the values for S/D equal to 2.5. This may be due to the reason that when S/D increases the perforation on the QBW surface will be less resulting in lesser values for K_l. In the case of QBW with S/D= 2, the more perforations on the QBW surface causes turbulence inside the chamber and results in increasing the reflection.
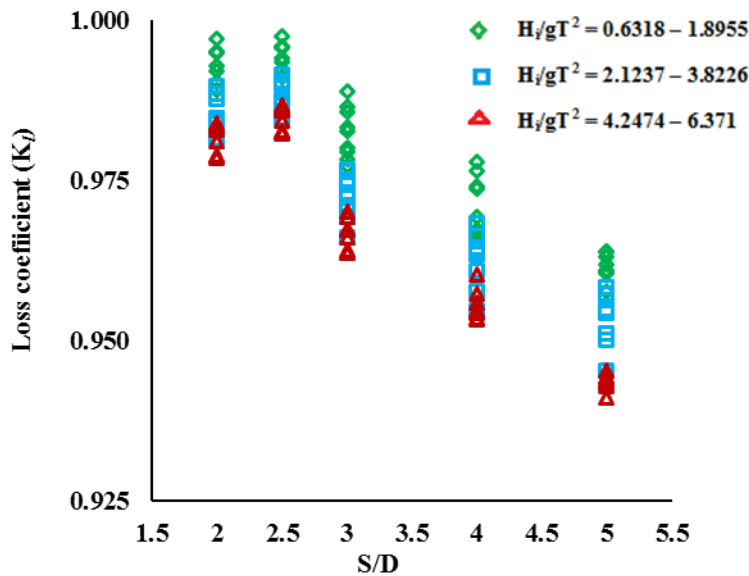
Fig. 4.50 Influence of S/D on K_l for d/h_s= 0.732

In the case of water depth of 0.45 m (d/h_s = 0.732), it is observed that for an S/D = 2, the range of variation of K_l is from 0.9784 to 0.9970 and S/D= 2.5, the range of variation of K_l is from 0.9822 to 0.9975 for $6.24 \times 10^{-4} < H_i/gT^2 < 6.4 \times 10^{-3}$. For the same radius of QBW and at the same water depth, for S/D = 3, the range of variation of K_l is found to be 0.9638 to 0.9889. The variation of K_l for S/D = 4 is observed to

be in the range 0.9553 to 0.9779 and for S/D = 5; the value of K_l varies in the range 0.9411 to 0.9639.
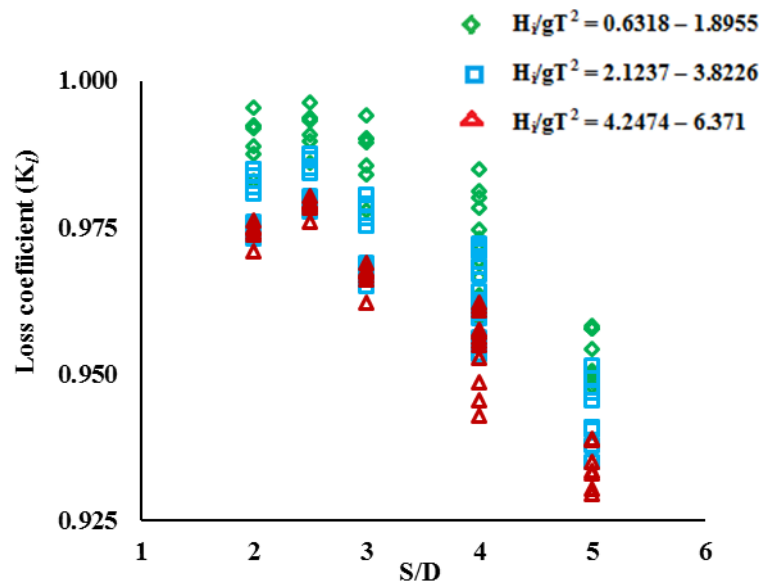
Fig. 4.51 Influence of S/D on K_l for d/h$_s$= 0.650

For water depth of 0.40 m (d/h$_s$ equal to 0.650) and S/D ratio equal to 2, K_l varies from 0.9662 to 0.9954 and for S/D ratio equal to 2.5; the range of variation of K_l is from 0.9721 to 0.9962 and for S/D ratio equal to 3 is from 0.9553 to 0.9848. The variation of K_l for S/D ratio equal to 4 is observed to be in the range 0.9429 to 0.9713 and for S/D ratio equal to 5; the value of K_l varies in the range 0.9238 to 0.9582.
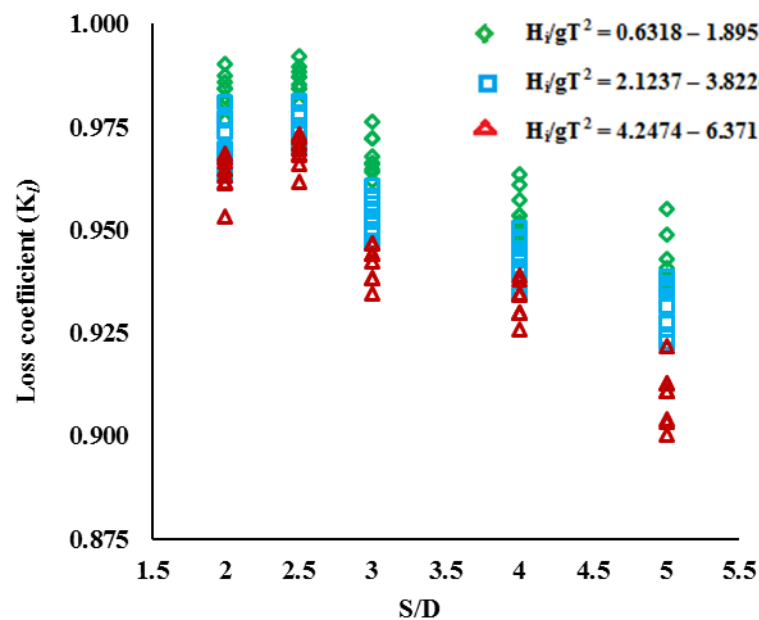
Fig. 4.52 Influence of S/D on K_l for d/h$_s$= 0.569

For a seaside perforated QBW of radius 0.55 m at water depth of 0.35 m (d/h_s equal to 0.569) and S/D ratio equal to 2, K_l varies from 0.9612 to 0.9904 and for S/D ratio equal to 2.5, K_l varies from 0.9615 to 0.9921. For S/D ratio equal to 3, the range of variation of K_l is found to be 0.9346 to 0.9762. For S/D ratio equal to 4, K_l varies from 0.9258 to 0.9635and for S/D ratio equal to 5; K_l varies in the range 0.9003 to 0.9551.

From the results, it is clear that the loss coefficient has higher values for S/D = 2.5 and for higher values of d/h_s. That means that the wave energy dissipation will be more at higher water depths for a constant breakwater radius.

The maximum value for K_l observed for d/h_s equal to 0.569 (0.35 m water depth) is 0.9921 corresponding to S/D equal to 2.5. For d/h_s equal to 0.650 (0.40 m water depth), the maximum value for K_l observed is 0.9962 when S/D is equal to 2.5. Further changing the $d/h_s = 0.732$ (0.45 m water depth), the maximum value for K_l observed is 0.9975 when S/D is equal to 2.5.

4.10 VARIATION OF LOSS COEFFICIENT (K_l) FOR QBW 0.575 m RADIUS

4.10.1 Influence of incident wave steepness on loss characteristics

Fig. 4.53 shows the variation of K_l for a constant S/D for different values of H_i/gT^2 and d/h_s (QBW radius 0.575 m). Similar to QBW of radius 0.55 m, K_l is found to be decreasing with increase in H_i/gT^2 for all values of S/D ratio and d/h_s.

Considering all values d/h_s for QBW of radius 0.575 m, K_l varies from 0.9529 to 0.9969 for $6.24 \times 10^{-4} < H_i/gT^2 < 6.4 \times 10^{-3}$ and S/D= 2. The maximum K_l observed is 0.9969 at a wave height of 0.03 m and a wave period of 2.2 s ($H_i/gT^2 = 6.318 \times 10^{-4}$) at water depth equal to 0.45 m ($d/h_s = 0.703$).

For S/D= 2.5, K_l varies from 0.9807 to 0.9975 for $6.24 \times 10^{-4} < H_i/gT^2 < 6.4 \times 10^{-3}$. The maximum value of K_l observed is 0.9975 at $H_i/gT^2 = 7.645 \times 10^{-4}$ and at water depth equal to 0.45 m ($d/h_s = 0.703$). Under similar conditions and for S/D ratio equal to 3, K_l varies from 0.9615 to 0.9886. The maximum value of K_l observed is 0.9886 for a wave height of 0.03 m and a wave period of 2s ($H_i/gT^2 = 7.645 \times 10^{-4}$) and at water depth equal to 0.45 m (d/h_s equal to 0.703).

(a) For S/D = 2

(b) For S/D = 2.5

(c) For S/D = 3

(d) For S/D = 4

(e) For S/D = 5
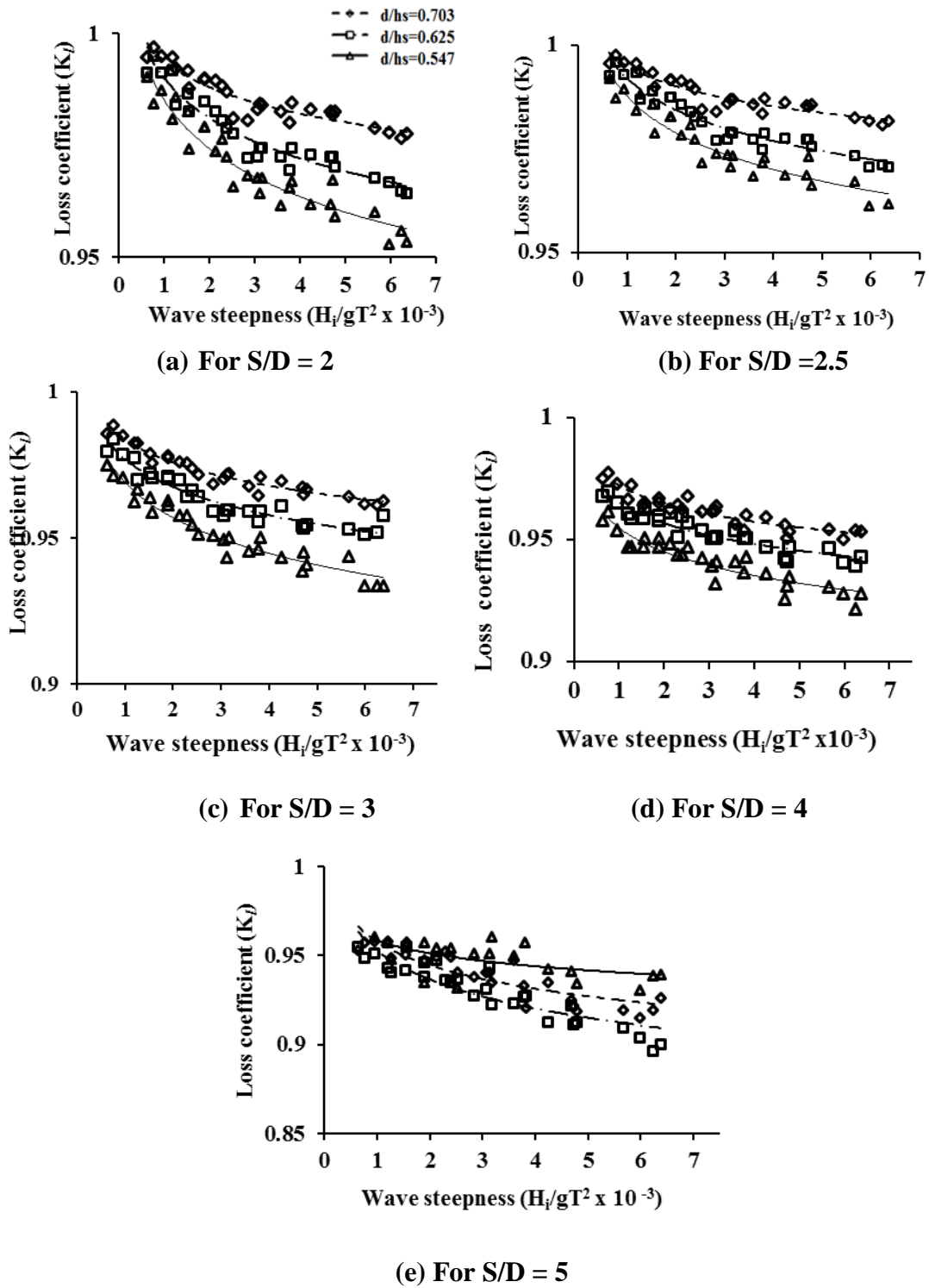
Fig. 4.53 Influence of H_i/gT^2 on K_l for various S/D (R= 0.575 m)

For S/D ratio equal to 4 and for all values d/h_s, K_l varies from 0.9502 to 0.9774. The maximum value of K_l observed is 0.9774 for a wave height of 0.03 m and a wave period of 2 s ($H_i/gT^2 = 7.645 \times 10^{-4}$) and at water depth equal to 0.45 m.

For S/D ratio equal to 5 and for all values d/h_s, K_l varies from 0.9306 to 0.9609 for

$6.24 \times 10^{-4} < H_i/gT^2 < 6.4 \times 10^{-3}$. The maximum value of K_l observed is 0.9609 for a wave height of 0.03 m and a wave period of 2 s ($H_i/gT^2 = 7.645 \times 10^{-4}$) and at water depth equal to 0.45 m.
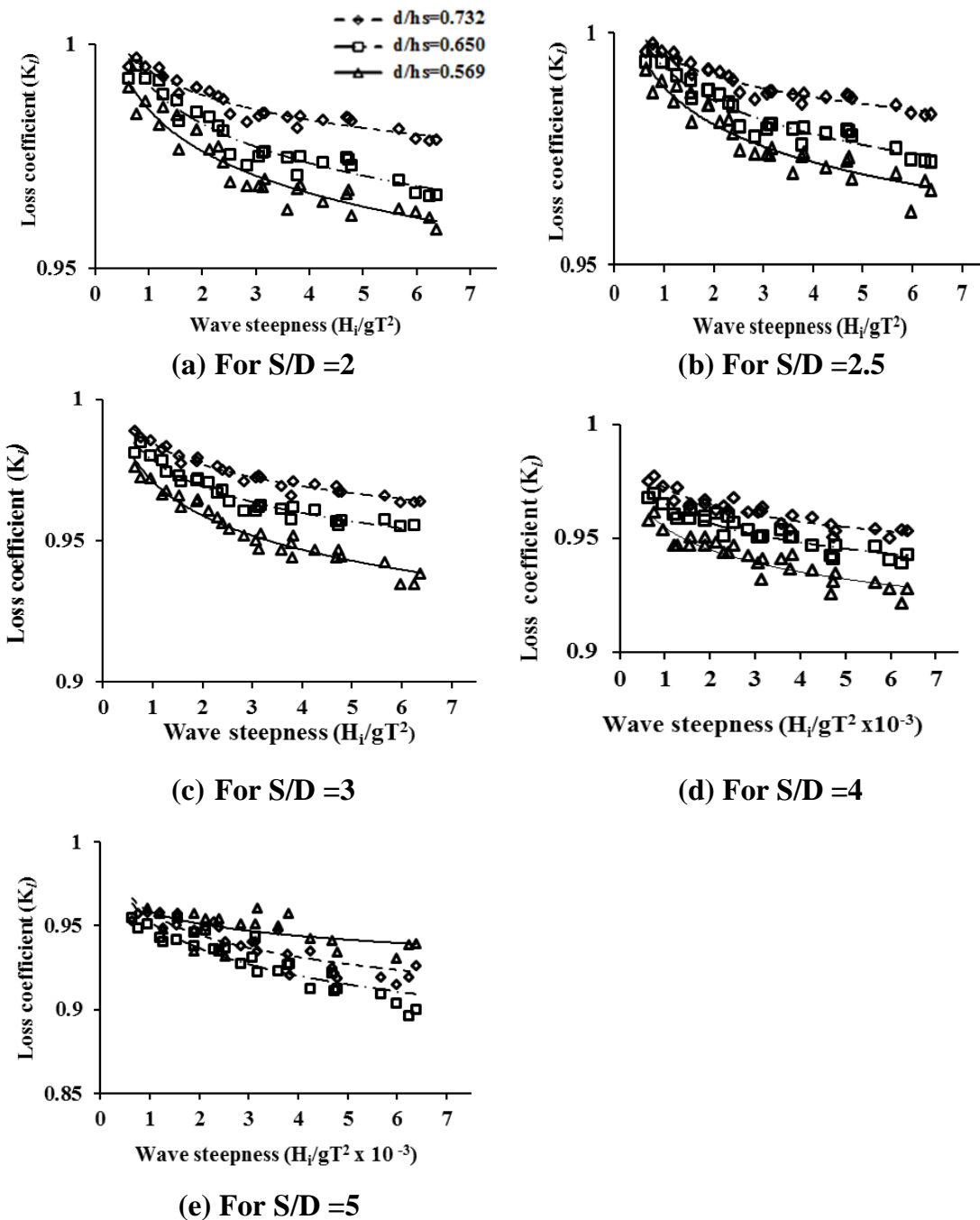
For $6.24 \times 10^{-4} < H_i/gT^2 < 6.4 \times 10^{-3}$ and water depth equal to 0.40 m for S/D ratio equal to 2, 2.5, 3, 4 and 5, K_l varies from 0.9950 to 0.9643, 0.9959 to 0.9705, 0.9839 to 0.9511, 0.9697 to 0.9393 and 0.9579 to 0.9152 respectively. For water depth equal to 0.35 m, $6.24 \times 10^{-4} < H_i/gT^2 > 6.4 \times 10^{-3}$ and S/D ratio equal to 2, 2.5, 3, 4 and 5, K_l varies from 0.9902 to 0.9529, 0.9919 to 0.9613, 0.9747 to 0.9334, 0.9614 to 0.9216 and 0.9549 to 0.8960 respectively.

The percentage decrease in K_l with H_i/gT^2 considering different values of d/h_s for S/D ratio equal to 2, 2.5, 3, 4 and 5 varying from 14.55% to 42.66%, 15.25% to 44.44%, 13.99% to 42.47%, 12.98% to 40.55% and 11.50% to 39.23% respectively.

4.10.2 Influence of water depth on loss characteristics

For QBW of radius 0.575 m and S/D ratio equal to 2, the maximum value for K_l observed is 0.9969 at a water depth of 0.45 m. Under same condition for water depth equal to 0.40 m, the maximum value observed for K_l is 0.9950 and for 0.35 m water depth, the maximum observed value for K_l is 0.9902.

In the case of S/D ratio equal to 2.5, the maximum value for K_l observed is 0.9975 at 0.45 m water depth. For water depth equal to 0.40 m, maximum K_l is 0.9959 and for a water depth equal to 0.35 m, the maximum observed value for K_l is 0.9919 respectively.

For S/D ratio equal to 3, the maximum observed values for K_l are 0.9886, 0.9839 and 0.9747 for water depths 0.45 m, 0.40 m and 0.35 m respectively. For S/D ratio equal to 4, the maximum observed values for K_l are 0.9774, 0.9697 and 0.9614 for water depths 0.45 m, 0.40 m and 0.35 m respectively.

For S/D ratio equal to 5, the maximum observed values for K_l are 0.9609, 0.9579 and 0.9549 for water depths 0.45 m, 0.40 m and 0.35 m respectively. Therefore it is concluded that the loss coefficient K_l increases with increase in relative water depth due to the fact that at higher water depths perforations encountered by the waves are more leading to greater energy dissipation.

(a) For S/D= 2 (b) For S/D =2.5

(c) For S/D= 3 (d) For S/D =4

(e) For S/D = 5
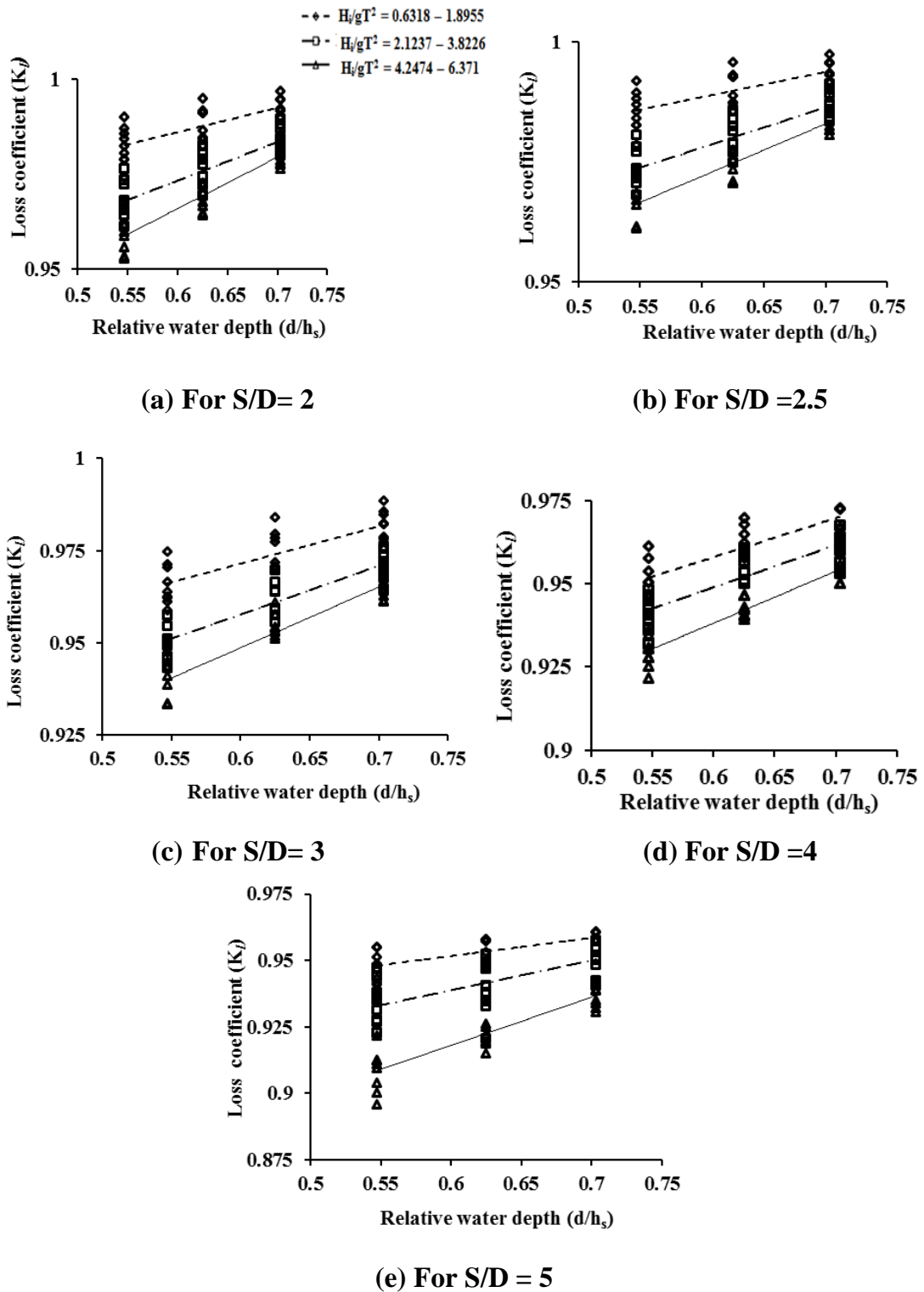
Fig. 4.54 Influence of d/h$_s$ on K$_l$ for various S/D values (R= 0.575 m)

4.10.3 Influence of S/D ratio on loss characteristics

Fig. 4.55 shows the variation of K$_l$ with H$_i$/gT^2 for different S/D ratios and under different water depths for a QBW of radius equal to 0.575 m. Similar to the other

QBW radius, it was observed that K_l increases with increase in S/D ratio for all ranges of H_i/gT^2.
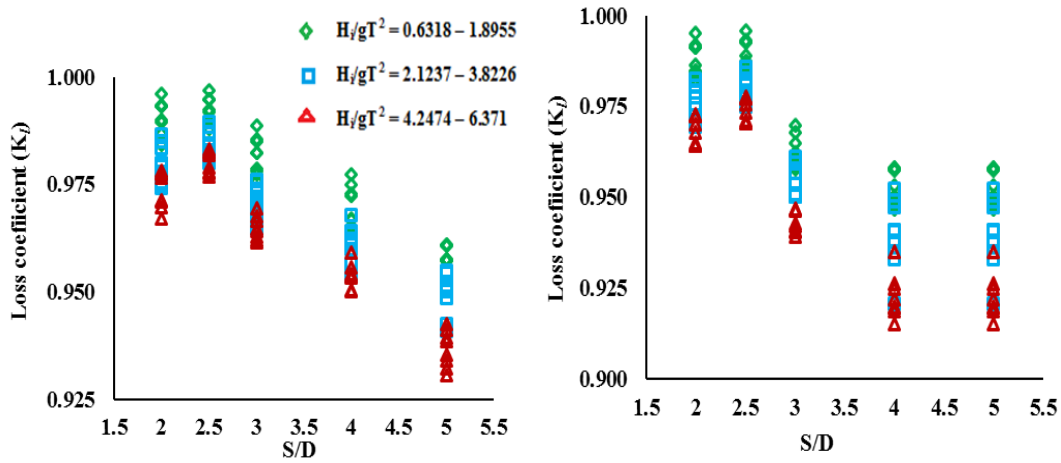
(a) For d/hs = 0.703

(b) For d/hs = 0.625
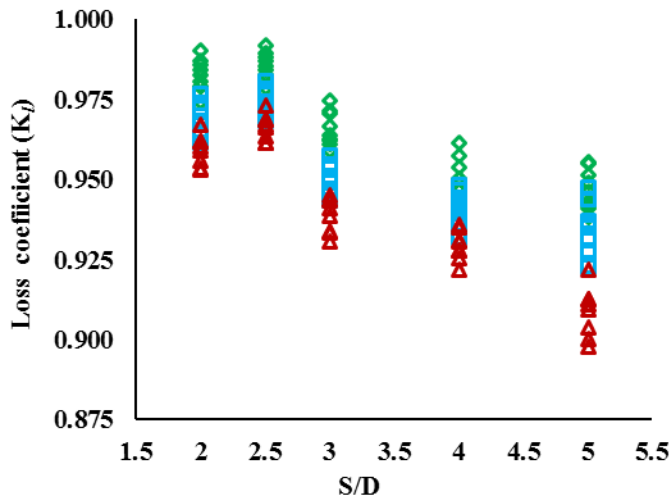
c) For d/hs = 0.547

Fig. 4.55 Influence of S/D on K_l for various d/h_s (for R= 0.575 m)

For a seaside perforated QBW of radius 0.575 m at water depth of 0.35 m (d/h$_s$ equal to 0.547), it is observed that for an S/D ratio equal to 2, 2.5, 3, 4 and 5, the range of variation of K_l is from 0.9529 to 0.9902, 0.9613 to 0.9919, 0.9334 to 0.9747, 0.9216 to 0.9614 and 0.8960 to 0.9549 respectively.

For water depth of 0.40 m (d/h$_s$ equal to 0.625), it is observed that for an S/D ratio equal to 2, 2.5, 3, 4 and 5; the range of variation of K_l is from 0.9643 to 0.9950, 0.9705 to 0.9959, 0.9511 to 0.9839, 0.9393 to 0.9697 and 0.9152 to 0.9579 respectively.

In the case of water depth of 0.45 m (d/h$_s$ = 0.703), it is observed that for an S/D = 2, 2.5 3, 4 and 5, the range of variation of K$_l$ is from 0.9766 to 0.9969, 0.9807to 0.9975, 0.9615 to 0.9886, 0.9502 to 0.9774 and 0.9306 to 0.9608 respectively.

4.11 VARIATION OF LOSS COEFFICIENT (K$_l$) FOR QBW 0.60 m RADIUS

4.11.1 Influence of incident wave steepness on loss characteristics

(a) For S/D = 2

(b) For S/D = 2.5

(c) For S/D = 3

(d) For S/D = 4

(e) For S/D = 5
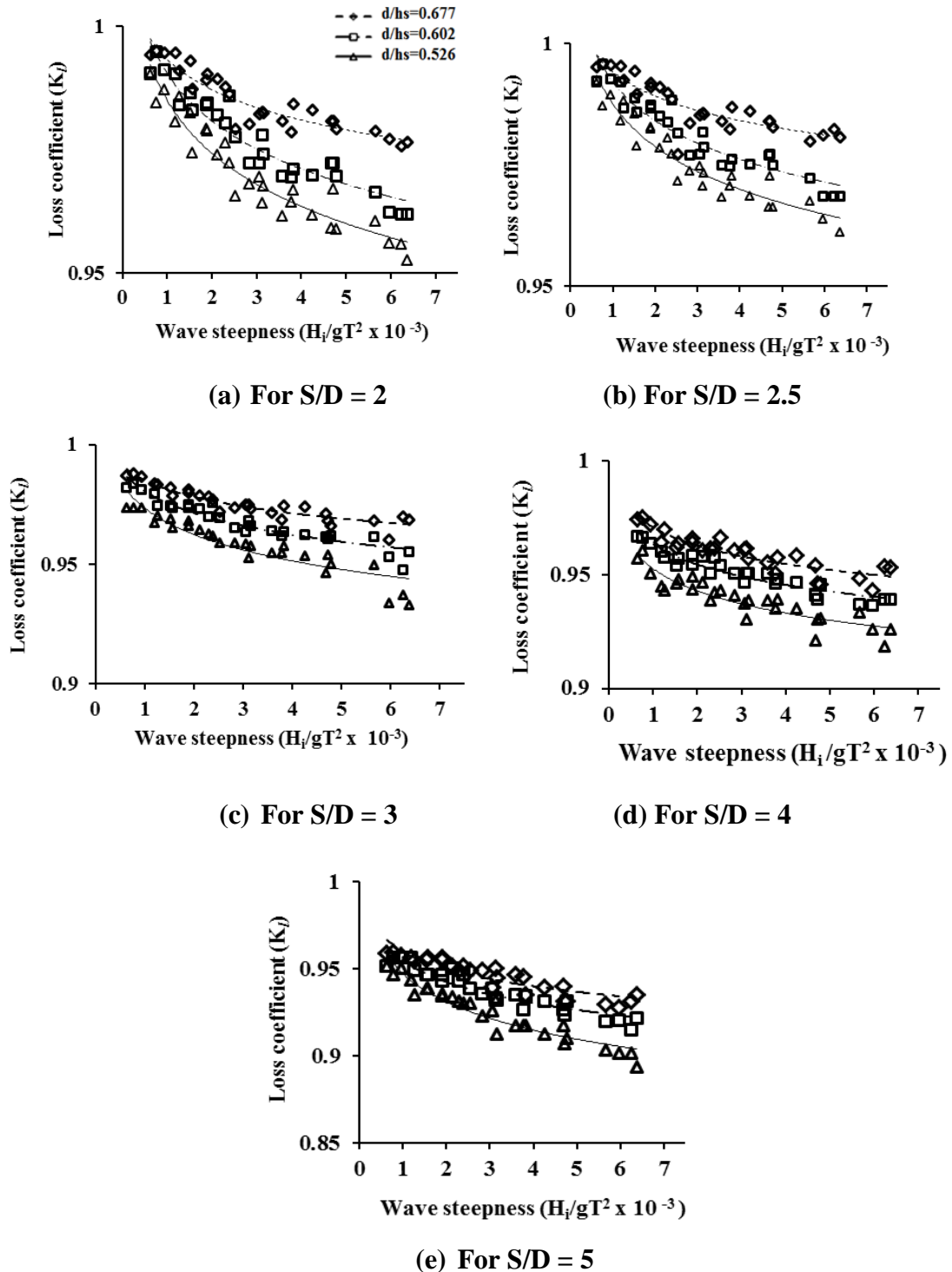
Fig. 4.56 Influence of H$_i$/gT^2 on K$_l$ for various S/D and d/h$_s$ (R= 0.60 m)

For QBW of radius 0.60 m, K_l varies from 0.9525 to 0.9951 for $6.24 \times 10^{-4} < H_i/gT^2 < 6.4 \times 10^{-3}$ and S/D= 2. The maximum K_l observed is 0.9951 at a wave height of 0.03 m and a wave period of 2 s ($H_i/gT^2 = 7.645 \times 10^{-4}$) and at 0.45 m water depth ($d/h_s = 0.677$).

When S/D= 2.5, K_l varies from 0.9772 to 0.9959 for $6.24 \times 10^{-4} < H_i/gT^2 < 6.4 \times 10^{-3}$. The maximum K_l observed is 0.9959 at a wave height of 0.03 m and a wave period of 2s ($H_i/gT^2 = 7.645 \times 10^{-4}$) and at $d/h_s = 0.677$. For S/D ratio equal to 3, 4 and 5, maximum K_l observed is 0.9877, 0.9750, 0.9594 for a $H_i/gT^2 = 7.645 \times 10^{-4}$ and at water depth equal to 0.45 m.

For water depth equal to 0.40 m at S/D ratio equal to 2, 2.5, 3, 4 and 5, optimum values of K_l are 0.9949, 0.9958, 0.9837, 0.9669 and 0.9564 respectively. For water depth equal to 0.35 m, $6.24 \times 10^{-4} < H_i/gT^2 < 6.4 \times 10^{-3}$ and S/D ratio equal to 2, 2.5, 3, 4 and 5, K_l varies 0.9901, 0.9918, 0.9737, 0.9605and 0.9514 respectively.

The percentage decrease in K_l with H_i/gT^2 is found out for different values of d/h_s and for various S/D. When S/D = 2, 2.5, 3, 4 and 5 the percentage reduction in K_l with H_i/gT^2 considering all values of d/h_s is observed to be varying from 14.58% to 44.96%, 15.22% to 45.86%, 14.35% to 44.08%, 13.25% to 43.12% and 11.99% to 41.76% respectively. The percentage variation in the values of K_l is found to be the decreasing for QBW of different radius or different values of d/h_s.

4.11.2 Influence of water depth on loss characteristics

For QBW of radius 0.60 m and S/D = 2, the maximum value for K_l observed is 0.9951 at a water depth of 0.45 m. At the same condition for water depth equal to 0.40 m, 0.9949 and for a water depth equal to 0.35 m, the maximum observed value for K_l is 0.9901.

When S/D = 2.5, maximum K_l observed is 0.9959 at 0.45 m water depth. At 0.40 m water depth, the maximum observed value for K_l is 0.9958 and for a water depth equal to 0.35 m, the maximum observed value for K_l is 0.9918. For S/D =3, the maximum observed values for K_l are 0.9877, 0.9837 and 0.9737 for water depths 0.45 m, 0.40 m and 0.35 m respectively. For S/D = 4, the maximum observed values for K_l are 0.9750, 0.9669 and 0.9605 for water depths 0.45 m, 0.40 m and 0.35 m

respectively. For S/D = 5, the maximum observed values for K_l are 0.9594, 0.9564 and 0.9514 for water depths 0.45 m, 0.40 m and 0.35 m respectively.

(a) For S/D = 2

(b) For S/D =2.5

(c) For S/D = 3

(d) For S/D =4

(e) For S/D = 5

Fig. 4.57 Influence of d/h$_s$ on K$_l$ for various S/D (R= 0.60 m)

4.11.3 Influence of S/D ratio on loss characteristics

Fig. 4.58 shows the variation of K_l with S/D for different d/h$_s$ and constant QBW radius equal to 0.60 m. For seaside perforated QBW of radius 0.60 m at water depth

of 0.35 m (d/h_s = 0.526), it is observed that for S/D = 2, 2.5, 3, 4 and 5, the range of variation of K_l is from 0.9525 to 0.9901, 0.9609 to 0.9919, 0.9334 to 0.9737, 0.9186 to 0.9605 and 0.8932 to 0.9514 respectively.
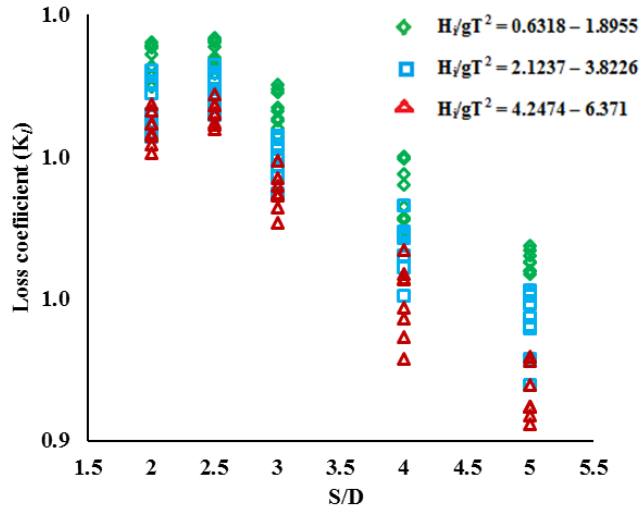
(a) For d/hs =0.677
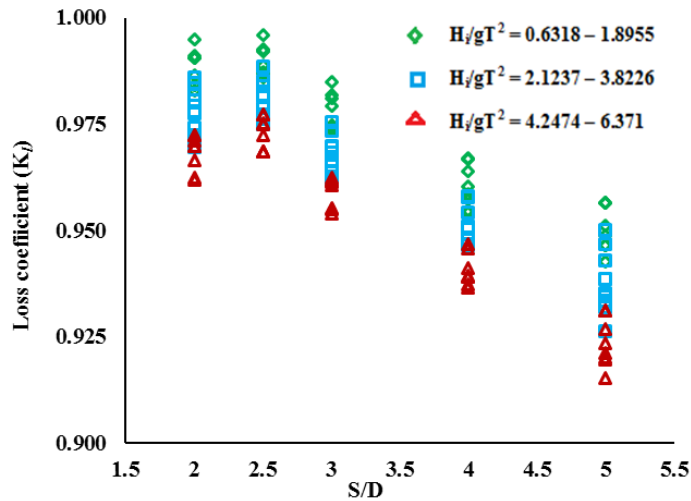
(b) For d/hs =0.602
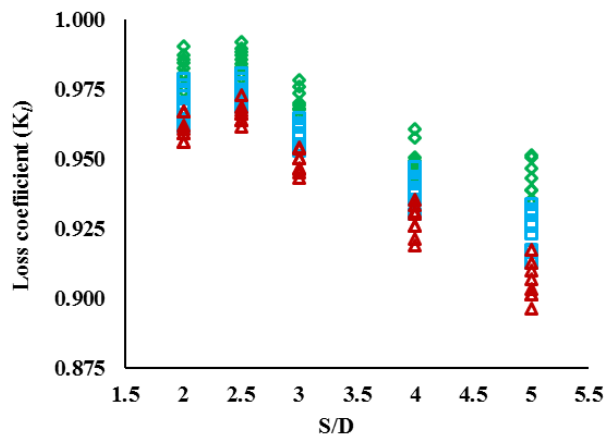
(c) For d/hs =0.526

Fig. 4.58 Influence of S/D on K_l for different d/h_s (R= 0.60 m)

Fig. 4.58 shows the variation of K_l with S/D for different d/h_s and constant QBW radius equal to 0.60 m. For seaside perforated QBW of radius 0.60 m at water depth of 0.35 m (d/h_s equal to 0.526), it is observed that for S/D ratio equal to 2, 2.5, 3, 4 and 5, the range of variation of K_l is from 0.9525 to 0.9901, 0.9609 to 0.9919, 0.9334 to 0.9737, 0.9186 to 0.9605 and 0.8932 to 0.9514 respectively.

For 0.40 m water depth (d/h_s equal to 0.602), it is observed that for an S/D ratio equal to 2, 2.5, 3, 4 and 5; the range of variation of K_l is from 0.9617 to 0.9949, 0.9685 to 0.9958, 0.9478 to 0.9837, 0.9363 to 0.9669 and 0.9149 to 0.9564 respectively. In the case of 0.45 m water depth (d/h_s equal to 0.677), it is observed that for an S/D ratio equal to 2, 2.5, 3, 4 and 5, the range of variation of K_l is from 0.9756 to 0.9951, 0.9772 to 0.9959, 0.9601 to 0.9877, 0.9432 to 0.9750 and 0.9149 to 0.9564 respectively.

From the studies on loss characteristics of seaside perforated QBW, it is observed that the K_l decreases with increase in H_i/gT^2 for all QBW models tested under different water depth (d/h_s) and S/D ratio. The maximum value for K_l observed is 0.9976 at H_i/gT^2 of 7.645 $\times 10^{-4}$ for S/D ratio equal to 2.5 and d/h_s ratio equal to 0.703(d= 0.45 m and QBW radius= 0.55 m).The decrease in K_l with H_i/gT^2 may be because when the waves of shorter wave period or wave length run over the curved surface, they feel the presence of perforations on the QBW for a shorter distance; because of this the energy dissipated due to turbulence is less and hence the K_l is lesser for higher wave steepness.

For all S/D ratio and H_i/gT^2, K_l increases with increase in values for d/h_s. For constant h_s and for S/D= 2, 2.5, 3, 4 and 5, K_l is found to be increasing with increase in d/h_s or increase in water depth. It is also observed that K_l decreases with increase in QBW radius for different ranges of d/h_s and all values of S/D ratio considered for the study. The value of K_l decreases with increase in QBW radius because the effect of curvature is less predominant when the breakwater radius is more and hence the waves encounter lesser perforations resulting in lesser dissipation.

4.12 COMPARITIVE ANALYSIS OF K_r AND K_l ON IMPERMEABLE AND SEASIDE PERFORATED QBW

From the experimental investigations on the reflection and loss characteristics of

impermeable and seaside perforated quarter circle breakwater, it is observed that the K_r is always increasing but K_l is decreasing with increase in wave steepness for all values of d/h_s and S/D ratio. The maximum value for K_l, 0.9976 and minimum K_r 0.0696 are observed for QBW of radius 0.55 m with S/D = 2.5 and d/h_s = 0.732 (0.45 m water depth). When depth of water increases the wave energy dissipation is more effective resulting in higher K_l and lower K_r. The maximum % reduction in K_r obtained is 44.5% for QBW of radius 0.55 m at 0.45 m water depth compared to 0.35 m water depth (d/h_s = 0569).
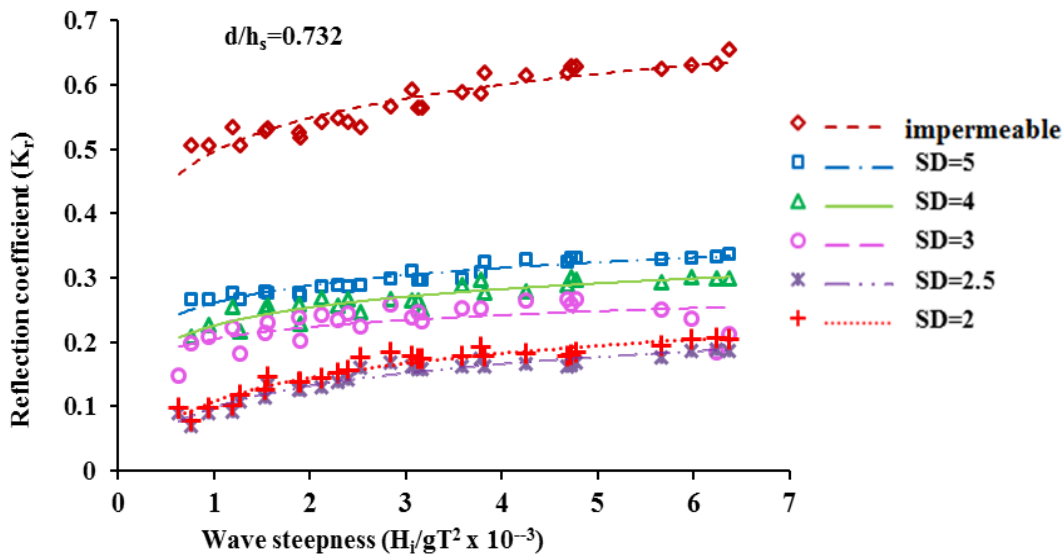
Fig. 4.59 Comparitive study of K_r on impermeable & perforated QBW (d/h_s=0.732)
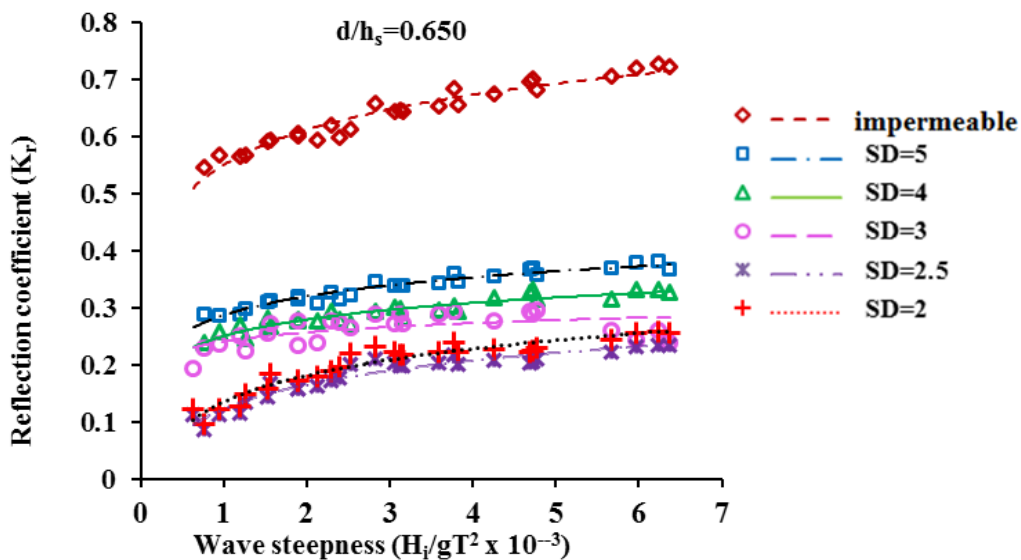
Fig. 4.60 Comparitive study of K_r on impermeable & perforated QBW (d/h_s= 0.650)
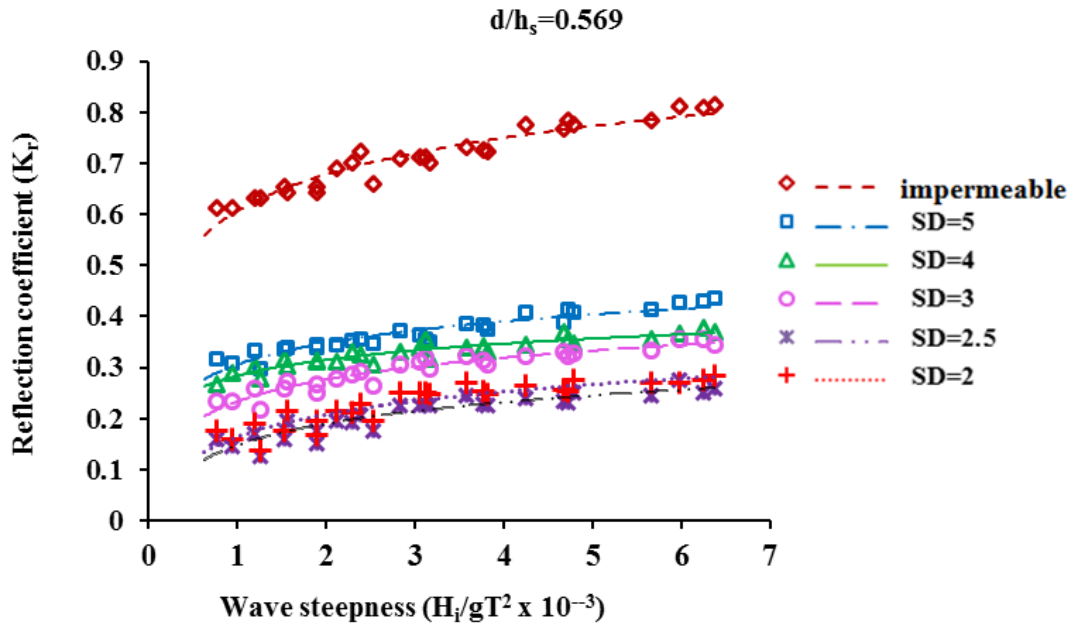
Fig. 4.61 Comparitive study of K_r on impermeable & perforated QBW (d/h$_s$= 0.569)

For QBW of 0.55 m radius and at 0.45 m water depth, the range of variation of K_r is found to be varying from 0.5054 to 0.6559 for impermeable QBW, 0.2660 to 0.3380 for S/D= 5, 0.2090 to 0.3018 for S/D= 4, 0.1480 to 0.2667 for S/D= 3, 0.0696 to 0.1876 for S/D= 2.5 and 0.0767 to 0.2063 for S/D= 2.

When compared to impermeable QBW, percentage reduction in K_r for S/D equal to 5, 4, 3, 2.5 and 2 is observed to be varying from 47% to 49%, 54% to 58%, 60% to 71%, 72% to 86% and 68 to 84% respectively. For impermeable QBW, the values for K_r will be higher compared to the perforated QBW due to less dissipation of wave energy.

The decrease in K_r with decrease in S/D ratio from 5 to 2.5 may be because of dissipation of wave energy due to turbulence inside the chamber. But in the case of S/D= 2, the values for K_r and K_l shows a reverse trend (K_r increases and K_l decreases) compared to that of S/D = 2.5. The slight increase in K_r for S/D = 2 with respect to S/D = 2.5 may be because of back propagation of reflected wave from the rear wall from inside the chamber. Therefore it was recommended that QBW of radius equal to 0.55 m and with S/D= 2.5 is more efficient in wave dissipation resulting in lower reflection.

From the studies on the reflection characteristics of seaside perforated quarter circle breakwater, it is observed that the K_r is always increasing with increase in H_i/gT^2 for all QBW models tested under different water depths (d/h_s) and S/D ratio. The maximum K_r observed is 0.4495 at H_i/gT^2 of 6.3710 x10^{-3} for S/D ratio equal to 5 and d/h_s ratio equal to 0.526 (0.35 m water depth and QBW radius 0.60 m). The minimum value for K_r observed is 0.0696 at H_i/gT^2 of 7.645 x10^{-4} for S/D = 2.5 and d/h_s ratio equal to 0.732 (0.45 m water depth and QBW radius 0.55 m).

The increase in reflection coefficient with wave steepness may be because when the waves of shorter wave period or wave length run over the curved surface, they feel the presence of perforations on the caisson for a shorter distance; because of this the energy dissipated due to turbulence is less and hence the reflection is greater for higher wave steepness.

For all S/D ratio and wave steepness, K_r decreases with increase in values for d/ h_s. In all cases, the height of the breakwater structure or breakwater radius is kept constant. For a constant height of the structure and for S/D values 2, 2.5, 3, 4 and 5, the reflection coefficient, K_r is found to be decreasing with increase in d/h_s ratio or increase in water depth.

Table 4.7 gives the percentage reduction in reflection coefficient for seaside perforated with S/D =2, 2.5, 3, 4 and 5 at water depths 0.45 m and 0.40m with respect to 0.35 m water depth.

Table 4.7 Percentage reduction in K_r with respect to 0.35 m water depth

S/D	Water depth (m)	Percentage reduction of K_r with respect to 0.35 m water depth (%)		
		QBW radius 0.55 m	QBW radius 0.575 m	QBW radius 0.60 m
2.00	0.45	44.38	29.63	29.41
	0.40	30.53	28.85	28.09
2.50	0.45	44.50	43.94	28.93
	0.40	30.54	28.82	28.07
3.00	0.45	31.70	32.77	39.76
	0.40	19.98	20.10	21.09
4.00	0.45	21.93	23.16	20.14
	0.40	11.09	11.27	8.27
5.00	0.45	10.20	6.67	8.44
	0.40	3.44	3.34	5.19

For QBW of radius 0.55 m and S/D = 2, when the water depth increases from 0.35 m to 0.40 m the percentage reduction in K_r is 30.53% and it further reduces to 44.38% when water depth increases to 0.45 m. Similarly from the table and graphs plotted so far for all values of wave steepness and S/D ratio considered for the study it is observed that the K_r decreases with increase in water depth.

Under higher water depth condition, in which case, the waves are exposed to greater area of perforations leading to greater dissipation of energy and, thereby, resulting in lesser reflection. In addition, the effect of curvature also plays a role in dissipating more energy by permitting waves to run over a longer distance.

The maximum % reduction in reflection coefficient is obtained for S/D ratio equal to 2.5 compared to other S/D values for QBW of radius 0.55 m. Similar trends are observed for QBW of radius equal to 0.575 m and 0.60 m under different conditions of water depths.

The decrease in K_r with decrease in S/D ratio may be because of higher dissipation of wave energy due to turbulence inside in the breakwater chamber when the spacing between the perforations is lesser or number of perforations is more.

The percentage reduction in K_r is 44.5% for QBW of radius 0.55 m and S/D ratio equal to 2.5, is about 43.94% for QBW of radius 0.575 m and 28.93% for QBW of radius 0.60 m respectively.

The values of K_r increase with increase in breakwater radius because effect of curvature is less predominant when the breakwater radius is more and hence the waves encounter lesser perforations resulting in lesser dissipation. Hence the QBW of radius equal to 0.55 m is more effective in reducing the reflection compared to QBW of radius equal to 0.575 m and 0.60 m.

4.13 EQUATIONS DEVELOPED FOR REFLECTION COEFFICIENT, K_r AND LOSS COEFFICIENT, K_l

The data obtained from the experiments conducted on reflection and loss characteristics of impermeable QBW for different breakwater radius at different water depths and wave conditions are combined into suitable dimensionless terms.

The equation for the best fit curve with a higher regression coefficient is obtained by using Excel statistical software - XLSTAT.

The equation for K_r for impermeable QBW with regression coefficient $R^2 = 0.924$ is derived as follows:

$$K_r = 0.0684(H_i/gT^2)^{0.685} - 0.747(d/h_s) + 0.976 \dots\dots\dots\dots\dots\dots\dots\dots\dots (4.1)$$

Fig. 4.62 shows the comparison between the measured and predicted values of K_r. The measured values for K_r are in good agreement with the predicted values for K_r.
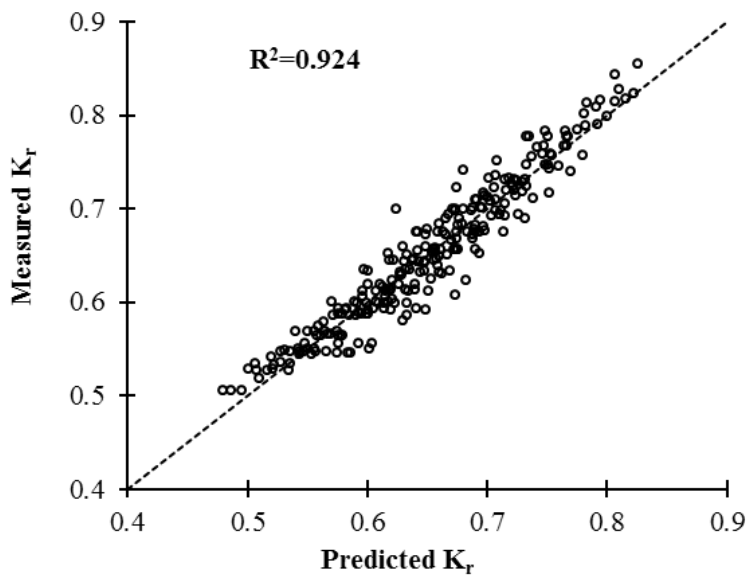
Fig 4.62 Comparison between measured and predicted K_r for impermeable QBW
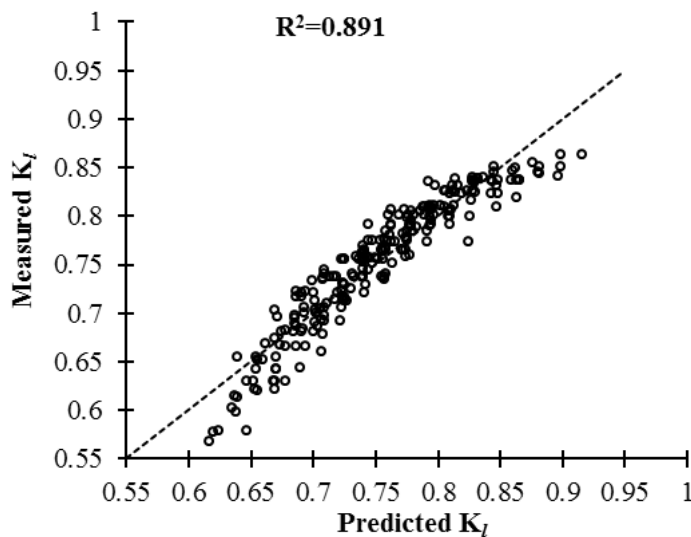
Fig. 4.63 Comparison between measured and predicted K_l for impermeable QBW

The equation for K_l for impermeable QBW with $R^2 = 0.891$ is derived as follows:

$$K_l = 10.289(H_i/gT^2)^{-0.0075} + 1.517(d/h_s)^{0.3187} - 10.767 \quad .... \quad (4.2)$$

Fig. 4.63 shows the comparison between the measured and predicted values of K_l for impermeable QBW.

Similarly the experimental results obtained for perforated QBW with different radius, S/D ratio at different water depths are combined into suitable dimensionless parameters. The curves with best fit for reflection and loss coefficient for perforated QBW are obtained.

Fig. 4.64 shows the comparison between the measured and predicted values of K_r in the case of seaside perforated QBW. The equation for K_r for seaside perforated QBW with $R^2 = 0.903$ is derived as follows:

$$K_r = 0.1850(H_i/gT^2)^{0.231} - 0.4915(d/h_s)^{0.741} + 0.181(S/D)^{0.522} + 0.0392 .... \quad (4.3)$$
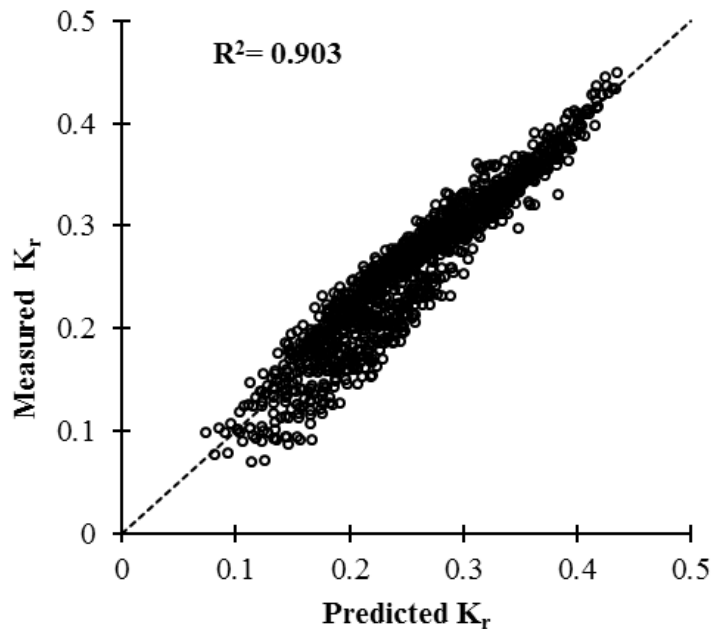
Fig 4.64 Comparison between measured and predicted K_r for perforated QBW

The equation for K_l for seaside perforated QBW with $R^2 = 0.890$ is derived as follows:

$$K_l = 0.1955(H_i/gT^2)^{-0.0692} + 0.377(d/h_s)^{0.198} + 0.2649(S/D)^{-0.2197} + 0.2299 .... \quad (4.4)$$

Fig 4.65 shows the comparison between the measured and predicted values of K_l for perforated quarter circle breakwater.
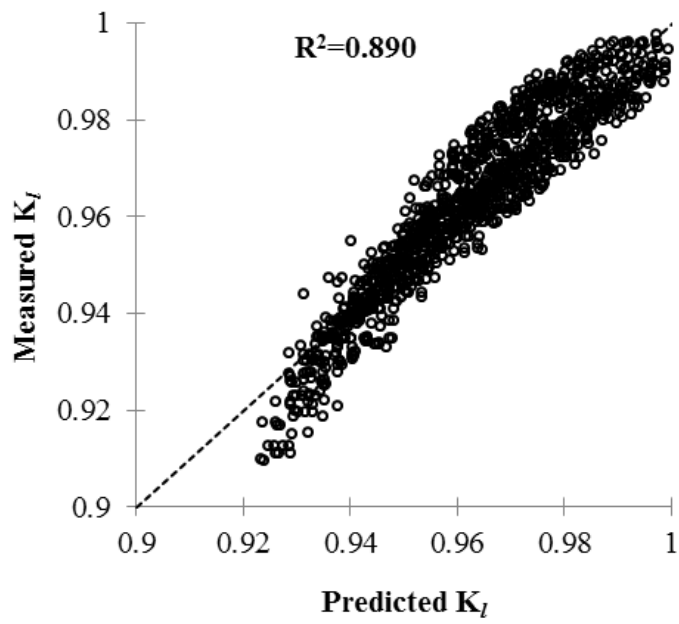
Fig. 4.65 Comparison between measured and predicted values of K_l

INVESTIGATIONS ON RUNUP AND RUNDOWN CHARACTERISTICS OF EMERGED IMPERMEABLE AND SEASIDE PERFORATED QBW

5.1 GENERAL

The results for the reflection and loss characteristics of both emerged impermeable and sea side perforated QBW's are analyzed separately by plotting non dimensional graphs as explained in the previous chapter.

The results obtained after analysis are tabulated and the QBW with good performance based on reflection and loss characteristics are identified. Studies are also conducted on runup and rundown characteristics of different QBW models; both impermeable and perforated to check the adequacy of the assumed QBW radius and height of the rubble mound base.

The main objective of the study is to investigate the effect of varying water depth, the spacing/diameter of perforations (S/D) under different wave conditions. The experiments are conducted on impermeable and seaside perforated QBW with radius 0.55 m, 0.575 m and 0.60 m (S/D ratios 2, 2.5, 3, 4 and 5).

In this chapter the effect of various sea state parameters as well as structural parameters on the wave runup and rundown characteristics of the emerged impermeable and sea side perforated QBW model with varying perforations are studied in detail.

Wave runup studies help in knowing the highest level a wave reaches while wave rundown studies aid us in relating the movement of rubble mound base and hence the stability of the breakwater.

The runup depends on many dimensionless parameters including the seaward slope angle, wave steepness, depth of toe, slope roughness and permeability. Understanding the effect of various sea state and structural parameters is essential in knowing the behavior of the structure and design an optimized structure which is safe as well as economical for the wave conditions considered.

5.2 STUDIES ON EMERGED IMPERMEABLE QBW

The results obtained from the studies on emerged impermeable QBW are analysed separately for different breakwater radii under different water depths (say 0.35 m, 0.40 m and 0.45 m) and varying wave conditions. The data collected from the experimental work are initially expressed as non dimensional parameters. The results are plotted as non-dimensional graphs to study the effect of influencing parameters and the percentage increase or decrease in wave runup and rundown characteristics with incident wave steepness, water depth, and breakwater radii.

5.3 VARIATION OF WAVE RUNUP FOR IMPERMEABLE QBW

The wave runup on QBW are usually expressed in terms of relative wave runup, R_u/H_i which depends on water depth, structure parameters like breakwater radii, percentage perforations and wave parameters. The results obtained from the experimental studies are plotted as non-dimensional graphs showing the variation of relative wave runup with wave steepness, H_i/gT^2 and relative water depth, d/h_s for each S/D ratio.

5.3.1 Influence of incident wave steepness on relative wave runup

Fig. 5.1 shows the variation of R_u/H_i with H_i/gT^2 for different d/h_s (radius of QBW 0.55 m, 0.575 m and 0.60 m). It is observed that R_u/H_i decreases with increase in H_i/gT^2 for all values of d/h_s.

For QBW of radius 0.55 m ($h_s = 0.615$ m), R_u/H_i varies from 1.767 to 3.870 for $6.318 \times 10^{-4} < H_i/gT^2 < 6.3710 \times 10^{-3}$. The maximum R_u/H_i observed is 3.870 at a wave height of 0.03 m and a wave period of 1.6 s ($H_i/gT^2 = 1.194 \times 10^{-3}$) and at 0.35 m water depth ($d/h_s = 0.569$). The minimum R_u/H_i observed is 1.767 at a wave height of 0.09 m and a wave period of 1.2s ($H_i/gT^2 = 6.371 \times 10^{-3}$) and at 0.45 m water depth ($d/h_s = 0.732$).

When QBW radius is increased to 0.575 m, R_u/H_i varies from 2.168 to 4.651 for $6.318 \times 10^{-4} < H_i/gT^2 < 6.3710 \times 10^{-3}$. Also the maximum R_u/H_i increases to 4.651 obtained at a wave height of 0.03 m and a wave period of 2 s ($H_i/gT^2 = 7.645 \times 10^{-4}$) and at water depth equal to 0.35 m. The minimum R_u/H_i observed is 2.168 obtained for a wave height of 0.12 m and a wave period of 1.4s ($H_i/gT^2 = 6.241 \times 10^{-3}$) and at

0.45 m water depth.

In the case of QBW of radius 0.60 m, R_u/H_i varies from 2.484 to 5.468 for 6.318 x $10^{-4} < H_i/gT^2 < 6.3710 \times 10^{-3}$. The maximum R_u/H_i observed is 4.772 for wave height of 0.03 m and a wave period of 2 s ($H_i/gT^2 = 7.645 \times 10^{-4}$) and at 0.35 m water depth. The minimum R_u/H_i observed is 2.305 at a wave height of 0.12 m and a wave period of 1.4s ($H_i/gT^2 = 6.241 \times 10^{-3}$) and at water depth equal to 0.45 m.
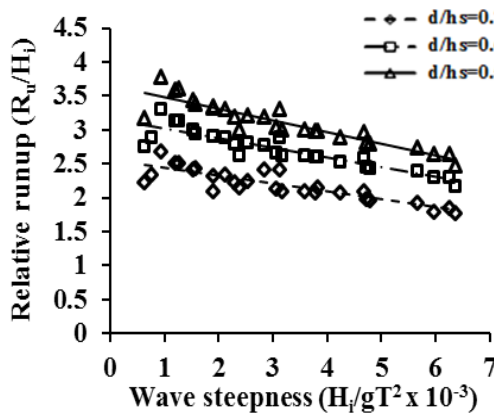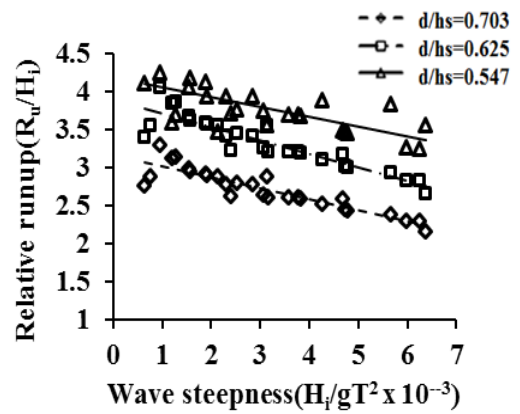
(a) For QBW radius 0.55 m   (b) For QBW radius 0.575 m
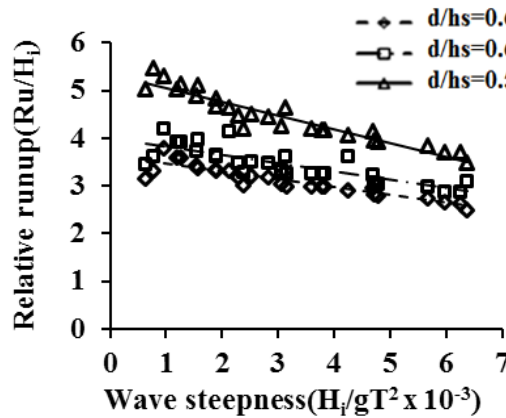
(c) For QBW radius 0.600 m

Fig. 5.1 Influence of H_i/gT^2 on R_u/H_i for different d/h_s

From all the graphs plotted and the results obtained it is observed that relative wave runup decreases with increase in wave steepness. The decrease in relative wave runup with wave steepness may be because when the waves of shorter wave period or wave length run over the curved surface, most of the energy of the incident waves is reflected and hence less energy will be available for the runup.

5.3.2 Influence of relative water depth on relative wave runup

Fig. 5.2 Variation of R_u/H_i with d/h_s for QBW of 0.55 m radius

Fig. 5.3 Variation of R_u/H_i with d/h_s for QBW of 0.575 m radius
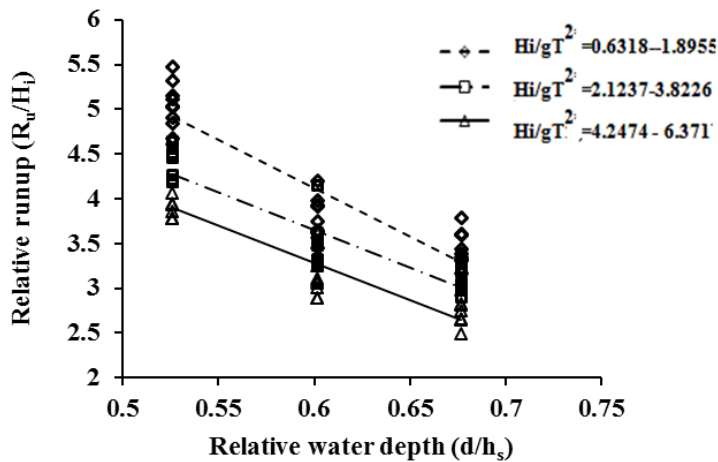
Fig. 5.4 Variation of R_u/H_i with d/h_s for QBW of 0.60 m radius

In all of the above cases, QBW is tested for varying water depths say 0.35 m, 0.40 m and 0.45 m, then non dimensional graphs are plotted for each condition at different wave steepness in order to obtain the effect of water depth on relative wave run up. From the plotted graphs and results, it is observed that R_u/H_i decreases with increase in water depth.

For QBW of radius 0.55 m and $6.318 \times 10^{-4} < H_i/gT^2 < 1.8955 \times 10^{-3}$, the minimum value for R_u/H_i is equal to 2.1006 corresponding to $d/h_s = 0.732$ (0.45 m water depth) and maximum R_u/H_i obtained is 3.870 corresponding to $d/h_s = 0.569$ (0.35 m water depth). Similar trends are observed for all the other ranges of wave steepness.

The variation of R_u/H_i with d/h_s for QBW of 0.55 m radius for different H_i/gT^2 is shown in Fig. 5.2. For $2.1237 \times 10^{-3} < H_i/gT^2 < 3.8226 \times 10^{-3}$, the minimum value for R_u/H_i is equal to 2.084 when $d/h_s = 0.732$ (0.45 m water depth) and maximum R_u/H_i obtained is 3.598 when $d/h_s = 0.569$ (0.35 m water depth). For $4.247 \times 10^{-3} < H_i/gT^2 < 6.371 \times 10^{-3}$, the minimum value for is equal to 1.767 corresponding to $d/h_s = 0.732$ and maximum R_u/H_i obtained is 3.107 corresponding to $d/h_s = 0.569$.

Fig. 5.3 shows the variation of R_u/H_i with d/h_s for QBW 0.575 m radius under varying conditions of wave steepness. It is observed that for $6.318 \times 10^{-4} < H_i/gT^2 < 1.8955 \times 10^{-3}$ the minimum value for R_u/H_i is equal to 2.765 when $d/h_s = 0.703$ (water depth of 0.45 m) and maximum R_u/H_i is 4.651 corresponding to $d/h_s = 0.547$ (water depth of 0.35 m).

The minimum and maximum values for R_u/H_i observed for $2.123 \times 10^{-3} < H_i/gT^2 < 3.8226 \times 10^{-3}$ are 2.608 and 3.946. For $4.247 \times 10^{-3} < H_i/gT^2 < 6.371 \times 10^{-3}$, the minimum value for is equal to 2.168 corresponding to $d/h_s = 0.703$ and maximum R_u/H_i obtained is 3.889 corresponding to $d/h_s = 0.547$ respectively.

Considering QBW of radius 0.60 m, for $6.318 \times 10^{-4} < H_i/gT^2 < 1.8955 \times 10^{-3}$, the minimum value for $R_u/H_i = 2.765$ for $d/h_s = 0.677$ and maximum R_u/H_i is 4.651 corresponding to $d/h_s = 0.526$ (Refer Fig. 5.4). The minimum and maximum values for R_u/H_i observed for $2.123 \times 10^{-3} < H_i/gT^2 < 3.8226 \times 10^{-3}$ are 2.608 and 3.946. For $4.247 \times 10^{-3} < H_i/gT^2 < 6.371 \times 10^{-3}$, the minimum value for is equal to 2.168 corresponding to $d/h_s = 0.677$ and maximum R_u/H_i obtained is 3.889 corresponding to $d/h_s = 0.526$ respectively.

In all cases it is observed that the relative wave runup decreases with increase in relative water depth (d/h_s). When d/h_s increases the effect of curvature is more pronounced and hence the vertical elevation attained is very less resulting in less runup.

In the case of QBW of 0.55 m radius, the percentage reduction in R_u/H_i for 0.40 m and 0.45 m water depth with respect to 0.35 m water depth are determined. For $6.318 \times 10^{-4} < H_i/gT^2 < 1.8955 \times 10^{-3}$ and considering 0.35 m water depth as reference, when $d/h_s = 0.650$ (0.40 m water depth) the percentage reduction in R_u/H_i varies from 17.10% to 19.52% and when $d/h_s = 0.732$ (0.45 m water depth) the percentage reduction in R_u/H_i varies from 25.19% to 38.04 %.

Similarly for $2.123 \times 10^{-3} < H_i/gT^2 < 3.8226 \times 10^{-3}$ and considering 0.35 m water depth as reference, when $d/h_s = 0.650$ (0.40 m water depth) the percentage reduction in R_u/H_i varies from 16.19% to 19.97% and when $d/h_s = 0.732$ (0.45 m water depth) the percentage reduction in R_u/H_i varies from 30% to 32%. It is observed that the maximum percentage reduction in R_u/H_i varies from 32% to 33% for $d/h_s = 0.732$ (water depth of 0.45 m) and when $4.247 \times 10^{-3} < H_i/gT^2 < 6.371 \times 10^{-3}$.

Considering the studies on QBW 0.575 m radius, the maximum percentage reduction in R_u/H_i is observed when $4.247 \times 10^{-3} < H_i/gT^2 < 6.371 \times 10^{-3}$ that varies from 33% to 34% $d/h_s = 0.703$ (water depth of 0.45 m). When the QBW radius is increased to 0.60 m, the maximum percentage reduction in R_u/H_i is observed when $4.247 \times 10^{-3} < H_i/gT^2 < 6.371 \times 10^{-3}$ that varies from 34% to 36% $d/h_s = 0.677$ (water depth of 0.45 m).

From the experiments conducted on QBW of different radius, it is clearly understood that R_u/H_i increases with increase in breakwater radius or decrease in d/h_s for different ranges of H_i/gT^2. When breakwater radius increases, the vertical height attained by the wave will be more or the effect of curvature becomes less predominant resulting in higher wave runup.

The percentage increase in R_u/H_i with decrease in d/h_s (increase in QBW radius) is more effective at a water depth of 0.45 m for $4.247 \times 10^{-3} < H_i/gT^2 < 6.371 \times 10^{-3}$ and it varies from 37.13% to 40.50 %. The minimum percentage reduction in R_u/H_i with decrease in d/h_s (increase in QBW radius) that varies 35.83% to 38.01% is observed

at a water depth equal to 0.35 m and for lower values of $6.318 \times 10^{-4} < H_i/gT^2 < 1.8955 \times 10^{-3}$.

5.4 VARIATION OF WAVE RUNDOWN FOR IMPERMEABLE QBW

The wave rundown characteristics on an emerged impermeable QBW are usually expressed in terms of relative wave rundown (R_d/H_i). Based on the experiments conducted on emerged impermeable QBW, the influence of parameters such as incident wave steepness (H_i/gT^2), relative water depth (d/h_s) are analyzed which are discussed in the following sections.

5.4.1 Influence of incident wave steepness on relative wave rundown

Fig. 5.5 shows the variation of R_d/H_i with H_i/gT^2 for different water depths with radius of QBW 0.55 m, 0.575 m and 0.60 m respectively. It is observed that R_d/H_i decreases with increase in H_i/gT^2 for all values of d/h_s.
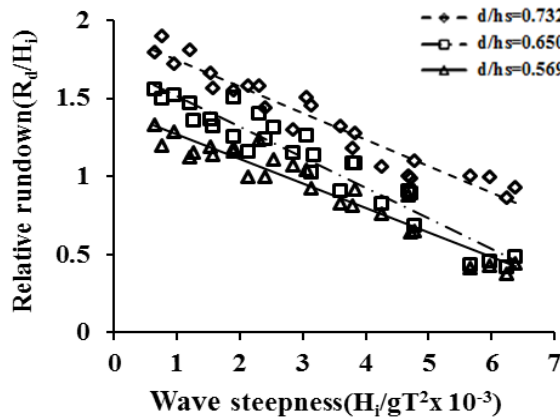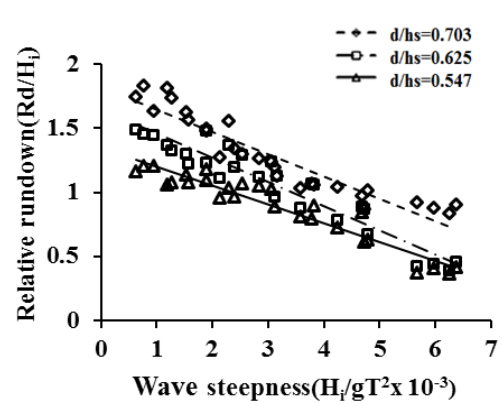
(a) For QBW of radius 0.55 m   **(b) For QBW of radius 0.575 m**
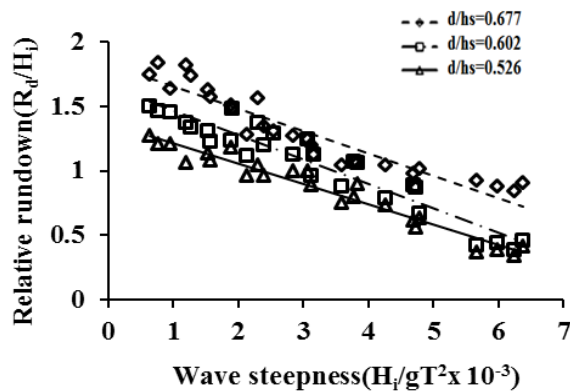
(c) For QBW of radius 0.600 m

Fig. 5.5 Influence of H_i/gT^2 on R_d/H_i for QBW of radius 0.55 m, 0.575 m and 0.60 m

For QBW of radius 0.55 m, R_d/H_i varies from 0.3762 to 1.904 for $6.318 \times 10^{-4} < H_i/gT^2 < 6.3710 \times 10^{-3}$. The maximum value for R_d/H_i observed is 1.904 at a wave height of 0.03 m and a wave period of 2s ($H_i/gT^2 = 7.645 \times 10^{-4}$) and at water depth equal to 0.45 m ($d/h_s = 0.732$). The minimum value for R_d/H_i observed is 0.3762 at a wave height of 0.12 m and a wave period of 1.4s ($H_i/gT^2 = 6.2410 \times 10^{-3}$) and at water depth equal to 0.35 m (d/h_s equal to 0.569).

When radius of QBW is increased to 0.575 m, R_d/H_i varies from 0.3643 to 1.904 for $6.318 \times 10^{-4} < H_i/gT^2 < 6.3710 \times 10^{-3}$. The maximum value for R_d/H_i observed is 1.904 at a wave height of 0.03 m and a wave period of 2s ($H_i/gT^2 = 7.645 \times 10^{-4}$) and at water depth equal to 0.45 m ($d/h_s = 0.703$). The minimum value for R_d/H_i observed is 0.3643 at a wave height of 0.12 m and a wave period of 1.4 s ($H_i/gT^2 = 6.2410 \times 10^{-3}$) and at water depth equal to 0.35 m (d/h_s equal to 0.547).

The values for R_d/H_i for QBW of radius equal to 0.60 m vary from 0.3417 to 1.845 for $6.318 \times 10^{-4} < H_i/gT^2 < 6.3710 \times 10^{-3}$. The maximum R_d/H_i observed is 1.845 at a wave height of 0.03 m and a wave period of 2s ($H_i/gT^2 = 7.645 \times 10^{-4}$) and at 0.45 m water depth ($d/h_s = 0.677$). The minimum R_d/H_i observed is 0.3417 at a wave height of 0.12 m and a wave period of 1.4 s ($H_i/gT^2 = 6.2410 \times 10^{-3}$) and at 0.35 m water depth.

### 5.4.2 Influence of relative water depth on rundown characteristics

From Fig. 5.6 for QBW of radius 0.55 m, the minimum value for R_d/H_i is equal to 0.3762 observed at a water depth of 0.35 m ($d/h_s = 0.569$) when $4.247 \times 10^{-3} < H_i/gT^2 < 6.371 \times 10^{-3}$ and maximum R_d/H_i obtained is 1.904 corresponding to a water depth of 0.45 m ($d/h_s = 0.732$) when $6.318 \times 10^{-4} < H_i/gT^2 < 1.8955 \times 10^{-3}$. In the case of QBW of radius 0.575 m, the minimum value for R_d/H_i is equal to 0.3643 observed at 0.35 m water depth when $4.247 \times 10^{-3} < H_i/gT^2 < 6.371 \times 10^{-3}$ and maximum R_d/H_i obtained is 1.8351 corresponding to 0.45 m water depth when $6.318 \times 10^{-4} < H_i/gT^2 < 1.8955 \times 10^{-3}$ (Refer Fig. 5.7).

For QBW of radius 0.60 m, the minimum value for R_d/H_i is equal to 0.5202 observed at a water depth of 0.35 m when $4.247 \times 10^{-3} < H_i/gT^2 < 6.371 \times 10^{-3}$ and maximum R_d/H_i obtained is 0.8443 corresponding to a water depth of 0.45 m when $6.318 \times 10^{-4} < H_i/gT^2 < 1.8955 \times 10^{-3}$ (Refer Fig.5.8).
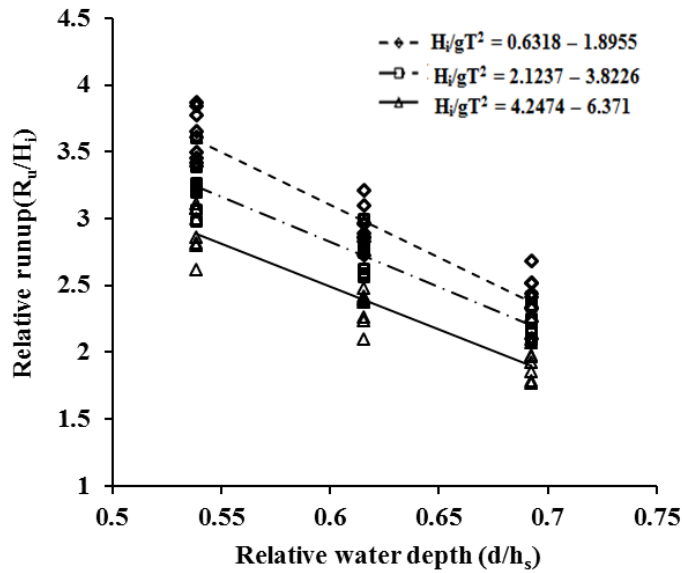
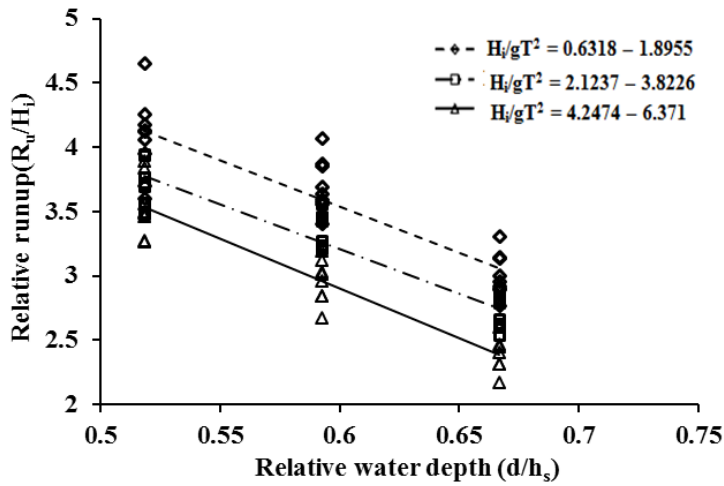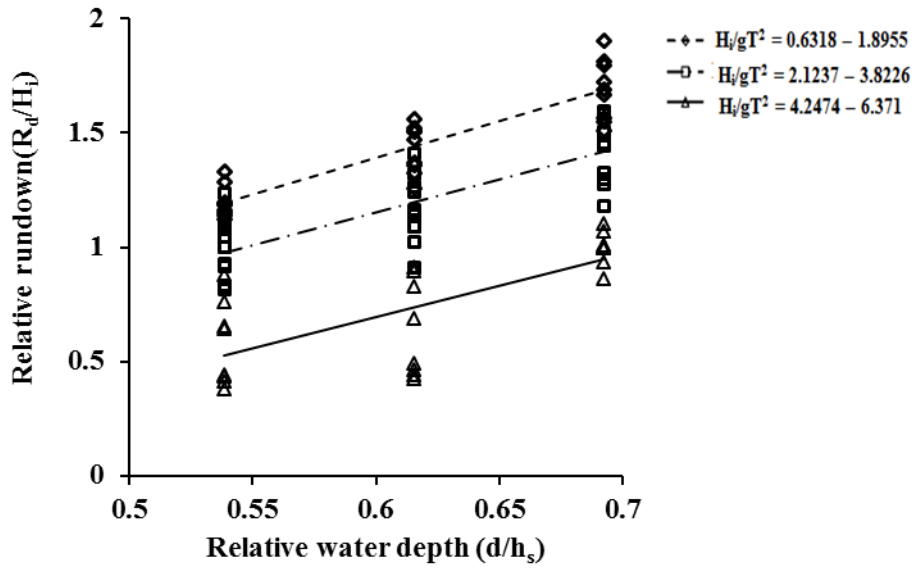**Fig. 5.6 Variation of R_d/H_i with d/h_s for QBW of radius 0.55 m**
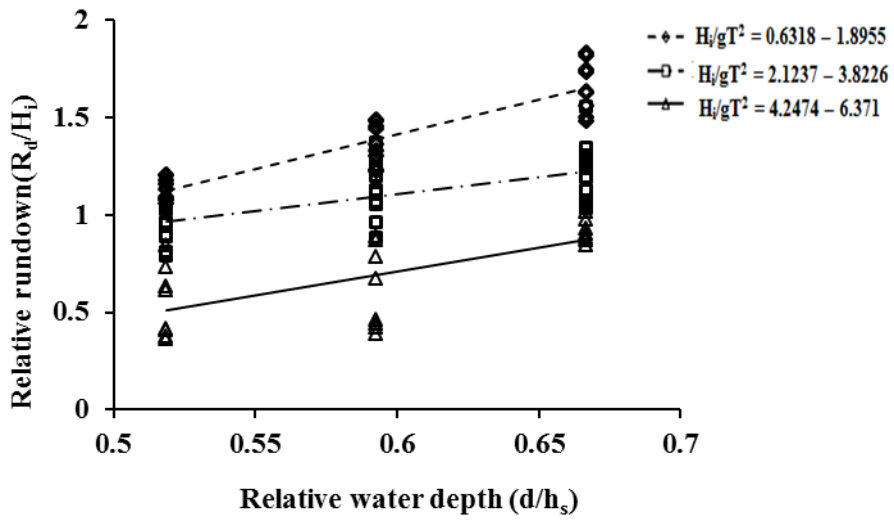
Fig. 5.7 Variation of R_d/H_i with d/h_s for QBW of radius 0.575 m
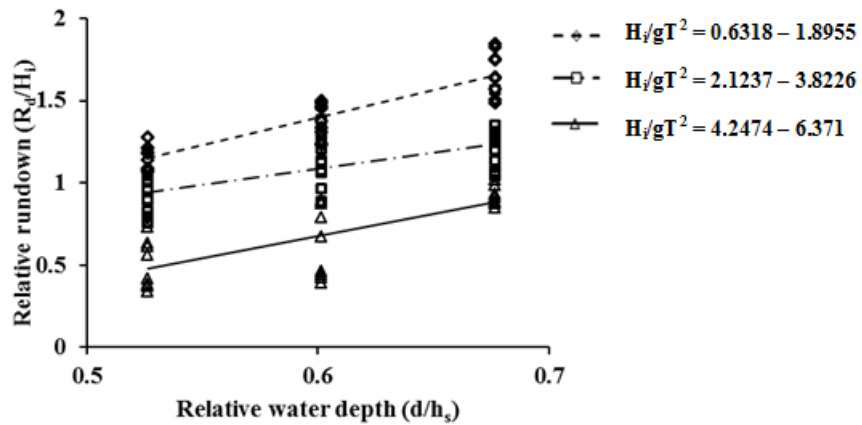
Fig. 5.8 Variation of R_d/H_i with d/h_s for QBW of radius 0.60 m

In all cases it is observed that the relative wave rundown increases with increase in relative water depth (d/h_s). When d/h_s increases the effect of curvature is more pronounced therefore the vertical height attained by the wave or wave runup will be very less and hence more wave energy is available for wave run down.

5.5 STUDIES ON EMERGED SEASIDE PERFORATED QBW

The results obtained from the studies on emerged seaside perforated QBW are analysed separately for different spacing to diameter (S/D) ratios as well as for different breakwater radii under different water depths (say 0.35, 0.40 and 0.45 m) and varying wave conditions.

The data collected from the experimental work are initially expressed as non dimensional parameters. The results are plotted as non-dimensional graphs to study the effect of influencing parameters and the percentage increase or decrease in wave runup and rundown characteristics with wave steepness, water depth, S/D ratio and breakwater radii are found out.

5.6 VARIATION OF RELATIVE WAVE RUNUP (R_u/H_i) FOR QBW OF 0.55 m RADIUS (h_s=0.615 m)

5.6.1 Influence of incident wave steepness on relative wave runup

5.6.1.1 Seaside perforated QBW with S/D ratio equal to 2.

Fig. 5.9 shows the variation of R_u/H_i with H_i/gT^2 for different water depths with radius of QBW 0.55 m and S/D ratio equal to 2. It is clear from the graphs that R_u/H_i decreases with increase in H_i/gT^2 for all values of d/h_s.

Considering all values d/h_s and R_u/H_i varies from 0.7790 to 1.8890 for $6.24 \times 10^{-4} < H_i/gT^2 < 6.4 \times 10^{-3}$ and S/D= 2. The maximum value for R_u/H_i observed is 1.8890 at a wave height of 0.03 m and a wave period of 2 s ($H_i/gT^2 = 7.645 \times 10^{-4}$) and at water depth equal to 0.35 m (d/h_s equal to 0.569).

The minimum value for R_u/H_i observed is 0.7790 at a wave height of 0.09 m and a wave period of 1.2 s ($H_i/gT^2 = 6.371 \times 10^{-3}$) and at water depth equal to 0.45 m ($d/h_s = 0.732$).
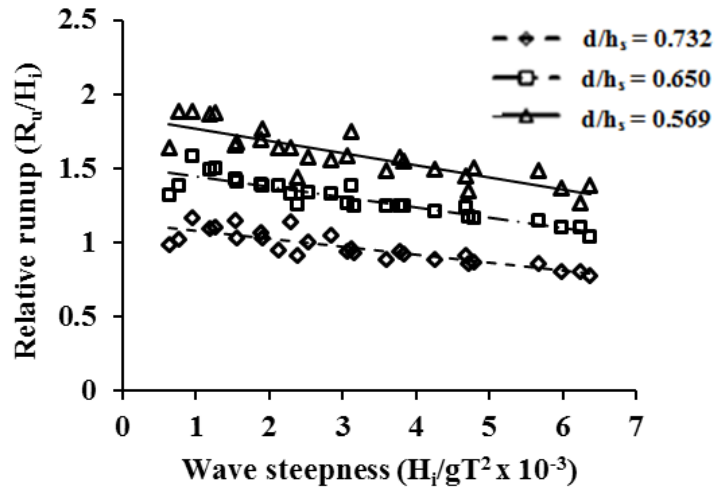
Fig. 5.9 Influence of H_i/gT^2 on R_u/H_i for S/D=2
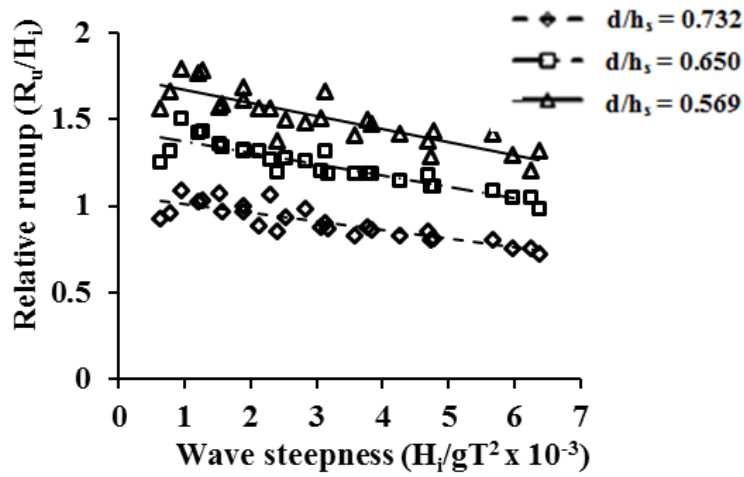
Fig. 5.10 Influence of H_i/gT^2 on R_u/H_i for S/D= 2.5
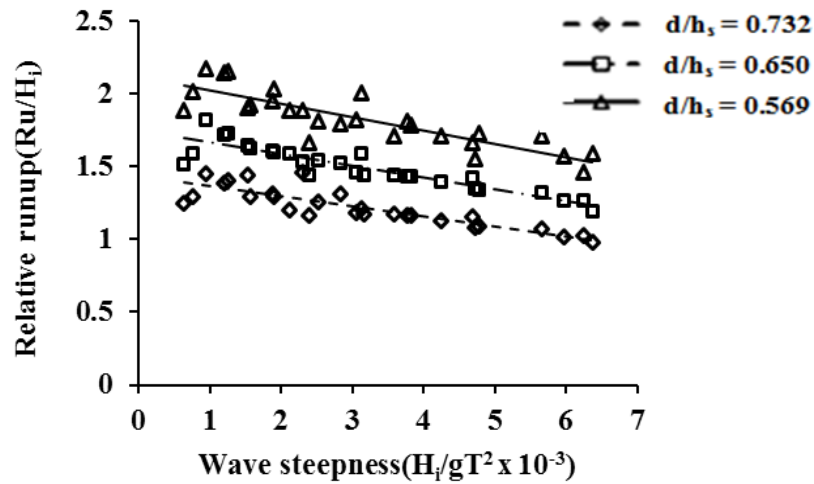
Fig. 5.11 Influence of H_i/gT^2 on R_u/H_i for S/D= 3
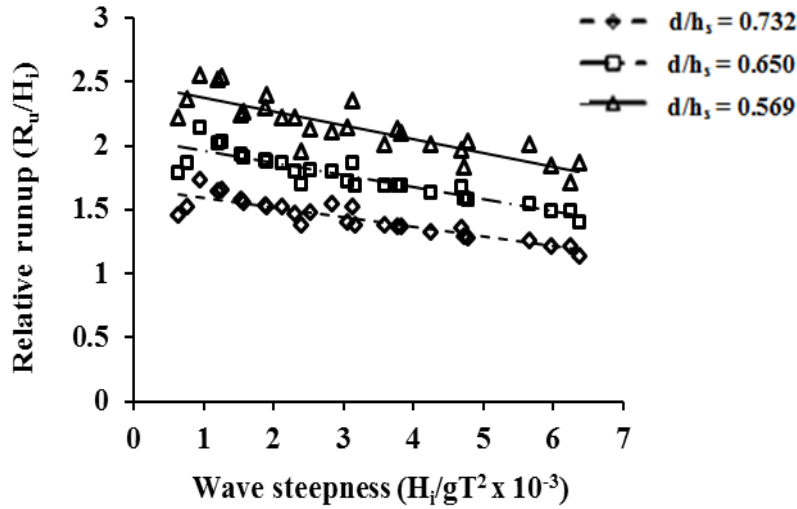
Fig. 5.12 Influence of H_i/gT^2 on R_u/H_i for S/D= 4
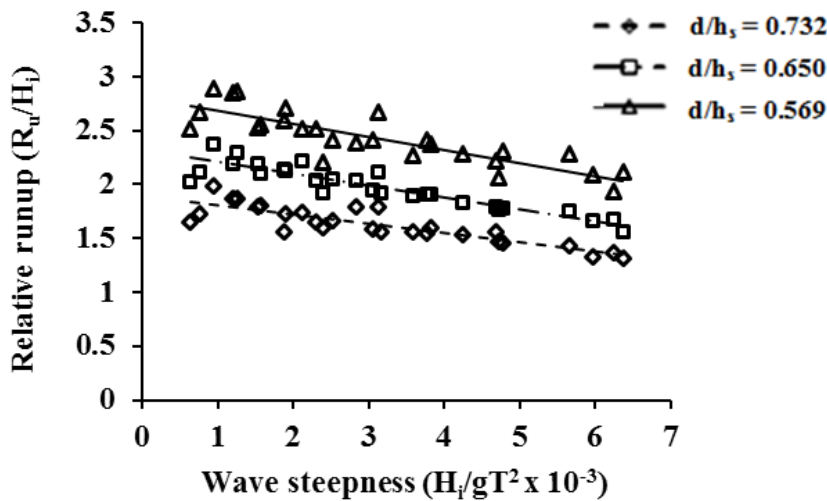
Fig. 5.13 Influence of H_i/gT^2 on R_u/H_i for S/D= 5

5.6.1.2 Seaside perforated QBW with S/D ratio equal to 2.5

In case of S/D equal to 2.5, the observed values for R_u/H_i varies from 0.7270 to 1.795 for $6.24 \times 10^{-4} < H_i/gT^2 < 6.4 \times 10^{-3}$. From Fig. 5.10, maximum value for R_u/H_i observed is 1.795 at a wave height of 0.03 m and a wave period of 2 s ($H_i/gT^2 = 7.645 \times 10^{-4}$) and at water depth equal to 0.35 m (d/h_s equal to 0.569). The minimum R_u/H_i observed is 0.7270 at a wave height of 0.09 m and a wave period of 1.2 s ($H_i/gT^2 = 6.371 \times 10^{-3}$) and at water depth equal to 0.45 m ($d/h_s = 0.732$).

5.6.1.3 Seaside perforated QBW with S/D ratio equal to 3

When S/D ratio is increased to 3, the values obtained from the experiments for R_u/H_i are observed to be varying from 0.9770 to 2.168 for $6.24 \times 10^{-4} < H_i/gT^2 < 6.4 \times 10^{-3}$.

159

The maximum R_u/H_i observed is 2.168 at a wave height of 0.03 m and a wave period of 1.8 s ($H_i/gT^2 = 9.439 \times 10^{-4}$ and at water depth equal to 0.35 m). The minimum R_u/H_i observed is 0.9770 at a wave height of 0.09 m and a wave period of 1.2s ($H_i/gT^2 = 6.371 \times 10^{-3}$ and at water depth equal to 0.45 m) (Refer Fig. 5. 11).

5.6.1.4 Seaside perforated QBW with S/D ratio equal to 4

Fig. 5.12 shows the variation of R_u/H_i with H_i/gT^2 for different water depths with radius of breakwater constant (R = 0.55 m or h_s= 0.615 m) and S/D ratio equal to 4. The values of the relative runup, R_u/H_i varies from 1.140 to 2.552 for $6.24 \times 10^{-4} < H_i/gT^2 < 6.4 \times 10^{-3}$.

The maximum R_u/H_i observed is 2.552 at a wave height of 0.03 m and a wave period of 1.8 s ($H_i/gT^2 = 9.439 \times 10^{-4}$) and at water depth equal to 0.35 m (d/h_s equal to 0.569). The minimum R_u/H_i observed is 1.140 at a wave height of 0.09 m and a wave period of 1.2s ($H_i/gT^2 = 6.3710 \times 10^{-3}$) and at water depth equal to 0.45 m (d/h_s equal to 0.732).

5.6.1.5 Seaside perforated QBW with S/D ratio equal to 5

From Fig. 5.13, it is observed that for S/D equal to 5 and for all values d/h_s and QBW of 0.55 m radius or h_s= 0.615 cm, R_u/H_i varies from 1.309 to 2.779 for $6.24 \times 10^{-4} < H_i/gT^2 < 6.4 \times 10^{-3}$.

The highest value for R_u/H_i observed is 2.779 at a wave height of 0.03 m and a wave period of 1.8 s ($H_i/gT^2 = 9.439 \times 10^{-4}$) and at water depth equal to 0.35 m (d/h_s equal to 0.569). The lowest R_u/H_i observed is 1.309 at a wave height of 0.09 m and a wave period of 1.2s ($H_i/gT^2 = 6.371 \times 10^{-3}$) and at water depth equal to 0.45 m (d/h_s equal to 0.732).

The variation of R_u/H_i with H_i/gT^2 for different d/h_s and S/D ratio are summarized in table From all the graphs plotted for different S/D ratio and H_i/gT^2, it is observed that relative wave runup decreases with increase in wave steepness.

The decrease in relative wave runup with wave steepness may be because when the waves of shorter wave period or wave length run over the curved surface, most of the energy of the incident waves is reflected and hence less energy will be available for the runup.

Table 5.1 Variation of relative wave runup, R_u/H_i (for R = 0.55 m, h_s= 0.615 m)

S/D ratio	Water depth in m	d/ h_s	Range of R_u/H_i values
2	0.45	0.732	0.7790- 1.1650
	0.40	0.650	1.0370 – 1.5820
	0.35	0.569	1.2680 – 1.8890
2.5	0.45	0.732	0.7270- 1.0890
	0.40	0.650	0.9853 – 1.5030
	0.35	0.569	1.2040 – 1.7950
3	0.45	0.732	0.9770 – 1.4560
	0.40	0.650	1.1920 – 1.8185
	0.35	0.569	1.4570 - 2.1690
4	0.45	0.732	1.140- 1.7390
	0.40	0.650	1.4020 - 2.1390
	0.35	0.569	1.7150 - 2.5520
5	0.45	0.732	1.3090 – 1.9870
	0.40	0.650	1.5550 – 2.3770
	0.35	0.569	1.9370 – 2.7790

5.6.2   Influence of water depth on relative wave runup

5.6.2.1 Seaside perforated QBW with S/D ratio equal to 2

For S/D ratio equal to 2 and at a water depth equal to 0.45 m (d/h_s equal to 0.732), the maximum value for R_u/H_i observed is 1.165 when H_i/gT^2 = 9.439 x10^{-4}. At the same water depth, the minimum value of R_u/H_i is 0.779 for H_i/gT^2 = 6.3710 x10^{-3} (Refer Fig. 5.14).

For water depth equal to 0.40 m (d/h_s = 0.650), the maximum value for R_u/H_i observed is 1.582 at H_i/gT^2 = 9.439 x10^{-4}. Under the same condition, the minimum value of R_u/H_i obtained is 1.037 for H_i/gT^2 = 6.3710 x10^{-3}. At water depth equal to 0.35 m (d/h_s = 0.569), the maximum and the minimum value for R_u/H_i observed are 1.889 and 1.268 for H_i/gT^2= 6.241 x10^{-3} and 7.645 x10^{-4} respectively.

As water depth increases from 0.35 m to 0.40 m there is a reduction in R_u/H_i by 16.55% to 18.3%.When water depth increases from 0.35 m to 0.45m there is a

reduction in R_u/H_i by 38.3% to 38.50%.
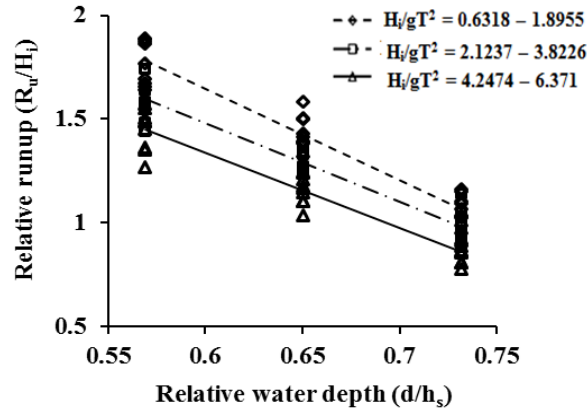
(a) For S/D = 2
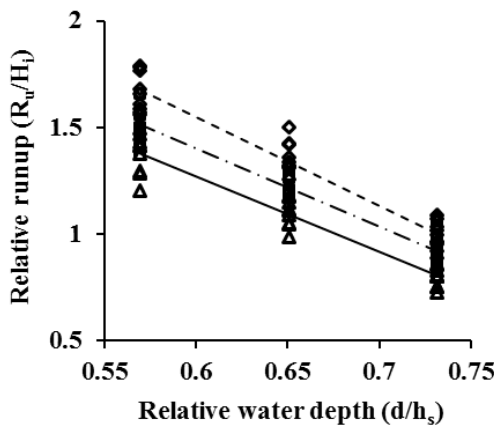
(b) For S/D = 2.5
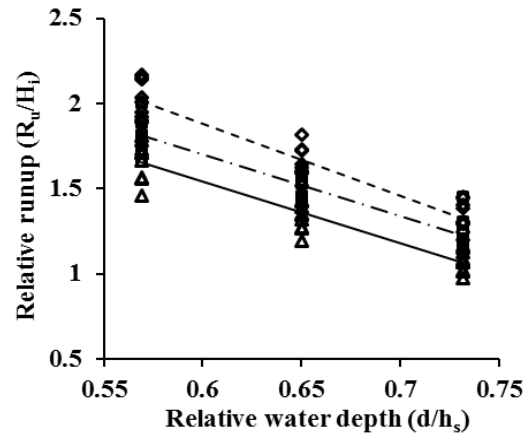
(c) For S/D = 3
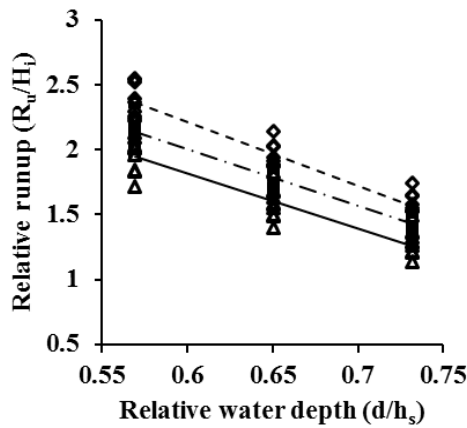
(d) For S/D = 4
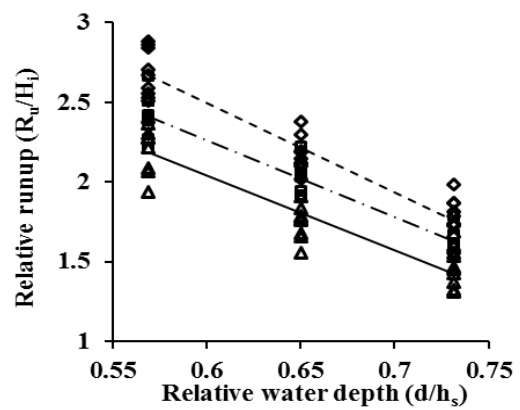
(e) For S/D = 5

Fig. 5.14 Variation of R_u/H_i with d/h_s, for S/D= 2, 2.5, 3, 4, 5

5.6.2.2 Seaside perforated QBW with S/D ratio equal to 2.5

From the plotted non- dimensional graphs Fig. 5.14 it is observed that for 0.45 m water depth ($d/h_s = 0.732$), the maximum value for R_u/H_i is 1.089 at a wave height of

0.03m and a wave period of 1.8 s (H_i/gT^2 = 9.439 $\times 10^{-4}$). At the same water depth, the minimum value of R_u/H_i obtained is 0.7270 for H_i/gT^2 = 6.3710 $\times 10^{-3}$. For 0.40 m water depth (d/h_s = 0.650), the maximum value for R_u/H_i observed is 1.5030 at H_i/gT^2 = 9.439 $\times 10^{-4}$. Under the same condition, the minimum R_u/H_i value of obtained is 0.9853 for H_i/gT^2 = 6.3710 $\times 10^{-3}$. At 0.35 m water depth (d/h_s equal to 0.569), the maximum and the minimum value for R_u/H_i observed is1.204 and 1.795 for H_i/gT^2 = 6.2410 $\times 10^{-3}$ and 7.645 $\times 10^{-4}$ respectively.

From the results, it is clear that as the water depth increases, the value of R_u/H_i decreases and the minimum value for R_u/H_i are observed at a water depth of 0.45 m. As water depth increases from 0.35 m to 0.40 m there is a reduction in relative wave runup by 16.27 % to 18.16%. When water depth increases from 0.35 m to 0.45 m there is a reduction in relative wave runup by 39 % to 40%.

5.6.2.3 Seaside perforated QBW with S/D ratio equal to 3

At a water depth equal to 0.45 m, the maximum and the minimum value for R_u/H_i are 1.456 and 0.977 at H_i/gT^2 = 2.2936 $\times 10^{-3}$ and H_i/gT^2 = 6.371 $\times 10^{-3}$. For water depth equal to 0.40 m (d/h_s = 0.650), the maximum R_u/H_i observed is 1.818 for H_i/gT^2 = 9.439 $\times 10^{-4}$. Under the same condition, the minimum R_u/H_i obtained is 1.192 for H_i/gT^2 = 6.371 $\times 10^{-3}$.

At 0.35 m water depth (d/h_s = 0.569), the maximum and the minimum value for R_u/H_i observed are 2.169 and 1.457 for H_i/gT^2 = 9.439 $\times 10^{-4}$ and 6.241 $\times 10^{-3}$ respectively. As water depth increases from 0.35 m to 0.40 m there is a reduction in R_u/H_i by 16.15% to 18.19% .When water depth increases from 0.35 m to 0.45m there is a reduction in R_u/H_i by 32.87 to 32.94%.

5.6.2.4 Seaside perforated QBW with S/D ratio equal to 4

For 0.45 m water depth and QBW of radius 0.55 m, the maximum R_u/H_i is 1.739 at a wave height of 0.03 m and a wave period of 1.8 s (H_i/gT^2 = 9.439 $\times 10^{-4}$). At the same water depth, the minimum value of R_u/H_i obtained is 1.140 for H_i/gT^2 = 6.371 $\times 10^{-3}$.

For water depth equal to 0.40 m (d/h_s equal to 0.650), the maximum value for R_u/H_i observed is 2.139 for H_i/gT^2 = 9.439 $\times 10^{-4}$. The minimum value of R_u/H_i obtained is 1.402 for H_i/gT^2 = 6.371 $\times 10^{-3}$.

At a water depth equal to 0.35 m (d/h_s equal to 0.569), the maximum and the minimum R_u/H_i observed are 2.552 and 1.715 for H_i/gT^2 = 9.439 $\times 10^{-4}$ and 6.241 $\times 10^{-3}$ respectively.

As water depth increases from 0.35 m to 0.40 m there is a reduction in R_u/H_i by 16.18% to 18.25% .When water depth increases from 0.35 m to 0.45m there is a reduction in R_u/H_i by 31.85 to 33.53%.

5.6.2.5 Seaside perforated QBW with S/D ratio equal to 5

At water depth equal to 0.45 m, the maximum value for R_u/H_i is 1.987 at a wave height of 0.03 m and a wave period of 1.8 s (H_i/gT^2 = 9.439 $\times 10^{-4}$). At the same water depth, the minimum value of R_u/H_i obtained is 1.309 for H_i/gT^2 = 6.371 $\times 10^{-3}$.

For water depth equal to 0.40 m (d/h_s equal to 0.650), the maximum value for R_u/H_i observed is 2.377 for H_i/gT^2 = 9.439 $\times 10^{-4}$. Under the same condition, the minimum value of R_u/H_i obtained is 1.555 for H_i/gT^2 = 6.371 $\times 10^{-3}$.

At a water depth equal to 0.35 m (d/h_s equal to 0.569), the maximum and the minimum value for R_u/H_i observed is 2.799 and 1.937 for H_i/gT^2 = 9.439 $\times 10^{-4}$ and 6.241 $\times 10^{-3}$ respectively.

As water depth increases from 0.35 m to 0.40 m there is a reduction in R_u/H_i by 17.55% to 19.72% .When water depth increases from 0.35 m to 0.45m there is a reduction in R_u/H_i by 31.08 to 32.42%.

5.6.3   Influence of S/D ratio on relative wave runup

At a constant QBW radius(R) and different water depths, variations of R_u/H_i for different values of S/D ratio are analyzed separately. It is observed that R_u/H_i decreases with decrease in S/D or increase in percentage of perforations for all values of d/h_s. Considering 0.45 m water depth (d/h_s = 0.693), for an S/D = 5, R_u/H_i varies in the range 1.309 to 1.987.for $6.24 \times 10^{-4} < H_i/gT^2 < 6.4 \times 10^{-3}$.

For S/D = 4, the range of variation of R_u/H_i is found to be 1.140 to 1.739; for S/D = 3 R_u/H_i is observed to be in the range 0.9770 to 1.456; for S/D = 2.5, the value of R_u/H_i varies in the range 0.7270 to 1.089 and for an S/D = 2, the range of variation of R_u/H_i is from 0.779 to 1.165 (Refer Fig. 5.15).
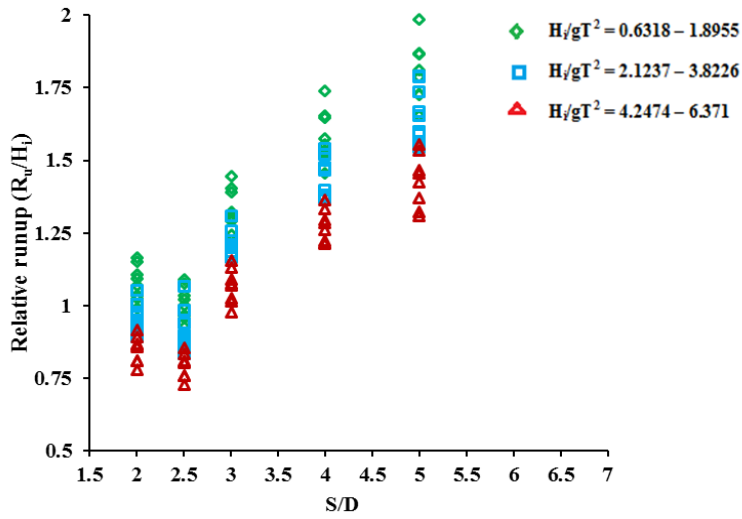
(a) For d/hs = 0.732
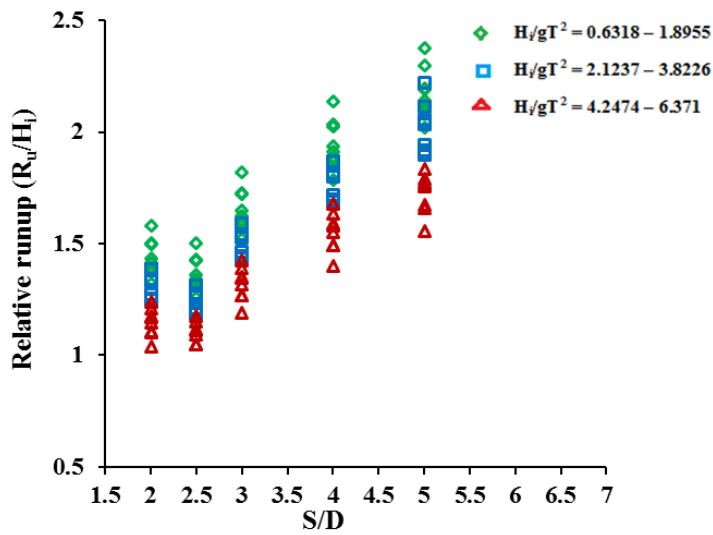
(b) For d/hs = 0.650
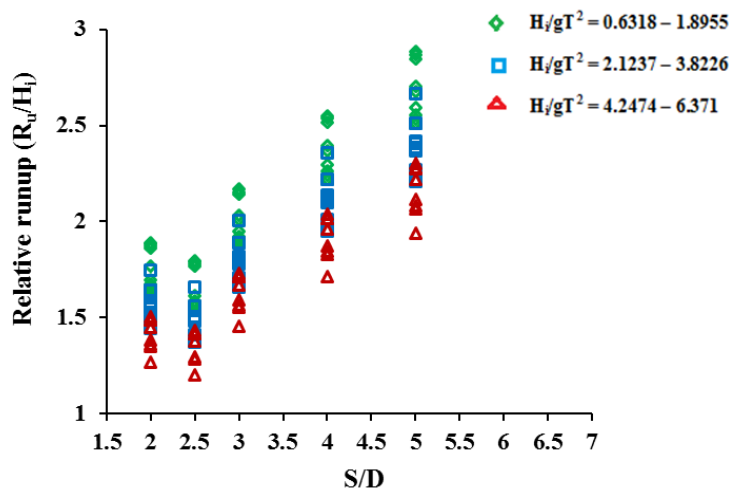
(c) For d/hs = 0.569

Fig. 5.15 Influence of S/D on R_u/H_i

When water depth is reduced to 0.40 m (d/h_s equal to 0.650), for an S/D ratio equal to 5, the value of R_u/H_i varies in the range 1.555 to 2.377.for $6.24 \times 10^{-4} < H_i/gT^2 < 6.4 \times 10^{-3}$. For S/D ratio equal to 4, the range of variation of R_u/H_i is found to be 1.402 to 2.139. The variation of R_u/H_i for S/D ratio equal to 3 is observed to be in the range 1.192 to 1.8185; for S/D ratio equal to 2.5, the value of R_u/H_i varies in the range 0.9853 to 1.503 and for an S/D ratio equal to 2, the range of variation of R_u/H_i is from 1.037 to 1.582.

For experiments conducted on seaside perforated QBW of radius 0.55 m at a water depth of 0.35 m (d/h_s equal to 0.569), it is observed that for S/D ratio equal to 5, the value of R_u/H_i varies in the range 1.937 to 2.799 for $6.24 \times 10^{-4} < H_i/gT^2 < 6.4 \times 10^{-3}$. For the same radius of QBW and at the same water depth, for S/D ratio equal to 4, R_u/H_i is observed to be in the range 1.715 to 2.552. The range of variation of R_u/H_i is from 1.457 to 2.169 for S/D ratio equal to 3, from 1.204 to 1.795 for S/D ratio equal to 2.5 and from 1.268 to 1.889 for S/D ratio equal to 2.

From the results for R_u/H_i, it is observed that at a water depth equal to 0.35 m , the percentage reduction in R_u/H_i for S/D = 4 is 8.17% to 11.46 % compared to S/D ratio equal to 5. The percentage reduction in R_u/H_i for S/D ratio equal to 3, 2.5 and 2 are 21.95% to 24.78% , 35.41% to 37.84% and 32.02% to 34.53% with respect to S/D= 5.

At a water depth equal to 0.40 m, the percentage reduction in R_u/H_i for S/D = 4, 3, 2.5 and 2 are 9.83% to 10.02% , 23.34% to 23.49% , 36.63% to 36.77% and 33.31% to 33.44% with respect to S/D = 5. At a water depth equal to 0.45 m ,the percentage reduction in R_u/H_i for S/D ratio equal to 4 is 12.48% to 12.91% compared to S/D ratio equal to 5. The percentage reduction in R_u/H_i for S/D = 3, 2.5 and 2 are 25.36% to 26.72%, 44.46% to 45.19% and 40.48% to 41.37% with respect to S/D = 5.

When S/D decreases, the spacing between the perforations also decreases resulting in more perforations on the QBW surface. Therefore decrease in S/D ratio causes higher dissipation of wave energy due to turbulence inside the QBW chamber resulting in lesser relative wave runup (R_u/H_i). When compared to S/D = 2.5, R_u/H_i values were higher for S/D=2 due to additional runup resulting from back propagation of waves.

5.7 VARIATION OF RELATIVE WAVE RUNUP (R_u/H_i) FOR QBW 0.575 m RADIUS (h_s= 0.640 m)

5.7.1 Influence of incident wave steepness on relative wave runup

(a) For S/D=2

(b) For S/D =2.5

(c) For S/D=3

(d) For S/D = 4

(e) For S/D = 5
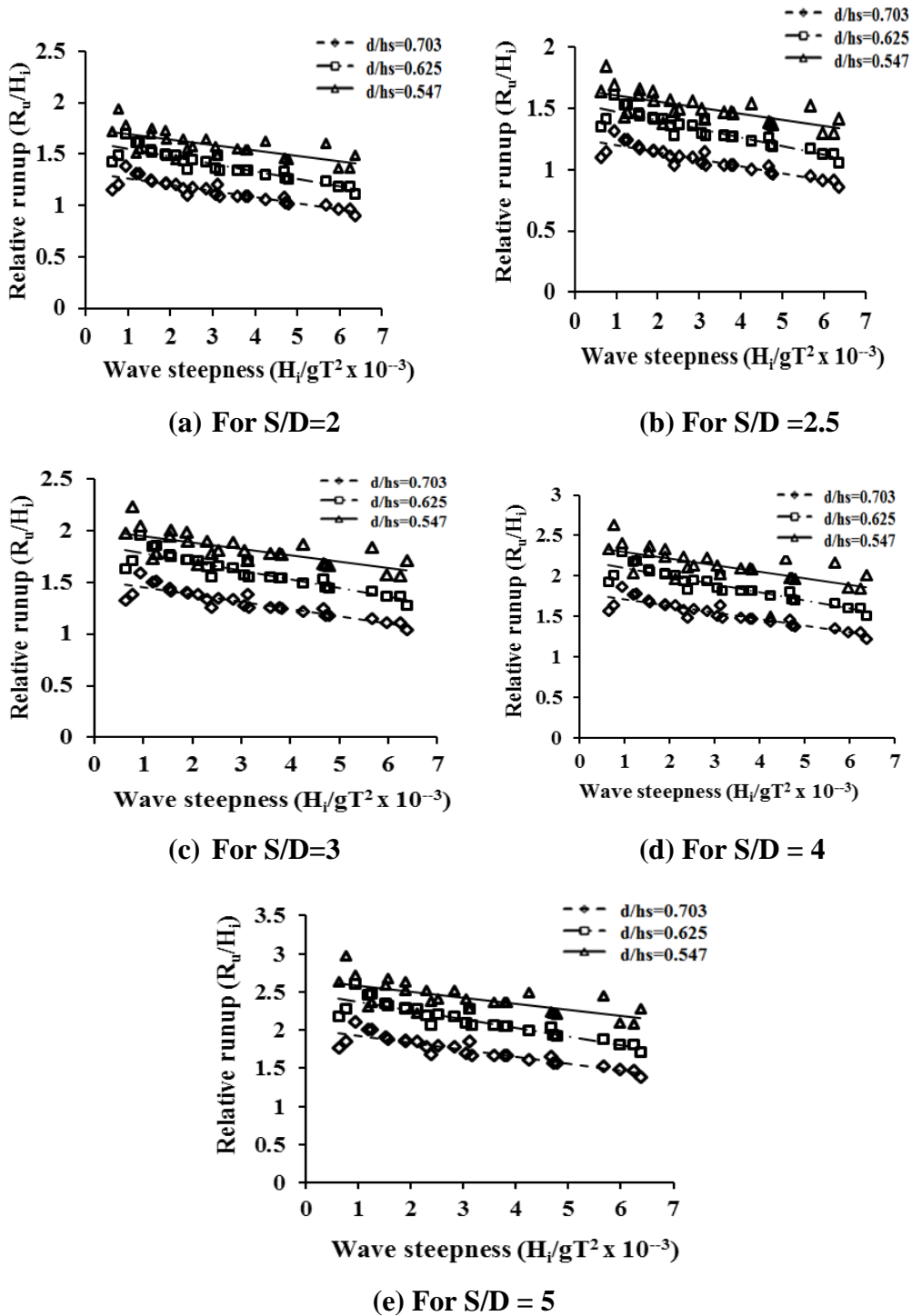
Fig. 5.16 Influence of H_i/gT^2 on R_u/H_i for different d/hs values and S/D ratio

5.7.1.1 Seaside perforated QBW with S/D ratio equal to 2

For S/D ratio equal to 2, considering all values d/h_s and for QBW radius of 0.575 m,

the relative wave runup, R_u/H_i varies from 0.9067 to 1.977 for $6.24 \times 10^{-4} < H_i/gT^2 <$ 6.4×10^{-3} (Refer Fig. 5.16 (a)). It is clear from the graph that R_u/H_i decreases with increase in H_i/gT^2 for all values of d/h_s. The maximum R_u/H_i observed is 1.977 at a wave height of 0.03 m and a wave period of 1.8 s ($H_i/gT^2 = 9.439 \times 10^{-4}$) and at water depth equal to 0.35 m (d/h_s equal to 0.547). The minimum value for R_u/H_i observed is 0.9067 at a wave height of 0.09 m and a wave period of 1.2 s ($H_i/gT^2 = 6.371 \times 10^{-3}$) and at water depth equal to 0.45 m ($d/h_s = 0.703$).

5.7.1.2 Seaside perforated QBW with S/D ratio equal to 2.5

From Fig. 5.16 (b) it was observed that for S/D ratio equal to 2.5, considering all values d/h_s, the values of R_u/H_i varies from 0.8613 to 1.886 for $6.24 \times 10^{-4} < H_i/gT^2 <$ 6.4×10^{-3}. The maximum value for R_u/H_i observed is 1.886 for wave height of 0.03 m and a wave period of 1.8 s ($H_i/gT^2 = 9.439 \times 10^{-4}$) and at water depth equal to 0.35 m (d/h_s equal to 0.547). The minimum value for R_u/H_i observed is 0.8163 for wave height of 0.09 m and a wave period of 1.2 s ($H_i/gT^2 = 6.371 \times 10^{-3}$) and at water depth equal to 0.45 m ($d/h_s = 0.703$).

5.7.1.3 Seaside perforated QBW with S/D ratio equal to 3

From the graph plotted for S/D= 3, it is clear that for all values d/h_s and for QBW of radius 0.575 m, R_u/H_i varies from 1.042 to 2.235 for $6.24 \times 10^{-4} < H_i/gT^2 < 6.4 \times 10^{-3}$ (Refer Fig. 5.16 (c)).

The maximum value for R_u/H_i observed is 2.235 for wave height of 0.03 m and a wave period of 2 s ($H_i/gT^2 = 7.645 \times 10^{-4}$) and at water depth equal to 0.35 m (d/h_s equal to 0.547). The minimum R_u/H_i observed is 1.042 for wave height of 0.09 m and a wave period of 1.2 s ($H_i/gT^2 = 6.371 \times 10^{-3}$) and at water depth equal to 0.45 m ($d/h_s = 0.703$).

5.7.1.4 Seaside perforated QBW with S/D ratio equal to 4

From Fig. 5.16 (d) values of R_u/H_i was observed to be varying from 1.226 to 2.629 for $6.24 \times 10^{-4} < H_i/gT^2 < 6.4 \times 10^{-3}$ for S/D ratio equal to 4. The maximum value for R_u/H_i observed is 2.629 for wave height of 0.03 m and a wave period of 2 s ($H_i/gT^2 = 7.645 \times 10^{-4}$) and at water depth equal to 0.35 m ($d/h_s = 0.547$). The minimum value for R_u/H_i observed is 1.226 for wave height of 0.09 m and a wave period of 1.2 s

$(H_i/gT^2 = 6.371 \times 10^{-3})$ and at water depth equal to 0.45 m $(d/h_s = 0.703)$.

5.7.1.5 Seaside perforated QBW with S/D ratio equal to 5

For S/D = 5, R_u/H_i for QBW of radius equal to 0.575 m varies from 1.385 to 2.971 for $6.24 \times 10^{-4} < H_i/gT^2 < 6.4 \times 10^{-3}$ (Refer Fig. 5.16 (e)). The maximum value for R_u/H_i observed is 2.889 at $H_i/gT^2 = 7.645 \times 10^{-4}$ and at water depth equal to 0.35 m. The minimum value for R_u/H_i observed is 1.385 at $H_i/gT^2 = 6.371 \times 10^{-3})$ and at 0.45 m water depth. The variation of R_u/H_i with wave steepness for different water depths and S/D ratio for QBW with 0.575 m radius are summarized in Table 5.2.

Table 5.2 Variation of R_u/H_i (R = 0.575 m or h_s= 0.640 m)

S/D ratio	Water depth in m	d/ h_s	Range of R_u/H_i values
2	0.45	0.703	0.9067 – 1.3830
	0.40	0.625	1.1150 – 1.7010
	0.35	0.547	1.3630 – 1.977
2.5	0.45	0.703	0.8613 – 1.3139
	0.40	0.625	1.0594 – 1.6161
	0.35	0.547	1.2950 – 1.886
3	0.45	0.703	1.0420 – 1.5890
	0.40	0.625	1.2820 – 1.9550
	0.35	0.547	1.5670 – 2.2350
4	0.45	0.703	1.2260 – 1.8700
	0.40	0.625	1.5080 - 2.3000
	0.35	0.547	1.8430 – 2.6290
5	0.45	0.703	1.3850 – 2.1130
	0.40	0.625	1.7040 – 2.555
	0.35	0.547	2.830 – 2.889

5.7.2 Influence of water depth on relative wave runup

For QBW of radius 0.575 m and S/D ratio equal to 2, the minimum value for R_u/H_i observed is 0.9067 when $d/h_s = 0.703$ (water depth = 0.45 m) (Refer Fig. 5.17). At the same condition for water depth equal to 0.40 m $(d/h_s = 0.625)$, the minimum

observed value for R_u/H_i is 1.1150 and for 0.35 m water depth ($d/h_s = 0.547$), the minimum observed value for R_u/H_i is 1.3630. The percentage decrease in R_u/H_i with increase in water depth from 0.35 m to 0.40 m is found to be 19.44% to 32.16%. Also the percentage decrease in R_u/H_i with increase in water depth from 0.35 m to 0.45 m is found to be 10.71% to 12.25%.

(a) For S/D =2

(b) For S/D =2.5

(c) For S/D =3
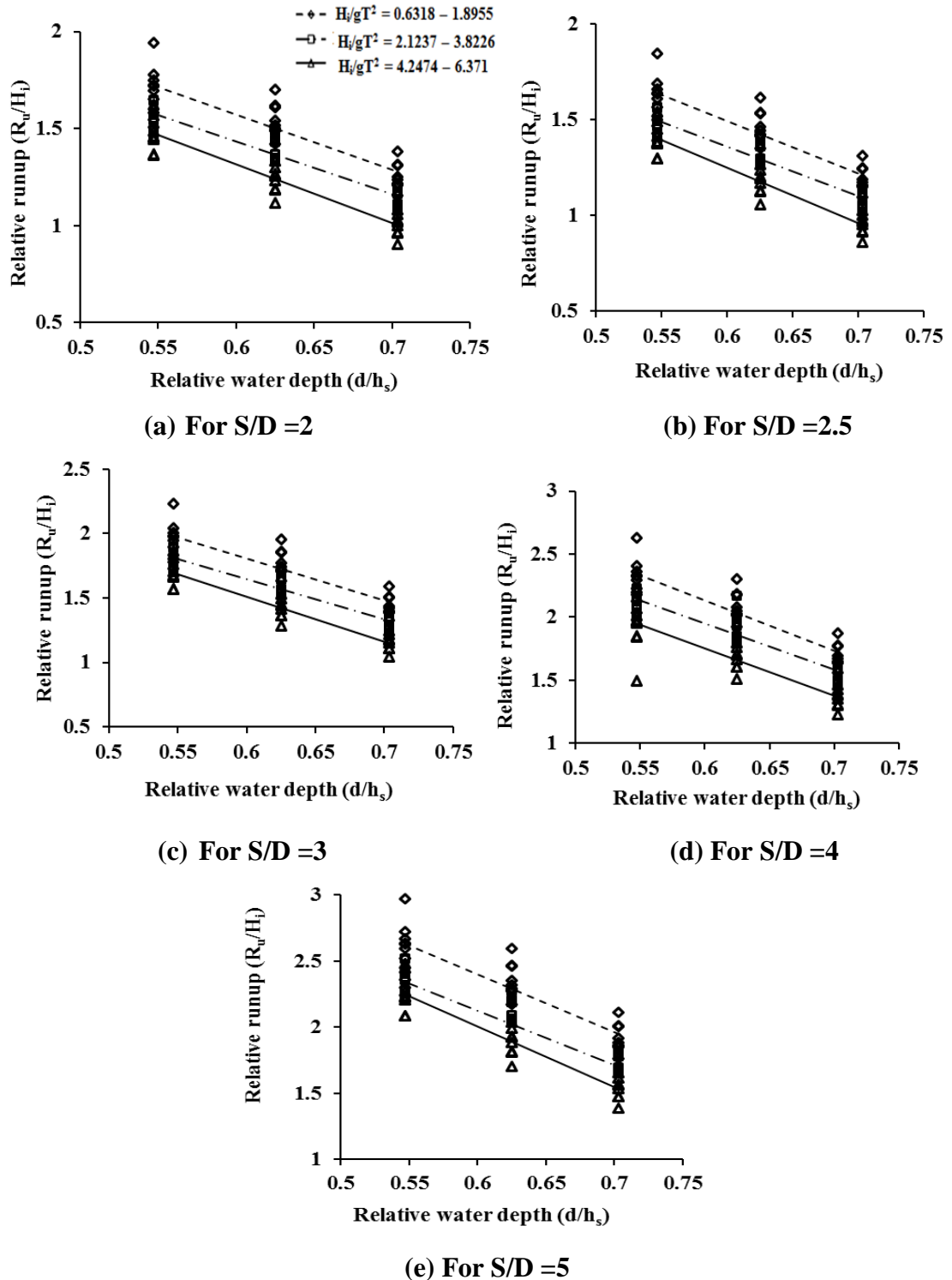
(d) For S/D =4

(e) For S/D =5

Fig. 5.17 Variation of R_u/H_i with d/h_s, for S/D= 2, 2.5, 3, 4, 5

For S/D ratio equal to 2.5, the minimum value observed for R_u/H_i is 0.8613 at a water depth of 0.45 m ($d/h_s = 0.703$). For 0.40 m water depth ($d/h_s = 0.625$), the minimum observed value for R_u/H_i is 1.0594 and for 0.35 m water depth ($d/h_s = 0.547$), the minimum observed value for R_u/H_i is 1.2950. The decrease in R_u/H_i with increase in water depth is more effective for 0.45 m water depth compared to 0.35m water depth i.e. from 28.57% to 32.16% and percentage reduction with increase in water depth from 0.35 m to 0.40 m water depth is found to be 10.65% to 12.50%.

For S/D ratio equal to 3 and under similar condition, the minimum observed value for R_u/H_i is 1.0420 at a water depth of 0.45 m. For water depth equal to 0.40 m, the minimum observed value for R_u/H_i is 1.2820 and for water depth equal to 0.35 m, the minimum observed value for R_u/H_i is 1.5670.When water depth is increased from 0.35 m to 0.40 m there is decrease in R_u/H_i from 10.71% to 12.26% and for increase in water depth from 0.35 m to 0.45 m there is a decrease in R_u/H_i from 28.57% to 32.16%.

For QBW of radius 0.575 m with S/D ratio equal to 4, the minimum observed value for R_u/H_i is 1.226 at a water depth of 0.45 m. At the same condition for water depth equal to 0.40 m, the minimum observed value for R_u/H_i is 1.5080 and for a water depth equal to 0.35 m, the minimum observed value for R_u/H_i is 1.8430. The percentage reduction in R_u/H_i with increase in water depth from 0.35 m to 0.40 m is found to vary from 10.71% to 12.25% and from 0.35 m to 0.45 m varies from 28.57% to 32.16%. When S/D ratio is increased to 5 and under similar condition, the minimum observed value for R_u/H_i is 1.3850 at a water depth of 0.45 m. For water depth equal to 0.40 m, the minimum observed value for R_u/H_i is 1.7040 and for water depth equal to 0.35m, the minimum observed value for R_u/H_i is 2.0830.

5.7.3 Influence of S/D ratio on relative wave runup

The variation of R_u/H_i with S/D ratios for different H_i/gT^2 and under different water depths for a QBW of radius equal to 0.575 m is plotted as non-dimensional graphs. From Fig. 5.18, it is observed that the value R_u/H_i decreases with decrease in S/D ratios for all values of d/h_s and different ranges of H_i/gT^2 considered for the study.
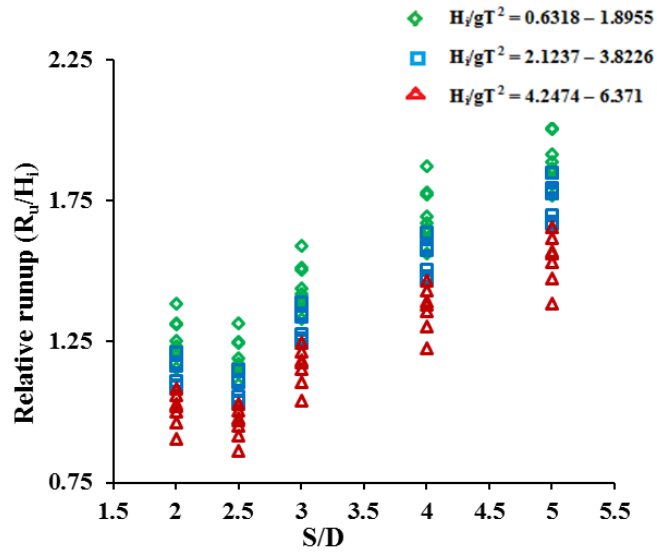
(a) For d/hs =0.703
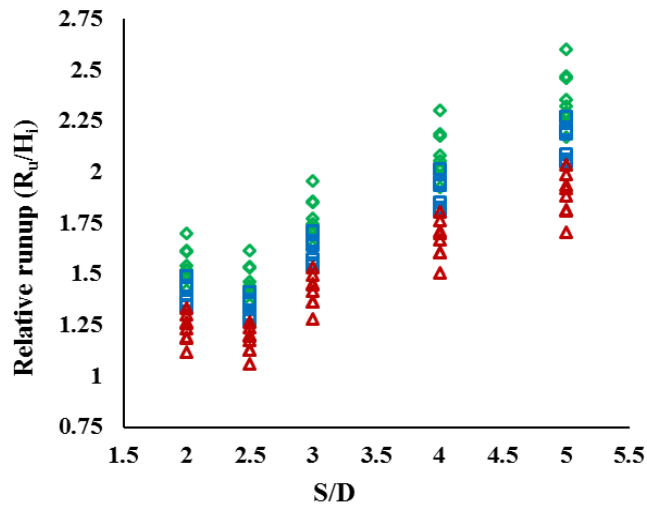
(b) For d/hs =0.625
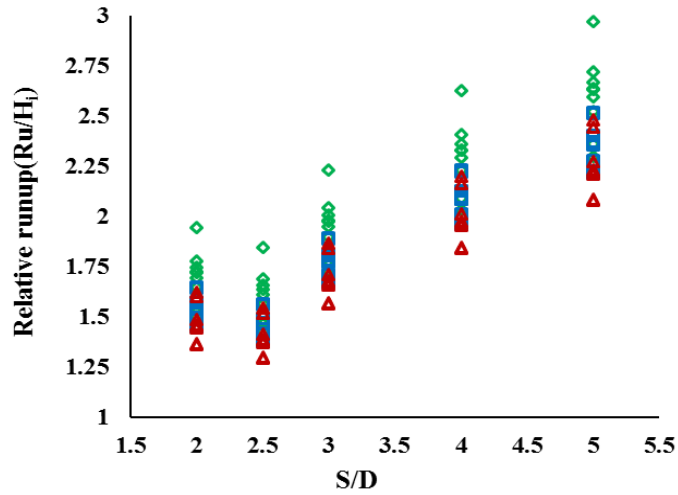
(c) For d/hs =0.547

Fig. 5.18 Influence of S/D on R_u/H_i

For a seaside perforated QBW of radius 0.575 m at a water depth of 0.45 m (d/h_s equal to 0.703) and S/D ratio equal to 2, R_u/H_i varies from 0.9067 to 1.3830 for $6.24 \times 10^{-4} < H_i/gT^2 < 6.4 \times 10^{-3}$. For the same radius of QBW and at the same water depth, for S/D ratio equal to 2.5, R_u/H_i varies from 0.8613 to 1.3139 and S/D ratio equal to 3, the range of variation of R_u/H_i is found to be 1.0420 to 1.5890.The variation of R_u/H_i for S/D ratio equal to 4 is observed to be in the range 1.2260 to 1.870 and for S/D ratio equal to 5, the value of R_u/H_i varies in the range 1.3850 to 2.1130.

For 0.40 m water depth (d/h_s equal to 0.625) and S/D ratio equal to 2, the range of variation of R_u/H_i is from 1.0594 to 1.6161. For the same radius of QBW and at the same water depth, S/D ratio equal to 2.5, the range of variation of R_u/H_i is found to be 1.1150 to 1.7010 and for S/D equal to 3 R_u/H_i varies from 1.2820 to 1.9550. The variation of R_u/H_i for S/D ratio equal to 4 is observed to be in the range 1.5080 to 2.300 and for S/D ratio equal to 5, the value of R_u/H_i varies in the range 1.7040 to 2.555.

Further reducing the water depth to 0.35 m (d/h_s equal to 0.547) and S/D ratio equal to 2, the range of variation of R_u/H_i is from 1.2950 to 1.886 for $6.24 \times 10^{-4} < H_i/gT^2 > 6.4 \times 10^{-3}$. For the same radius of QBW and at the same water depth, S/D ratio equal to 2.5, the range of variation of R_u/H_i is found to be 1.363 to 1.977 and for S/D ratio equal to 3, R_u/H_i varies from 1.567 to 2.235.The variation of R_u/H_i for S/D ratio equal to 4 is observed to be in the range 1.843 to 2.629 and for an S/D ratio equal to 5, the value of R_u/H_i varies in the range 2.083 to 2.889.

From the analysis of data for R_u/H_i, it is observed that at a water depth equal to 0.35 m, the percentage reduction in R_u/H_i for S/D ratio equal to 4 varies from 8.99% to 11.52% compared to S/D ratio equal to 5. The percentage reduction in R_u/H_i for S/D ratio equal to 3, 2.5 and 2 varies from 22.64% to 24.77%, 31.56% to 34.57% and 34.71 % to 37.83% with respect to S/D equal to 5.

Similarly at a water depth equal to 0.40 m, the percentage reduction in R_u/H_i for S/D ratio equal to 4, 3, 2.5 and 2 varies from 9.98% to 11.50 %, 23.48% to 24.76% , 33.42% to 34.56% and 36.74 % to 37.82% with respect to S/D = 5. At a water depth equal to 0.45 m ,the percentage reduction in R_u/H_i for S/D ratio equal to 4

varies from 11.48% to 11.50% compared to S/D ratio equal to 5. The percentage reduction in R_u/H_i for S/D ratio equal to 3, 2.5 and 2 varies from 24.76% to 24.79%, 34% to 34.54% and 37% to 37.81% with respect to S/D equal to 5.

The value of relative water depth (R_u/H_i) decreases with decrease in S/D ratio or increase in the perforations on QBW surface. This may be due to the reason that when S/D decreases the more perforations on the surface causes greater dissipation of wave energy resulting in lower values of R_u/H_i.

5.8 VARIATION OF RELATIVE WAVE RUNUP (R_u/H_i) FOR QBW 0.60 m RADIUS (h_s= 0.665 m)

5.8.1 Influence of incident wave steepness on relative wave runup

Fig. 5.19 shows the variation of R_u/H_i with H_i/gT^2 for different values of d/h_s and corresponding to S/D= 2, 2.5, 3, 4 and 5.

5.8.1.1 Seaside perforated QBW with S/D ratio equal to 2

For S/D = 2, R_u/H_i varies from 0.9855 to 2.2160 for $6.24 \times 10^{-4} < H_i/gT^2 < 6.4 \times 10^{-3}$. The maximum R_u/H_i observed is 2.2160 for wave height of 0.03 m and a wave period of 1.8 s ($H_i/gT^2 = 9.439 \times 10^{-4}$) and at 0.35 m water depth ($d/h_s = 0.526$). The minimum R_u/H_i observed is 0.9855 for wave height of 0.09 m and a wave period of 1.2 s ($H_i/gT^2 = 6.371 \times 10^{-3}$) and at 0.45 m water depth ($d/h_s = 0.677$).

5.8.1.2 Seaside perforated QBW with S/D ratio equal to 2.5

For S/D = 2.5, R_u/H_i varies from 0.9360 to 2.105 for $6.24 \times 10^{-4} < H_i/gT^2 < 6.4 \times 10^{-3}$. The maximum R_u/H_i observed is 2.216 for wave height of 0.03 m and a wave period of 1.8 s ($H_i/gT^2 = 9.439 \times 10^{-4}$) and at 0.35 m water depth ($d/h_s = 0.526$). The minimum R_u/H_i observed is 0.9855 for wave height of 0.09 m and a wave period of 1.2 s ($H_i/gT^2 = 6.371 \times 10^{-3}$) and at water depth equal to 0.45 m ($d/h_s = 0.677$).

5.8.1.3 Seaside perforated QBW with S/D ratio equal to 3

The values for R_u/H_i vary from 1.132 to 2.547 for $6.24 \times 10^{-4} < H_i/gT^2 < 6.4 \times 10^{-3}$ and S/D = 3. The maximum R_u/H_i observed is 2.547 for wave height of 0.03 m and a wave period of 1.8 s ($H_i/gT^2 = 9.439 \times 10^{-4}$) and at 0.35 m water depth ($d/h_s = 0.526$). The minimum R_u/H_i observed is 1.132 for $H_i/gT^2 = 6.371 \times 10^{-3}$ and 0.45 m water depth ($d/h_s = 0.677$).

(a) For S/D =2

(b) For S/D =2.5

(c) For S/D =3

(d) For S/D =4

(e) For S/D = 5
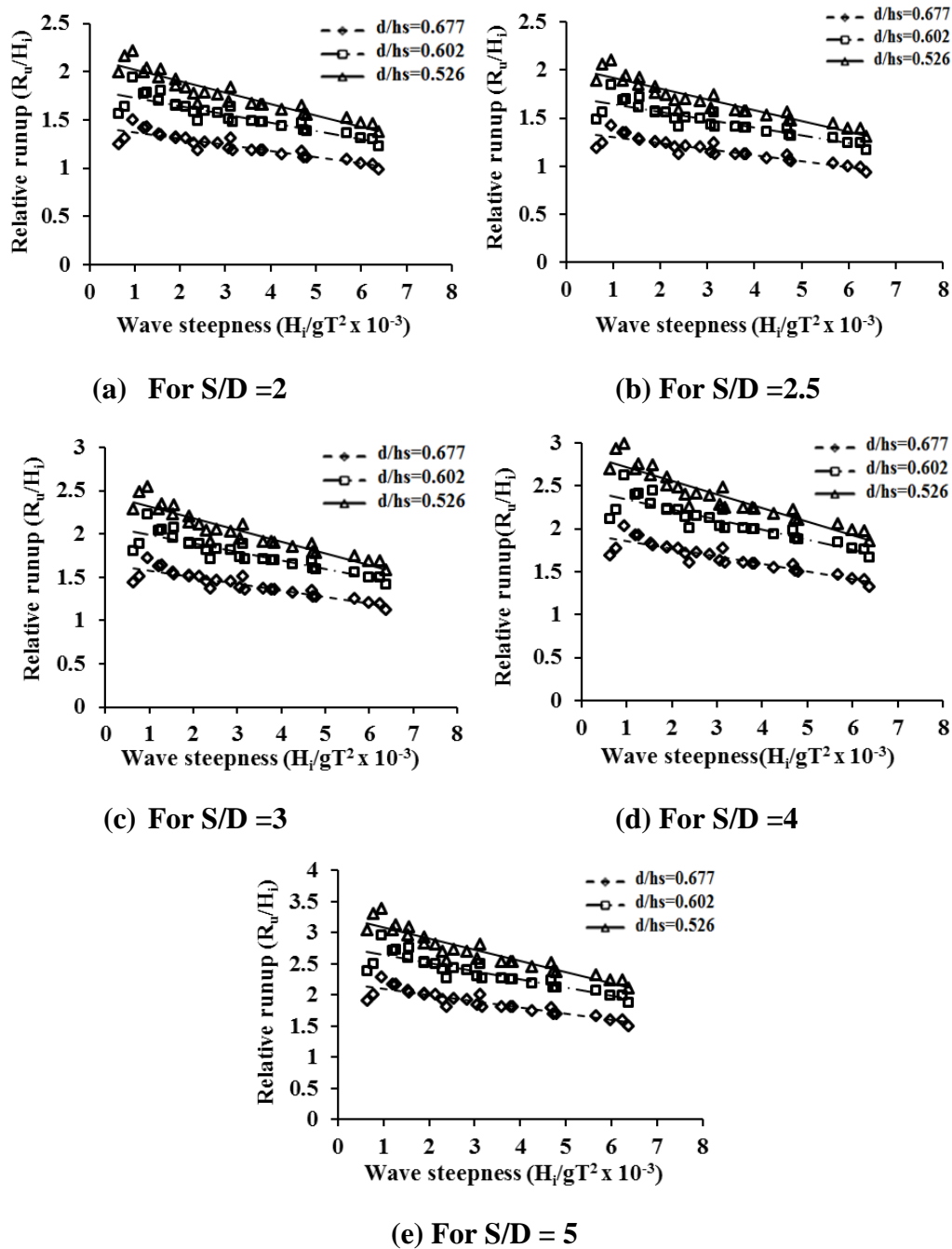
Fig. 5.19 Influence of H_i/gT^2 on R_u/H_i for different d/hs values and S/D ratio

5.8.1.4 Seaside perforated QBW with S/D ratio equal to 4

The maximum value for R_u/H_i observed is 2.996 at a wave height of 0.03 m and a wave period of 1.8 s ($H_i/gT^2 = 9.439 \times 10^{-4}$) and at water depth equal to 0.35 m ($d/h_s = 0.526$). The minimum value for R_u/H_i observed is 1.332 at a wave height of 0.09 m and a wave period of 1.2 s ($H_i/gT^2 = 6.371 \times 10^{-3}$) and at water depth equal to 0.45 m ($d/h_s = 0.677$).

5.8.1.5 Seaside perforated QBW with S/D ratio equal to 5

The maximum value for R_u/H_i observed is 3.222 at a wave height of 0.03 m and a wave period of 1.8 s ($H_i/gT^2 = 9.439 \times 10^{-4}$) and at water depth equal to 0.35 m. The minimum value for R_u/H_i observed is 1.505 at a wave height of 0.09 m and a wave period of 1.2 s ($H_i/gT^2 = 6.371 \times 10^{-3}$) and at 0.45 m water depth.

From the results, it was observed that R_u/H_i decreases with increase in H_i/gT^2 for all values of d/h_s. Therefore it was clear that when H_i/gT^2 increases, major portion of the wave energy is reflected and only less energy available for wave runup or R_u/H_i.

The variation of R_u/H_i with wave steepness for different water depths and S/D ratio for QBW with 0.60 m radius are summarized in Table 5.3. From Table 5.3 it was clear that the values for R_u/H_i increases with decrease in d/h_s and increases with increase in S/D values.

Table 5.3 Variation of R_u/H_i (for R = 0.60 m or h_s= 0.665 m)

S/D ratio	Water depth in m	d/ h_s	Range of R_u/H_i values
2	0.45	0.677	0.9855 – 1.5034
	0.40	0.602	1.2318 – 1.9440
	0.35	0.526	1.3790 – 2.2160
2.5	0.45	0.677	0.9360 – 1.4280
	0.40	0.602	1.170 – 1.8470
	0.35	0.526	1.310 – 2.1050
3	0.45	0.677	1.1320 – 1.7280
	0.40	0.602	1.4159 – 2.2340
	0.35	0.526	1.5850 – 2.5470
4	0.45	0.677	1.3320 – 2.0330
	0.40	0.602	1.6650 - 2.6290
	0.35	0.526	1.8650 – 2.9960
5	0.45	0.677	1.5050 – 2.2970
	0.40	0.602	1.8820 – 2.9150
	0.35	0.526	2.1080 – 3.2220

5.8.2 Influence of water depth on relative wave runup

(a) For S/D = 2

(b) For S/D = 2.5

(c) For S/D = 3

(d) For S/D = 4
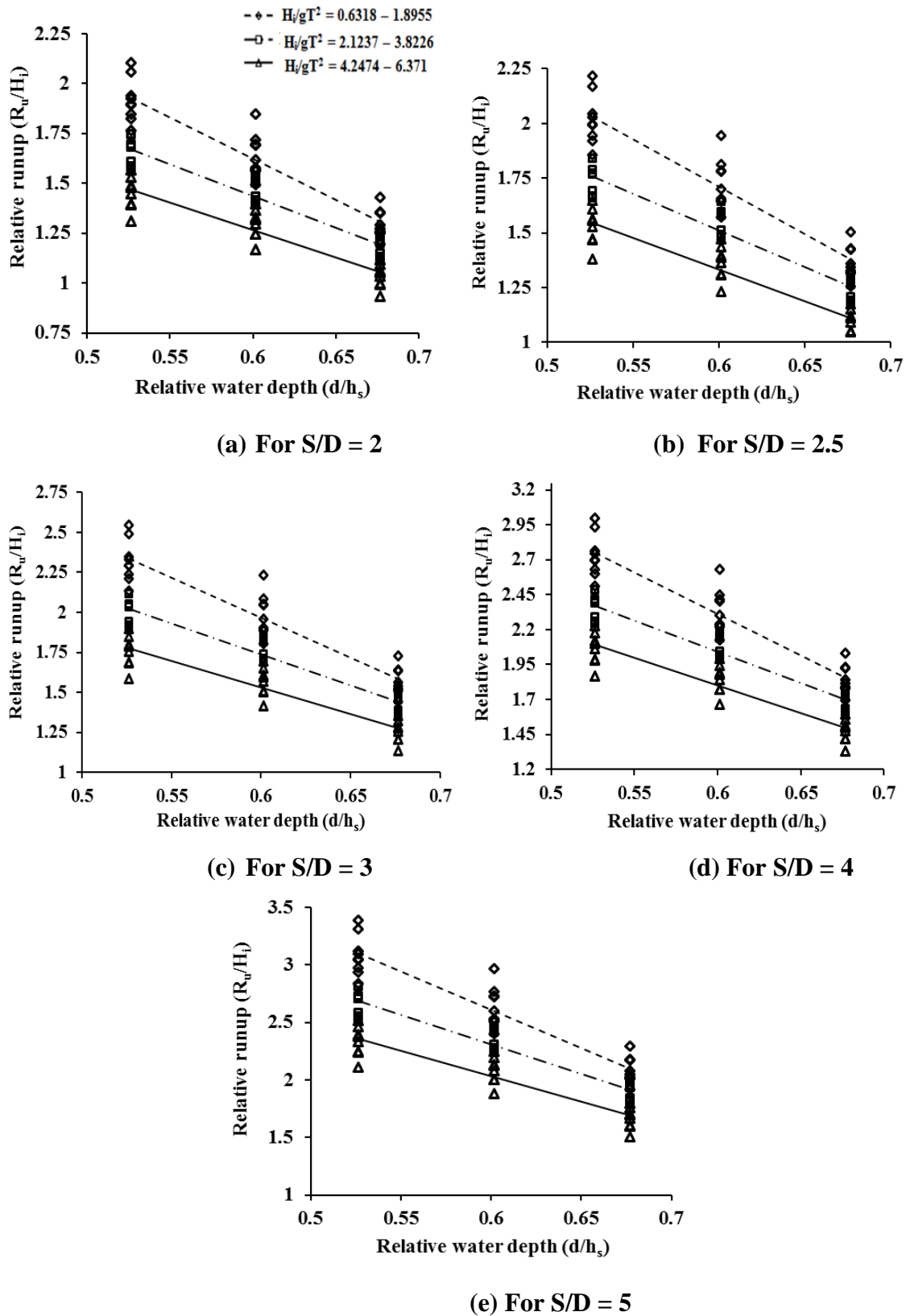
(e) For S/D = 5

**Fig. 5.20 Variation of R_u/H_i with d/h_s for S/D= 2, 2.5, 3, 4 and 5**

For QBW of radius 0.60 m and S/D ratio equal to 2, the minimum value for R_u/H_i observed is 0.9885 at a water depth of 0.45 m. At the same condition for water depth equal to 0.40 m, the minimum observed value for R_u/H_i is 1.2318 and for a water depth equal to 0.35 m, the minimum observed value for R_u/H_i is 1.3790 (Refer Fig. 5.20).

When S/D ratio is changed to 2.5 and under similar condition, the minimum observed value for R_u/H_i is 0.9360 at a water depth of 0.45 m. For water depth equal to 0.40 m, the minimum observed value for R_u/H_i is 1.170 and for water depth equal to 0.35 m, the minimum observed value for R_u/H_i is 1.310.

Further increasing S/D ratio to 3 and under similar condition, the minimum observed value for R_u/H_i is 1.1320 at a water depth of 0.45 m. For water depth equal to 0.40 m, the minimum observed value for R_u/H_i is 1.4159 and for water depth equal to 0.35 m, the minimum observed value for R_u/H_i is 1.5850.

When S/D ratio is equal to 4, the minimum observed value for R_u/H_i is 1.332 at a water depth of 0.45 m. At the same condition for water depth equal to 0.40 m, the minimum observed value for R_u/H_i is 1.6650 and for a water depth equal to 0.35 m, the minimum observed value for R_u/H_i is 1.8650.

For S/D ratio equal to 5 and under similar condition, the minimum observed value for R_u/H_i is 1.5050 at a water depth of 0.45 m. For water depth equal to 0.40 m, the minimum observed value for R_u/H_i is 1.8820 and for water depth equal to 0.35 m, the minimum observed value for R_u/H_i is 2.1080.

5.8.3 Influence of S/D ratio on relative wave runup

The variation of R_u/H_i with H_i/gT^2 for different S/D ratios and under different water depths for a QBW of radius equal to 0.60 m are plotted as non-dimensional graphs.

From Fig.5.21, it is observed that the value R_u/H_i decreases with decrease in S/D ratios 5, 4, 3 and 2.5 but increases for S/D= 2 for all values of d/h_s and different ranges of H_i/gT^2 considered for the study.

When S/D ratio decreases the perforations on the QBW will increase and the wave dissipation will be more resulting in lower values of S/D.
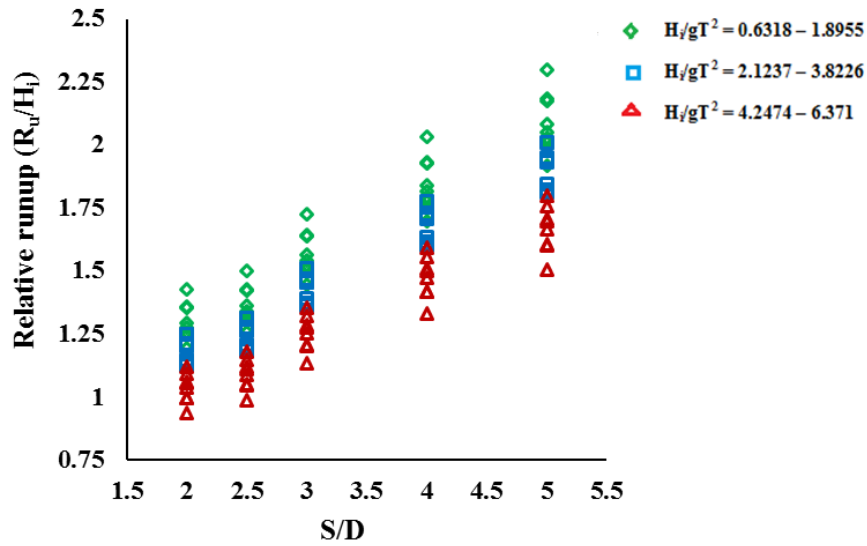
(a) For d/hs = 0.677
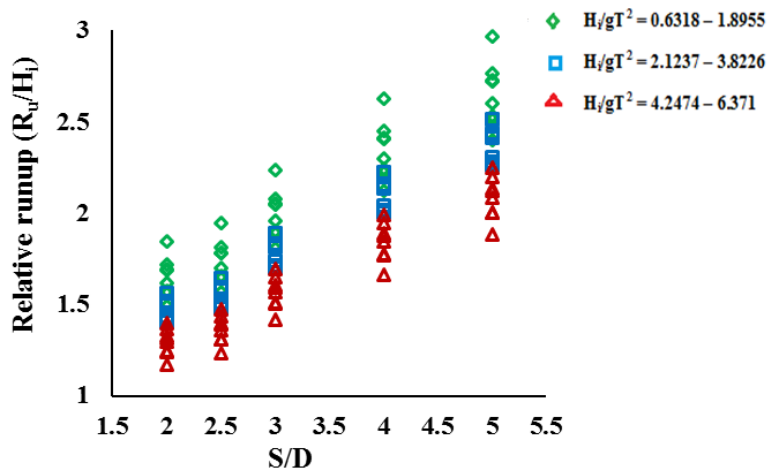
(b) For d/hs = 0.602
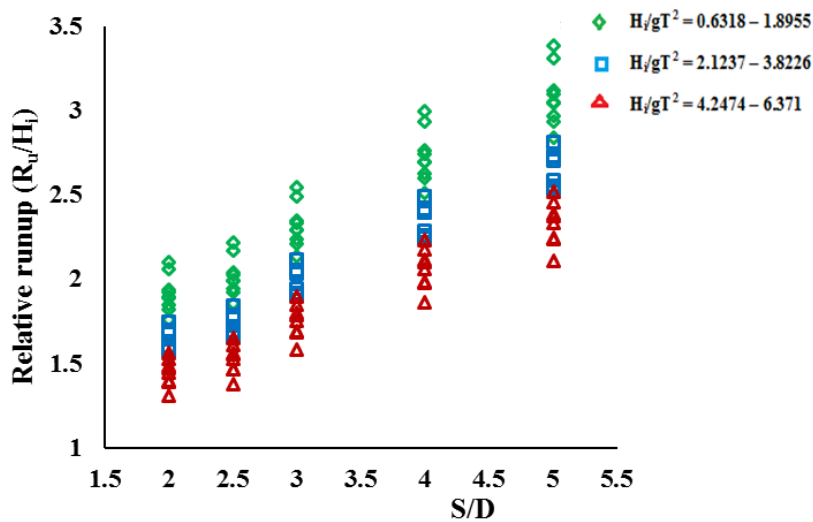
(c) For d/hs = 0.526

Fig. 5.21 Influence of R_u/H_i with S/D for various H_i/gT^2

For a seaside perforated QBW of radius 0.60 m at a water depth of 0.45 m (d/h_s equal to 0.677) and S/D ratio equal to 2, R_u/H_i varies from 0.9855 to 1.3830 for $6.24 \times 10^{-4} < H_i/gT^2 < 6.4 \times 10^{-3}$. For the same radius of QBW and at the same water depth, for S/D ratio equal to 2.5, R_u/H_i varies from 0.9360 to 1.4280 and S/D ratio equal to 3, the range of variation of R_u/H_i is found to be 1.1320 to 1.7280. The variation of R_u/H_i for S/D ratio equal to 4 is observed to be in the range 1.3320 to 2.033 and for S/D ratio equal to 5, the value of R_u/H_i varies in the range 1.5050 to 2.2970.

For QBW of radius 0.60 m at a water depth of 0.40 m (d/h_s equal to 0.602) and S/D ratio equal to 2, the range of variation of R_u/H_i is from 1.2318 to 1.9440. For the same radius of QBW and at the same water depth, S/D ratio equal to 2.5, the range of variation of R_u/H_i is found to be 1.170 to 1.8470 and for S/D equal to 3, R_u/H_i varies from 1.4159 to 2.2340. The variation of R_u/H_i for S/D ratio equal to 4 is observed to be in the range 1.6650 to 2.629 and for S/D ratio equal to 5, the value of R_u/H_i varies in the range 1.8820 to 2.915.

For a water depth of 0.35 m (d/h_s equal to 0.526) and S/D ratio equal to 2, the range of variation of R_u/H_i is from 1.379 to 2.216 for $6.24 \times 10^{-4} < H_i/gT^2 < 6.4 \times 10^{-3}$. For the same radius of QBW and at the same water depth, S/D ratio equal to 2.5, the range of variation of R_u/H_i is found to be 1.310 to 2.105 and for S/D ratio equal to 3, R_u/H_i varies from 1.585 to 2.547. The variation of R_u/H_i for S/D ratio equal to 4 is observed to be in the range 1.865 to 2.996 and for an S/D ratio equal to 5, the value of R_u/H_i varies in the range 2.108 to 3.222.

The percentage reduction in R_u/H_i for different S/D ratios and at different water depths are foundout seperately. It is observed that the maximum perentage redution in R_u/H_i is observed for S/D ratio equal to 2; at a water depth equal to 0.45 m. From the analysis of data for R_u/H_i, it is observed that at a water depth equal to 0.35 m ,the percentage reduction in R_u/H_i for S/D ratio equal to 4 varies from 7.01% to 11.52% compared to S/D ratio equal to 5. The percentage reduction in R_u/H_i for S/D ratio equal to 3, 2.5 and 2 varies from 20.95% to 24.81%, 31.22% to 34.58% and 34.66% to 37.86% with respect to S/D equal to 5. At a water depth equal to 0.40 m ,the percentage reduction in R_u/H_i for S/D ratio equal to 4 varies from 9.81% to

11.53% compared to S/D ratio equal to 5. The percentage reduction in R_u/H_i for S/D ratio equal to 3, 2.5 and 2 varies from 23.36% to 24.76%, 33.31% to 34.55% and 36..63% to 37.83% respectively. When the water depth is increased to 0.45 m ,the percentage reduction in R_u/H_i for S/D ratio equal to 4 varies from 11.49% to 11.51% compared to S/D ratio equal to 5. The percentage reduction in R_u/H_i for S/D ratio equal to 3, 2.5 and 2 varies from 24.70% to 24.80%, 34.5% to 34.6% and 37.80% to 37.84% respectively.

5.9 COMPARITIVE STUDY OF R_u/H_i ON QBW WITH DIFFERENT RADII

From the studies on runup characteristics of seaside perforated quarter circle breakwater, it is observed that the R_u/H_i is always decreasing with increase in wave steepness for all QBW models tested under different water depth (d/h_s) and S/D ratio.

The maximum value for relative wave runup observed is 3.222 at a wave steepness of 9.439 $x10^{-4}$ for S/D ratio equal to 5 and d/h_s ratio equal to 0.526 (d= 0.35 m and QBW radius= 0.60 m) . The minimum value for R_u/H_i observed is 0.727 at a wave steepness of 6.3710 $x10^{-3}$ for S/D ratio equal to 2 and d/h_s ratio equal to 0.732 (d= 0.45 m and QBW radius= 0.55 m).

From graphs plotted so far for all values of wave steepness and S/D ratio considered for the study it is observed that the relative wave runup decreases with increase in water depth. Under higher water depth condition, in which case, the waves are exposed to greater area of perforations leading to greater dissipation of energy and, thereby, resulting in lesser wave runup.

The decrease in R_u/H_i with increase in the perforations or decrease in S/D ratio may be because of higher dissipation of wave energy due to turbulence inside in the breakwater chamber when the perforations are higher.

The values of R_u/H_i increases with increase in breakwater radius or height of the breakwater structure (h_s) because the front face of QBW acts as nearly vertical and effect of curvature is less predominant. Also when the QBW radius increases, the waves encounter lesser perforations resulting in lesser dissipation of wave energy and hence more wave runup.

5.10   VARIATION OF RELATIVE WAVE RUNDOWN (R_d/H_i) FOR QBW 0.55 m RADIUS (h_s= 0.615 m)

The results obtained from the experimental studies are plotted as non-dimensional graphs showing the variation of relative wave rundown with wave steepness and d/ h_s for each S/D ratio.
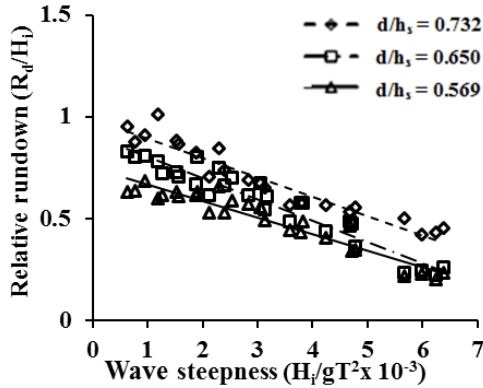
(a) For S/D = 2
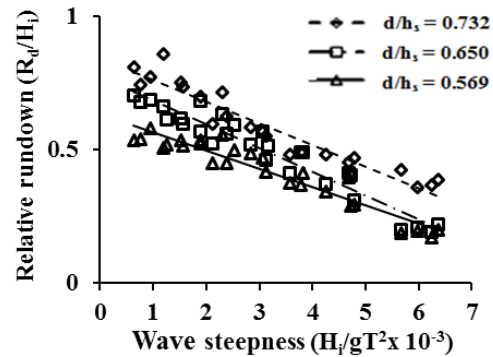
(b) For S/D =2.5
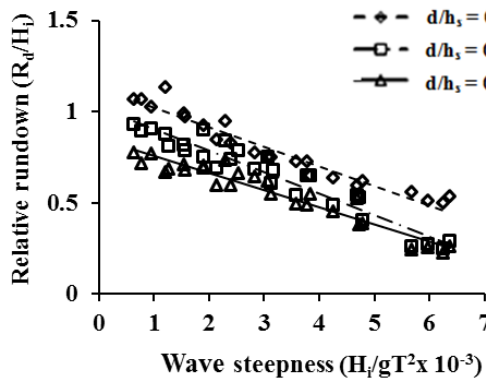
(c) For S/D = 3

(d) For S/D =4

(d) For S/D = 5

Fig. 5.22 Influence of H_i/gT^2 on R_d/H_i for different d/hs values and S/D ratio

Fig. 5.22(a) shows the variation of R_d/H_i with H_i/gT^2 at different water depths for QBW of radius 0.55 m and S/D equal to 2. The maximum value of R_d/H_i observed is 1.101 for wave height of 0.03 m and a wave period of 1.6 s ($H_i/gT^2 = 1.1946 \times 10^{-3}$) and at water depth equal to 0.45 m ($d/h_s = 0.732$). The maximum value of R_d/H_i observed is 0.8284 at a wave height of 0.03 m and a wave period of 2.2 s ($H_i/gT^2 = 6.318 \times 10^{-4}$) and at water depth equal to 0.40 m ($d/h_s = 0.650$). The maximum value of R_d/H_i observed is 0.6839 at a wave height of 0.03 m and a wave period of 1.8 s ($H_i/gT^2 = 9.439 \times 10^{-4}$) and at water depth equal to 0.35 m ($d/h_s = 0.569$).

The variation of R_d/H_i with H_i/gT^2 at different water depths for QBW of radius 0.55 m and S/D = 2.5 is shown in Fig. 5.22(b). The maximum value of R_d/H_i observed is 0.8590 for wave height of 0.03 m and a wave period of 1.6 s ($H_i/gT^2 = 1.1946 \times 10^{-3}$) and at water depth equal to 0.45 m ($d/h_s = 0.732$). The maximum value of R_d/H_i observed is 0.7040 at a wave height of 0.03 m and a wave period of 2.2 s ($H_i/gT^2 = 6.318 \times 10^{-4}$) and at water depth equal to 0.40 m ($d/h_s = 0.650$). The maximum value of R_d/H_i observed is 0.5813 at a wave height of 0.03 m and a wave period of 1.8 s ($H_i/gT^2 = 9.439 \times 10^{-4}$) and at water depth equal to 0.35 m ($d/h_s = 0.569$).

When S/D ratio is increased to 3, the maximum value of R_d/H_i observed is 1.137 at a wave height of 0.03 m and a wave period of 1.6 s ($H_i/gT^2 = 1.1946 \times 10^{-3}$) and at water depth equal to 0.45 m ($d/h_s = 0.732$) (Refer Fig. 5.22(c)). When the water depth is increased to 0.40 m, the maximum value of R_d/H_i observed is 0.9320 at a wave height of 0.03 m and a wave period of 2.2 s ($H_i/gT^2 = 6.318 \times 10^{-4}$). The maximum value of R_d/H_i observed is 0.7694 at a wave height of 0.03 m and a wave period of 1.8 s ($H_i/gT^2 = 9.439 \times 10^{-4}$) and at water depth equal to 0.35 m ($d/h_s = 0.569$).

For S/D equal to 4, the maximum R_d/H_i observed is 1.2643 at a wave height of 0.03 m and a wave period of 1.6 s ($H_i/gT^2 = 1.1946 \times 10^{-3}$) at water depth equal to 0.45 m ($d/h_s = 0.732$). The maximum R_d/H_i observed is 1.0350 at a wave height of 0.03 m and a wave period of 2.2 s ($H_i/gT^2 = 6.318 \times 10^{-4}$) and at water depth equal to 0.40 m ($d/h_s = 0.650$). The maximum R_d/H_i observed is 0.8549 at a wave height of 0.03 m and a wave period of 1.8 s ($H_i/gT^2 = 9.439 \times 10^{-4}$) and at water depth equal to 0.35 m

$(d/h_s = 0.569)$ (Refer Fig. 5.22(d)).

When S/D is increased to 5, the maximum value of R_d/H_i observed is 1.4170 at a wave height of 0.03 m and a wave period of 1.6 s ($H_i/gT^2 = 1.1946 \times 10^{-3}$) and at water depth equal to 0.45 m ($d/h_s = 0.732$). The maximum value of R_d/H_i observed is 1.2183 at a wave height of 0.03 m and a wave period of 2.2 s ($H_i/gT^2 = 6.318 \times 10^{-4}$) and at water depth equal to 0.40 m ($d/h_s = 0.650$). At a water depth equal to 0.35 m ($d/h_s = 0.569$), maximum value of R_d/H_i observed is 1.005 at a wave height of 0.03 m and a wave period of 1.8 s ($H_i/gT^2 = 9.439 \times 10^{-4}$) (Refer Fig. 5.22(e)).

The percentage reduction in R_d/H_i for different S/D ratios and at different water depths are analysed seperately. It is observed that for a water depth of 0.35 m, R_d/H_i varies from 0.2940 to 1.005 for S/D= 5; 0.2498 to 0.8549 for S/D= 4; 0.2248 to 0.7694 for S/D= 3; 0.1699 to 0.5813 for S/D= 2.5 and 0.1998 to 0.6839 for S/D= 2. The percentage reduction in R_d/H_i with respect to S/D= 5 is obtained as 15.03% for S/D= 4, 23.53% for S/D= 3, 42.21% for S/D= 2.5 and 32.04% for S/D= 2.

At a water depth of 0.40 m, R_d/H_i varies from 0.3294 to 1.2183 for S/D= 5; 0.2799 to1.035 for S/D= 4; 0.2519 to 0.9320 for S/D= 3; 0.1903 to 0.7040 for S/D= 2.5 and 0.2239 to 0.8284 for S/D= 2. The percentage reduction in R_d/H_i with respect to S/D= 5 is obtained as 22.62% for S/D= 4, 34.19% for S/D= 3, 53.89% for S/D= 2.5 and 45.75% for S/D= 2.

For a water depth of 0.45 m, R_d/H_i varies from 0.7780 to 1.4170 for S/D= 5; 0.6020 to 1.2643 for S/D= 4; 0.5120 to 1.1379 for S/D= 3; 0.3587 to 0.8590 for S/D= 2.5 and 0.4220 to 1.0115 for S/D=2. The percentage reduction in R_d/H_i with respect to S/D=5 is obtained as 22.62% for S/D= 4, 34.19% for S/D= 3, 53.89% for S/D= 2.5 and 45.75% for S/D= 2.

5.11 VARIATION OF RELATIVE WAVE RUNDOWN (R_d/H_i) FOR QBW 0.575 m RADIUS (h_s=0.640 m)

Fig. 5.23 shows the variation of R_d/H_i with H_i/gT^2 at different water depths for QBW of radius 0.575 m and S/D equal to 2, 2.5, 3, 4 and 5. For S/D= 2, the maximum value of R_d/H_i observed is 0.8352 for wave height of 0.03 m and a wave period of 2 s ($H_i/gT^2 = 7.645 \times 10^{-4}$) and at water depth equal to 0.45 m ($d/h_s = 0.703$). The

maximum value of R_d/H_i observed is 0.6632 at a wave height of 0.03 m and a wave period of 2 s ($H_i/gT^2 = 7.645 \times 10^{-4}$) and at water depth equal to 0.40 m ($d/h_s = 0.625$). The maximum value of R_d/H_i observed is 0.5486 at a wave height of 0.03 m and a wave period of 2 s ($H_i/gT^2 = 7.645 \times 10^{-4}$) and at water depth equal to 0.35 m ($d/h_s = 0.547$).

(a) For S/D = 2

(b) For S/D = 2.5

(c) For S/D = 3

(d) For S/D = 4

(e) For S/D = 5

Fig. 5.23 Influence of H_i/gT^2 on R_d/H_i for different d/h_s values and S/D ratio

From the graphs plotted for the variation of R_d/H_i with S/D = 2.5, maximum value of R_d/H_i observed is 0.7099 at a wave height of 0.03 m and a wave period of 2 s ($H_i/gT^2 = 7.645 \times 10^{-4}$) and at water depth equal to 0.45 m ($d/h_s = 0.703$). Considering 0.40 m water depth ($d/h_s = 0.625$), the maximum value of R_d/H_i observed is 0.5637 for wave height of 0.03 m and a wave period of 2 s ($H_i/gT^2 = 7.645 \times 10^{-4}$). The maximum value of R_d/H_i observed is 0.5486 at a wave height of 0.03 m and a wave period of 2 s ($H_i/gT^2 = 7.645 \times 10^{-4}$) and at water depth equal to 0.35 m ($d/h_s = 0.547$).

When S/D is equal to 3, maximum value of R_d/H_i observed is 1.044 for wave height of 0.03 m and a wave period of 2 s ($H_i/gT^2 = 7.645 \times 10^{-4}$) and at water depth equal to 0.45 m ($d/h_s = 0.703$). The maximum value of R_d/H_i observed is 0.8290 at a wave height of 0.03 m and a wave period of 2 s ($H_i/gT^2 = 7.645 \times 10^{-4}$) and at water depth equal to 0.40 m ($d/h_s = 0.625$). But for water depth equal to 0.35 m ($d/h_s = 0.547$), maximum value of R_d/H_i observed is 0.6857 at a wave height of 0.03 m and a wave period of 2 s ($H_i/gT^2 = 7.645 \times 10^{-4}$).

Considering QBW of radius 0.575 m and S/D equal to 4, maximum value of R_d/H_i observed is 1.2282 at a wave height of 0.03 m and a wave period of 2 s ($H_i/gT^2 = 7.645 \times 10^{-4}$) and at 0.45 m water depth ($d/h_s = 0.703$). The maximum value of R_d/H_i observed is 0.9753 at a wave height of 0.03 m and a wave period of 2 s ($H_i/gT^2 = 7.645 \times 10^{-4}$) and at water depth equal to 0.40 m ($d/h_s = 0.625$). The maximum value of R_d/H_i observed is 0.8067 at a wave height of 0.03 m and a wave period of 2 s ($H_i/gT^2 = 7.645 \times 10^{-4}$) and at water depth equal to 0.35 m ($d/h_s = 0.547$).

When S/D ratio is increased to 5, maximum value of R_d/H_i observed is 1.4450 at a wave height of 0.03 m and a wave period of 2 s ($H_i/gT^2 = 7.645 \times 10^{-4}$) and at water depth equal to 0.45 m ($d/h_s = 0.703$). The maximum value of R_d/H_i observed is 1.1475 at a wave height of 0.03 m and a wave period of 2 s ($H_i/gT^2 = 7.645 \times 10^{-4}$) a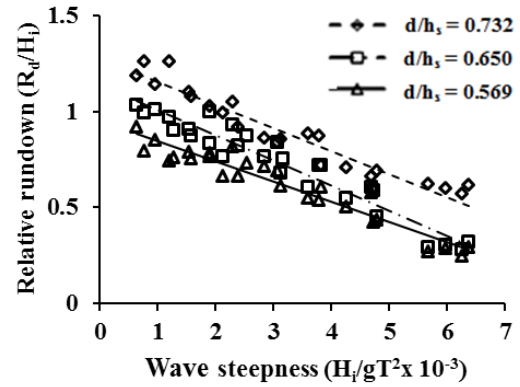nd at water depth equal to 0.40 m ($d/h_s = 0.625$). For water depth equal to 0.35 m ($d/h_s = 0.547$), maximum value of R_d/H_i observed is 0.9492 at a wave height of 0.03 m and a wave period of 2 s ($H_i/gT^2 = 7.645 \times 10^{-4}$).

The range of variation and the percentage reduction in R_d/H_i different S/D ratios and at different water depths and for QBW of radius 0.575 m are shown in Table 5.4.

Table 5.4 Range of variation and percentage reduction in R_d/H_i ($h_s= 0.640$ m)

d/h_s	S/D	Variation in R_d/H_i	% Reduction in R_d/H_i
0.526	5	0.2689 to 0.9492	
	4	0.2438 to 0.8067	14.85 % to 15.03%
	3	0.2072 to 0.6857	26.76% to 27.79%
	2.5	0.1409 to 0.4663	49.87% to 50.88%
	2	0.1658 to 0.5486	40.20% to 42.21%
0.602	5	0.3081 to 1.1475	
	4	0.2619 to 0.9753	12.99% to 15.01%
	3	0.2262 to 0.8290	26.58% to 27.75%
	2.5	0.1780 to 0.6632	48.23% to 51.22%
	2	0.1513 to 0.5637	42.20% to 43.02%
0.677	5	0.6622 to 1.4450	
	4	0.5629 to 1.2282	14.99% to 15.18%
	3	0.4785 to 1.0440	25.74% to 27.75%
	2.5	0.3828 to 0.8352	48.12% to 52.80%
	2	0.3253 to 0.7099	41.75% to 42.88%

5.12 VARIATION OF RELATIVE WAVE RUNDOWN (R_d/H_i) FOR QBW 0.60 m RADIUS (h_s=0.665 m)

The results obtained from the experimental studies are plotted as non-dimensional graphs showing the variation of relative wave rundown with wave steepness and d/h_s for each S/D ratio.
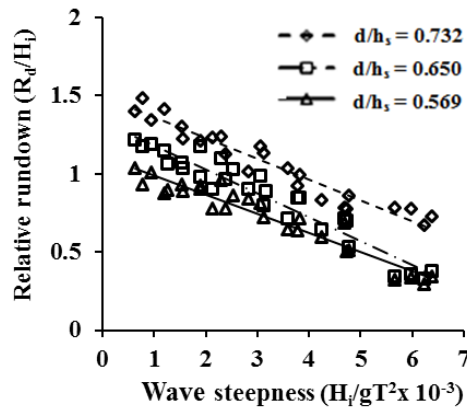
The variation of R_d/H_i with H_i/gT^2 at different water depths for QBW of radius 0.60 m and S/D equal to 2 is plotted and the maximum value of R_d/H_i observed is 0.8059 at a wave height of 0.03 m and a wave period of 2 s ($H_i/gT^2 = 7.645 \times10^{-3}$) and at water depth equal to 0.45 m ($d/h_s = 0.677$).

The maximum value of R_d/H_i observed is 0.6558 at a wave height of 0.06 m and a wave period of 2.2 s ($H_i/gT^2 = 1.2637 \times10^{-3}$) and at water depth equal to 0.40 m ($d/h_s = 0.602$). Further at water depth equal to 0.35 m ($d/h_s = 0.526$), maximum value of R_d/H_i observed is 0.5294 at a wave height of 0.03 m and a wave period of 2 s ($H_i/gT^2 = 7.645 \times10^{-3}$).

Fig. 5.24 shows the variation of R_d/H_i with H_i/gT^2 at different water depths for QBW of radius 0.60 m and S/D equal to 2, 2.5, 3, 4 and 5.

(a) For S/D = 2

(b) For S/D=2.5

(c) For S/D = 3

(d) For S/D= 4

(e) For S/D= 5
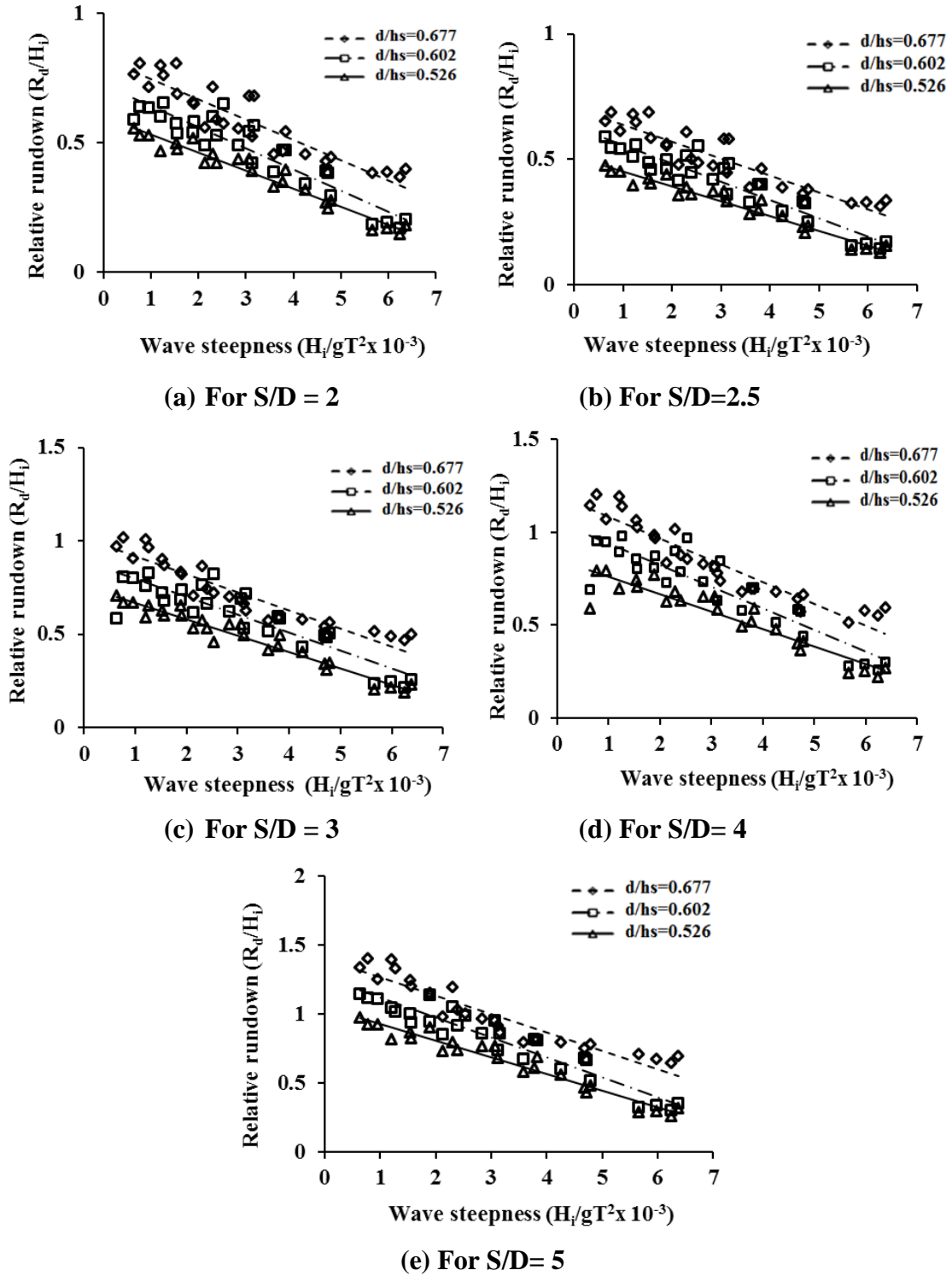
Fig. 5.24 Influence of H_i/gT^2 on R_d/H_i for different d/hs values and S/D ratio

The maximum value of R_d/H_i observed is 0.6886 at a wave height of 0.03 m and a wave period of 2 s ($H_i/gT^2 = 7.645 \times 10^{-3}$) and at water depth equal to 0.45 m ($d/h_s = 0.677$). The maximum value of R_d/H_i observed is 0.5603 at a wave height of 0.06 m and a wave period of 2.2 s ($H_i/gT^2 = 1.2637 \times 10^{-3}$) and at 0.40 m water depth ($d/h_s =$

0.602). The maximum value of R_d/H_i observed is 0.4523 at a wave height of 0.03 m and a wave period of 2 s ($H_i/gT^2 = 7.645 \times 10^{-3}$) and at water depth equal to 0.35 m ($d/h_s = 0.526$).

From the results for the variation of R_d/H_i with H_i/gT^2 at different water depths for QBW of radius 0.60 m and S/D equal to 3, maximum value of R_d/H_i observed is 1.020 at a wave height of 0.03 m and a wave period of 2 s ($H_i/gT^2 = 7.645 \times 10^{-3}$) and at water depth equal to 0.45 m. The maximum value of R_d/H_i observed is 0.8300 at a wave height of 0.06 m and a wave period of 2.2 s ($H_i/gT^2 = 1.2637 \times 10^{-3}$) and at water depth equal to 0.40 m. The maximum value of R_d/H_i observed is 0.6700 at a wave height of 0.03 m and a wave period of 2 s ($H_i/gT^2 = 7.645 \times 10^{-3}$) and at water depth equal to 0.35 m.

For S/D equal to 4, the maximum value of R_d/H_i observed is 1.2643 at a wave height of 0.03 m and a wave period of 1.6 s ($H_i/gT^2 = 1.1946 \times 10^{-3}$) and at water depth equal to 0.45 m ($d/h_s = 0.677$). The maximum value of R_d/H_i observed is 1.0350 at a wave height of 0.03 m and a wave period of 2.2 s ($H_i/gT^2 = 6.318 \times 10^{-4}$) and at water depth equal to 0.40 m ($d/h_s = 0.602$). The maximum value of R_d/H_i observed is 0.8549 at a wave height of 0.03 m and a wave period of 1.8 s ($H_i/gT^2 = 9.439 \times 10^{-4}$) and at water depth equal to 0.35 m ($d/h_s = 0.526$).

When S/D ratio was increased to 5, maximum value of R_d/H_i observed is 1.4170 at a wave height of 0.03 m and a wave period of 1.6 s ($H_i/gT^2 = 1.1946 \times 10^{-3}$) and at water depth equal to 0.45 m ($d/h_s = 0.677$). The maximum value of R_d/H_i observed is 1.2183 at a wave height of 0.03 m and a wave period of 2.2 s ($H_i/gT^2 = 6.318 \times 10^{-4}$) and at water depth equal to 0.40 m ($d/h_s = 0.602$). The maximum value of R_d/H_i observed is 1.005 at a wave height of 0.03 m and a wave period of 1.8 s ($H_i/gT^2 = 9.439 \times 10^{-4}$) and at water depth equal to 0.35 m ($d/h_s = 0.526$). The percentage reduction in R_d/H_i different S/D ratios and at different water depths and for QBW of radius 0.60 m are shown in Table 5.5

From the studies, it is observed that R_u/H_i and R_d/H_i decreases with increase in breakwater radius for different ranges of H_i/gT^2 and all values of S/D ratio. The relative runup, R_u/H_i and relative rundown R_d/H_i decreases with increase in breakwater radius because effect of curvature is less predominant when the

breakwater radius is more and hence the waves encounter lesser perforations resulting in lesser dissipation.

Table 5.5 Range of variation and percentage reduction in R_d/H_i (for R = 0.60 m or h_s= 0.665 m)

d/h_s	S/D	Variation in R_d/H_i	% Reduction in R_d/H_i
0.677	5	0.2940 to 1.005	
	4	0.2498 to 0.8549	14.93% to 15.03%
	3	0.2248 to 0.7694	22.44% to 23.53%
	2.5	0.1998 to 0.6839	40.15% to 42.21%
	2	0.1699 to 0.5813	31.95% to 32.04%
0.602	5	0.3294 to 1.2183	
	4	0.2799 to 1.035	13.02% to 15.14%
	3	0.2519 to 0.9320	21.49% to 23.53%
	2.5	0.2239 to 0.8284	41.15% to 42.21%
	2	0.1903 to 0.7040	30.01% to 32.03%
0.526	5	0.7780 to 1.4170	
	4	0.6020 to 1.2643	10.77% to 22.62%
	3	0.5120 to 1.1379	19.69% to 34.19%
	2.5	0.4220 to 1.0115	39.37% to 53.89%
	2	0.3587 to 0.8590	28.62% to 45.75%

5.13   COMPARITIVE STUDY OF R_u/H_i and R_d/H_i ON IMPERMEABLE AND PERFORATED QBW

From experimental investigations on runup and rundown characteristics of impermeable and seaside perforated quarter circle breakwater, it is observed that the relative runup R_u/H_i and relative rundown R_d/H_i are always decreasing with increase in wave steepness for all values of d/h_s and S/D ratio. In the case of impermeable QBW, the highest value for R_u/H_i is equal to 4.772 observed for QBW of radius equal to 0.60 m at a wave height of 0.03 m and a wave period of 2 s ($H_i/gT^2 = 7.645 \times 10^{-4}$) and at water depth equal to 0.35 m. But the minimum $R_u/H_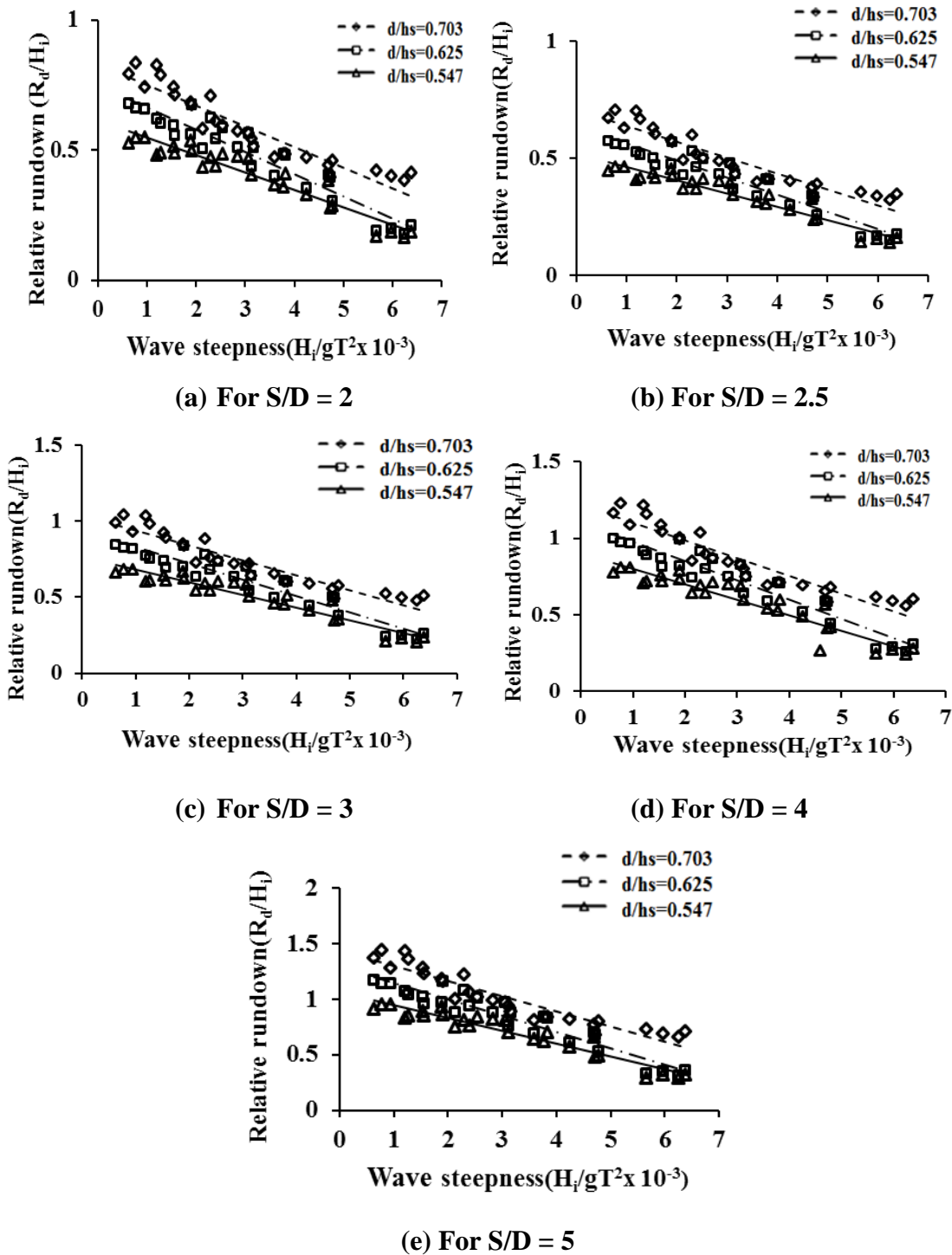i$ observed is 1.767 at a wave height of 0.09 m and a wave period of 1.2s ($H_i/gT^2 = 6.371 \times 10^{-3}$) and at water depth equal to 0.45 m ($d/h_s = 0.732$) for QBW of radius equal to 0.55 m. In the case of waves of low period or higher wave steepness, QBW structure is exposed to wave action only for a short interval of time resulting in higher reflection and hence only less energy available for runup or rundown.

For seaside perforated QBW, the highest value for R_u/H_i is equal to 3.222 observed for QBW of radius equal to 0.60 m and S/D= 5 at a water depth equal to 0.35 m, $H_i/gT^2 = 9.439 \times 10^{-4}$. But the minimum R_u/H_i observed is 0.727 at a wave height of 0.09 m and a wave period of 1.2s ($H_i/gT^2 = 6.371 \times 10^{-3}$) and at water depth equal to 0.45 m ($d/h_s = 0.732$) for QBW of radius equal to 0.55 m.

In the case of impermeable QBW 0.55 m radius, for $6.318 \times 10^{-4} < H_i/gT^2 < 1.8955 \times 10^{-3}$ and considering 0.35 m water depth as reference, when $d/h_s = 0.650$ (0.40 m water depth) the percentage reduction in R_u/H_i varies from 17.10% to 19.52% and when $d/h_s = 0.732$ (0.45 m water depth) the percentage reduction in R_u/H_i varies from 25.19% to 38.04 %. Similarly for $2.123 \times 10^{-3} < H_i/gT^2 < 3.8226 \times 10^{-3}$ and considering 0.35 m water depth as reference, when $d/h_s = 0.650$ (0.40 m water depth) the percentage reduction in R_u/H_i varies from 16.19% to 19.97% and when $d/h_s = 0.732$ (0.45 m water depth) the percentage reduction in R_u/H_i varies from 30% to 32%. It is observed that the maximum percentage reduction in R_u/H_i varies from 32% to 33% $d/h_s = 0.732$ (water depth of 0.45 m) and when $4.247 \times 10^{-3} < H_i/gT^2 < 6.371 \times 10^{-3}$.

For seaside perforated QBW of radius 0.55 m, considering water depth of 0.45 m (d/h_s equal to 0.732), for an S/D ratio equal to 5, R_u/H_i varies in the range 1.309 to 1.987 for $6.24 \times 10^{-4} < H_i/gT^2 < 6.4 \times 10^{-3}$. For S/D ratio equal to 4, the range of variation of R_u/H_i is found to be 1.140 to 1.739; for S/D ratio equal to 3, R_u/H_i is observed to be in the range 0.9770 to 1.456; for S/D ratio equal to 2.5, the value of R_u/H_i varies in the range 0.727 to 1.089 and for an S/D ratio equal to 2, the range of variation of R_u/H_i is from 0.779 to 1.165. At a water depth equal to 0.45 m ,the percentage reduction in R_u/H_i for S/D ratio equal to 4 is 12.48% to 12.91% compared to S/D ratio equal to 5. The percentage reduction in R_u/H_i for S/D ratio equal to 3, 2.5 and 2 are 25.36% to 26.72%, 44.46% to 45.19% and 40.48% to 41.37% with respect to S/D equal to 5.

In the case of impermeable QBW of radius equal to 0.55 m, R_d/H_i varies from 0.3762 to 1.904 for $6.318 \times 10^{-4} < H_i/gT^2 < 6.3710 \times 10^{-3}$. The maximum value for R_d/H_i observed is 1.904 at a wave height of 0.03 m and a wave period of 2s ($H_i/gT^2 = 7.645 \times 10^{-4}$) and at water depth equal to 0.45 m ($d/h_s = 0.732$). The minimum value

for R_d/H_i observed is 0.3762 at a wave height of 0.12 m and a wave period of 1.4s ($H_i/gT^2 = 6.2410 \times 10^{-3}$) and at water depth equal to 0.35 m (d/h_s equal to 0.569).

For perforated QBW, at a water depth of 0.45 m, R_d/H_i varies from 0.7780 to 1.4170 for S/D= 5; 0.6020 to 1.2643 for S/D= 4; 0.5120 to 1.1379 for S/D= 3; 0.3587 to 0.8590 for S/D= 2.5 and 0.4220 to 1.0115 for S/D= 2.

The percentage reduction in R_d/H_i with respect to S/D= 5 is obtained as 22.62% for S/D= 4, 34.19% for S/D= 3, 53.89% for S/D= 2.5 and 45.75% for S/D= 2. Hence it is concluded that the seaside perforated QBW with radius equal to 0.55 m is more effective in reducing wave runup and rundown compared to impermeable QBW.

5.14 EQUATIONS DEVELOPED FOR RELATIVE WAVE RUNUP, R_u/H_i AND RUNDOWN, R_d/H_i

The results obtained from the experimental studies on the runup and rundown characteristics for impermeable QBW with different breakwater radius at different water depths and wave conditions are combined into suitable dimensionless terms. The regression analysis is done by using Excel statistical software – XLSTAT and the equation for the best fit curve is obtained.

The equation for R_u/H_i for impermeable QBW was derived as follows:

$$R_u/H_i = 8.621 \ - 0.1468(H_i/gT^2) - 7.938(d/h_s) \dots\dots\dots\dots\dots\dots\dots\dots\dots\dots \text{ (5.1)}$$

Fig. 5.25 shows the comparison between the measured and predicted values of relative wave runup R_u/H_i for impermeable QBW.

The equation for R_d/H_i for impermeable QBW was derived as follows:

$$R_d/H_i = 0.03276 \ - 0.1725(H_i/gT^2) + 2.562(d/h_s) \dots\dots\dots\dots\dots\dots\dots\dots \text{ (5.2)}$$

Fig. 5.26 shows the comparison between the measured and predicted values of R_d/H_i for impermeable QBW.
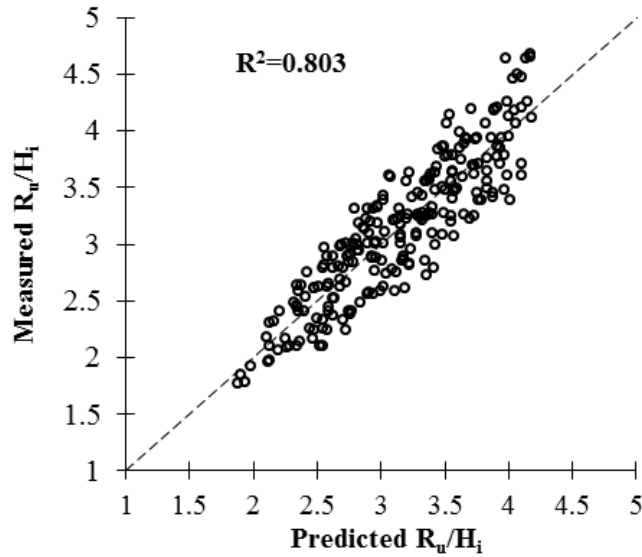
Fig. 5.25 Comparison between measured and predicted values of R_u/H_i for impermeable QBW
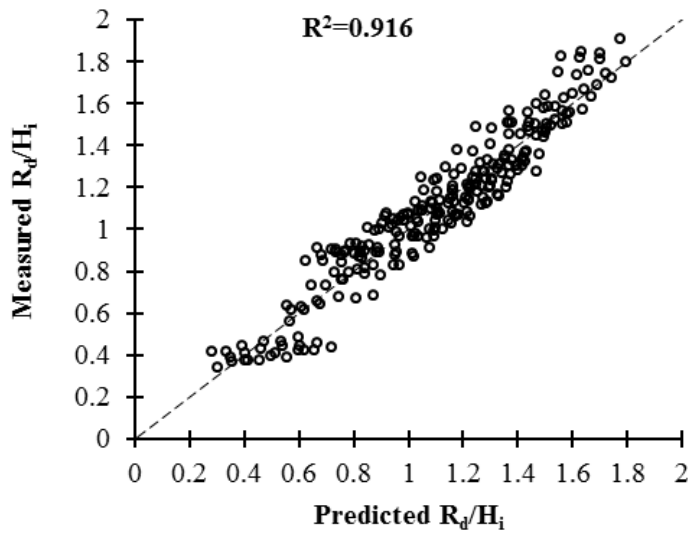
Fig. 5.26 Comparison between measured and predicted values of R_d/H_i for impermeable QBW

The experimental results obtained for perforated QBW with different radius, S/D ratio at different water depths were combined into suitable dimensionless parameters. The curves with best fit for R_u/H_i and R_d/H_i for perforated QBW were obtained. Fig 5.27 shows the comparison between the measured and predicted values of R_u/H_i. The equation for R_u/H_i for seaside perforated QBW was derived as follows:

$$R_u/H_i = 3.523 + 0.0873(H_i/gT^2) - 4.019(d/h_s) + 0.2835 (S/D) \ldots\ldots\ldots\ldots\ldots\ldots \quad (5.3)$$
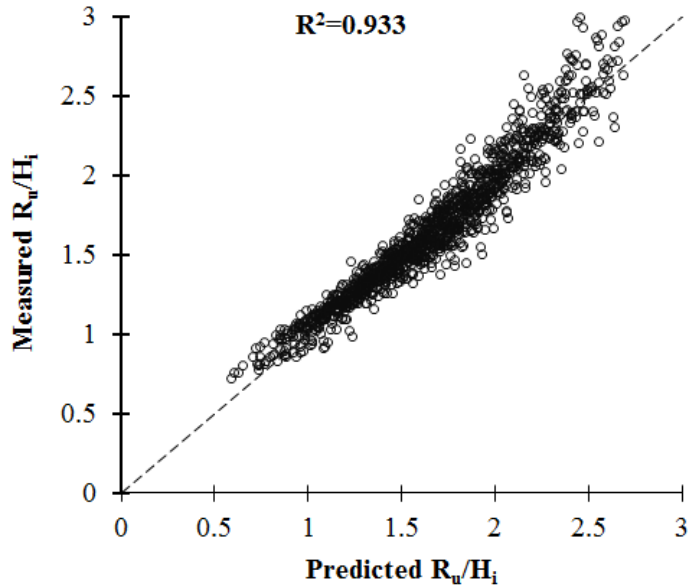
Fig. 5.27 Comparison between measured and predicted values of R_u/H_i for perforated QBW

The equation for R_d/H_i for seaside perforated QBW was derived as follows:

$$R_d/H_i= -0.4549 - 0.1005(H_i/gT^2) + 1.525(d/h_s) + 0.1352(S/D) \dots\dots\dots\dots\dots \text{ (5.4)}$$

Fig. 5.28 shows the comparison between the measured and predicted values of R_d/H_i for perforated quarter circle breakwater.
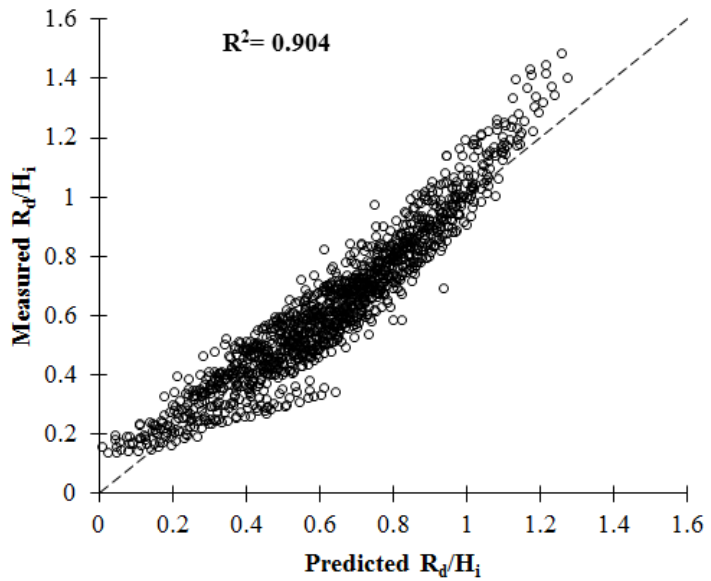
Fig. 5.28 Comparison between measured and predicted values of R_d/H_i for perforated QBW

SLIDING STABILITY ANALYSIS OF EMERGED IMPERMEABLE AND SEASIDE PERFORATED QBW

6.1 GENERAL

In the previous chapters details of investigations on performance characteristics of both emerged impermeable and seaside perforated QBW's are summarized briefly. The results are tabulated systematically and the QBW with good performance based on reflection and loss characteristics, run up and rundown characteristics are identified. Later experiments are also conducted to determine the sliding stability of different models of non-overtopped emerged QBW; both impermeable and seaside perforated.

In the present chapter, experiments conducted to study the minimum (critical) weight required to resist the sliding of emerged impermeable and seaside perforated quarter circle breakwater models with radius 0.55 m, 0.575 m and 0.60 m (S/D ratios 2, 2.5, 3, 4 and 5) are discussed in detail . Based on the behavior of different models under varying wave conditions, water depths and S/D ratios, interpretations are made on the sliding stability characteristics and finally a comparative study is conducted based on the results obtained.

6.2 STUDIES ON EMERGED IMPERMEABLE QBW

Studies are conducted on emerged impermeable QBW with different breakwater radii under different water depths (0.35 m, 0.40 m and 0.45 m) and varying wave conditions. Variations of minimum weight required for sliding stability with different wave specific and structural specific parameters are studied, and the variations are then plotted graphically using non-dimensional parameters obtained from a dimensional analysis by Buckingham's π theorem.

The stability based on sliding performance is represented by a non-dimensional stability parameter ($W/\gamma H_i^2$), where W is the minimum weight of the QBW required (including the additional weight) to resist the sliding per unit length of the

breakwater, γ is the specific weight of water and H_i is the incident wave height. The sliding of QBW occurs when the wave force exceeds the frictional resistance offered by the QBW. The stability of QBW against wave force increases with increase in the total weight of the structure. Therefore the experiment is repeated by the addition of weight in increments till the structure stops sliding.

6.3 VARIATION OF STABILITY PARAMETER ($W/\gamma H_i^2$) FOR IMPERMEABLE QBW

Variation of $W/\gamma H_i^2$ with incident wave steepness (H_i/gT^2) for different relative water depth (d/h_s) and for a constant radius and a constant spacing to diameter of perforations (S/D) ratio is studied. The results obtained are plotted as non-dimensional graphs showing the variation of stability parameter, $W/\gamma H_i^2$ with wave steepness, H_i/gT^2 and relative water depth, d/h_s for each S/D ratio.

6.3.1 Influence of incident wave steepness on stability parameter

The graphs of non-dimensional stability parameter ($W/\gamma H_i^2$) against the incident wave steepness (H_i/gT^2) are plotted for different values of relative water depth, d/h_s and a constant spacing to diameter of perforation ratio (S/D). Fig. 6.1 shows the variation of $W/\gamma H_i^2$ with H_i/gT^2 for different d/h_s (radius of QBW 0.55 m, 0.575 m and 0.60 m). It is observed that $W/\gamma H_i^2$ decreases with increase in H_i/gT^2 for all values of d/h_s.
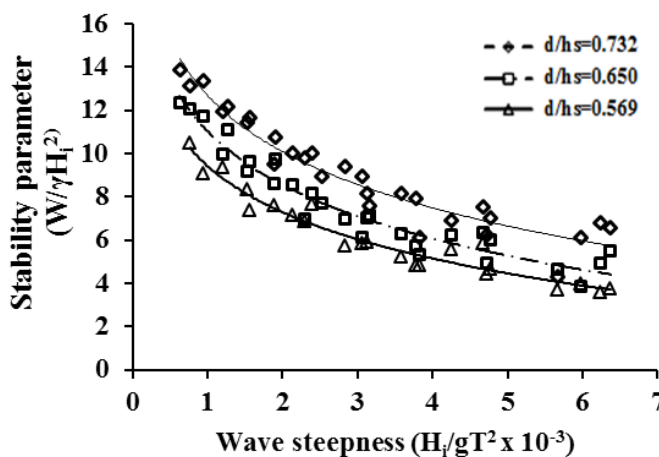
Fig. 6.1 Influence of H_i/gT^2 on $W/\gamma H_i^2$ at different d/h_s for QBWof 0.55 m radius

First of all, QBW of radius equal to 0.55 m (h_s equal to 0.615 m) is analysed for different value of incident wave steepness and it is observed that $W/\gamma H_i^2$ is varying

from 3.557 to 13.889 for $6.318 \times 10^{-4} < H_i/gT^2 < 6.3710 \times 10^{-3}$. The maximum value for $W/\gamma H_i^2$ observed is 13.889 for wave height of 0.03 m and a wave period of 2.2s ($H_i/gT^2 = 6.318 \times 10^{-4}$) and at water depth equal to 0.45 m (d/h_s equal to 0.732). The minimum $W/\gamma H_i^2$ observed is 3.557 for wave height of 0.12 m and a wave period of 1.4s ($H_i/gT^2 = 6.241 \times 10^{-3}$) and at water depth equal to 0.35 m ($d/h_s = 0.538$).

When QBW radius is increased to 0.575 m, the values for $W/\gamma H_i^2$ is observed to be varying from 3.450 to 13.223 for $6.318 \times 10^{-4} < H_i/gT^2 < 6.3710 \times 10^{-3}$. The maximum value obtained for $W/\gamma H_i^2$ is 13.223 corresponding to a wave height of 0.03 m and a wave period of 2.2 s ($H_i/gT^2 = 6.318 \times 10^{-4}$) and at water depth equal to 0.45 m. The minimum $W/\gamma H_i^2$ observed is 3.450 obtained for a wave height of 0.12 m and a wave period of 1.4s ($H_i/gT^2 = 6.241 \times 10^{-3}$) and at water depth equal to 0.35 m.
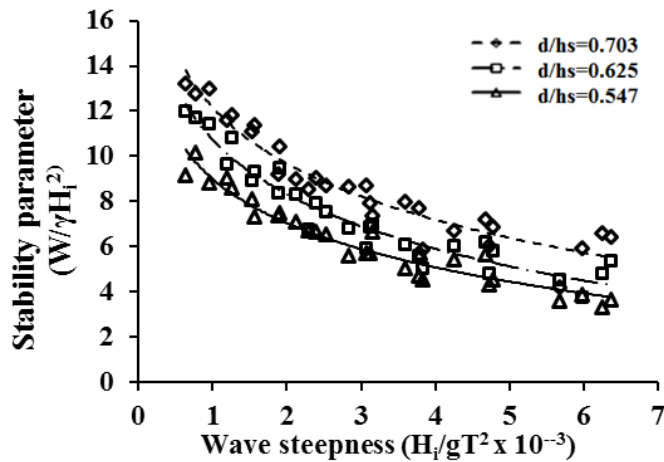
Fig. 6.2 Influence of H_i/gT^2 on $W/\gamma H_i^2$ at different d/h_s for QBW of radius 0.575m
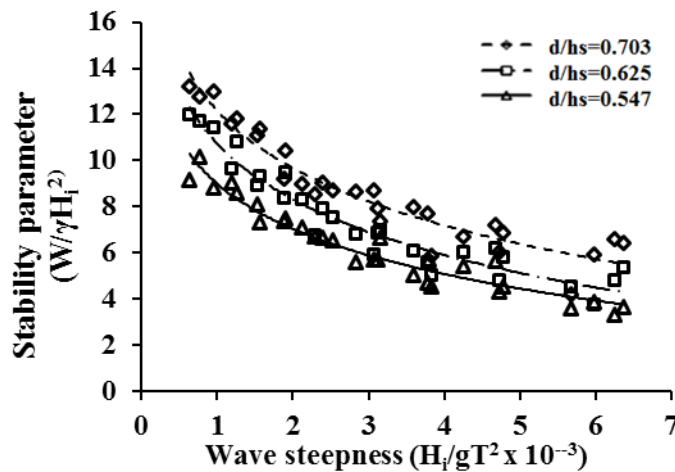
Fig. 6.3 Influence of H_i/gT^2 on $W/\gamma H_i^2$ at different d/h_s for QBW of radius 0.60 m

In the case of QBW of radius equal to 0.60 m, $W/\gamma H_i^2$ varies from 3.112 to 12.439 for $6.318\times10^{-4} < H_i/gT^2 < 6.3710\times10^{-3}$. The maximum for $W/\gamma H_i^2$ observed is 12.439 at a wave height of 0.03 m and a wave period of 2.2 s ($H_i/gT^2 = 6.318\times10^{-4}$) and at water depth equal to 0.45 m. The minimum $W/\gamma H_i^2$ observed is 3.112 at a wave height of 0.12 m and a wave period of 1.4s ($H_i/gT^2 = 6.241\times10^{-3}$) and at water depth equal to 0.35 m.

For all models tested, it is observed when the incident wave steepness increases, the dimensionless stability parameter decreases. Therefore the minimum weight required for resisting sliding also decreases. This is because long period waves (low steepness) exert more force on the caisson demanding more minimum weight and short period (steep) waves transfer less force, hence low minimum weight. The sliding due to increase in wave force is overcome by increasing the weight of breakwater by adding additional weight into the caisson.

6.3.2 Influence of water depth on stability parameter

The QBW models of three different radii are analysed under varying water depths say 0.35 m, 0.40 m and 0.45 m and at different ranges of wave steepness. Non-dimensional graphs are then plotted in order to evaluate the influence of relative water depth on stability parameter and it is observed that $W/\gamma H_i^2$ increases with increase in water depth for all ranges of wave steepness.
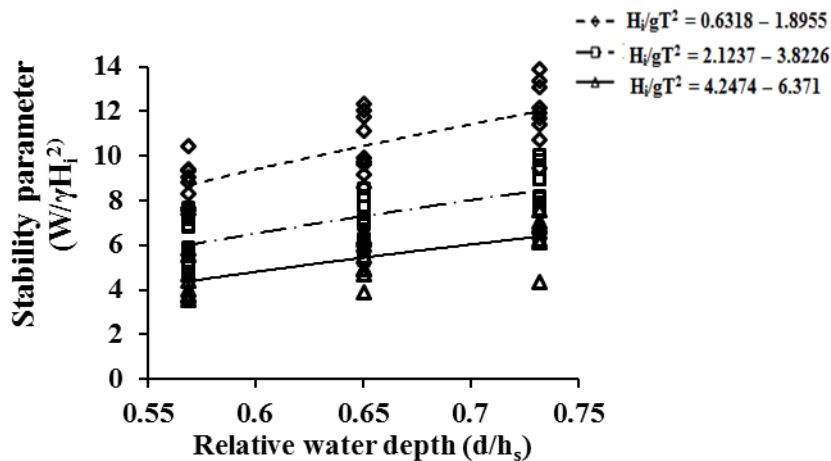
Fig. 6.4 Variation of $W/\gamma H_i^2$ with d/h$_s$ for QBW of 0.55 m radius

From Fig. 6.4, for QBW of radius 0.55 m and $6.318\times10^{-4} < H_i/gT^2 < 1.8955\times10^{-3}$, the minimum value for $W/\gamma H_i^2$ is equal to 7.388 corresponding to d/h$_s$= 0.569 (water

depth of 0.35 m) and maximum $W/\gamma H_i^2$ obtained is 13.889 corresponding to $d/h_s=$ 0.732 (water depth of 0.45 m). For $2.1237 \times 10^{-3} < H_i/gT^2 < 3.8226 \times 10^{-3}$,the minimum value for is equal to 4.804 when $d/h_s=$ 0.569 and maximum $W/\gamma H_i^2$ obtained is 10.032 when $d/h_s=$ 0.732. For $4.247 \times 10^{-3} < H_i/gT^2 < 6.371 \times 10^{-3}$,the minimum value for $W/\gamma H_i^2$ is equal to 3.557 corresponding to $d/h_s=$ 0.569 and maximum $W/\gamma H_i^2$ obtained is 7.545 corresponding to $d/h_s=$ 0.732.

Fig. 6.5 shows the variation of $W/\gamma H_i^2$ with d/h_s for QBW 0.575 m radius under varying conditions of wave steepness. It is observed that for $6.318 \times 10^{-4} < H_i/gT^2 < 1.8955 \times 10^{-3}$ the minimum value for $W/\gamma H_i^2$ is equal to7.322 when $d/h_s=$ 0.547 (water depth of 0.35 m) and maximum $W/\gamma H_i^2$ is 13.223corresponding to $d/h_s=$ 0.703(water depth of 0.45 m).

The minimum and maximum values for $W/\gamma H_i^2$observed for $2.123 \times 10^{-3} < H_i/gT^2 < 3.8226 \times 10^{-3}$ are 4.528 and 9.052. For $4.247 \times 10^{-3} < H_i/gT^2 < 6.371 \times 10^{-3}$,the minimum value for $W/\gamma H_i^2$ is equal to 3.333 corresponding to $d/h_s=$ 0.547 and maximum $W/\gamma H_i^2$obtained is 7.225 corresponding to $d/h_s=$ 0.703 respectively.
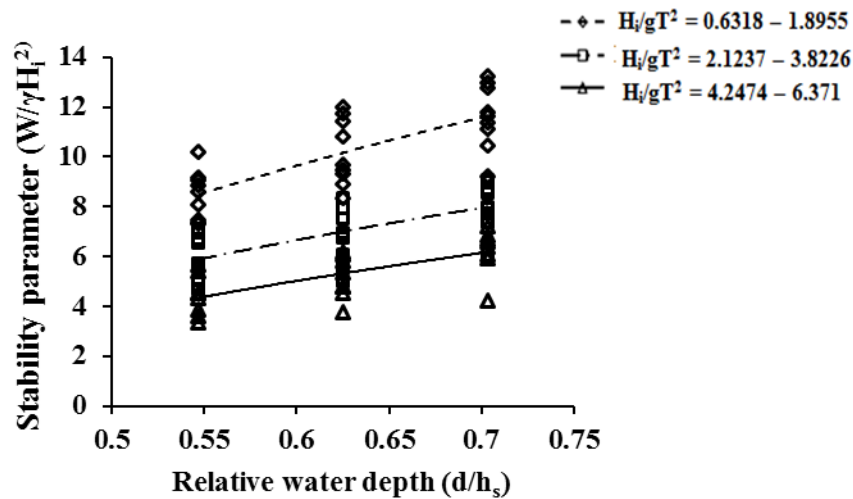
Fig. 6.5 Variation of $W/\gamma H_i^2$ with d/h_s for QBW of 0.575 m radius

When QBW radius is equal to 0.60 m, for $6.318 \times 10^{-4} < H_i/gT^2 < 1.8955 \times 10^{-3}$ the minimum value for $W/\gamma H_i^2$ is equal to 7.056 for $d/h_s=$ 0.526 and maximum $W/\gamma H_i^2$ is 12.439 corresponding to $d/h_s=$ 0.677.

The minimum and maximum values for $W/\gamma H_i^2$ observed for $2.123 \times 10^{-3} < H_i/gT^2 < 3.8226 \times 10^{-3}$ are 4.476 and 8.332. For $4.247 \times 10^{-3} < H_i/gT^2 < 6.371 \times 10^{-3}$,the minimum

value for $W/\gamma H_i^2$ is equal to 3.112 corresponding to $d/h_s=0.526$ and maximum $W/\gamma H_i^2$ obtained is 6.665 corresponding to $d/h_s=0.643$ respectively.
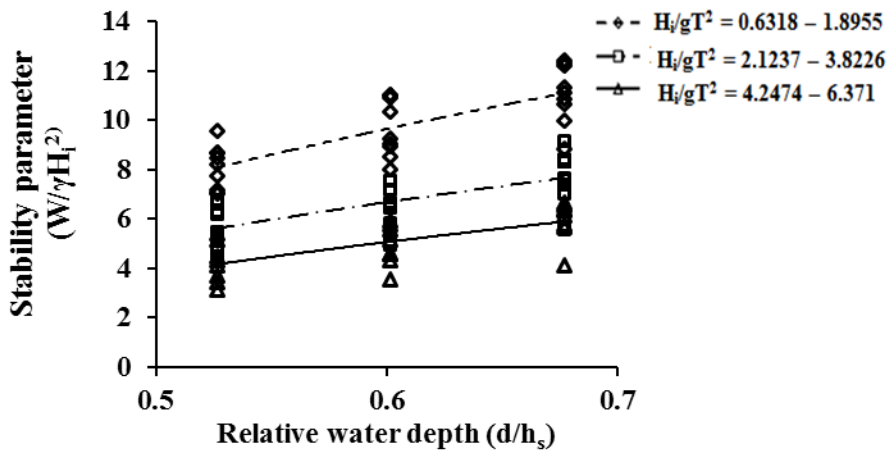
Fig. 6.6 Variation of $W/\gamma H_i^2$ with d/h_s for QBW of 0.60 m radius

In all cases it is observed that the stability parameter $W/\gamma H_i^2$ increases with increase in relative water depth (d/h_s). This is because higher the water depth, greater is the area of the QBW model structure exposed to wave action, and hence, the increase in d/h_s imparts more force and therefore increase in $W/\gamma H_i^2$. This means more structure weight is required for sliding stability in larger depths.

For QBW of radius equal to 0.55 m, the minimum value for $W/\gamma H_i^2$ is observed when $4.247 \times 10^{-3} < H_i/gT^2 < 6.371 \times 10^{-3}$ at 0.35 m water depth. The percentage increase in $W/\gamma H_i^2$ for 0.40 m water depth compared to 0.35 m water depth varies from 9.20% to 9.40% and for 0.45 m water depth; $W/\gamma H_i^2$ varies from 21.78% to 29.73%.

Considering the studies on QBW of radius 0.575 m, the minimum values for $W/\gamma H_i^2$ is observed for $4.247 \times 10^{-3} < H_i/gT^2 < 6.371 \times 10^{-3}$ and at 0.35 m water depth. The percentage increase in $W/\gamma H_i^2$ for 0.40 m water depth compared to 0.35 m water depth varies from 9.24% to 12.32% and for 0.45 m water depth; $W/\gamma H_i^2$ varies from 26.64% to 27.51%.

When the QBW radius is increased to 0.60 m, the percentage increase in $W/\gamma H_i^2$ for a $4.247 \times 10^{-3} < H_i/gT^2 < 6.371 \times 10^{-3}$ and at 0.40 m water depth compared to 0.35 m water depth varies from 9.41% to 14.58% and for 0.45 m water depth, $W/\gamma H_i^2$ varies from 22.99% to 31.68%.

From the graphs plotted, the non-dimensional parameter $W/\gamma H_i^2$ was found to be decreasing with increase in QBW radius for all values of wave steepness and at different water depths. This may be because for higher QBW radius or lower relative water depth (d/h_s), the interaction of the structure with the wave will be less and the wave force exerted on the structure will be minimum resulting in lesser values for $W/\gamma H_i^2$.

From the results, it is observed the values for a water depth of 0.45 m $W/\gamma H_i^2$ varies from 4.098 to 12.439, 4.221 to 13.223 and 4.332 to 13.889 respectively for QBW of radius 0.60 m, 0.575 m and 0.55 m. Similarly the values obtained for $W/\gamma H_i^2$ varies from 3.566 to 11.023, 3.746 to 12.00 and 3.885 to 12.336 for QBW of radius 0.60 m, 0.575 m and 0.5 m and at 0.40 m water depth. At water depth equal to 0.35 m $W/\gamma H_i^2$ varies from 4.098 to 12.439, 3.456 to 10.182 and 3.557 to 10.467 for QBW of radius 0.60 m, 0.575 m and 0.55 m and at 0.40 m water depth.

The minimum value of $W/\gamma H_i^2$ obtained is 3.112 corresponding to $H_i/gT^2 = 6.241 \times 10^{-3}$ for QBW of radius equal to 0.60 m and at 0.35 m water depth. The percentage increase in $W/\gamma H_i^2$ for QBW of 0.575 m radius is 2.91% to 5.93% and for QBW of 0.55 m radius 5.40% to 10.44% compared to that of QBW of radius 0.60 m observed at a water depth equal to 0.45 m.

Similarly at a water depth of 0.40 m, the percentage of increase in $W/\gamma H_i^2$ for QBW of 0.575 m radius is 4.81% to 8.14% and for QBW of 0.55 m radius 8.21% to 10.64% compared to that of QBW of radius 0.60 m. At 0.35 m water depth, the percentage of increase in $W/\gamma H_i^2$ for QBW of 0.575 m radius is 6.07% to 6.63% and for QBW of 0.55 m radius 8.62% to 12.51% compared to that of QBW of radius 0.60 m.

6.4 STUDIES ON EMERGED SEASIDE PERFORATED QBW

The results obtained from the studies on emerged QBW are analysed separately for different spacing to diameter (S/D) ratios as well as for different breakwater radii under different water depths (say 0.35 m, 0.40 m and 0.45 m) and varying wave conditions. The results are plotted as non-dimensional graphs to study the effect of influencing parameters such as wave steepness, water depth, S /D ratio and breakwater radii.

6.5 VARIATION OF STABILITY PARAMETER ($W/\gamma H_i^2$) FOR QBW 0.55 m RADIUS (h_s= 0.615 m)

6.5.1 Influence of incident wave steepness on stability parameter

(a) For S/D = 2

(b) For S/D= 2.5

(c) For S/D = 3

(d) For S/D= 4

(e) For S/D= 5
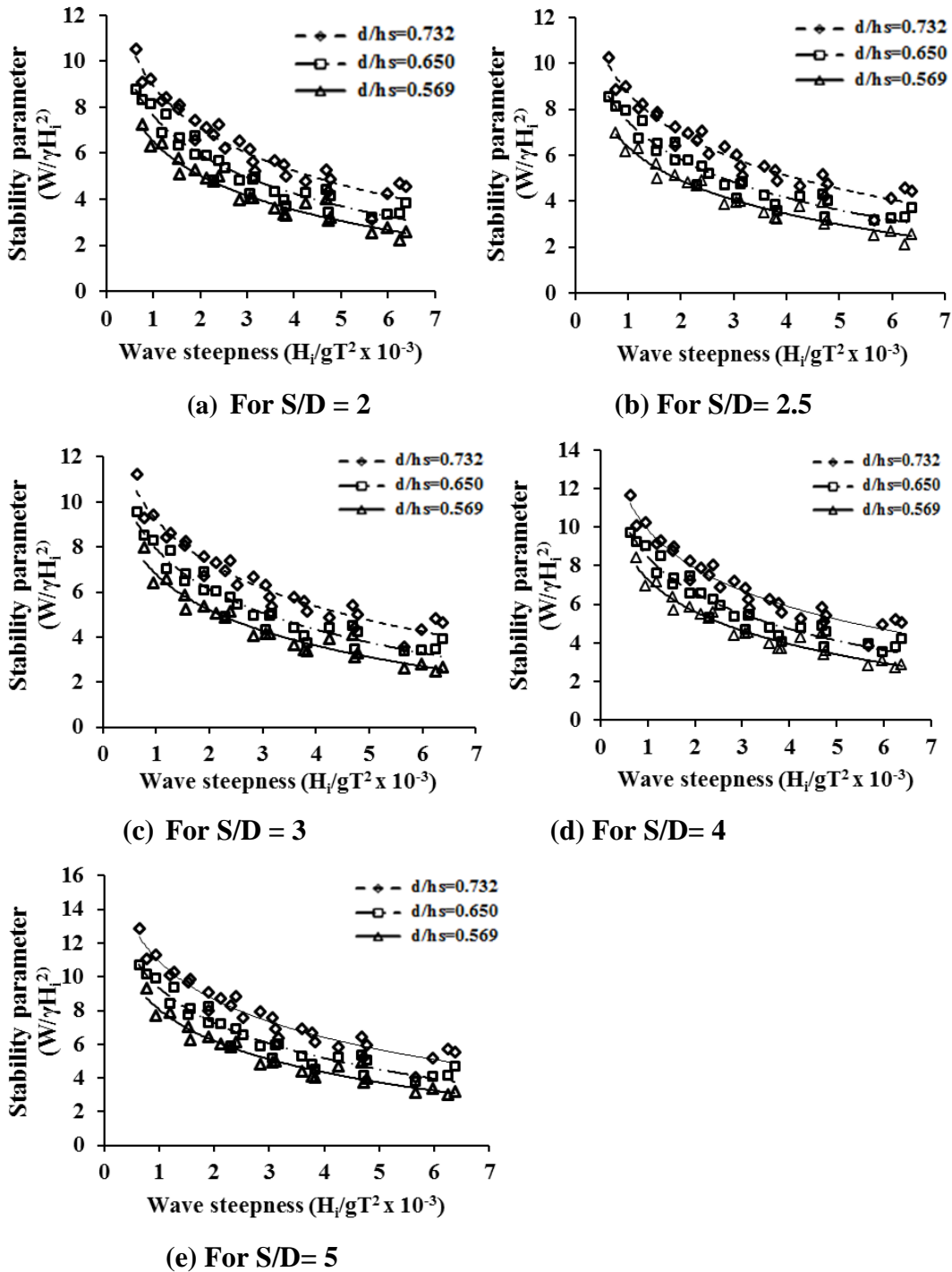
Fig. 6.7 Influence of H_i/gT^2 on $W/\gamma H_i^2$ for different d/h_s and S/D ratio

6.5.1.1 Seaside perforated QBW with S/D = 2.

The variation of $W/\gamma H_i^2$ with H_i/gT^2 at different water depths for QBW radius 0.55 m and S/D ratio equal to 2 are plotted as shown in Fig. 6.7(a). It is clear from the

graphs that $W/\gamma H_i^2$ decreases with increase in H_i/gT^2 for all values of d/h_s. This may be due to the reason that waves of higher steepness (lower wave period for a given wave height) interacts with the QBW surface only for short interval of time causing lesser wave force. Therefore lesser weight has to be added to prevent sliding and hence lower values of $W/\gamma H_i^2$.

Considering all values d/h_s, $W/\gamma H_i^2$ varies from 2.225 to 10.532 for $6.24 \times 10^{-4} < H_i/gT^2 < 6.4 \times 10^{-3}$ and S/D= 2. The maximum value for $W/\gamma H_i^2$ observed is 10.532 for $H_i/gT^2 = 6.318 \times 10^{-4}$ and at 0.45 m water depth (d/h_s equal to 0.732). The minimum value for $W/\gamma H_i^2$ observed is 2.225 for $H_i/gT^2 = 6.241 \times 10^{-3}$ and at water depth equal to 0.35 m ($d/h_s = 0.569$).

6.5.1.2 Seaside perforated QBW with S/D = 2.5
When S/D ratio is increased to 2.5, the observed values for $W/\gamma H_i^2$ varies from 2.110 to 10.269 for $6.24 \times 10^{-4} < H_i/gT^2 < 6.4 \times 10^{-3}$. The maximum value for $W/\gamma H_i^2$ observed is 10.269 for $H_i/gT^2 = 6.318 \times 10^{-4}$ and at water depth equal to 0.45 m (d/h_s equal to 0.732). The minimum $W/\gamma H_i^2$ observed is 2.110 for $H_i/gT^2 = 6.241 \times 10^{-3}$ and at water depth equal to 0.35 m ($d/h_s = 0.569$) (Refer Fig. 6.7 (b)).

6.5.1.3 Seaside perforated QBW with S/D = 3
For S/D = 3, the values obtained from the experiments for $W/\gamma H_i^2$ are observed to be varying from 2.472 to 11.223 for $6.24 \times 10^{-4} < H_i/gT^2 < 6.4 \times 10^{-3}$ (Refer Fig. 6.7 (c)). The maximum $W/\gamma H_i^2$ observed is 11.223 for $H_i/gT^2 = 6.318 \times 10^{-4}$ and at water depth equal to 0.45 m. The minimum $W/\gamma H_i^2$ observed is 2.472 for $H_i/gT^2 = 6.241 \times 10^{-3}$ and at 0.35 m water depth.

6.5.1.4 Seaside perforated QBW with S/D = 4
From Fig. 6.7 (d) showing the variation of $W/\gamma H_i^2$ with H_i/gT^2 for different water depths with radius of breakwater constant (R = 0.55 m or h_s= 0.615 m) and S/D ratio equal to 4, the values of $W/\gamma H_i^2$ is found to be varying from 2.729 to 11.668 for $6.24 \times 10^{-4} < H_i/gT^2 < 6.4 \times 10^{-3}$. The maximum $W/\gamma H_i^2$ observed is 11.688 for wave height of 0.03 m and a wave period of 2.2 s ($H_i/gT^2 = 6.318 \times 10^{-4}$) and at water depth equal to 0.45 m (d/h_s equal to 0.732). The minimum $W/\gamma H_i^2$ observed is 2.729 for wave height of 0.12 m and a wave period of 1.4s ($H_i/gT^2 = 6.2410 \times 10^{-3}$) and at water depth equal to 0.35 m (d/h_s equal to 0.569).

6.5.1.5 Seaside perforated QBW with S/D = 5

From Fig. 6.7(e), it is observed that for S/D equal to 5 and for all values d/h_s and QBW of 0.55 m radius, $W/\gamma H_i^2$ varies from 3.006 to 12.850 for $6.24 \times 10^{-4} < H_i/gT^2 < 6.4 \times 10^{-3}$. The highest value for $W/\gamma H_i^2$ observed is 12.850 for $H_i/gT^2 = 9.439 \times 10^{-4}$ and at water depth equal to 0.45 m. The lowest $W/\gamma H_i^2$ observed is 3.006 for wave height of 0.12 m and a wave period of 1.4s ($H_i/gT^2 = 6.241 \times 10^{-3}$) and at water depth equal to 0.35 m.

Table 6.1 Range of variation of $W/\gamma H_i^2$ (for R = 0.55 m or h_s= 0.615 m)

S/D ratio	Water depth in m	d/ h_s	Range of variation in $W/\gamma H_i^2$
2	0.45	0.732	3.335 – 10.532
	0.40	0.650	3.236 – 8.766
	0.35	0.569	2.225 – 7.249
2.5	0.45	0.732	3.198 – 10.269
	0.40	0.650	3.155 – 8.546
	0.35	0.569	2.110 – 6.967
3	0.45	0.732	3.566 – 11.223
	0.40	0.650	3.385– 9.566
	0.35	0.569	2.472 – 7.989
4	0.45	0.732	3.882 – 11.668
	0.40	0.650	3.555 – 9.711
	0.35	0.569	2.729 – 8.412
5	0.45	0.732	4.056 – 12.850
	0.40	0.650	3.779 – 10.695
	0.35	0.569	3.006 – 9.355

The variation of $W/\gamma H_i^2$ with wave steepness for different water depths and S/D ratio for QBW with 0.55 m radius are summarized in Table 6.1.

For all models, it is observed when the incident wave steepness increases, the dimensionless stability parameter decreases. This is because for a given wave height and long period waves (low steepness) exert more force on the caisson demanding more minimum weight and short period (steep) waves transfer less force, hence low

minimum weight. The sliding due to increase in wave force is overcome by increasing the weight of breakwater by adding additional weight into the caisson.

6.5.2 Influence of water depth on stability parameter

Fig. 6.8 represents the variation of non-dimensional stability parameter $(W/\gamma H_i^2)$, with relative water depth, d/h_s for different ranges of incident wave steepness (H_i/gT^2), for a constant QBW radius and S/D values. It is found that when the relative water depth d/h_s increases, the value of $W/\gamma H_i^2$ also increases for all values of wave steepness. This is because higher the water depths, greater the QBW model exposed to wave action, and hence, imparts more force and therefore increase in $W/\gamma H_i^2$.

For S/D = 2, the minimum $W/\gamma H_i^2$ observed is 2.225 for $H_i/gT^2 = 6.2410 \times 10^{-3}$ at a water depth equal to 0.35 m (d/h_s = 0.569). At the same water depth, the maximum $W/\gamma H_i^2$ obtained is 7.249 for $H_i/gT^2 = 7.645 \times 10^{-4}$. At a water depth equal to 0.40 m (d/h_s = 0.650), the minimum and the maximum value for $W/\gamma H_i^2$ observed is 3.236 and 8.766 for $H_i/gT^2 = 5.972 \times 10^{-3}$ and 7.645×10^{-4} respectively. Further increase in water depth to 0.45 m, the minimum and the maximum value for $W/\gamma H_i^2$ observed is 3.335 and 10.532 for $H_i/gT^2 = 5.663 \times 10^{-3}$ and 6.318×10^{-4} respectively.

From all these results, it is clear that as the water depth increases, the value of $W/\gamma H_i^2$ increases and the minimum value for $W/\gamma H_i^2$ are observed at a water depth of 0.35 m. As water depth increases from 0.35 m to 0.40 m there is an increase in $W/\gamma H_i^2$ by 17.30 % to 31.24%. When water depth increases from 0.35 m to 0.45m there is an increase in $W/\gamma H_i^2$ by 31.17 % to 33.28%. Therefore it is clear that the structure is safe against sliding with minimum weight including additional weight at lower water depths.

When S/D = 2.5 and at a water depth equal to 0.35 m (d/h_s equal to 0.569), minimum value for $W/\gamma H_i^2$ observed is 2.110 when $H_i/gT^2 = 6.2410 \times 10^{-3}$ and the maximum value of $W/\gamma H_i^2$ is 6.967 for $H_i/gT^2 = 7.645 \times 10^{-4}$. For water depth equal to 0.40 m (d/h_s = 0.650), the minimum value for $W/\gamma H_i^2$ observed is 3.155 at $H_i/gT^2 = 5.972 \times 10^{-3}$. Under the same condition, the maximum value of $W/\gamma H_i^2$ obtained is 8.546 for $H_i/gT^2 = 6.318 \times 10^{-4}$.
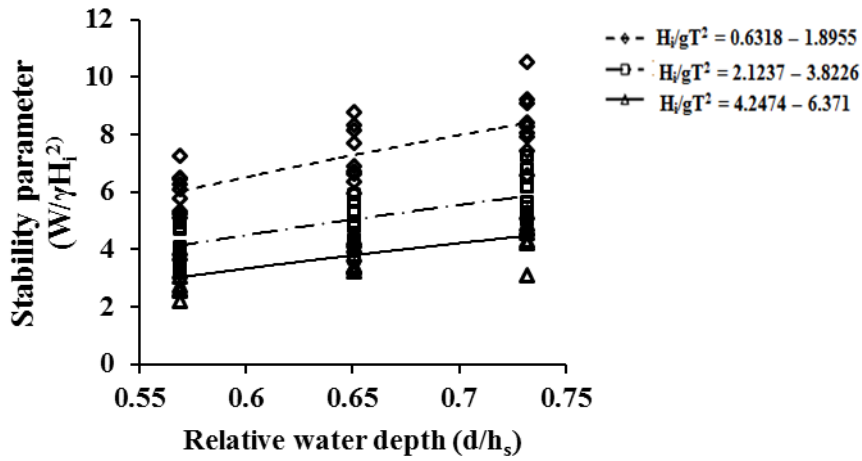
(a) For S/D = 2
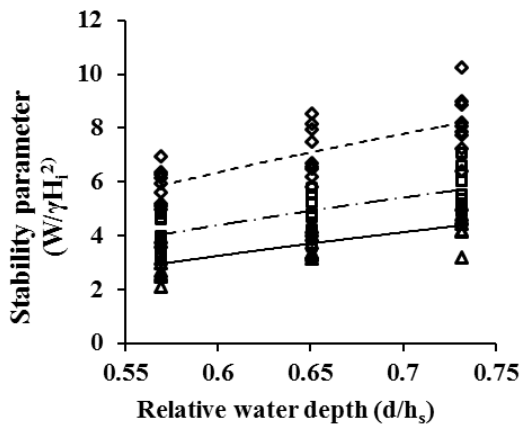
(b) For S/D = 2.5
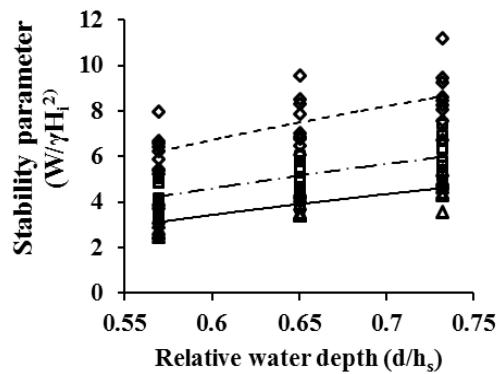
(c) For S/D = 3
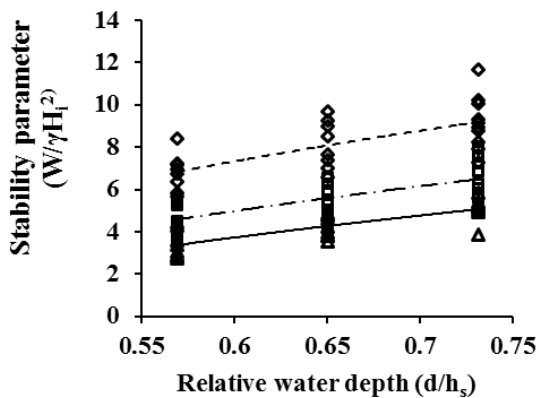
(d) For S/D = 4
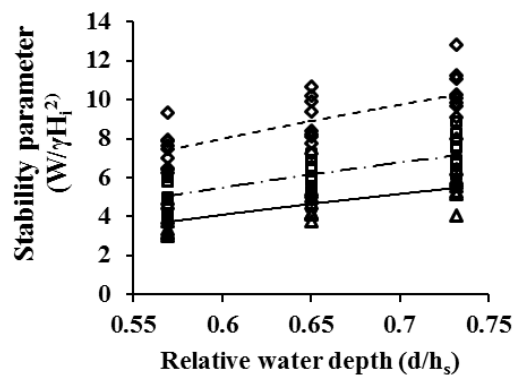
(e) For S/D = 5

Fig. 6.8 Variation of $W/\gamma H_i^2$ with d/h_s for various S/D values (for R= 0.55 m)

At a water depth equal to 0.45 m (d/h_s = 0.732), the minimum and the maximum value for $W/\gamma H_i^2$ observed is 3.198 and 10.269 for H_i/gT^2 = 5.663 x10^{-3} and 6.318 x10^{-4} respectively. When water depth increases from 0.35 m to 0.40 m there is an

increase in $W/\gamma H_i^2$ by 18.47% to 33.12%. When water depth increases from 0.35 m to 0.45m there is an increase in $W/\gamma H_i^2$ by 32.15% to 34.02%.

For S/D= 3 and at a water depth equal to 0.35 m, minimum value for $W/\gamma H_i^2$ observed is 2.472 when $H_i/gT^2 = 6.2410$ x10^{-3} and the maximum value of $W/\gamma H_i^2$ is 7.989 for $H_i/gT^2 = 7.645$ x10^{-4}. For 0.40 m water depth ($d/h_s = 0.650$), the minimum value for $W/\gamma H_i^2$ observed is 3.385 at $H_i/gT^2 = 5.972$ x10^{-3}. Under the same condition, the maximum value of $W/\gamma H_i^2$ obtained is 9.566 for $H_i/gT^2 = 6.318$ x10^{-4}. At a water depth equal to 0.45 m ($d/h_s= 0.732$), the minimum and the maximum value for $W/\gamma H_i^2$ observed is 3.556 and 11.223 for $H_i/gT^2= 5.663$ x10^{-3} and 6.318 x10^{-4} respectively. When water depth increases from 0.35 m to 0.40 m there is an increase in $W/\gamma H_i^2$ by 16.48% to 26.97%. When water depth increases from 0.35 m to 0.45 m there is an increase in $W/\gamma H_i^2$ by 28.81% to 30.48%.

Considering S/D= 4 and at 0.35 m water depth, minimum value for $W/\gamma H_i^2$ observed is 2.472 when $H_i/gT^2 = 6.2410$ x10^{-3} and the maximum value of $W/\gamma H_i^2$ is 7.989 for $H_i/gT^2 = 7.645$ x10^{-4}. For water depth equal to 0.40 m ($d/h_s =0.650$), the minimum value for $W/\gamma H_i^2$ observed is 3.555 at $H_i/gT^2 = 5.972$ x10^{-3} and the maximum $W/\gamma H_i^2$ observed is 9.711 for $H_i/gT^2 = 6.318$ x10^{-4}. At a water depth equal to 0.45 m ($d/h_s = 0.732$), the minimum and the maximum value for $W/\gamma H_i^2$ observed is 3.882 and 11.668 for $H_i/gT^2= 5.663$ x10^{-3} and 6.318 x10^{-4} respectively. When water depth increases from 0.35 m to 0.40 m there is an increase in $W/\gamma H_i^2$ by 13.37% to 23.23%.When water depth increases from 0.35 m to 0.45m there is an increase in $W/\gamma H_i^2$ by 27.90% to 29.70%.

Further increasing S/D ratio to 5, the minimum $W/\gamma H_i^2$ observed is 3.006 for 0.35 m water depth when $H_i/gT^2 = 6.2410$ x10^{-3} and the maximum value of $W/\gamma H_i^2$ is 9.355 for $H_i/gT^2 = 7.645$ x10^{-4}. For water depth equal to 0.40 m, the minimum and the maximum $W/\gamma H_i^2$ observed is 3.779 and 10.695 respectively. At a water depth equal to 0.45 m ($d/h_s = 0.732$), the minimum and the maximum value for $W/\gamma H_i^2$ observed is 4.056 and 12.850 for $H_i/gT^2= 5.663$ x10^{-3} and 6.318 x10^{-4} respectively. The increase in $W/\gamma H_i^2$ when water depth increases from 0.35 m to 0.40 m is found to be varying from 12.52% to 20.46%. When water depth increases from 0.35 m to 0.45 m there is an increase in $W/\gamma H_i^2$ by 25.88% to 27.19%.

In all of the above cases for different wave steepness and for a constant S/D value, it is observed that the stability parameter $W/\gamma H_i^2$ increases with increase in relative water depth (d/h_s). This is because higher the water depth, greater is the area of the QBW model structure exposed to wave action, and hence, the increase in d/h_s imparts more force and therefore increase in $W/\gamma H_i^2$. This means that for a constant S/D ratio more structure weight is required for sliding stability in larger depths compared to smaller water depth.

6.5.3 Influence of S/D ratio on stability parameter

For a constant QBW radius (say 0.55 m) and different water depths, variations of $W/\gamma H_i^2$ for different values of S/D ratio are analyzed separately. It is observed that $W/\gamma H_i^2$ increases with increase in S/D for all values of d/h_s.
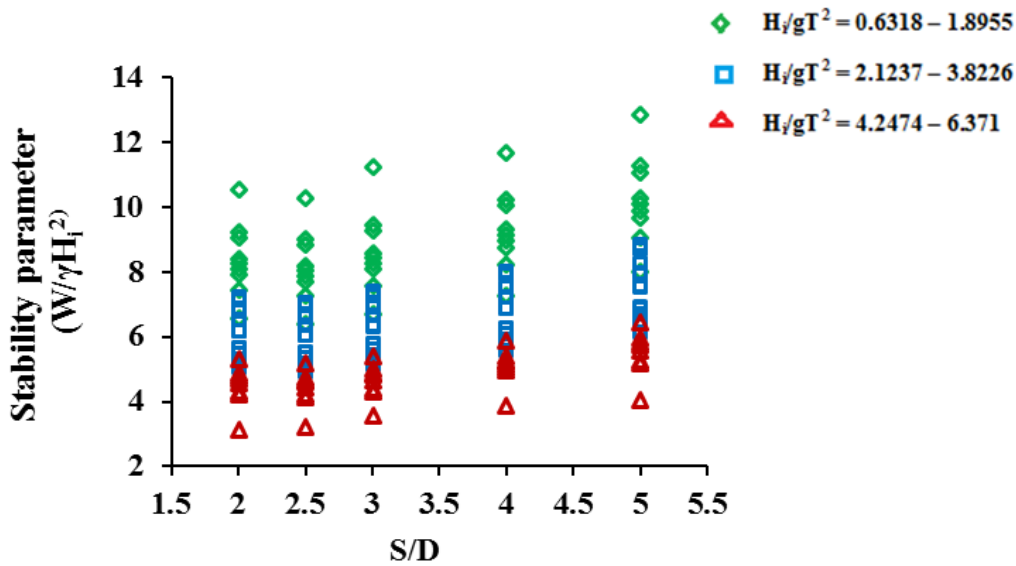
Fig. 6.9 Influence of S/D on $W/\gamma H_i^2$ for d/h_s = 0.732 (water depth = 0.45m)

Considering water depth of 0.45 m (d/h_s = 0.732), for an S/D = 5, $W/\gamma H_i^2$ varies in the range 4.056 to 12.850 for $6.24 \times 10^{-4} < H_i/gT^2 < 6.4 \times 10^{-3}$.

For S/D= 4, the range of variation of $W/\gamma H_i^2$ is found to be 3.882 to 11.668; for S/D = 3 $W/\gamma H_i^2$ is observed to be in the range 3.566 to 11.223; for S/D = 2.5, the value of $W/\gamma H_i^2$ varies in the range 3.198 to 10.269. But for S/D = 2, the range of variation of $W/\gamma H_i^2$ is from 3.335 to 10.532 (Refer Fig. 6.9).
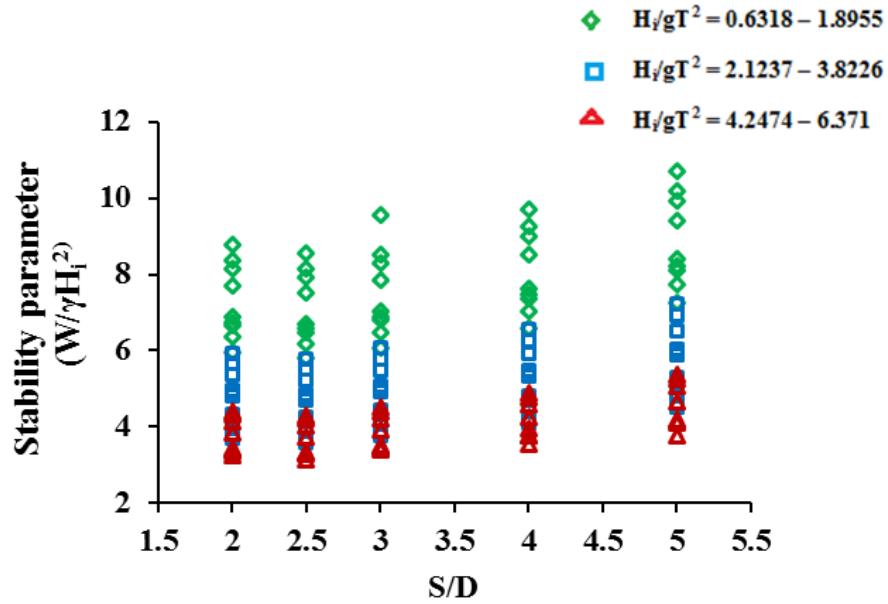
Fig. 6.10 Influence of S/D on W/γH$_i^2$ for d/h$_s$ = 0.650 (water depth = 0.40 m)

When water depth is reduced to 0.40 m (d/h$_s$ = 0.650), for an S/D = 5, the value of W/γH$_i^2$ varies in the range 3.779 to 10.699 for $6.24 \times 10^{-4} <$ H$_i$/gT$^2 < 6.4 \times 10^{-3}$. For S/D ratio = 4, the range of variation of W/γH$_i^2$ is found to be 3.555 to 9.711. The variation of W/γH$_i^2$ for S/D = 3 is observed to be in the range 3.385 to 9.566; for S/D = 2.5, the value of W/γH$_i^2$ varies in the range 3.155 to 8.546 and for S/D ratio = 2, the range of variation of W/γH$_i^2$ is from 3.236 to 8.766 (Refer Fig. 6.10).
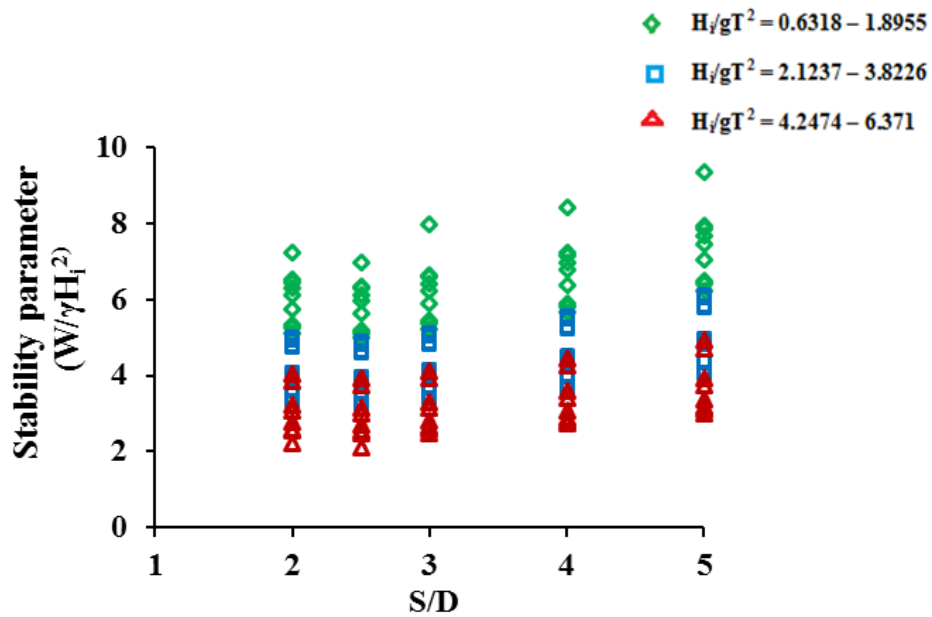
Fig. 6.11 Influence of S/D on W/γH$_i^2$ for d/h$_s$ = 0.569 (water depth = 0.35 m)

Fig. 6.11 shows the variation of $W/\gamma H_i^2$ for different values of S/D ratio for a seaside perforated QBW of radius 0.55 m at a water depth of 0.35 m (d/h_s equal to 0.569). It is observed that for S/D = 5, the value of $W/\gamma H_i^2$ varies in the range 3.006 to 9.355 for $6.24 \times 10^{-4} < H_i/gT^2 < 6.4 \times 10^{-3}$. For the same radius of QBW and at the same water depth, for S/D = 4, $W/\gamma H_i^2$ is observed to be in the range 2.729 to 8.412. The range of variation of $W/\gamma H_i^2$ is observed to be from 2.472 to 7.989 for S/D = 3, from 2.110 to 6.967 for S/D ratio equal to 2.5 and from 2.225 to 7.249 for S/D = 2.

From the results for $W/\gamma H_i^2$, it is observed that at a water depth equal to 0.35 m , the percentage reduction in $W/\gamma H_i^2$ for S/D = 4 is 9.21% to 10.08 % compared to S/D ratio equal to 5. The percentage reduction in $W/\gamma H_i^2$ for S/D = 3, 2.5 and 2 are 14.60% to 17.76% , 25.52% to 29.80% and 22.51% to 25.98% with respect to S/D= 5.

At a water depth equal to 0.40 m, the percentage reduction in $W/\gamma H_i^2$ for S/D = 4 , 3, 2.5 and 2 are 5.92% to 9.20% , 10.42% to 10.55% , 16.51% to 20.09% and 14.36% to 18.04% with respect to S/D = 5. At a water depth equal to 0.45 m, the percentage reduction in $W/\gamma H_i^2$ for S/D = 4 is 4.29% to 9.19% compared to S/D = 5. The percentage reduction in $W/\gamma H_i^2$ for S/D = 3, 2.5 and 2 are 12.32% to 12.66%, 20.08% to 21.15% and 17.77% to 18.03% with respect to S/D = 5.

From the results for $W/\gamma H_i^2$ for varying ranges of H_i/gT^2, it is observed that $W/\gamma H_i^2$ increases with increase in S/D ratio. For lower values of S/D, $W/\gamma H_i^2$ is found to very less compared to higher values except in the case of S/D ratio equal to 2. For lower values of S/D perforations encountered are more resulting in dissipating of major portion of the wave energy and hence force exerted on the QBW caisson will be very less. Therefore the weight required for resisting sliding stability will be very less and resulting in lower values for $W/\gamma H_i^2$.

6.6 VARIATION OF $W/\gamma H_i^2$ FOR QBW OF 0.575 m RADIUS (h_s= 0.640 m)

6.6.1   Influence of incident wave steepness on stability

Fig. 6.12 shows the variation of stability parameter $W/\gamma H_i^2$ with wave steepness for different S/D values and at different water depths. For S/D = 2, the dimensionless stability parameter, $W/\gamma H_i^2$ varies from 2.127 to 9.798 for $6.24 \times 10^{-4} < H_i/gT^2 < 6.4 \times 10^{-3}$.
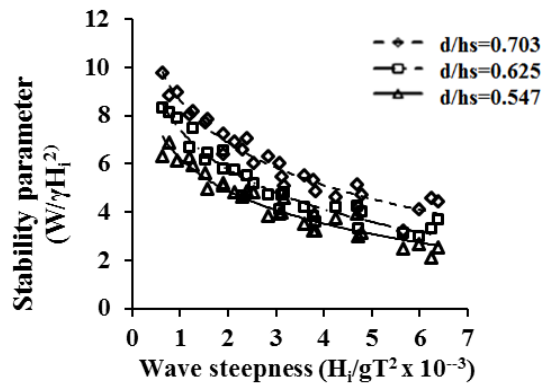
(a) For S/D = 2
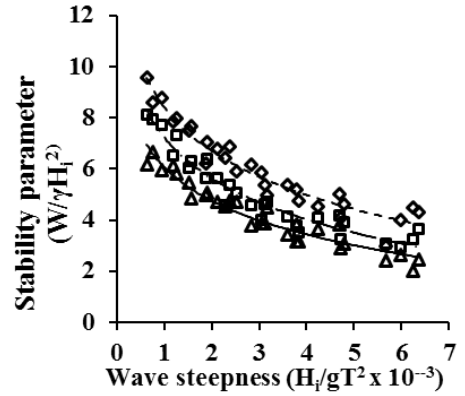
(b) For S/D =2.5
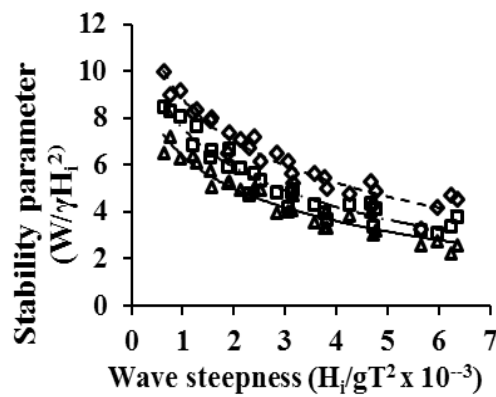
(c) For S/D = 3
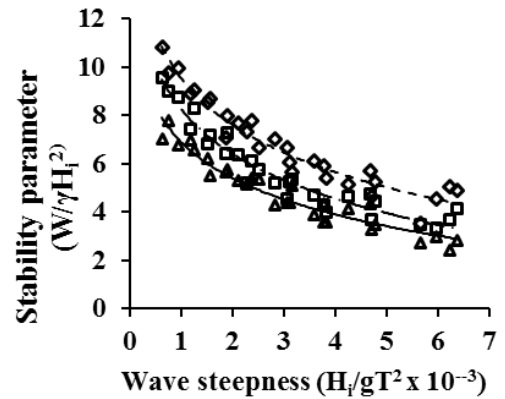
(d) For S/D = 4
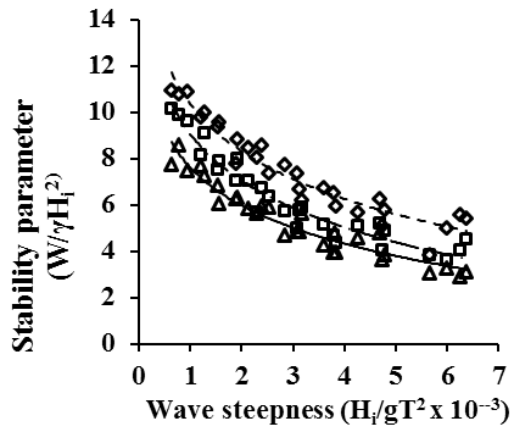
(e) For S/D = 5

Fig. 6.12 Influence of H_i/gT^2 on $W/\gamma H_i^2$ for different d/h_s and S/D ratio

It is clear from the graph that $W/\gamma H_i^2$ decreases with increase in H_i/gT^2 for all values of d/h_s. The maximum value for $W/\gamma H_i^2$ observed is 9.798 at $H_i/gT^2 = 6.318$ x10^{-4} and at water depth equal to 0.45 m (d/h_s equal to 0.703). The minimum value for $W/\gamma H_i^2$ observed is 2.127 at $H_i/gT^2 = 6.241$ x10^{-3} and at water depth equal to 0.35 m ($d/h_s = 0.547$).

When S/D ratio is increased to 2.5, considering all values d/h_s, $W/\gamma H_i^2$ varies from 1.998 to 9.553 for $6.24 \times 10^{-4} < H_i/gT^2 < 6.4 \times 10^{-3}$. The maximum value for $W/\gamma H_i^2$ observed is 9.553 when $H_i/gT^2 = 6.318 \times 10^{-4}$ and at water depth equal to 0.45 m ($d/h_s = 0.703$). The minimum value for $W/\gamma H_i^2$ observed is 1.998 at $H_i/gT^2 = 6.241 \times 10^{-3}$ and at water depth equal to 0.35 m ($d/h_s = 0.547$).

Considering all values d/h_s and for S/D= 3, $W/\gamma H_i^2$ varies from 2.225 to 10.008 for $6.24 \times 10^{-4} < H_i/gT^2 < 6.4 \times 10^{-3}$. The maximum value for $W/\gamma H_i^2$ observed is 10.008 when $H_i/gT^2 = 6.318 \times 10^{-4}$ and at water depth equal to 0.45 m ($d/h_s = 0.703$). The minimum value for $W/\gamma H_i^2$ observed is 2.225 at $H_i/gT^2 = 6.241 \times 10^{-3}$ and at 0.35 m water depth ($d/h_s = 0.547$).

Table 6.2 Range of variation of $W/\gamma H_i^2$ (for R = 0.575 m or h_s= 0.640 m)

S/D ratio	Water depth in m	d/ h_s	Range of variation in $W/\gamma H_i^2$
2	0.45	0.703	3.228 – 9.798
	0.40	0.625	3.008 – 8.310
	0.35	0.547	2.127 – 6.889
2.5	0.45	0.703	3.005 – 9.553
	0.40	0.625	2.925 – 8.103
	0.35	0.547	1.998 – 6.668
3	0.45	0.703	3.289 – 10.008
	0.40	0.625	3.065– 8.489
	0.35	0.547	2.225 – 7.203
4	0.45	0.703	3.523 – 10.855
	0.40	0.625	3.324 – 9.588
	0.35	0.547	2.445 – 7.812
5	0.45	0.703	3.856 – 10.954
	0.40	0.625	3.661 – 10.140
	0.35	0.547	2.924 – 8.603

When S/D= 4, $W/\gamma H_i^2$ varies from 2.445 to 10.855 for all values d/h_s and $6.24 \times 10^{-4} < H_i/gT^2 < 6.4 \times 10^{-3}$. The maximum value for $W/\gamma H_i^2$ observed is 10.855 when at

$H_i/gT^2 = 6.318 \times 10^{-4}$ and at water depth equal to 0.45 m ($d/h_s = 0.703$). The minimum value for $W/\gamma H_i^2$ observed is 2.445 at $H_i/gT^2 = 6.241 \times 10^{-3}$ and at water depth equal to 0.35 m ($d/h_s = 0.547$).

Further increasing S/D to 5, $W/\gamma H_i^2$ varies from 2.924 to 10.954 for $6.24 \times 10^{-4} < H_i/gT^2 < 6.4 \times 10^{-3}$. The maximum $W/\gamma H_i^2$ observed is 10.954 when at $H_i/gT^2 = 6.318 \times 10^{-4}$ and at water depth equal to 0.45 m (d/h_s equal to 0.703). The minimum value for $W/\gamma H_i^2$ observed is 2.924 at $H_i/gT^2 = 6.241 \times 10^{-3}$ and at water depth equal to 0.35 m ($d/h_s = 0.547$). The variation of $W/\gamma H_i^2$ with wave steepness for different water depths and S/D ratio for QBW with 0.575 m radius are summarized in Table 6.2.

6.6.2 Influence of water depth on stability parameter

The variation of non-dimensional stability parameter ($W/\gamma H_i^2$), with relative water depth, d/h_s for different ranges of incident wave steepness (H_i/gT^2), for a constant QBW radius and S/D value is shown in Fig. 6.13. It is found that when the relative water depth d/h_s increases, the value of $W/\gamma H_i^2$ also increases for all values of wave steepness.

For QBW of radius 0.575 m and S/D ratio equal to 2, the minimum value for $W/\gamma H_i^2$ observed is 2.127 when $d/h_s = 0.547$ (water depth = 0.35 m). At the same condition for water depth equal to 0.40 m ($d/h_s = 0.625$), the minimum observed value for $W/\gamma H_i^2$ is 3.008 and for a water depth equal to 0.45 m ($d/h_s = 0.703$), the minimum observed value for $W/\gamma H_i^2$ is 3.228.

The percentage increase in $W/\gamma H_i^2$ with increase in water depth from 0.35 m to 0.40 m is found to be varying from 17.09% to 29.28%. Also the percentage increase in $W/\gamma H_i^2$ with increase in water depth from 0.35 m to 0.45 m is found to be 29.68% to 34.10%.

For S/D ratio equal to 2.5, the minimum value observed for $W/\gamma H_i^2$ is 1.998 at a water depth of 0.35 m ($d/h_s = 0.547$). For 0.40 m water depth ($d/h_s = 0.625$), the minimum observed value for $W/\gamma H_i^2$ is 2.925 and for 0.45 m water depth ($d/h_s = 0.703$), the minimum observed value for $W/\gamma H_i^2$ is 3.005.
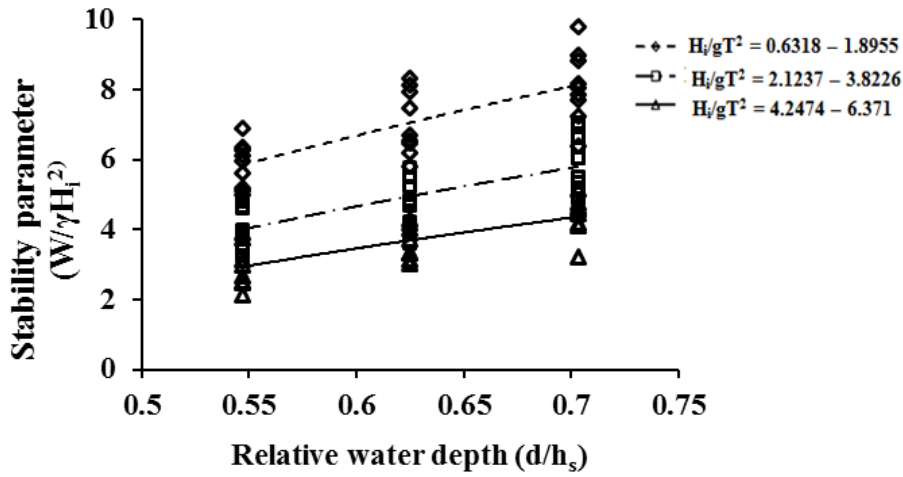
(a) For S/D = 2
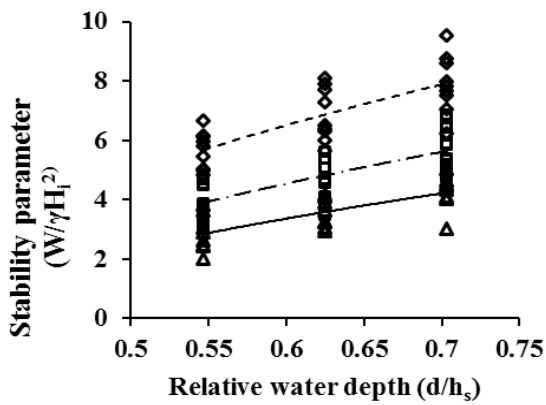
(b) For S/D = 2.5
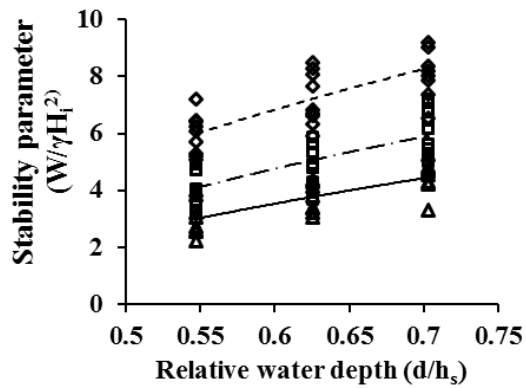
(c) For S/D = 3
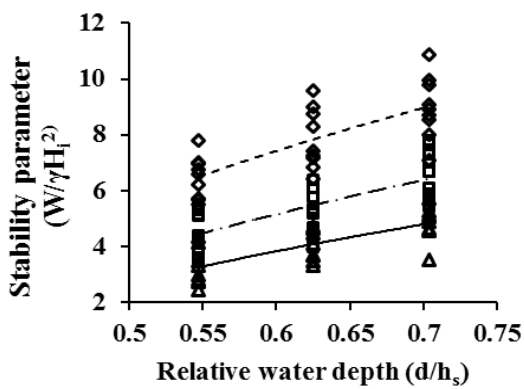
(d) For S/D = 4
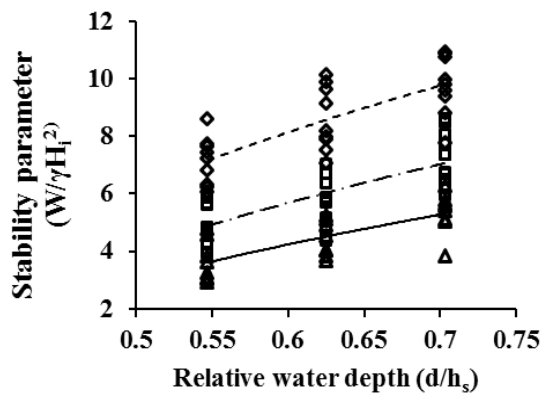
(e) For S/D = 5

Fig. 6.13 Influence of d/h_s on $W/\gamma H_i^2$ for S/D= 2, 2.5, 3, 4 and 5

The increase in $W/\gamma H_i^2$ with increase in water depth is more effective for 0.45 m water depth compared to 0.35 m water depth i.e. from 17.71% to 31.69% and percentage reduction with increase in water depth from 0.35 m to 0.40 m water depth is found to be 30.19% to 33.51%.

For S/D ratio equal to 3 and under similar condition, the minimum observed value for $W/\gamma H_i^2$ is 2.225 at a water depth of 0.35 m. For water depth equal to 0.40 m, the minimum observed value for $W/\gamma H_i^2$ is 3.065 and for water depth equal to 0.45 m, the minimum observed value for $W/\gamma H_i^2$ is 3.289. When water depth is increased from 0.35 m to 0.40 m there is increase in $W/\gamma H_i^2$ from 15.14% to 27.41% and for increase in water depth from 0.35 m to 0.45 m there is an increase in $W/\gamma H_i^2$ from 28.03% to 32.35%.

When S/D ratio is increased to 4, the minimum observed value for $W/\gamma H_i^2$ is 2.445 at a water depth of 0.45 m. At the same condition for water depth equal to 0.40 m, the minimum observed value for $W/\gamma H_i^2$ is 3.324 and for a water depth equal to 0.35 m, the minimum observed value for $W/\gamma H_i^2$ is 3.523. The percentage reduction in $W/\gamma H_i^2$ with increase in water depth from 0.35 m to 0.40 m is found to vary from 18.52% to 26.44% and from 0.35 m to 0.45 m varies from 28.03% to 30.59%.

Further increasing S/D ratio to 5 and under similar condition, the minimum observed value for $W/\gamma H_i^2$ is 2.924 at a water depth of 0.45 m. For water depth equal to 0.40 m, the minimum observed value for $W/\gamma H_i^2$ is 3.661 and for water depth equal to 0.35 m, the minimum observed value for $W/\gamma H_i^2$ is 3.856. The percentage reduction in $W/\gamma H_i^2$ with increase in water depth from 0.35 m to 0.40 m is found to vary from 15.15% to 20.13% and from 0.35 m to 0.45 m varies from 21.46% to 24.17%.

6.6.3   Influence of S/D ratio on stability parameter

The variation of $W/\gamma H_i^2$ with S/D ratios for different H_i/gT^2 and under different water depths for a QBW of radius equal to 0.575 m is plotted as non-dimensional graphs (Refer Fig. 6.14). It is observed that the value $W/\gamma H_i^2$ decreases with decrease in S/D ratios for all values of d/h_s and different ranges of H_i/gT^2 considered for the study.

At a water depth of 0.45 m (d/h_s equal to 0.703) and S/D ratio equal to 2, $W/\gamma H_i^2$ varies from 3.228 to 9.798 for $6.24 \times 10^{-4} < H_i/gT^2 < 6.4 \times 10^{-3}$. For the same radius of QBW and at the same water depth, for S/D ratio equal to 2.5, $W/\gamma H_i^2$ varies from 3.005 to 9.553 and S/D ratio equal to 3, the range of variation of $W/\gamma H_i^2$ is found to be 3.289 to 10.008. The variation of $W/\gamma H_i^2$ for S/D ratio equal to 4 is observed to

be in the range 3.523 to 10.855 and for S/D ratio equal to 5, the value of $W/\gamma H_i^2$ varies in the range 3.856 to 10.954.
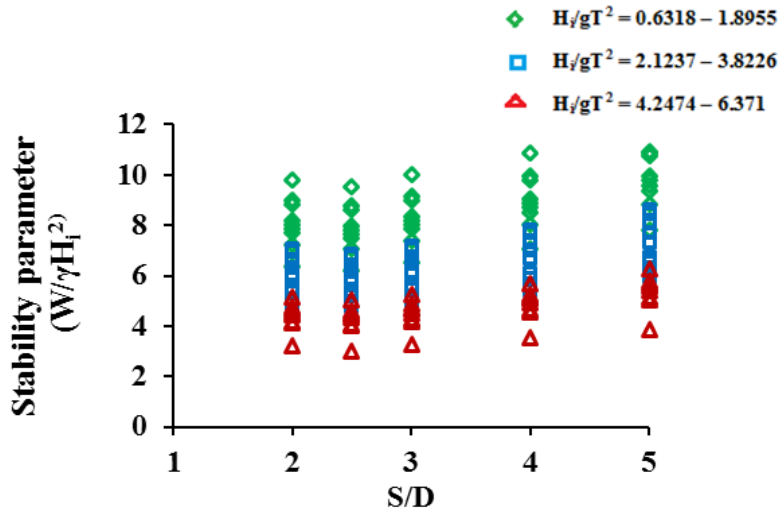
(a) For $d/h_s = 0.703$
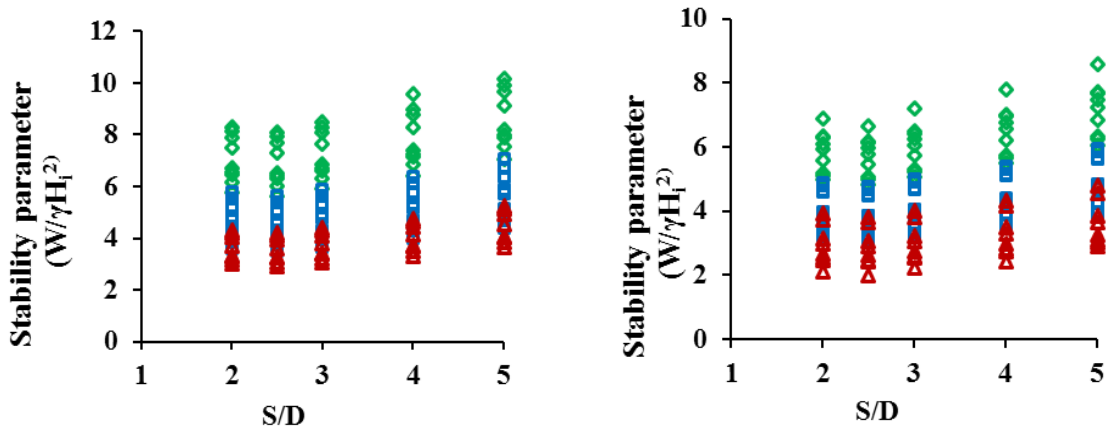
(b) For $d/h_s = 0.625$

(c) For $d/h_s = 0.547$

Fig. 6.14 Influence of S/D on $W/\gamma H_i^2$ for various d/h_s

Considering 0.40 m water depth ($d/h_s = 0.625$) and S/D =2, the range of variation of $W/\gamma H_i^2$ is from 3.008 to 8.310. For the same radius of QBW and at the same water depth, S/D = 2.5, the range of variation of $W/\gamma H_i^2$ is found to be 2.925 to 8.103 and for S/D = 3, $W/\gamma H_i^2$ varies from 3.065 to 8.489. The variation of $W/\gamma H_i^2$ for S/D = 4 is observed to be in the range 3.324 to 9.588 and for S/D = 5, the value of $W/\gamma H_i^2$ varies in the range 3.661 to 10.140.

Further reducing the water depth to 0.35 m (d/h_s = 0.547) and S/D = 2, the range of variation of W/γH_i^2 is from 2.127 to 6.889 for 6.24x10^{-4}< H_i/gT^2 < 6.4x10^{-3}. For the same radius of QBW and at the same water depth for S/D = 2.5, the range of variation of W/γH_i^2 is found to be 1.998 to 6.668 and for S/D = 3, W/γH_i^2 varies from 2.225 to 7.203. The variation of W/γH_i^2 for S/D = 4 is observed to be in the range 2.445 to 7.812 and for an S/D = 5, the value of W/γH_i^2 varies in the range 2.924 to 8.603.

From the analysis of data for W/γH_i^2, it is observed that at 0.35 m water depth, the percentage reduction in W/γH_i^2 for S/D = 4 varies from 9.19% to 16.38% compared to S/D = 5. The percentage reduction in W/γH_i^2 for S/D = 3, 2.5 and 2 varies from 16.27% to 23.90%, 22.49% to 31.67% and 19.92% to 27.25% with respect to S/D = 5. Similarly at water depth equal to 0.40 m, the percentage reduction in W/γH_i^2 for S/D ratio equal to 4, 3, 2.5 and 2 varies from 5.44% to 9.20 %, 16.20% to 16.28% , 20.08 % to 20.10% and 17.83% to 18.05% with respect to S/D = 5. At 0.45 m water depth, the percentage reduction in W/γH_i^2 for S/D = 4 varies from 0.09% to 8.63% compared to S/D =5. The percentage reduction in W/γH_i^2 for S/D = 3, 2.5 and 2 varies from 8.64% to 14.70% , 12.78% to 22.07% and 10.55% to 16.36% with respect to S/D = 5.

6.7 VARIATION OF STABILITY PARAMETER (W/γH_i^2) FOR QBW 0.60 m RADIUS (h_s= 0.665 m)

6.7.1   Influence of incident wave steepness on stability

The variation of stability parameter, W/γH_i^2 with wave steepness H_i/gT^2 for different values of d/h_s and S/D ratio are shown in Fig. 6.15. For S/D= 2, W/γH_i^2 varies from 2.096 to 9.385 for 6.24x10^{-4}< H_i/gT^2 < 6.4x10^{-3}. The maximum value for W/γH_i^2 observed is 9.385 at H_i/gT^2 = 6.318 x10^{-4} and at water depth equal to 0.45 m (d/h_s equal to 0.677). The minimum value for W/γH_i^2 observed is 2.096 at H_i/gT^2 = 6.241 x10^{-3} and at water depth equal to 0.35 m (d/h_s = 0.526).

The values for W/γH_i^2 for S/D = 2.5, varies from 1.967 to 9.150 for 6.24x10^{-4}< H_i/gT^2 < 6.4x10^{-3}. The maximum W/γH_i^2 observed is 9.150 at H_i/gT^2 = 6.318 x10^{-4} and at water depth equal to 0.45 m (d/h_s equal to 0.677). The minimum W/γH_i^2 observed is 1.967 at H_i/gT^2 = 6.241 x10^{-3} and at water depth equal to 0.35 m (d/h_s = 0.526).

(a) For S/D =2

(b) For S/D =2.5

(c) For S/D = 3

(d) For S/D = 4

(e) For S/D = 5
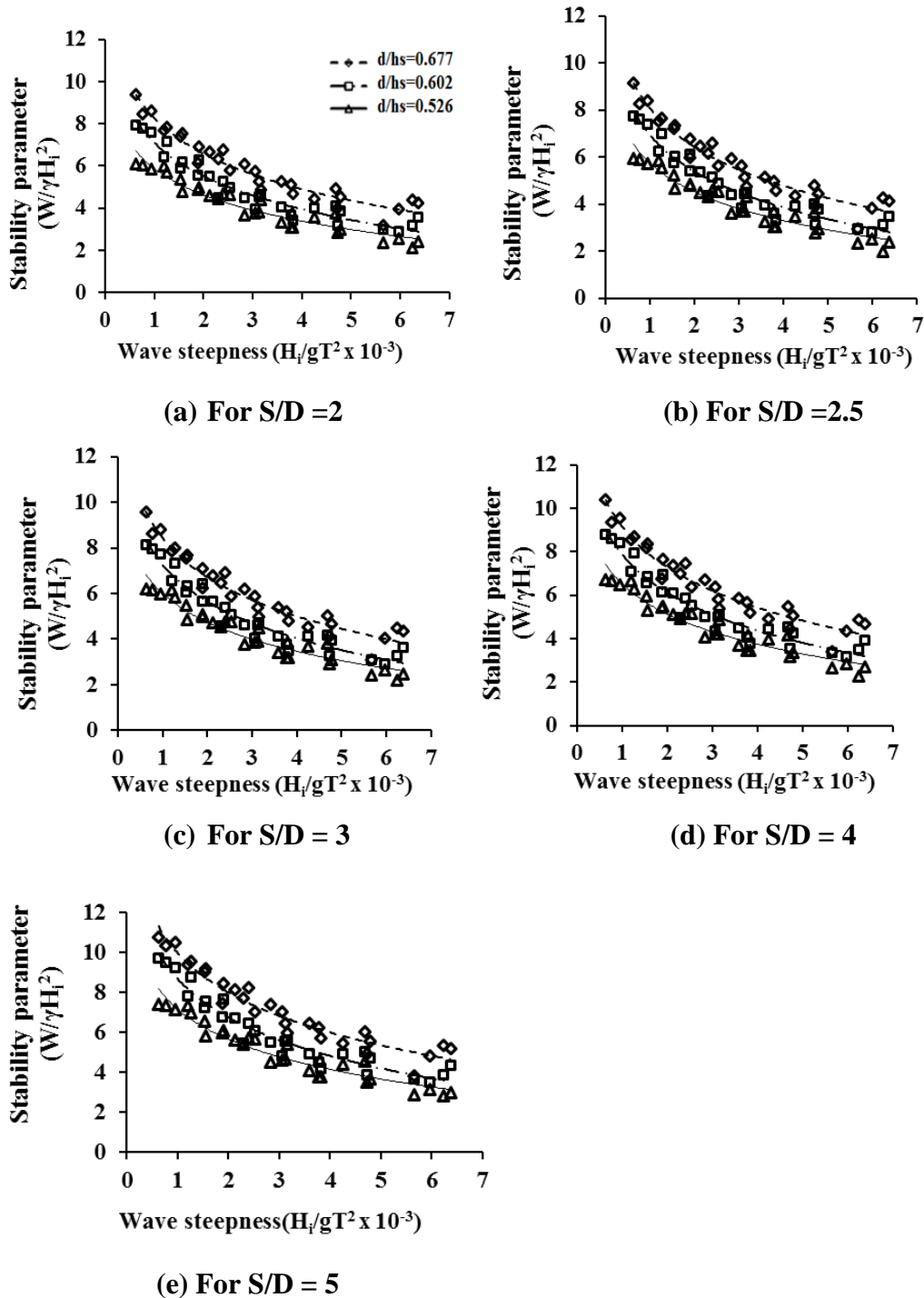
Fig. 6.15 Influence of H_i/gT^2 on $W/\gamma H_i^2$ for different d/h_s and S/D ratio

From Fig. 6.15, it is observed that the values for S/D= 3, $W/\gamma H_i^2$ varies from 2.187 to 9.586 for $6.24 \times 10^{-4} < H_i/gT^2 < 6.4 \times 10^{-3}$. The maximum $W/\gamma H_i^2$ observed is 9.586 at $H_i/gT^2 = 6.318 \times 10^{-4}$ and at water depth equal to 0.45 m (d/h_s equal to 0.677). The minimum $W/\gamma H_i^2$ observed is 2.187 at $H_i/gT^2 = 6.241 \times 10^{-3}$ and at water depth equal to 0.35 m ($d/h_s = 0.526$).

When S/D=4, $W/\gamma H_i^2$ varies from 2.256 to 10.397 for $6.24 \times 10^{-4} < H_i/gT^2 < 6.4 \times 10^{-3}$.

The maximum $W/\gamma H_i^2$ observed is 10.397 at $H_i/gT^2 = 6.318 \times 10^{-4}$ and at water depth equal to 0.45 m (d/h_s equal to 0.677). The minimum $W/\gamma H_i^2$ observed is 2.256 at $H_i/gT^2 = 6.241 \times 10^{-3}$ and at 0.35 m water depth ($d/h_s = 0.526$).

Further when increasing S/D = 5, maximum $W/\gamma H_i^2$ observed is 10.777 at $H_i/gT^2 = 6.318 \times 10^{-4}$ and at water depth equal to 0.45 m ($d/h_s = 0.677$). The minimum $W/\gamma H_i^2$ observed is 2.801 at $H_i/gT^2 = 6.241 \times 10^{-3}$ and at water depth equal to 0.35 m ($d/h_s = 0.526$). The variation of $W/\gamma H_i^2$ with wave steepness for different water depths and S/D ratio for QBW with 0.60 m radius are summarized in Table 6.3.

Table 6.3 Range of variation of $W/\gamma H_i^2$ (for R = 0.60 m or h_s = 0.665 m)

S/D ratio	Water depth in m	d/ h_s	Range of variation in $W/\gamma H_i^2$
2	0.45	0.643	3.189 – 9.385
	0.40	0.571	2.874 – 7.960
	0.35	0.500	2.096 – 6.075
2.5	0.45	0.643	2.967 – 9.150
	0.40	0.571	2.802 – 7.761
	0.35	0.500	1.967 – 5.923
3	0.45	0.643	3.115– 9.586
	0.40	0.571	2.935 – 8.131
	0.35	0.500	2.187 – 6.205
4	0.45	0.643	3.427 – 10.397
	0.40	0.571	3.340 – 8.819
	0.35	0.500	2.256 – 6.730
5	0.45	0.643	3.815 – 10.777
	0.40	0.571	3.506 – 9.712
	0.35	0.500	2.801 – 7.412

6.7.2   Influence of water depth on stability parameter

The variation of stability parameter, $W/\gamma H_i^2$ with relative water depth d/h_s for different values of H_i/gT^2 and S/D ratio are shown in Fig. 6.16. For QBW of radius 0.60 m and S/D = 2, the minimum value for $W/\gamma H_i^2$ observed is 3.189 at a water depth of 0.45 m. At the same condition for water depth equal to 0.40 m, the

minimum observed value for $W/\gamma H_i^2$ is 2.874 and for a water depth equal to 0.35 m, the minimum observed value for $W/\gamma H_i^2$ is 2.096.
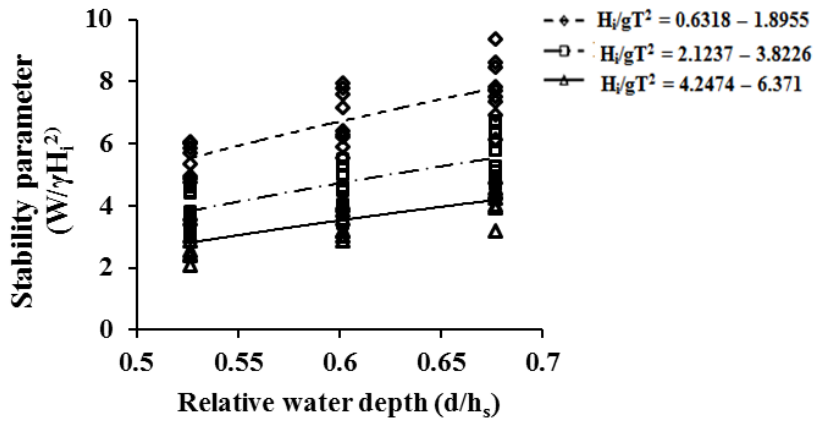
(a) For S/D =2
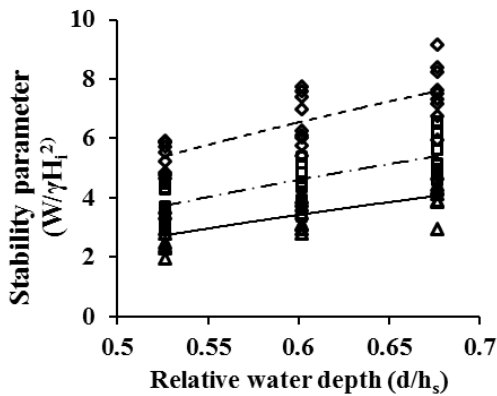
(b) For S/D =2.5
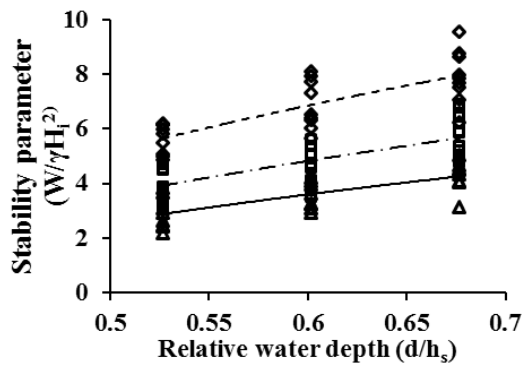
(c) For S/D = 3
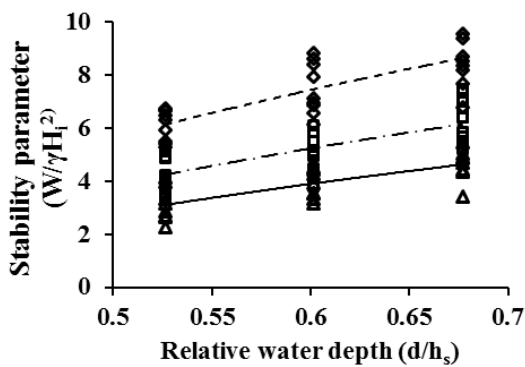
(d) For S/D = 4
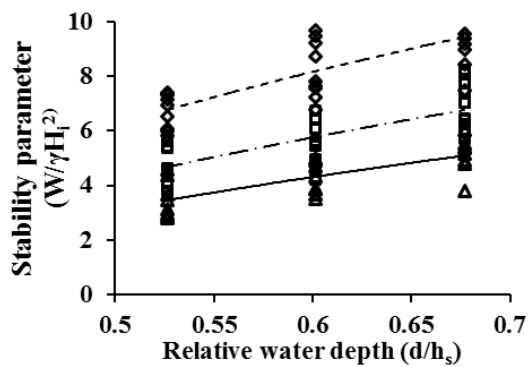
(e) For S/D = 5

Fig. 6.16 Variation of $W/\gamma H_i^2$ with d/h_s , for different S/D values

The percentage increase in $W/\gamma H_i^2$ with increase in water depth from 0.35 m to 0.40 m is found to be varying from 23.68% to 27.07% and 0.35 m to 0.45 m is found to be varying from 32.15% to 35.27%.

For S/D = 2.5 and under similar condition, the minimum observed value for $W/\gamma H_i^2$ is 2.967 at water depth of 0.45 m. For water depth equal to 0.40 m, the minimum observed value for $W/\gamma H_i^2$ is 2.802 and for water depth equal to 0.35 m, the minimum observed value for $W/\gamma H_i^2$ is 1.967. The percentage increase in $W/\gamma H_i^2$ with increase in water depth from 0.35 m to 0.40 m is found to be varying from 21.68% to 27.07%. Also the percentage increase in $W/\gamma H_i^2$ with increase in water depth from 0.35 m to 0.45 m is found to be 32.15% to 34.27%.

For S/D ratio equal to 3 and under similar condition, the minimum observed value for $W/\gamma H_i^2$ is 3.115 at a water depth of 0.45 m. For water depth equal to 0.40 m, the minimum observed value for $W/\gamma H_i^2$ is 2.935 and for water depth equal to 0.35 m, the minimum observed value for $W/\gamma H_i^2$ is 2.187.

The percentage increase in $W/\gamma H_i^2$ with increase in water depth from 0.35 m to 0.40 m is found to be varying from 24.00% to 25.49%. Also the percentage increase in $W/\gamma H_i^2$ with increase in water depth from 0.35 m to 0.45 m is found to be 29.79% to 35.30%.

When S/D ratio is increased to 4, the minimum observed value for $W/\gamma H_i^2$ is 3.427 at a water depth of 0.45 m. At the same condition for water depth equal to 0.40 m, the minimum observed value for $W/\gamma H_i^2$ is 3.340 and for a water depth equal to 0.35 m, the minimum observed value for $W/\gamma H_i^2$ is 2.256.

The percentage increase in $W/\gamma H_i^2$ with increase in water depth from 0.35 m to 0.40 m is found to be varying from 22.64% to 32.45%. Also the percentage increase in $W/\gamma H_i^2$ with increase in water depth from 0.35 m to 0.45 m is found to be 34.16% to 35.45%.

For S/D ratio equal to 5 and under similar condition, the minimum observed value for $W/\gamma H_i^2$ is 3.815 at a water depth of 0.45 m. For water depth equal to 0.40 m, the minimum observed value for $W/\gamma H_i^2$ is 3.506 and for water depth equal to 0.35 m, the minimum observed value for $W/\gamma H_i^2$ is 2.801.

The percentage increase in $W/\gamma H_i^2$ with increase in water depth from 0.35 m to 0.40 m is found to be varying from 20.10% to 23.23%. Also the percentage increase in $W/\gamma H_i^2$ with increase in water depth from 0.35 m to 0.45 m is found to be 26.57% to 31.22%.

6.7.3 Influence of S/D ratio on stability parameter
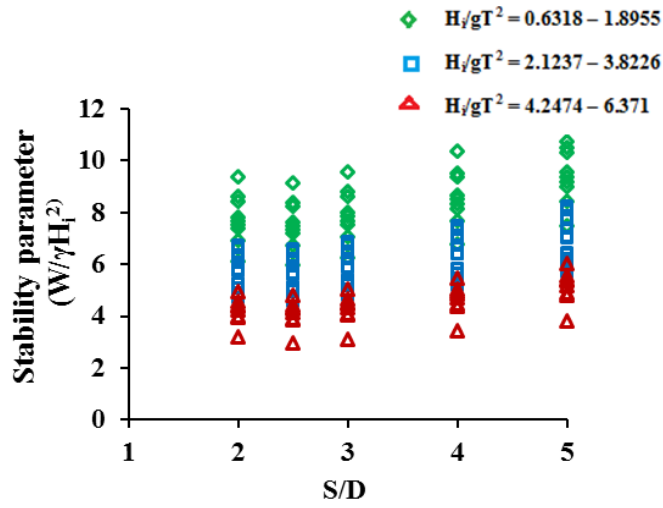
(a) For $d/h_s = 0.677$
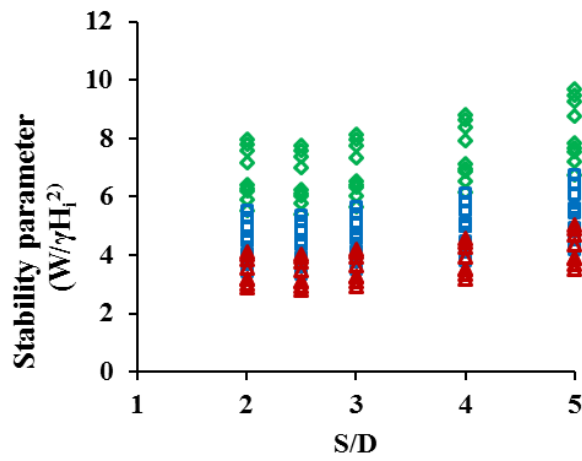
(b) For $d/h_s = 0.602$
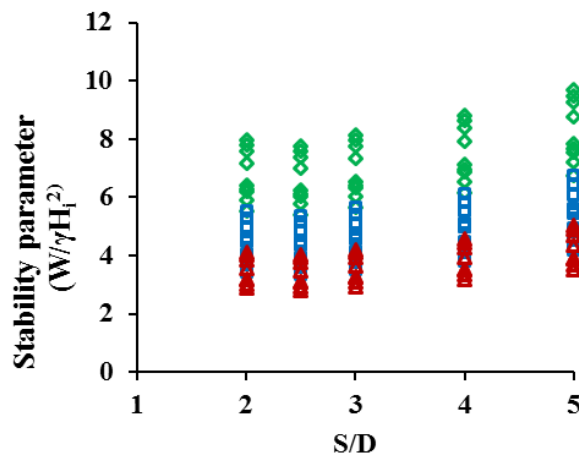
(c) For $d/hs = 0.526$

Fig 6.17 Influence of S/D on $W/\gamma H_i^2$ for various H_i/gT^2 and d/h_s

The variation of $W/\gamma H_i^2$ with S/D for different H_i/gT^2 and under different water depths for a QBW of radius equal to 0.60 m are plotted as non-dimensional graphs shown in Fig. 6.17. It is observed that the value $W/\gamma H_i^2$ decreases with decrease in S/D ratios 5, 4, 3 and 2.5 and then slightly increases for S/D= 2 for all values of d/h_s and different ranges of H_i/gT^2 considered for the study.

For a seaside perforated QBW of radius 0.60 m at a water depth of 0.45 m (d/h_s = 0.677) and S/D = 2, $W/\gamma H_i^2$ varies from 3.189 to 9.385 for $6.24\times10^{-4}< H_i/gT^2 < 6.4\times10^{-3}$. For the same radius of QBW and at the same water depth, for S/D = 2.5, $W/\gamma H_i^2$ varies from 2.967 to 9.150 and S/D = 3, the range of variation of $W/\gamma H_i^2$ is found to be 3.115 to 9.586. The variation of $W/\gamma H_i^2$ for S/D = 4 is observed to be in the range 3.427 to 10.397 and for S/D = 5, the value of $W/\gamma H_i^2$ varies in the range 3.815 to 10.777.

When water depth is reduced to 0.40 m (d/h_s = 0.602), for S/D = 2, the range of variation of $W/\gamma H_i^2$ is from 2.874 to 7.960. For the same radius of QBW and at the same water depth, S/D = 2.5, the range of variation of $W/\gamma H_i^2$ is found to be 2.802 to 7.761 and for S/D =3, $W/\gamma H_i^2$ varies from 2.935 to 8.131.The variation of $W/\gamma H_i^2$ for S/D = 4 is observed to be in the range 3.340 to 8.819 and for S/D = 5, the value of $W/\gamma H_i^2$ varies in the range 3.506 to 9.712.

For a water depth of 0.35 m (d/h_s = 0.526) and S/D = 2, the range of variation of $W/\gamma H_i^2$ is from 2.096 to 6.075 for $6.24\times10^{-4}<H_i/gT^2 >6.4\times10^{-3}$. For the same radius of QBW and at the same water depth, S/D = 2.5, the range of variation of $W/\gamma H_i^2$ is found to be varying from 1.967 to 5.923 and for S/D = 3, $W/\gamma H_i^2$ varies from 2.187 to 6.205. The variation of $W/\gamma H_i^2$ for S/D = 4 is observed to be in the range 2.256 to 6.730 and for an S/D = 5, the value of $W/\gamma H_i^2$ varies in the range 2.801 to 7.412. The percentage reduction in $W/\gamma H_i^2$ for different S/D ratios and at different water depths are foundout seperately. It is observed that the maximum percentage redution in $W/\gamma H_i^2$ is observed for S/D ratio equal to 2.5; at a water depth equal to 0.35 m.

From the analysis of data for $W/\gamma H_i^2$, it is observed that at a water depth equal to 0.35 m, the percentage reduction in $W/\gamma H_i^2$ for S/D ratio equal to 4 varies from 9.20% to 19.45% compared to S/D = 5. The percentage reduction in $W/\gamma H_i^2$ for S/D = 3, 2.5 and 2 varies from 16.28% to 21.92%, 20.08% to 29.77% and 18.03% to

25.17% with respect to S/D = 5. At a water depth equal to 40 cm ,the percentage reduction in $W/\gamma H_i^2$ for S/D = 4 varies from 4.73% to 9.19% compared to S/D ratio equal to 5. The percentage reduction in $W/\gamma H_i^2$ for S/D = 3, 2.5 and 2 varies from 16.20% to 16.28%, 19.98% to 20.08% and 18.02% to 18.11% respectively. When the water depth is increased to 45 cm ,the percentage reduction in $W/\gamma H_i^2$ for S/D = 4 varies from 3.52% to 10.17% compared to S/D = 5. The percentage reduction in $W/\gamma H_i^2$ for S/D ratio equal to 3,2.5 and 2 varies from 11.05% to 18.35%, 15.09% to 22.22% and 12.91% to 16.40% respectively.

From the results of the experiments conducted on QBW of different radii, it was observed that $W/\gamma H_i^2$ decreases with increase in QBW radius for all values of wave steepness for different S/D ratios and at different water depths. This may be because for lesser wave period, the interaction of the structure with the wave will be less and the wave force exerted on the structure will be minimum resulting in lesser values for $W/\gamma H_i^2$.

From the plotted non-dimensional graphs, it is observed the values for a water depth of 0.45 m and S/D= 2.5,$W/\gamma H_i^2$ varies from 2.967 to 9.150, 3.005 to 9.553 and 3.198 to 0.269 respectively for QBW of radius 0.60 m, 0.575 m and 0.55 m. Similarly the values for $W/\gamma H_i^2$ varies from 2.802 to 7.761, 2.925 to 8.103 and 3.155 to 8.546 for QBW of radius 0.60 m, 0.575 m and 0.55 m and at 0.40 m water depth. At water depth equal to 0.35 m $W/\gamma H_i^2$ varies from 1.967 to 5.923, 1.998 to 6.668 and 2.110 to 6.967 for QBW of radius 0.60 m, 0.575 m and 0.575 m.

The minimum value of $W/\gamma H_i^2$ obtained is 1.967 corresponding to $H_i/gT^2 = 6.241 \times 10^{-3}$ for QBW of radius 0.60 m and at 0.35 m water depth. The percentage increase in $W/\gamma H_i^2$ for QBW of 0.575 m radius is 1.26% to 4.21% and for QBW of 0.55 m radius 7.22% to 10.89% compared to that of QBW of radius 0.60 m observed at 0.45 m water depth. Similarly at 0.40 m water depth, the % increase in $W/\gamma H_i^2$ for QBW of 0.575 m radius is 4.20% to 4.22% and for QBW of 0.55 m radius 9.18% to 11.17% compared to that of QBW of radius 0.60 m. At 0.35 m water depth, the percentage increase in $W/\gamma H_i^2$ for QBW of 0.575 m radius is 1.55% to 11.20% and for QBW of 0.55 m radius is 6.77% to 14.98% compared to that of QBW of radius 0.60 m.

6.8 COMPARITIVE STUDY OF STABILITY ON EMERGED IMPERMEABLE AND SEASIDE PERFORATED QBW

From experimental investigations on sliding stability of impermeable and seaside perforated quarter circle breakwater, it is observed that the stability $W/\gamma H_i^2$ decreases with increase in wave steepness for all values of d/h_s and S/D ratio. In the case of impermeable QBW, the highest value for $W/\gamma H_i^2$ is equal to 13.889 observed for QBW of radius equal to 0.55 m for wave height of 0.03 m and a wave period of 2.2 s ($H_i/gT^2 = 6.318 \times 10^{-4}$) and at water depth equal to 0.45 m. But the minimum $W/\gamma H_i^2$ observed is 3.112 for wave height of 0.12 m and a wave period of 1.4 s ($H_i/gT^2 = 6.241 \times 10^{-3}$) and at water depth equal to 0.35 m for QBW of radius equal to 0.60 m.

For seaside perforated QBW, the highest value for $W/\gamma H_i^2$ is equal to 12.850 observed for QBW of radius equal to 0.55 m and S/D= 5 at a water depth equal to 0.45 m, $H_i/gT^2 = 6.318 \times 10^{-4}$. But the minimum $W/\gamma H_i^2$ observed is 1.967 at a wave height of 0.12 m and a wave period of 1.4 s ($H_i/gT^2 = 6.241 \times 10^{-3}$) and at water depth equal to 0.35 m for QBW of radius equal to 0.60 m. Therefore in the case of both impermeable as well as seaside perforated QBW, minimum values for $W/\gamma H_i^2$ is observed when higher wave steepness and hence minimum weight required preventing sliding of QBW for steep waves.

Fig. 6.18, 6.19 and 6.20 shows the comparison between impermeable and seaside perforated QBW with different S/D ratio for QBW of radius 0.55 m, 0.575 m and 0.60 m at 0.45 m water depth. In the case of impermeable QBW 0.60 m radius, for $6.318 \times 10^{-4} < H_i/gT^2 < 6.371 \times 10^{-3}$ and considering 0.45 m water depth as reference, the percentage reduction in $W/\gamma H_i^2$ varies from 11.38% to 12.98% for 0.40 m water depth and the percentage reduction in $W/\gamma H_i^2$ varies from 23.11% to 24.06% for 0.35 m water depth.

For sea side perforated QBW maximum reduction in $W/\gamma H_i^2$ is observed for S/D= 2.5 and for 0.35 m water depth. For QBW 0.60 m radius and S/D= 2.5, with reference to 0.45 m water depth the percentage reduction in $W/\gamma H_i^2$ varies from 5.56% to 15.18% for 0.40 m water depth and the percentage reduction in $W/\gamma H_i^2$ varies from 33.70% to 35.27% for 0.35 m water depth.
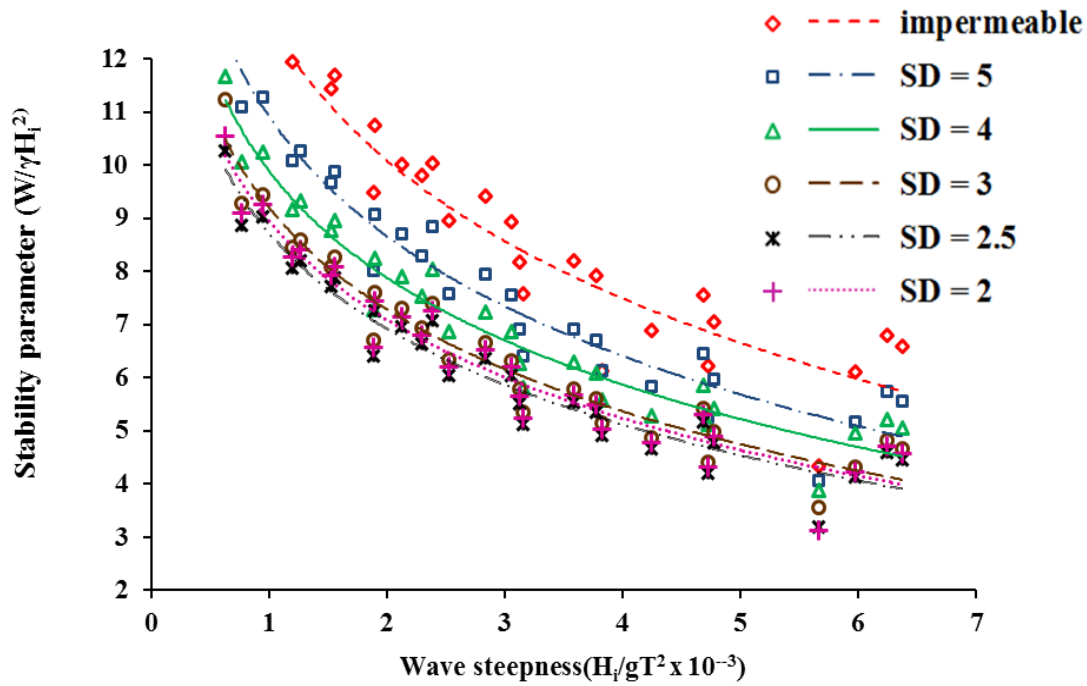
Fig. 6.18 Comparison of Stability paramerter for impermeable and seaside perforated QBW (d/h$_s$= 0.732)
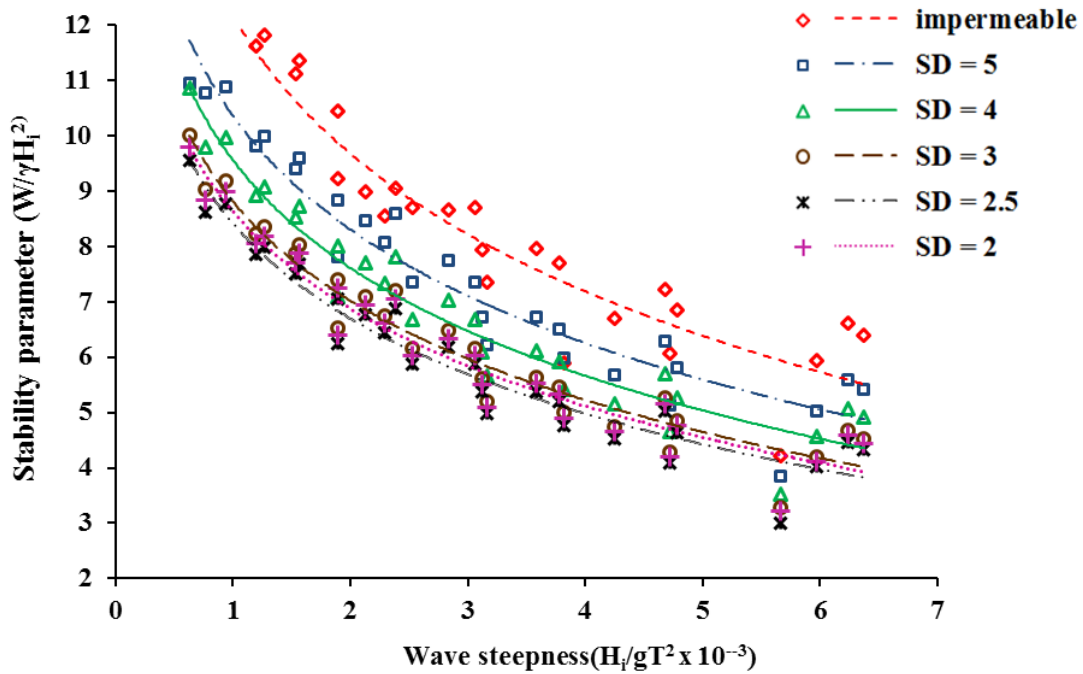
Fig 6.19 Comparison of Stabilty parameter for impermeable and seaside perforated QBW (d/h$_s$= 0.703)
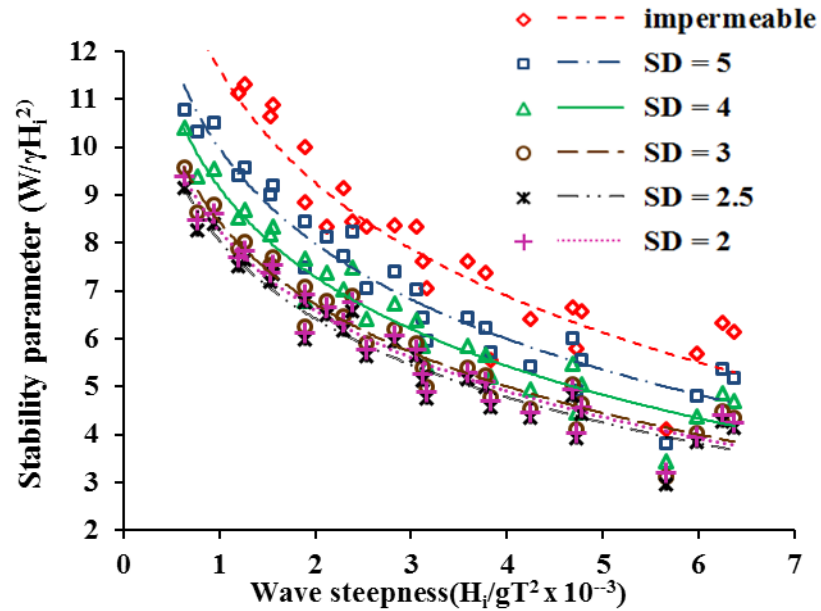
Fig 6.20 Comparison of Stability parameter for impermeable and seaside perforated QBW (d/h$_s$= 0.677)

Therefore it is seen that both impermeable and seaside perforated QBW has shown a similar trend of increase in $W/\gamma H_i^2$ with increase in water depth and the percentage reduction will be more for seaside perforated QBW with S/D= 2.5.

Considering water depth of 0.35 m and for impermeable QBW of radius 0.60 m, the values for $W/\gamma H_i^2$ varies in the range 3.112 to 9.564 for $6.24 \times 10^{-4} < H_i/gT^2 < 6.4 \times 10^{-3}$. For seaside perforated QBW of radius 0.60 m and considering water depth of 0.35 m, for an S/D = 5, $W/\gamma H_i^2$ varies in the range 2.801 to 7.412 for $6.24 \times 10^{-4} < H_i/gT^2 < 6.4 \times 10^{-3}$. For S/D ratio equal to 4, the range of variation of $W/\gamma H_i^2$ is found to be 2.256 to 6.730; for S/D = 3 $W/\gamma H_i^2$ is observed to be in the range 2.187 to 6.205; for S/D ratio equal to 2.5, the value of $W/\gamma H_i^2$ varies in the range 1.967 to 5.923 and for an S/D = 2, the range of variation of $W/\gamma H_i^2$ is from 2.096 to 6.075.

At a water depth equal to 0.45 m, when compared to impermeable QBW, the percentage reduction in $W/\gamma H_i^2$ for S/D ratio equal to 5 varies from 9.99% to 22.50%. The percentage reduction in $W/\gamma H_i^2$ for S/D ratio equal to 4, 3, 2.5 and 2 are found to be varying from 27.50% to 29.63%, 29.72% to 35.12% ,32.64% to 36.48% and 36.79% to 38.07% with respect impermeable QBW.

The minimum value of $W/\gamma H_i^2$ obtained for impermeable QBW of radius 0.55 m and at 0.35 m water depth is 3.557 and that for QBW of radius equal to 0.575 m and

0.60 m radius at the same water depth are 3.333 and 3.112 respectively. The percentage reduction in $W/\gamma H_i^2$ for impermeable QBW of radius 0.575 m and 0.60 m are found to be 6.29% and 12.51% respectively compared to QBW of radius 0.55 m. The minimum $W/\gamma H_i^2$ obtained for seaside perforated QBW of radius 0.55 m at S/D = 2.5 and at 0.35 m water depth is 2.110 and that for QBW of radius equal to 0.575 m and 0.60 m radius at the same water depth are 1.998 and 1.967 respectively. The percentage reduction in $W/\gamma H_i^2$ for impermeable QBW of radius 0.575 m and 0.60 m are found to be 5.30% and 6.77% respectively compared to QBW of radius 0.55 m. Therefore the effect of breakwater radius in reducing the values for $W/\gamma H_i^2$ is found to be negligible compared to that of S/D ratio.

6.9   EQUATIONS DEVELOPED FOR STABILITY PARAMETER

The results for the experimental studies on stability characteristics for impermeable QBW for different breakwater radius at different water depths and wave conditions are combined into suitable dimensionless terms. The regression analysis is done by using Excel statistical software – XLSTAT and the equation for the best fit curve is obtained.

The equation for $W/\gamma H_i^2$ for impermeable QBW is derived as follows:

$$W/\gamma H_i^2 = 16.731(H_i/gT^2)^{-0.236} + 20.126(d/h_s)^{5.22} - 7.944 \ldots\ldots\ldots\ldots\ldots\ldots\ldots\ldots (6.1)$$

Fig. 6.21 shows the comparison between the measured and predicted values of stability parameter $W/\gamma H_i^2$ for impermeable QBW.

Similarly the experimental results obtained for perforated QBW with different radius, S/D ratio at different water depths are combined into suitable dimensionless parameters. The curves with best fit for $W/\gamma H_i^2$ for perforated QBW are obtained.

The equation for $W/\gamma H_i^2$ for seaside perforated QBW was derived as follows:

$$W/\gamma H_i^2 = 6.813(H_i/gT^2)^{-0.503} + 31.580(d/h_s)^{8.357} + 0.0008(d/h_s)^{4.524} - 0.0841 \ldots (6.2)$$

Fig 6.22 shows the comparison between the measured and predicted values of stability parameter $W/\gamma H_i^2$ for perforated QBW.
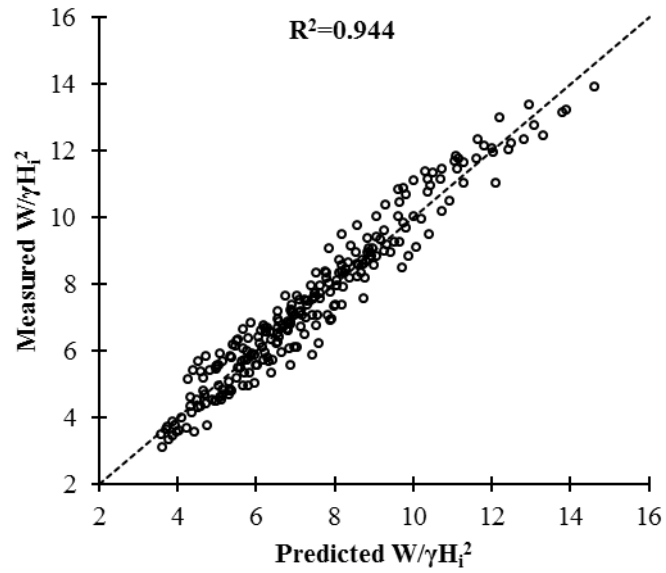
Fig 6.21 Comparison between measured and predicted values of $W/\gamma H_i^2$ for impermeable QBW
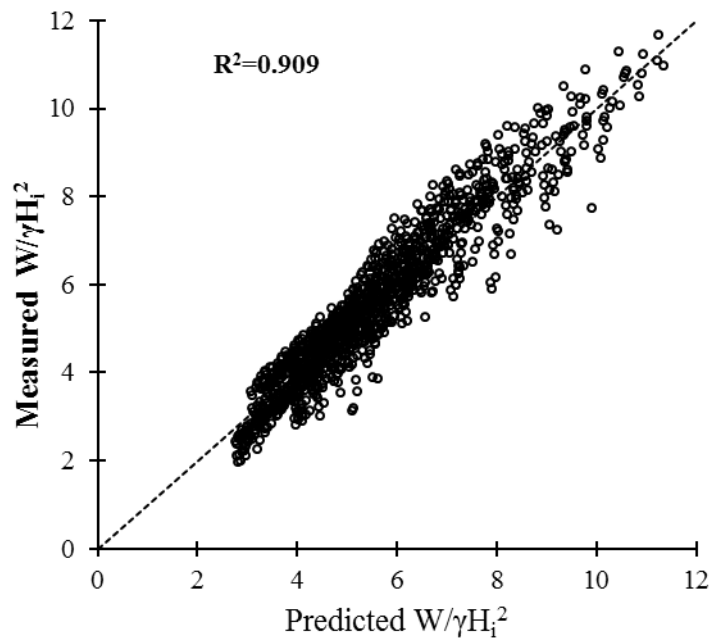
Fig 6.22 Comparison between measured and predicted values of $W/\gamma H_i^2$ for perforated QBW

SUMMARY AND CONCLUSIONS

7.1 SUMMARY

The physical model studies are conducted on emerged impermeable and seaside perforated QBW with different radii and S/D ratio using the facilities available in the wave flume in Marine Structures Laboratory of Applied Mechanics Department, National Institute of Technology Karnataka, Surathkal, India. First of all, impermeable and seaside perforated QBW models are tested for its performance such as reflection and loss characteristics, runup and rundown characteristics with varying structural and sea state parameters.

In the second phase, impermeable and seaside perforated models are tested for its sliding stability under varying water depths, wave conditions, S /D ratio and breakwater radii. The main aim of the study is to investigate the effect of water depth, perforations and breakwater radii on the hydrodynamic performance characteristics of impermeable and seaside perforated QBW under varying wave conditions. The conclusions drawn based on the present experimental work are listed in this chapter.

7.2 CONCLUSIONS FOR IMPERMEABLE QBW

Based on the present experimental study on impermeable quarter circle breakwater the following conclusions are drawn:

1. The reflection coefficient, K_r increases but the loss coefficient K_l decreases with increase in Hi/gT^2 for all values of d/h_s. The minimum K_r and the maximum K_l observed are 0.5054 and 0.8629 respectively for QBW of radius equal to 0.55 m at $Hi/gT^2 = 9.439 \times 10^{-4}$ and at water depth equal to 0.45 m ($d/h_s = 0.732$).

2. The reflection coefficient K_r decreases and loss coefficient K_l increases with increase in water depth (d/h_s). With respect to a water depth of 0.35 m, the maximum percentage reduction in K_r is observed at 0.45 m water depth and is found to vary from 17.35% to 19.27%, 12.37% to 19.59% and 12.69% to

17.01% for QBW of radius equal to 0.55 m, 0.575 m and 0.60 m respectively.

3 The reflection coefficient K_r increases and the loss coefficient K_l decreases with increase in QBW radius for all values of H_i/gT^2 and at all water depths. The percentage increase in K_r or percentage reduction in loss coefficient K_l with increase in QBW radius is very less compared to the effect of increase in d/h_s and H_i/gT^2.

4 The relative wave run up, R_u/H_i and the relative wave run down R_d/H_i decreases with increase in H_i/gT^2 for all values of d/h_s. For QBW of radius equal to 0.55 m, 0.575 m and 0.60 m, the maximum value for R_u/H_i observed is equal to 3.870, 4.651 and 5.468 at $H_i/gT^2 = 7.645 \times 10^{-4}$ and at water depth equal to 0.35 m. The maximum value for R_d/H_i observed are 1.904, 1.835, 1.845 at $H_i/gT^2 = 7.645 \times 10^{-4}$ and at water depth equal to 0.45 m for QBW of radius equal to 0.55 m, 0.575 m and 0.60 m respectively.

5 From the plotted non-dimensional graphs, it is observed that R_u/H_i decreases and R_d/H_i increases with increase in water depth (d/h_s). In the case of QBW 0.55 m radius, the percentage reduction in R_u/H_i with respect to 0.35 m water depth is observed to be varying from 25.19% to 38.04% when $d/h_s= 0.732$ (0.45 m water depth). Similarly for QBW 0.575 m radius and 0.60 m radius the percentage reduction in R_u/H_i varies from 33% to 34% and 34% to 36% when water depth of 0.45 m.

6 The non-dimensional stability parameter ($W/\gamma H_i^2$) decreases with increase in H_i/gT^2 for all values of d/h_s. For QBW of radius equal to 0.55 m, 0.575 m and 0.60 m, minimum $W/\gamma H_i^2$ observed are 3.557, 3.450 and 3.112 respectively at $H_i/gT^2 = 6.241 \times 10^{-3}$ and at water depth equal to 0.35 m.

7 The values for $W/\gamma H_i^2$ increases with increase in d/h_s for all ranges of H_i/gT^2. The percentage increase in $W/\gamma H_i^2$ for a water depth equal to 0.45 m compared to 0.35 m varies from 21.78% to 29.73%, 26.64% to 27.51% and 22.99% to 31.68% for QBW of radius equal to 0.55 m, 0.575 m and 0.60 m respectively.

7.3 CONCLUSIONS FOR SEASIDE PERFORATED QBW

Based on the experimental investigations on seaside perforated QBW, following conclusions are drawn:

1. For a constant S/D ratio and QBW radius, the values of K_r increases but K_l decreases with increase in H_i/gT^2 for all d/h_s. For QBW of 0.55 m radius, the minimum K_r and the maximum K_l observed are 0.0696 and 0.9980 respectively at $H_i/gT^2 = 7.645 \times 10^{-4}$ and 0.45 m water depth ($d/h_s = 0.732$) for S/D = 2.5.

2. The value of K_r decreases but K_l increases as the water depth (d/h_s) increases for all values of H_i/gT^2 and S/D ratio. The maximum percentage reduction in the value of K_r is observed for QBW 0.55 m radius S/D= 2.5 and varies from 31.66% to 44.50% when the d/h_s increases from 0.569 to 0.732.

3. For a constant breakwater radius and at different water depths, it is observed that K_r decreases but K_l increases with decrease in S/D for all values of H_i/gT^2. But in the case of seaside perforated QBW with S/D= 2, the values of K_r is found to be slightly more when compared to that of S/D =2.5. This may be because when S/D decreases there will be more perforations on the QBW surface resulting in higher dissipation of wave energy caused by the turbulence inside the QBW chamber and hence lower K_r values. But when S/D ratio is further reduced beyond 2.5, there will be back propagation of waves from the chamber to the front side of QBW resulting in increased reflection.

4. For seaside perforated QBW with $d/h_s = 0.732$, percentage reduction in K_r for S/D equal to 5, 4, 3, 2.5, 2 varies from 47% to 49%, 54% to 58%, 60% to 71%, 72% to 86% and 68% to 84% when compared to impermeable QBW.

5. Both relative wave runup R_u/H_i and relative wave rundown R_d/H_i decreases with increase in H_i/gT^2 for all values of d/h_s and S/D ratio. The maximum values for R_u/H_i observed are 1.795, 1.886 and 2.105 for QBW of radius equal to 0.55 m, 0.575 m and 0.60 m respectively with S/D= 2.5 when $H_i/gT^2 = 9.439 \times 10^{-4}$ and at 0.35 m water depth. For QBW of radius equal to 0.55 m, 0.575 m and 0.60 m, maximum value of R_d/H_i observed are 0.8590, 0.7099

and 0.6886 when $H_i/gT^2 = 7.645 \times 10^{-4}$ and at 0.45 m water depth.

6. The value of relative wave runup R_u/H_i decreases but relative wave rundown R_d/H_i increases with increase in d/h_s for all values of H_i/gT^2 and S/D ratio.

7. For all d/h_s and H_i/gT^2, the values for relative wave runup R_u/H_i and relative wave rundown R_d/H_i decreases with decrease in S/D ratio. In the case of seaside perforated QBW with S/D=2 the values of relative wave runup R_u/H_i and relative wave rundown R_d/H_i are found to be higher when compared that of S/D = 2.5. This is because when S/D decreases there will be more dissipation of wave energy due to more perforations on QBW surface causing turbulence inside the chamber and hence lower values for R_u/H_i and R_d/H_i. But for S/D= 2, the more perforation on QBW surface causes back propagation of waves from inside the chamber resulting in higher wave profile in front side of QBW or higher values for R_u/H_i and R_d/H_i.

8. For seaside perforated QBW of d/h_s= 0.732, % reduction in R_u/H_i for S/D= 5, 4, 3, 2.5 and 2 are 25.01% to 25.92%, 34.91% to 35.48%, 44.70% to 45.72%, 58.8% to 59.4% and 55.91% to 56.56% when compared to impermeable QBW.

9. The percentage reduction in R_u/H_i varies from 53.61% to 58.85%, 59.44% to 60.27% and 61.50% to 69.85% for d/h_s equal to 0.732, 0.703 and 0.677 (QBW of radius equal to 0.55 m, 0.575 m and 0.60 m) respectively with S/D= 2.5 when compared to impermeable QBW.

10. For all values of d/h_s and S/D ratio, the stability parameter $W/\gamma H_i^2$ decreases with increase in H_i/gT^2. The minimum values for $W/\gamma H_i^2$ for QBW of radius 0.55 m, 0.575 m and 0.60 m with S/D= 2.5 are 2.110,1.998 and 1.967 respectively for H_i/gT^2= 6.241 $\times10^{-3}$ and at 0.35 m water depth.

11. For sea side perforated QBW with S/D= 2.5, % reduction in $W/\gamma H_i^2$ varies from 5.56% to 15.18% for 0.40 m water depth and the % reduction in $W/\gamma H_i^2$ varies from 33.70% to 35.27% for 0.35 m water depth.

12. For various S/D, $W/\gamma H_i^2$ increases with increase in water depth for all ranges of H_i/gT^2. The percentage increase in $W/\gamma H_i^2$ for a water depth equal to 0.45

m compared to 0.35 m varies from 32.15% to 34.02%, 30.19% to 33.51% and 32.15% to 34.27% for QBW of radius 0.55 m, 0.575 m and 0.60 m with S/D= 2.5

13. The stability parameter $W/\gamma H_i^2$ decreases with decrease in S/D ratio for all values of H_i/gT^2 and d/h_s. When compared to seaside perforated QBW with S/D =2.5, the values of stability parameter $W/\gamma H_i^2$ is found to be higher in the case of QBW with S/D= 2. When S/D is reduced there will be more dissipation of wave energy and QBW is subjected to less wave force resulting in less weight of QBW to prevent sliding or lesser values of $W/\gamma H_i^2$. Further decreasing S/D to 2 causes back propagation of wave and hence exert more force on QBW resulting in higher values for $W/\gamma H_i^2$.

14. The percentage reduction in stability parameter $W/\gamma H_i^2$ varies from 33.43% to 40.68%, 34.51% to 40.05% and 36.79% to 38.06% for QBW of radius equal to 0.55 m, 0.575 m and 0.60 m respectively with S/D= 2.5 when compared to impermeable QBW.

15. Uncertainty analysis was done for the various tests conducted and the equation for the best fit curve with a good regression coefficient ($R^2 = 0.9$) was found out.

16. From the experiments conducted and the comparative analysis, it is clear that the perforated QBW of S/D = 2.5 has better performance characteristics and can be adopted in the site with favourable condition.

7.4 SCOPE FOR FUTURE WORK

The following studies may be carried out in future on the QBW:

1. Studies on the same models with random waves.
2. Studies on overturning stability.
3. Optimization of QBW cross section.
4. Studies on overtopping of QBW

MEASUREMENT OF WAVE REFLECTION

AI-1 GENERAL

The present section describes the measurement of regular wave reflection carried by Michael Isaacson (1991). There are three methods for measuring wave reflection by using either two or three fixed probes which will give for the incident wave height, reflection coefficient, and the phase of the reflected wave train. The method involving three height measurements is the most common one. By the use of three probes, recommendations are made for the relative probe spacing so as to avoid conditions at which the methods fail or become inaccurate.

The three methods used are

Method I: two fixed probes—two heights and one phase angle measured.

Method II: three fixed probes—three heights and two phase angles measured.

Method III: three fixed probes—three heights measured.

AI-2 REFLECTION USING THREE FIXED PROBES

For reflection of regular waves, free surface elevation results from the superposition of sinusoidal incident and reflected wave trains (Refer Fig. AI-1). The free surface elevation η is generally given by the equation AI-1
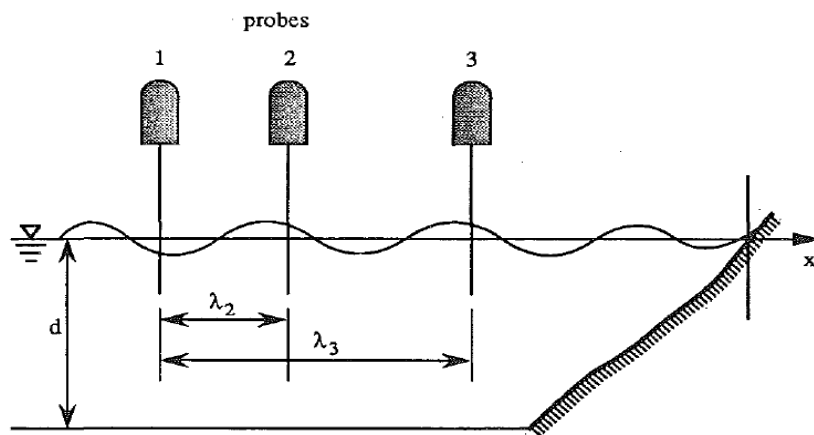
Fig. AI-1 Typical sketch for wave reflection

$$\eta = a_i \cos(kx - \omega t) + a_r \cos(-kx - \omega t + \beta) \ldots\ldots\ldots\ldots\ldots\ldots\ldots\ldots\ldots\ldots\ldots\ldots \text{(AI-1)}$$

Where a_i and a_r are the amplitudes of the incident and reflected wave trains, respectively; and β = phase angle that describes the phase of the reflected waves by accounting for the phase difference between the incident and reflected wave trains at $x = 0$ or $t = 0$. Also k = wave number and ω the wave angular frequency, respectively that are related by the equation AI-2.

$$\omega^2 = g\, k\, tanh\, (kd) \quad\text{...} \quad \text{(AI-2)}$$

Where d = the still water depth; and g = the gravitational constant.

The incident wave height H and reflection coefficient K are given in terms of a_i and a_r as $H = 2a_i$ and $K = a_r/a_i$.

Considering a series of probe locations x_n, $n = 1, 2, 3$ . .. The interval between the probes with respect to the location of first probe x_1 can be obtained given in equation (AI-3).

$$x_n = x_1 + \lambda_n \quad\text{...} \quad \text{(AI-3)}$$

Where λ_n is the distance between the nth probe and the first probe and $\lambda_1 = 0$.

$$kx_n = kx_1 + \Delta_n \quad\text{...} \quad \text{(AI-4)}$$

$$\eta = a_i\, cos(\, kx_1 + \Delta_n - \omega t) + a_r\, cos(\, kx_1 + \Delta_n + \omega t - \beta\,) \quad\text{.........................} \quad \text{(AI-5)}$$

The assumed form of free surface elevation at the nth probe is given by equation (AI-6) as follows

$$\eta_n = A'_n cos(\, \omega t - \phi'_n\,) \quad\text{...} \quad \text{(AI-6)}$$

Where A'_n is the assumed amplitude and ϕ'_n the assumed phase angle

$$A'^2_n = a_i^2 + a_r^2 + 2a_i a_r\, cos(\, 2x_n - \beta) \quad\text{.................................} \quad \text{(AI-7)}$$

The elevation in terms of the incident and reflected wave parameters may be written in complex form as:

$$\eta_n = \{\, a_i\, exp(\, ikx_n\,) + a_r\, exp[\, -i(\, kx_n - \beta\,)]\}\, exp(\, -i\omega t) \quad\text{.......................} \quad \text{(AI-8)}$$

In the case of three height measurements, probes are placed at sections 1, 2, and 3 as indicated in Fig. AI-1. Since only the heights are measured, the assumed form of the free surface elevation is expressed in the form of equation AI-6 and the assumed

amplitude $A'n$ at each probe location is given in terms of the incident and reflected wave amplitudes as in (AI-7).

The three values of A'_n are equated to the three measured wave amplitudes A_n in order to provide three equations for the unknowns to be determined.

$$A_1{}^2 = a_i{}^2 + a_r{}^2 + 2a_i a_r \cos(\chi) \dots\dots\dots\dots\dots\dots\dots\dots\dots\dots\dots\dots\dots\dots\dots\dots\dots\dots \quad \text{(AI-9)}$$

$$A_2{}^2 = a_i{}^2 + a_r{}^2 + 2a_i a_r \cos(\chi + 2\Delta_2) \dots\dots\dots\dots\dots\dots\dots\dots \dots\dots\dots\dots \quad \text{(AI-10)}$$

$$A_3{}^2 = a_i{}^2 + a_r{}^2 + 2a_i a_r \cos(\chi + 2\Delta_3) \dots\dots\dots\dots\dots\dots\dots\dots \dots\dots\dots\dots \quad \text{(AI-11)}$$

Where $\chi = 2x_1 - \beta$

$\cos(\chi) = f_1$

$$\sin(\chi) = \frac{f_1(\cos(2\Delta_2) - f_2)}{\sin(2\Delta_2)} \qquad \dots\dots\dots\dots\dots\dots\dots\dots\dots\dots\dots\dots\dots\dots\dots\dots\dots\dots\text{(AI-12)}$$

$$\sin(\chi) = \frac{f_1(\cos(2\Delta_3) - f_3)}{\sin(2\Delta 3)} \qquad \dots\dots\dots\dots\dots\dots\dots\dots\dots\dots\dots\dots\dots\dots\dots\dots\dots\text{(AI-13)}$$

Where $fn = \dfrac{A_n^2 - a_i^2 - a_r^2}{2a_i a_r} \qquad \dots\dots\dots\dots\dots\dots\dots\dots\dots\dots\dots\dots\dots\dots\dots\dots\dots\dots\dots\text{(AI-14)}$

From the above sets of equations a_i and a_r are obtained as given in equations AI-15 and AI-16.

$$a_i^2 + a_r^2 = \Lambda \dots\dots\dots\dots\dots\dots\dots\dots\dots\dots\dots\dots\dots\dots\dots\dots\dots\dots\dots\dots\dots\text{(AI-16)}$$

$$2a_i a_r = \Gamma \dots\dots\dots\dots\dots\dots\dots\dots\dots\dots\dots\dots\dots\dots\dots\dots\dots\dots\dots\dots\dots\dots\dots\text{(AI-17)}$$

Where $\Lambda = \dfrac{A_1^2 \sin[2(\Delta_3 - \Delta_2)] - A_2^2 \sin 2(\Delta_3) + A_3^2 \sin 2(\Delta_2)}{\sin[2(\Delta_3 - \Delta_2)] + \sin 2(\Delta_2) - \sin 2(\Delta_3)} \dots\dots\dots\dots\dots\text{(AI-18)}$

$$\Gamma = \frac{1}{2}\left[\frac{A_1^2 + A_3^2 - 2\Lambda^2}{\cos(\Delta_3)} + \frac{A_1^2 - A_3^2}{\sin(\Delta_3)} \right] \qquad \dots\dots\dots\dots\dots\dots\dots\dots\dots\dots\dots\dots \quad \text{(AI-19)}$$

Where Λ and Γ are functions in terms of which a_i and a_r are obtained from equations AI-20 and AI-21.

$$a_i = \frac{1}{2}\left(\sqrt{\Lambda + \Gamma} + \sqrt{\Lambda + \Gamma} \right) \dots\dots\dots\dots\dots\dots\dots\dots\dots\dots\dots\dots\dots\dots\dots \quad \text{(AI-20)}$$

$$a_r = \frac{1}{2}\left(\sqrt{\Lambda + \Gamma} - \sqrt{\Lambda + \Gamma} \right) \dots\dots\dots\dots\dots\dots\dots\dots\dots\dots\dots\dots\dots\dots \quad \text{(AI-21)}$$

$$H^2 = 2\left(\Lambda + \sqrt{\Lambda^2 - \Gamma^2}\right) \dots \dots \dots \dots \dots \dots \dots \dots \dots \quad \text{(AI-22)}$$

$$K^2 = \frac{4\Lambda}{H^2} - 1 \dots \dots \dots \dots \dots \dots \dots \dots \dots \dots \quad \text{(AI-23)}$$

Then reflected wave height H and the reflection coefficient K are obtained as given in equations AI-22 and AI-23.

UNCERTAINITY ANALYSIS

AII-1 GENERAL

The hydrodynamic test facilities differ from one another with regard to facilities, instrumentation, experimental procedures and scale. Hence, it becomes necessary for a test facility to provide with possible lower and upper margins, which can be adopted with a fair confidence level. Such a study for an experimental test procedure in a particular facility is termed as uncertainty analysis.

Uncertainty describes the degree of goodness of a measurement or experimentally determined result. It is an estimate of experimental error. It is possible to conduct experiments in a scientific manner and predict the accuracy of the result (Misra, 2001) with the help of uncertainty analysis. Experimental error sources should be identified and the error (δ) should be determined from manufactures brochures, from calibration and conducting simple experiments respectively (Kline, 1985).

The use of uncertainty analysis is indispensable in physical model studies. There is no single way to describe uncertainty in measurements and there are many different situations that demand somewhat differing description. The distribution of uncertainty between precision and bias is arbitrary. Whatever may the method used for calculating uncertainty, but the method used should be reported in some appropriate way and that the report includes the method employed (Kline, 1985). It is also generally agreed that the inaccuracies can be appropriately expressed by an "uncertainty" and these values could be obtained by an "Uncertainty analysis".

The confidence interval gives an estimated range of values, which is likely to include an unknown population parameter. From a given set of observations the estimated range is calculated. The 95% confidence interval limits must always be estimated and this concept of confidence level is fundamental to uncertainty analysis (Misra, 2001).

AII-2 PROCEDURE FOR UNCERTAINITY ANALYSIS

A best-fit curve can include both 95% confidence band and the 95% prediction band. Confidence band tells about 95% sure that the true best fit curve (if an infinite number of data points are available) lies within the confidence band. The prediction band tells about the scatter of the data. If data points are considered, 95% points are expected to fall within the prediction band. Since the prediction band has to an account for uncertainty in the curve itself as well as scatters around the curve, it is much wider than the confidence band.

Fig. AII-1 shown below, confidence bands contain a minority of data points. The confidence bands shown have a 95% chance of containing the true best fit curve and the dashed prediction bands include 95% of the data points. Also the 95% confidence and prediction bands have been accepted to be reliable enough for usage under the adoption of uncertainty analysis.
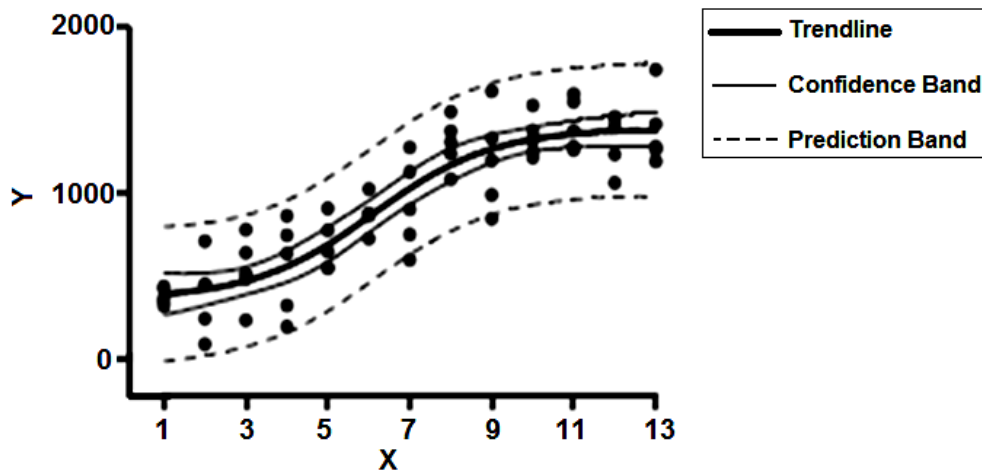
Fig. AII-1 Graph example for 95% confidence and prediction band

A 100(1-α) percent confidence interval about the mean response at the value of x = x_1, say Y_1 is given by Montgomery and Runger (1999) as follows:

$$Y_1 = Y_0 \pm t_{(\alpha/2, n-2)} \sqrt{\left(\sigma^2 \left[\frac{1}{n} + \left(\frac{(x_0 - \bar{x})^2}{S_{xx}} \right) \right] \right)} \quad \dots\dots\dots\dots\dots\dots\dots\dots\dots \text{(AII-1)}$$

Where $Y_0 = \beta_0 + \beta_1 X_0$ computed from regression model, α = significance level used to compute the confidence level, σ^2 = variance, n= sample size, $\bar{x}$ = sample mean, x = variable, S_{xx} = standard deviation, $t_{(\alpha/2, n-2)}$ = t-distribution values for n –2 degrees

of freedom.

A 100(1-α) percent prediction interval on a feature observation Y_o at given value x_o is given by:

$$Y_1 = Y_0 \pm t_{(\alpha/2, n-2)} \sqrt{\left(\sigma^2 \left[1 + \frac{1}{n} + \left(\frac{(x_0 - \bar{x})^2}{S_{xx}} \right) \right] \right)} \quad \dots\dots\dots\dots\dots\dots\dots\dots\dots\dots \text{(AII-2)}$$

AI-3 CONFIDENCE AND PREDICTION INTERVAL FOR REFLECTION COEFFICIENT ON QBW
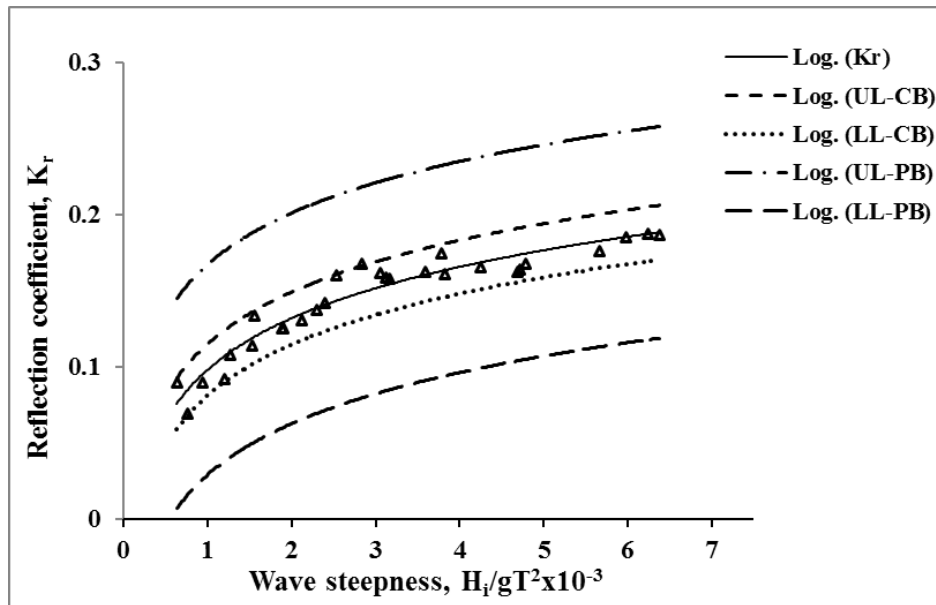
Fig. AII-2 Plot of 95% confidence and prediction bands for variation of K_r

The 95% confidence and prediction band for variation of reflection coefficient K_r with incident wave steepness for emerged quarter circle breakwater models tested with T = 1.2 s to 2.2 s, H = 0.06 m to 0.18 m and d = 0.35 m to 0.45 m is shown in Fig. AII-2. It is observed that more than 92% of experimental data lie within the 95% confidence bands. The regression coefficient, R^2, is found to be 0.9247.

From the figure it is observed that the trend line showing the variation of K_r with H_i/gT^2 lie within the 95% confidence bands and data points lie within the 95% prediction bands drawn. Therefore the results obtained may be analyzed with 95% confidence i.e. the conclusions drawn from these graphs are 95% reliable. Also from the figure it was observed that experimental data points lie within the 95% prediction band which strengthens the results obtained from the graph.

AII-4 CONFIDENCE AND PREDICTION INTERVAL FOR LOSS COEFFICIENT ON QBW

The 95% confidence and prediction band for variation of loss coefficient K_l with incident wave steepness H_i/gT^2 for emerged quarter circle breakwater models tested with T = 1.2 s to 2.2 s, H = 0.06 m to 0.18 m and d = 0.35 m to 0.45 m is shown in Fig. AII-3.
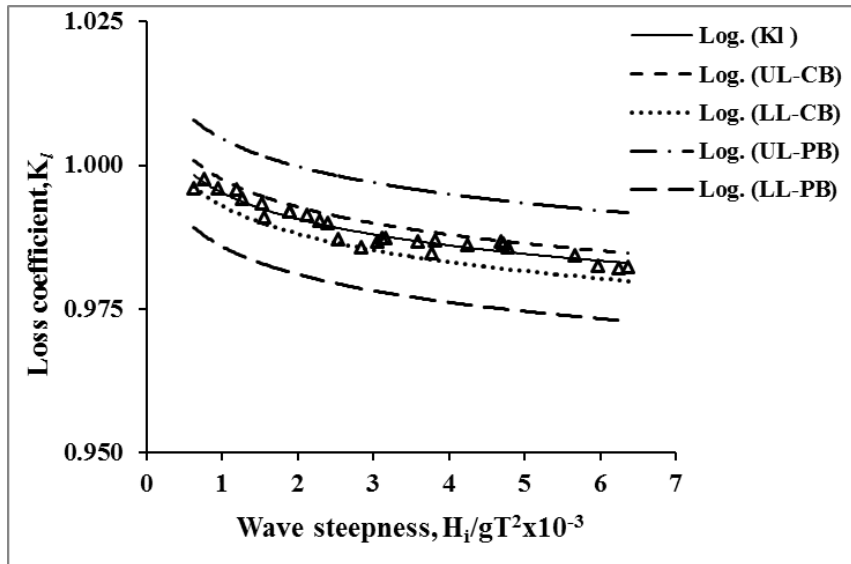
Fig. AII-3 Plot of 95% confidence and prediction bands for the variation of K_l

It is observed that more than 90% of experimental data lie within the 95% confidence bands. The regression coefficient, R^2, is found to be 0.9255. The trend line for the graph drawn on variation of K_l with H_i/gT^2 lie within 95% confidence bands and data points lie within the 95% prediction bands drawn. Therefore the results obtained are so far reliable.

AII-5 CONFIDENCE AND PREDICTION INTERVAL FOR RELATIVE WAVE RUNUP ON QBW

The 95% confidence and prediction band for variation of relative wave runup R_u/H_i with incident wave steepness for emerged quarter circle breakwater models tested with T = 1.2 to 2.2 s, H = 0.06 m to 0.18 m and d = 0.35 m to 0.45 m is shown in Fig. AII- 4. It is observed that more than 90% of experimental data lie within the 95% confidence bands. The regression coefficient, R^2, is found to be 0.9278.
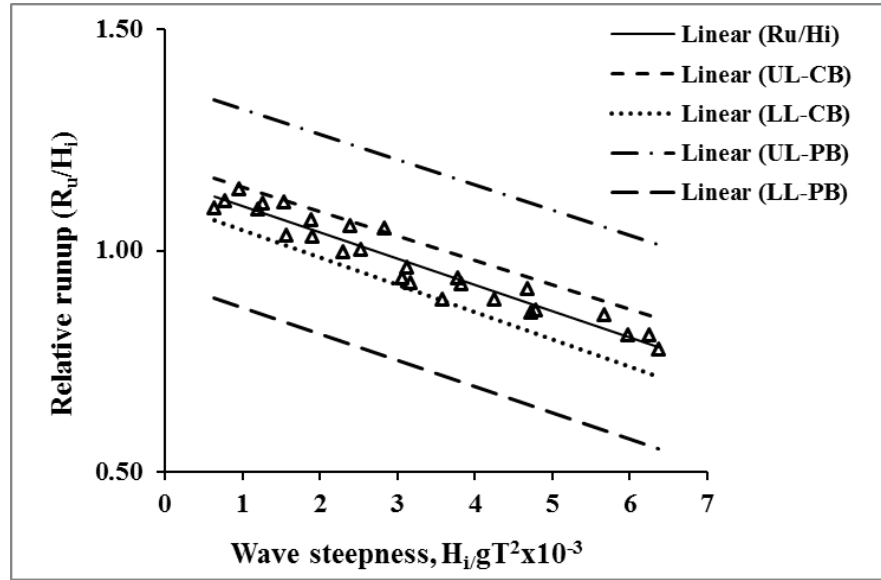
Fig. AII-4 Plot of 95% confidence and prediction bands for variation of R_u/H_i

AII-6 CONFIDENCE AND PREDICTION INTERVAL FOR RELATIVE WAVE RUNDOWN ON QBW

The 95% confidence and prediction band for variation of relative wave rundown R_d/H_i with incident wave steepness for emerged quarter circle breakwater models tested with T = 1.2 to 2.2 s, H = 0.06 m to 0.18 m and d = 0.35 m to 0.45 m is shown in Fig. AII-5.
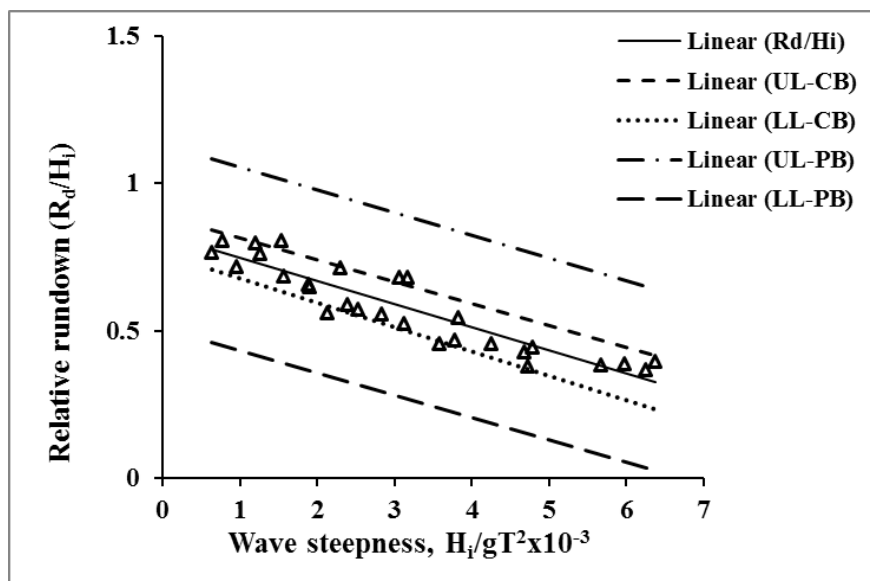
Fig. AII-5 Plot of 95% confidence and prediction bands for variation of R_d/H_i

As it can be observed about 84% data points lie within the confidence band and all the points are within prediction band. The scatter is because of different wave

conditions and water depths considered during the study. The wave rundown resulting from both down rush of a wave and backward flow of water from the pores made in the quarter circle breakwater which in turn depends on S/D ratio. This combined flow increases the variation in the rundown for considered parameters.

AII-7 CONFIDENCE AND PREDICTION INTERVAL FOR STABILITY PARAMETER ON QBW

The 95% confidence and prediction band for variation of stability parameter $W/\gamma H_i^2$ with incident wave steepness for emerged quarter circle breakwater models tested with T = 1.2 to 2.2 s, H = 0.06 m to 0.18 m and d = 0.35 m to 0.45 m is shown in Fig. AII-6. It is observed that more than 85% of experimental data lie within the 95% confidence bands. The regression coefficient, R^2, is found to be 0.850.
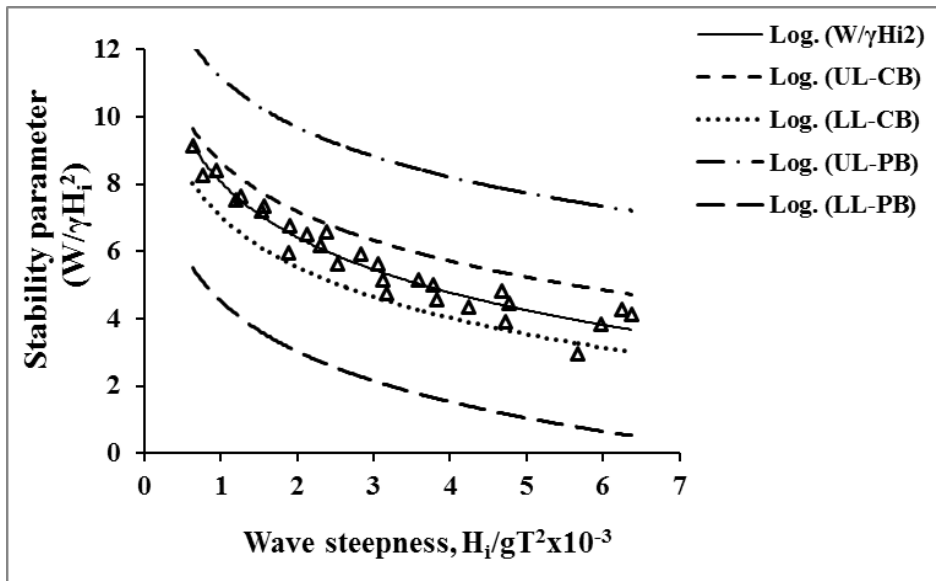
Fig. AII-6 Plot of 95% confidence and prediction bands for variation of $W/\gamma H_i^2$

AII-8 SAMPLE CALCULATION OF CONFIDENCE AND PREDICTION INTERVALS

Sample calculation for the plot K_r vs. H_i/gT^2 for different depths of water is shown in Table AII-1 with the 95% upper and lower confidence band values and 95% upper and lower prediction band values. The values are computed using equations AII-1 and AII-2.

Table AII-1 Data points with 95% confidence band and 95% prediction band

X_i (H_i/gT^2)	Y_i (K_r)	Confidence band		Prediction band	
		upper limit	lower limit	Upper limit	Lower limit
2.124	0.135	0.150	0.120	0.203	0.066
4.247	0.169	0.184	0.153	0.237	0.100
6.371	0.1883	0.216	0.161	0.261	0.116
1.560	0.120	0.137	0.103	0.189	0.051
3.121	0.154	0.166	0.141	0.222	0.085
4.681	0.173	0.191	0.156	0.243	0.104
6.241	0.187	0.214	0.161	0.259	0.115
1.195	0.107	0.126	0.088	0.176	0.037
2.389	0.141	0.154	0.127	0.209	0.072
3.584	0.160	0.174	0.147	0.229	0.092
4.778	0.174	0.192	0.157	0.244	0.105
5.973	0.185	0.210	0.160	0.257	0.114
0.944	0.095	0.116	0.075	0.165	0.025
1.88	0.129	0.145	0.114	0.198	0.060
2.832	0.149	0.162	0.136	0.217	0.081
3.775	0.163	0.177	0.149	0.231	0.095
4.719	0.174	0.191	0.156	0.243	0.105
5.663	0.183	0.206	0.160	0.253	0.112
0.765	0.085	0.107	0.063	0.155	0.015
1.529	0.119	0.136	0.102	0.188	0.050
2.294	0.139	0.153	0.125	0.207	0.070
3.058	0.153	0.165	0.140	0.221	0.085
3.823	0.164	0.177	0.150	0.232	0.095
0.632	0.076	0.098	0.053	0.146	0.005
1.264	0.110	0.128	0.091	0.179	0.040
1.896	0.129	0.145	0.114	0.198	0.061
2.527	0.143	0.157	0.130	0.212	0.075
3.159	0.154	0.167	0.142	0.222	0.086

SAMPLE DESIGN CALCULATION

AIII-1 GENERAL

From the physical model studies conducted on QBW, it is clear that the seaside perforated QBW is more effective in dissipating wave energy and thereby reducing the reflection. The seaside perforated QBW with S/D=2.5 has good performance characteristics within the design wave conditions and water depths assumed while conducting the model tests. Considering this a QBW cross section is designed for the site conditions of the Mangalore coast assumed while selecting the physical model. This chapter explains the details of design of prototypes and sliding stability analysis of typical QBW cross section.

AIII-2 DESIGN OF QBW CROSS SECTION

AIII-2.1 Site conditions

The wave climates off the Mangalore coast are considered while conducting the physical model tests and from the available conditions suitable parameters are assumed for the design. For the design, a wave height of 4.5 m and wave period of 10 s is taken into consideration since the maximum recorded wave height off Mangalore coast is about 4.5 m to 5.4 m and the predominant wave period is 8 s to 11 s. Also for the design a water depth of 10 m is used based on the water depth available at the site considered.

AIII-2.2 Design parameters

The design parameters assumed while conducting the experimental studies on the wave flume for the seaside perforated QBW models are given below.

Incident wave height, H_i : 4.5 m

Wave period : 10 s

Water depth	: 10 m

Incident wave steepness, H_i/gT^2 : 4.587 x10^{-3}

Considering a perforated QBW model with scale 1:30 and with breakwater radius equal to 0.55 m (Height of the structure, h_s= 0.615 m) with S/D= 2.5, corresponding to a wave height of 0.15 m and wave period of 1.8 s (H_i/gT^2= 4.719 x10^{-3}) and at 0.35 m water depth, the results obtained from the experimental studies are as follows:

Reflection coefficient, K_r	: 0.2296
Loss coefficient, K_l	: 0.9733
Relative wave runup, R_u/H_i	: 1.285
Relative wave rundown, R_d/H_i	: 0.289
Stability parameter, $W/\gamma H_i^2$	: 2.996

The above results for the values for loss coefficient implies that the wave dissipation characteristics of perforated QBW with S/D = 2.5 is good and the reflection coefficient is within the permissible limit which can be recommended for the site.

The actual wave conditions available in the site in front of the seaside perforated quarter circle breakwater are taken from the data's available. Therefore the corresponding design wave parameters and the structural parameters for the prototype can be determined from the results for experiments on the QBW model.

Reflected wave height, H_r	: 1.033 m (say 1m)
Wave runup, R_u	: 5.782 m $\approx$ 5.8 m above SWL
Wave rundown, R_d	: 1.30 m below SWL
Radius of QBW, R	: 16.5 m
Height of the structure, h_s	: 18.45 m

The reflected wave height is less 1m which is within the permissible limits for the safety of the nearby structures and maintains a calm area inside the harbor basin.

AIII-2.3 QBW crest level

The crest level of the QBW can be determined from the maximum wave runup depending on the available wave conditions at the site. As per the assumed breakwater radius, the crest level of the QBW prototype can be determined from the expression given below.

QBW crest level = Still water level + Wave run up + Tidal range + free board (assumed for safety)

Still water level : +0.0

Wave runup, R_u : 5.8 m

Tidal range : 1.5 m

Therefore assuming a free board of 1 m, the required minimum QBW crest height is equal to 8.3 m above the SWL which is less than the provided QBW height of 8.45 m above SWL. Hence the QBW structure radius provided is adequate.

AIII-2.4 Height of the rubble mound base

The height of the rubble mound should be adequate for the stability of the entire QBW structure due to foundation failure and to minimize the scouring in front of the breakwater.

AIII-2.5 Weight required for sliding stability of QBW

While conducting the experiment with the sea side perforated QBW it was observed that the model was moving under severe wave conditions and in order to avoid sliding, additional weight was provided inside the QBW model. For the prototype the corresponding weight required was determined and has to provide in addition to the QBW weight.

Stability parameter, $W/\gamma H_i^2$: 2.996

Incident wave height, H_i : 4.5m

Density of sea water, γ : 10.105 KN/m^3

Therefore the weight to be required to resist sliding was obtained as 613.06 KN and if a factor of safety of 1.5 is taken into consideration, the weight required to resist sliding will be equal to 920 KN per m length of the breakwater.

For QBW of radius 16.5 m and thickness 1.2 m,

Weight per metre length of Quarter circular top portion: $\dfrac{\pi}{4}$ (16.5^2- 15.3^2) x 1x 25

                                                                      : 749.26 KN $\approx$ 750 KN

Weight per metre length of the base slab   : 19.5 x 0.45 x 1 x 25

                                                                      : 219.375 KN $\approx$ 220 KN

Total weight per metre length of QBW structure   : 970 KN

Therefore the weight per metre length of QBW provided is greater than that of the weight per metre length of QBW required to prevent sliding. Hence cross section of QBW with quarter circular top portion of radius 16.5 m with thickness 1.2 m and base slab of dimension 19.5 m x 1m x 0.45 m is safe against sliding and can be adopted in the site with similar wave conditions.

AII-3 DETAILS OF QBW CROSS SECTION

From the results after the analysis and design of perforated QBW using the available site condition selected for the design, QBW of radius equal to 0.55 m with S/D=2.5 is adequate under the criteria required for the performance. Based on the sliding stability analysis performed under varying wave conditions and water depth on a seaside perforated QBW, the minimum weight per metre length of QBW required to prevent sliding can be obtained.

The details of the typical cross section considering SWL as the reference datum are given below and are shown in Fig.AIII-1.

1. Breakwater crest level   : +8.45m

2. Still water level   : +0.00m

3. Sea bed level   : -10.00 m

4. Top level of base slab   : -8.05 m

5. Top level of foundation   : -8.50m
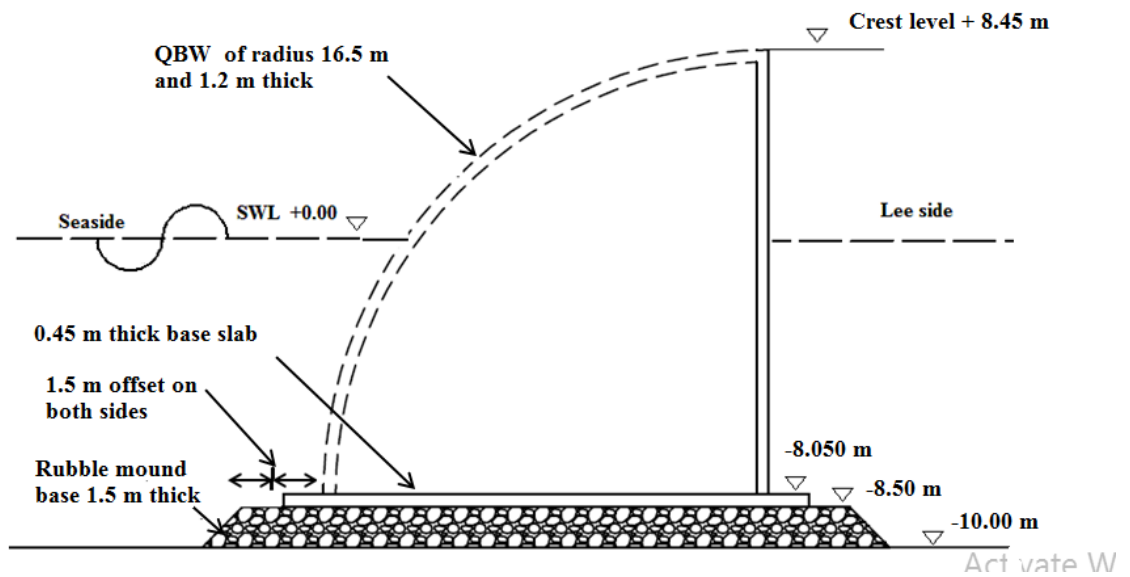
Fig. AIII-1 Typical QBW section

- Aburatani, S., Koizuka, T. and Sasayama, H. (1996). "Field test on a semi-circular caisson breakwater." *Coastal Engineering Japan,* 39(1), 59–78.

- Arkal, Vittal Hegde and L, Ravikiran. (2013). "Quarter-Circle Breakwaters of Different Radii Reflection Characteristics." *World Academy of Science, Engineering and Technology*, 79, 2013.

- Bruun, P. (1985) "Design and Construction of Mound for Breakwater and Coastal Protection" *Access online via Elsevie*r, 938p.

- D'Angremond, K. and Van Roode, F. C. (2004). "Breakwaters and Closure Dams." *Taylor & Francis*, e-Library.

- Danel, P. (1953). "Tetrapods." *Proc. Fourth Int. Conf. Coastal Eng.,* ASCE, Chicago, USA, pp. 390 – 398.

- Dattatri, J. (1993). "Waves off Mangalore harbour-west coast of India." *Journal of Waterway, port, coastal, and Ocean Engineering*, ASCE, 99(2), 39-57.

- Dhinakaran, G., Sundar, V.,Sundaravadivelu, R.and Graw, K. U. (2002). "Hydrodynamic characteristics of submerged impermeable and sea side perforated semicircular breakwaters."*21st International Conference on Offshore Mechanics and Arctic Engineering*, June 23-28, Oslo, Norway, pp 1 – 8.

- Dhinakaran, G., Sundar, V., Sundaravadivelu, R. and Graw, K.U.(2008). "Hydrodynamic characteristics of seaside perforated semicircular breakwaters due to random waves*." Journal Waterway, Port, Coastal Ocean Engg*, 134(4), 237–251.

- Dhinakaran, G., Sundar, V., Sundaravadivelu, R. and Graw, K. U. (2009). "Effect of perforations and rubble mound height on wave transformation characteristics of surface piercing semicircular breakwaters*." Ocean Engineering*, 36 (2009), 1182–1198.

- Dhinakaran, G., Sundar, V., Sundaravadivelu. R. and Graw, K.U. (2010). "Regular wave measurements on submerged semicircular breakwater." *J Offshore Mech Arctic Engineering, 132* (3), 034501-1–034501-6.

- Franco, L. (1996). "History of Coastal Engineering in Italy", *History and Heritage of Coastal Engineering,* ASCE, New York, USA, 275-335

- Fugazza, M., and L. Natale. (1992). Hydraulic design of perforated breakwaters, Journal of Waterway, Port, Coastal, and Ocean Engineering., ASCE. Vol.118, No.l,pp.l-14.

- Gu, H., Jiang, X. and Li, Y. (2008). "Research on hydraulic performances of quarter circular breakwater." *Chinese-German Joint Symposium on Hydraulic and Ocean Engineering*, August 24-30, 2008.

- Gunaydın, K. and Kabdasli, M.S. (2004). "Performance of solid and perforated U-type breakwaters under regular and irregular waves." *Ocean Engineering*, 31, 1377–1405.

- Hughes, S. A. (1993). "Physical models and laboratory techniques in coastal Engineering." *Advanced series on Ocean Engineering*, World Scientific, Singapore

- Issacson, M. (1991). "Measurement of regular wave reflection", *Journal of Waterway, Port, Coastal and Ocean Engineering*, ASCE, 117(6), 553 –569.

- Jarlan, G.E. (1961). "A perforated vertical wall breakwater". *The Dock and Harbor Authority* 41(486), 394-398.

- Jia, D.H. (1999). "Study on the interaction of water waves with semi-circular breakwater." *China Ocean Engineering,* 13(1), 73–80.

- Jiang, X. L., Gu, H. B. and Li, Y. B. (2008). "Numerical simulation on hydraulic performances of quarter circular breakwater", *China Ocean Engineering,* 22(4), 585-594.

- Kakuno, S., K. Oda, and P.L.-F. Liu. (1992). "Scattering of Water Waves by Vertical Cylinders with a Back wall," *Proc of the 23rd Int.conference*, Coastal Engg, Venice, pp 1258-1271.

- Kondo, H. and Toma, S. (1972). "Reflection and transmission for a porous structure." *Proc.13$^{.th}$ Coastal Engineering Conf.*, 3, 1847-1866.

- Krishna Priya, Roopsekhar, M., Sundar, V., Sundaravadivelu, R. and Graw, K.U. (2000). "Hydrodynamic Pressures On Submerged Semicircular Breakwaters", *Proceedings of International Conference on Coasts, Ports and Marine structures*, Iran, Bandar Abbas,21-24, November 2000, Paper No.562, pp 551 – 560.

- Li, Y., Dong, G., Liu, H. and Sun, D. (2003). "The reflection of oblique incident waves by breakwaters with double-layered perforated wall." *Coastal Engineering*, 50 (2003) 47–60.

- Liu and Tao (2004)."Modeling the interaction of solitary waves and Semi circular breakwater by using unsteady Reynolds Equations." *Applied Mathematics and Mechanics*, Shanghai University, China, Volume25, No.10.Oct 2004.

- Liu, Y. and Li, H-J. (2012). "Analysis of wave interaction with submerged perforated semi-circular breakwaters through multipole method." *Appl Ocean Res 2012*,34, 164–172.

- Luwen, Qie., Xiang, Zhang., Xuelian, Jiang and Yinan,Qin. (2013). "Research on partial coefficients for design of quarter-circular caisson breakwater." *Journal of Marine Science and Application*, 12, 65-71.

- N-C, Zhang., Li-qin, Wang. and Yu-xiu, Yu. (2005). "Oblique irregular waves load on semicircular breakwater," *Coastal Engineering Journal*, Vol. 47, 183 – 204.

- Sasajima, H., Koizuka, T. and Sasayama, H. (1994). "Field demonstration test of a semicircular breakwater". *International conference on hydro-technical engineering for port and harbor construction,* Yokosuka, Japan, 9–21 October 1994, pp. 593–615.

- SHI Yan-Jiao., Mi-ling, W.U., Jiang, X., and Li Yan-bao. (2011). "Experimental researches on reflective and transmitting performances of quarter circular breakwater under regular and irregular waves." *China Ocean Engineerin*g, 25(3), 469 – 478.

- Suh, K.D. and Park, W.S. (1995) "Wave reflection from perforated wall breakwaters." *Coastal Engineering*, 26 (1995) 177-193.

- Suh, K.D., Choi, J.D., Kim, B.H., Park, W.S. and Lee, K.S. (2001)."Reflection of irregular waves from perforated-wall caisson breakwaters." *Coastal Engineering*, 44 (2001), 141– 151.

- Suh, K.D., Park, J.K. and Park, W.S.(2005), "Wave reflection from partially perforated-wall caisson breakwater.", *Ocean Engineering*, 33 (2006),264–280.

- Sundar, V. and Raghu, D. (1997)."Wave Induced pressures on Semicircular Breakwater." *Proceedings of 2nd Indian National Conference on Harbor and Ocean Engineering*, Dec 7-10, 278 - 297.

- Sundar, V., and Raghu, D. (1998*).* "Dynamic pressures and run-up on semicircular breakwaters due to random waves." *Ocean Engineering Journal*, vol. 25, pp 221 - 241.

- Sundar, V. and Subbarao, B.V.V. (2002). "Hydrodynamic Performance Characteristics of Quadrant Front-Face Pile-Supported Breakwater*." J. Waterway, Port, Coastal, Ocean Engg,* 129, 22-33.

- Takahashi, S. (1996). "Design of Vertical Breakwaters." *Port and Airport Research Institute*, Japan, Document No.34, PHRI.

- Tanimoto, K., and Goda, Y. (1992). "Historical development of breakwater structures in the world." *Coastal Structures and Breakwaters*, Thomas Telford Ltd., London, pp 193 – 206.

- Tanimoto, K. and Takahashi, S. (1994). "Japanese experience on composite breakwaters." *International workshop on wave barriers in deep waters*, Yokosuka, Japan, 10–14 January 1994, pp. 1–24.

- Vijayalakshmi, K., Neelamani, S., Sundaravadivelu, R. and Murali, K. (2007). "Wave runup on a concentric twin perforated circular cylinder." *Ocean Engineering*, 34, 327–336.

- Xie, S.L. (1999), *"Wave forces on submerged semi-circular breakwater and similar structures." China Ocean Engineering*,13 (1), pp 63– 72.

- Xie, S.L., Li, Y.B., Wu,Y.Q and Gu, H.B. (2006). "Preliminary research on wave forces on quarter circular breakwater." *Ocean Engineering*, 24(1), 14-18.

- Yogesh K. R., Ravikiran L.and Arkal Vittal Hegde.(2012). "Reflection and loss characteristics of quarter-circle and semicircular submerged breakwaters." *Proceedings of National Conference on Hydraulic and Water Resources (HYDRO 2012),* IIT Bombay, India, 7 & 8 December 2012.

- Young, D.M. and Testik, F.Y. (2009). "Onshore scour characteristics around submerged vertical and semicircular breakwaters." *Coastal Engineering Journal*, 56(2009), 856–875.

- Young, D.M. and Testik, F.Y. (2011). "Wave reflection by submerged vertical and semicircular breakwaters." *Ocean Engineering Journal*, 38(2011), 1269–1276.

- Yuan, D. and Tao, J. (2003). "Wave forces on submerged, alternately, submerged, and emerged semicircular breakwaters." *Coastal Engineering Journal*; Volume 48: 75–93.

- Zhu, S. and Chwang, A.T. (2001). "Investigations on the reflection behaviour of a slotted seawall." *Coastal Engineering*, 43 (2001), 93–104.

INTERNATIONAL JOURNAL

1. **Binumol. S,** Subba Rao and Arkal Vittal Hegde (2017). "Hydrodynamic performance characteristics of an emerged perforated quarter circle breakwater**".** International *Journal of Innovative Research in Science Engineering and Technology* (IJIRSET)*,* ISSN (Online): 2319 – 8753, Vol. 6, Special issue 4, March 2017, pp. 45-48.

2. **Binumol. S,** Arkal Vittal Hegde and Subba Rao (2016). "Effect of water depth on wave reflection and loss characteristics of an emerged perforated Quarter circle breakwater". *International Journal of Ecology and development*, ISSN (Online): 0973-7308, Vol. 31(03), September, pp. 13-22.

3. V. Hafeeda**, S.Binumol**, A.V Hegde and Subba Rao (2014). "Wave reflection by emerged seaside perforated quarter circle breakwater."*International Journal of Earth Sciences and Engineering,* ISSN 0974-5904**,** Vol. 07(02), April, pp. 454 - 460.

NATIONAL JOURNAL

1. **Binumol. S,** Subba Rao and Arkal Vittal Hegde (2017). **"**Wave reflection and loss characteristics of an emerged quarter circle breakwater with varying seaside perforations**".** *Journal of Institution of Engineers - Series A* ISSN 2250-2149, DOI 10.1007/ s40030-017-0198-y (Published online).

2. **Binumol. S,** Arkal Vittal Hegde and Subba Rao (2017). "Sliding stability analysis of emerged quarter circle breakwater with varying seaside perforations". *Indian Journal of Geo-Marine Sciences,* ISSN 0975-1033, Vol. 46(07), August, pp 1428-1435.

INTERNATIONAL CONFERENCES

1. **Binumol. S**, Subba Rao and Arkal Vittal Hegde (2015). "Wave run up and rundown characteristics of an emerged seaside perforated quarter circle

breakwater." *International Conference on Water resources, Coastal and Ocean engineering (*ICWROE), NITK Surathkal, 12- 14   March 2015, paper published in Elsevier Aquatic Procedia , 4 (2015), pp. 234-239.

2. **Binumol. S**, Subba Rao and Arkal Vittal Hegde (2016) "Studies on the stability of an emerged seaside perforated quarter circle breakwater." *International conference on development of minor ports*, AMET University, Chennai, 26 August 2016.

NATIONAL CONFERENCES

1. **Binumol. S,** Subba Rao and Arkal Vittal Hegde (2017). "Hydrodynamic performance characteristics of an emerged perforated quarter circle breakwater**".** National Conference on Technological Advancements in Civil and Mechanical Engineering (NCTACME'17)*,* KMEA Engineering College, Kerala, 17-18 March 2017.

RESUME

Name   :   Binumol.S

Date of Birth   :   11-03-1977

Address   :   Shamu Nivas,

                           Peoples Nagar, House no.62,

                           Near Fire station, Kadappakkada,

                           Kollam -691001

                           Kerala

Mobile   :   (+91) 9656989721

Email   :   binus12@gmail.com

Qualification   :   B.Tech. (Civil), M.Tech. (Marine structures)

Journal Publications   :   International: 3   National: 2

No. of Conference Presentations   :   International: 2   National: 1